5-11-2015

# Quantitative Proteomic Analysis and Gene Expression Profiling Microarray Re-analysis of Uveal Melanoma

Pathma Ramasamy
*Royal College of Surgeons in Ireland*, pathmaramasay@rcsi.ie

# Quantitative Proteomic Analysis and Gene Expression Profiling Microarray Re-analysis of Uveal Melanoma

Pathma Ramasamy
MB BCh BAO MRCSI

Department of Ophthalmology
Faculty of Medicine and Health Sciences
Royal College of Surgeons in Ireland

Thesis submitted to the Royal College of Surgeons in Ireland for the degree of Doctor of Medicine


RCSI

May 2015

Supervisors: Dr Paula Meleady[a], Prof Susan Kennedy[a], Prof Martin Clynes[a], Prof Conor Murphy[b]

[a] National Institute for Cellular Biotechnology, Dublin City University
[b] Royal College of Surgeons Ireland

# Candidate thesis declaration

I declare that this thesis, which I submit to RCSI for examination in consideration of the award of a higher degree MD is my own personal effort. Where any of the content presented is the result of input or data from a related collaborative research programme this is duly acknowledged in the text such that it is possible to ascertain how much of the work is my own. I have not already obtained a degree in RCSI or elsewhere on the basis of this work. Furthermore, I took reasonable care to ensure that the work is original, and, to the best of my knowledge, does not breach copyright law, and has not been taken from other sources except where such work has been cited and acknowledged within the text.

Signed _____

Student Number _____

Date _____

Table of Contents

# List of abbreviations

| | |
|---|---|
| 2D-DIGE | Two-dimensional difference gel electrophoresis |
| 2-DE | Two-dimensional gel electrophoresis |
| 3HIDH | 3-Hydroxyisobutyrate Dehydrogenase1 |
| ADAM10 | A disintegrin and metalloproteinase domain 10 |
| AKT | Protein kinase B |
| ANOVA | Analysis of variance |
| ANXA5 | Annexin A5 |
| AP-2 | Activator protein-2 |
| APC | Antigen presenting cells |
| APEX | Absolute protein expression |
| APOE | Apolipoprotein E |
| APOH | Apolipoprotein H |
| AQUA | Absolute QUAntification of protein |
| AUC | Area under curve |
| BAP1 | BRCA1 associated protein-1 |
| BARD1 | BRCA1-associated RING domain protein 1 |
| BCAT1 | Branched chain aminotransferase 1, cytosolic |
| BCL2 | B-cell CLL/lymphoma 2 |
| BET | Bromodomain and extraterminal domain |
| BRAF | v-Raf murine sarcoma viral oncogene homolog B |
| BRD4 | Bromodomain-containing protein 4 |
| CELF2 | Elav-like family member 2 |
| CHL1 | Cell adhesion molecule with homology to L1CAM |
| CID | Collision induced dissociation |
| CNDP2 | Cytosolic non-specific dipeptidase |
| CNTN3 | Contactin 3 |
| CNTN3 | Contactin 3 (plasmacytoma associated) |
| COL1A1 | Collagen, type I, alpha 1 |
| CRYAB | Crystallin, alpha B |

| | |
|---|---|
| CTLA4 | Cytotoxic T-lymphocyte-associated protein 4 |
| CXCR3 | Chemokine (C-X-C motif) receptor 3 |
| D3NM | Disomy 3 uveal melanoma tumour that did not develop metastasis |
| DAG | Diacylglycerol |
| DCN | Decorin |
| DJ-1 | Parkinson protein 7 |
| DLC1 | Deleted in liver cancer 1 |
| ECD | Electron capture dissociation |
| EF1G | Elongation factor 1 gamma |
| EIF1AX | Eukaryotic translation initiation factor 1A, X-linked |
| ENOA | Enolase 1 |
| ERK | Extracellular signal-regulated kinase |
| ESI | Electrospray ionization |
| ET-3 | Endothelin-3 |
| ETD | Electron transfer dissociation |
| FABP3 | Fatty acid-binding protein, heart-type |
| FFPE | Formalin-fixed paraffin-embedded |
| FISH | Fluorescence in situ hybridization |
| FXR1 | Fragile X mental retardation, autosomal homolog 1 |
| G6PI | Glucose-6-phosphate isomerase |
| GEP | Gene expression profiling |
| GNA11 | Guanine nucleotide-binding protein subunit alpha-11 |
| GNAQ | Guanine nucleotide-binding protein G(q) subunit alpha |
| GNAS | Gs-α protein |
| GNB2 | Guanine nucleotide-binding protein G(I)/G(S)/G(T) subunit beta-2 |
| GnRH | Gonadotropin releasing hormone |
| GRB2 | Growth factor receptor-bound protein 2 |
| GRP78 | G protein-coupled receptor 78 |
| H&E | Hematoxylin and eosin stain |
| H2A | Histone A2 |
| H2O2 | Hydrogen peroxide |
| HDAC | Histone deacetylase |

| | |
|---|---|
| HEXB | Hexosaminidase B (beta polypeptide) |
| HGF | Hepatocyte growth factor |
| HGF | Hepatocyte growth factor |
| HMG-1 | High mobility group 1 |
| HSP-27 | Heat shock protein 27 |
| HSP60β | Heat shock 60 kDa protein B |
| HSP71 | Heat Shock 70kDa Protein 8 |
| HSPA1A | Heat shock 70 kDa protein 1A |
| HSPD1 | Heat shock 60kDa protein 1 |
| HTR2B | 5-hydroxytryptamine (serotonin) receptor 2B, G protein-coupled |
| ICAT | Isotope-coded affinity tags |
| ID2 | Inhibitor of DNA binding 2, dominant negative helix-loop-helix protein |
| IGF1 | Insulin-like growth factor 1 |
| INF | Interferon |
| IP3 | Inositol 1,4,5-trisphosphate |
| IRS | Insulin receptor substrate |
| ITGB1 | Integrin β1 |
| iTRAQ | Isobaric Tag for Relative and Absolute Quantification |
| JUN | V-jun sarcoma virus 17 oncogene homolog |
| KIT | Mast/stem cell growth factor receptor |
| LC | Liquid chromatography |
| LDHB | Lactate dehydrogenase B |
| LMCD1 | LIM and cysteine-rich domains 1 |
| LOH | Loss of heterozygosity of chromosome 3 |
| LZTS1 | Leucine zipper tumour suppressor-1 |
| M | Primary uveal melanoma tissue from patient that developed metastasis used for proteomic analysis |
| M3M | Monosomy 3 uveal melanoma tumour that developed metastasis |
| MALDI | Matrix-assisted laser desorption/ionization |
| MAPK | Mitogen-activated protein kinase |
| MAX | MYC associated factor X |

| | |
|---|---|
| MEGF10 | Multiple Epidermal Growth Factor 10 |
| MET | Met proto-oncogene |
| MMP11 | Matrix metallopeptidase 11 (stromelysin 3) |
| MnSOD | Mn2+ dependent superoxide dismutase |
| MRM | Multiple reaction monitoring |
| MS | Mass spectrometry |
| MTOR | Mechanistic target of rapamycin |
| MTUS1 | Microtubule associated tumor suppressor 1 |
| MUC18 | Melanoma cell adhesion molecule |
| NDKA | NME/NM23 nucleoside diphosphate kinase 1 |
| NFkB | Nuclear factor kappa-light-chain-enhancer of activated B cells |
| NM | Primary uveal melanoma tissue from patient that did not develop metastasis used for oroteomic analysis |
| nmUM | Full-face formalin-fixed paraffin-embedded primary uveal melanoma tissue from patient that did not develop metastasis |
| NRAS | Neuroblastoma RAS viral (v-ras) oncogene homolog |
| NSAF | Normalised spectral abundance factor |
| $O2^{\cdot -}$ | Superoxide |
| PAK1 | p21 protein (Cdc42/Rac)-activated kinase 1 |
| PDGF | Platelet-derived growth factor |
| PFKM | Phosphofructokinase |
| PGAM1 | Phosphoglycerate mutase 1 (brain) |
| PGM2 | Phosphoglucomutase 2 |
| PHB1 | Prohibitin |
| PHB2 | Prohibitin 2 |
| pI | Isoelectric point |
| PI3K | Phosphatidylinositol-4,5-bisphosphate 3-kinase |
| PIP2 | Phosphatidylinositol 4,5-bisphosphate |
| PKC | Protein kinase C |
| PKM2 | Pyruvate kinase, muscle |
| PLC | Phospholipase C |
| PPP | Picropodophyllin |

| | |
|---|---|
| PPP1CB | Protein Phosphatase 1, Catalytic Subunit, Beta Isozyme |
| PPP1R3C | Protein phosphatase 1, regulatory (inhibitor) subunit 3C |
| PPP1R3C | Protein phosphatase 1, regulatory subunit 3C |
| PRDX | Peroxiredoxin |
| PRDX3 | Thioredoxin-dependant peroxidase reductase, mitochondrial |
| PRELP | Proline/arginine-rich end leucine-rich repeat protein |
| PTEN | Phosphatase and tensin homolog |
| PTP4A3 | Protein tyrosine phosphatase type IV A member 3 |
| PTPRG | Receptor-type protein-tyrosine phosphatase gamma |
| PYGB | Phosphorylase, glycogen; brain |
| PYGL | Phosphorylase, glycogen, liver |
| Q-TOF | Quadrupole-time of flight |
| RAB31 | RAB31, member RAS oncogene family |
| ROBO1 | Roundabout, axon guidance receptor, homolog 1 (Drosophila) |
| ROS | Reactive oxygen species |
| SATB1 | SATB homeobox 1 |
| SCF | Stem cell-derived factor |
| SDC2 | Syndecan 2 |
| SF3B1 | Splicing factor 3B subunit 1 |
| SID | Surface induced dissociation |
| SILAC | Stable Isotope Labelling by Amino acids in Cell culture |
| SIN | Normalised spectral index |
| SIPA1L2 | Signal-induced proliferation-associated 1 like 2 |
| SIPA1L2 | Signal-induced proliferation-associated 1 like 2 |
| SNA | Standardised normalised abundances |
| SORBS2 | Arg/Abl-interacting protein ArgBP2 |
| SRC | -src avian sarcoma (Schmidt-Ruppin A-2) viral oncogene homolog |
| SRM | Selected reaction monitoring |
| STAT3 | Signal transducer and activator of transcription 3 |
| SYUA | Synuclein, Alpha |
| TFAP2A | Transcription factor activator protein-2 alpha |
| TFAP2C | Transcription factor activator protein-2 gamma |

| | |
|---|---|
| THBS2 | Thrombospondin 2 |
| TIC | Total ion chromatogram |
| TIMP3 | TIMP metallopeptidase inhibitor 3 |
| TLN1 | Talin 1 |
| TMA | Tissue microarray |
| TNF | Tumour necrosis factor |
| TOF | Time of flight |
| TPI1 | Triosephosphate isomerase |
| TRX | Thioredoxin |
| UM | Uveal Melanoma |
| VEGF | Vascular endothelial growth factor |
| WARS | Tryptophanyl-tRNA synthetase |

# List of figures

# List of tables

Table 36: Complete list of gene ontology (GO) molecular function, GO biological process, Protein ANalysis THrough Evolutionary Relationships (PANTHER) protein class and pathway details of 94 differentially expressed proteins with $p \leq 0.05$ and ≥ 2 peptides assigned to proteins, identified by quantitative label-free LC-MS proteomic analysis of 8 primary uveal melanoma tissues from patients who developed metastasis compared to 8 primary tumours of patients that did not develop metastasis. Data are presented in alphabetical order.___ Supplementary data

Table 37: Table showing 246 genes that were upregulated in monosomy 3 tumours with metastasis (M3M) compared to disomy 3 tumours without metastasis (D3NM). Bioinformatic reanalysis of publically available gene expression microarray profiling datasets of 11 M3M and 9 D3NM was performed. A fold change of > 1.3 and $p \leq 0.05$ was used. Genes are presented by ascending p value. _____ Supplementary data

Table 38: Table showing 203 genes that were downregulated in monosomy 3 tumours with metastasis (M3M) compared to disomy 3 tumours without metastasis (D3NM). Bioinformatic reanalysis of publically available gene expression microarray profiling datasets of 11 M3M and 9 D3NM was performed. A fold change of > 1.3 and $p < 0.05$ was used. Genes are presented by ascending p value. _____ Supplementary data

Table 39: Complete list of gene ontology (GO) molecular function, GO biological process, Protein ANalysis THrough Evolutionary Relationships (PANTHER) protein class and pathway details of 449 differentially expressed genes with fold change of > 1.3 and $p < 0.05$. Bioinformatic reanalysis of publically available gene expression microarray profiling datasets of 11 monosomy 3 tumours with metastasis (M3M) and 9 disomy 3 tumours without metastasis (D3NM) was performed. Data are presented in alphabetical order. _____ Supplementary data

Table 40: Clinical and histopathologic details of 92 uveal melanoma tissue samples used for tissue microarray immunohistochemistry _ Supplementary data

# Summary

Uveal melanoma (UM) is the most common primary intraocular malignancy in adults and 40% develop fatal metastatic disease. Compared to tumours with chromosome 3 disomy, monosomy 3 tumours will nearly exclusively develop metastasis. To identify differentially expressed proteins, quantitative label-free LC-MS proteomic profiling of 8 primary UM tissues from patients with metastasis (M) and 8 from patients without metastasis (NM) was performed. Fifty proteins with ≥ 3 peptides matched and $p < 0.05$ between the two patient groups were differentially expressed. Thioredoxin-dependant peroxidase reductase (PRDX3) was upregulated and cytosolic non-specific dipeptidase (CNDP2) was downregulated in M compared to NM. To identify differentially expressed genes, bioinformatic reanalysis of publically available gene expression microarray datasets of 63 primary UM tumours was performed. Samples with confounding factors (chromosome 3 disomy with metastasis and chromosome 3 monosomy without metastasis) and outlying samples in principal component analysis were excluded. Eleven monosomy 3 tumours with metastasis (M3M) versus 9 disomy 3 tumours without metastasis (D3NM) were compared. A total of 449 differentially expressed genes with fold change of ≥ 1.3 and $p < 0.05$ were found between the two patient groups. Signal-induced proliferation-associated 1-like protein 2 (SIPA1L2) was upregulated and contactin 3 (CNTN3) was downregulated in M3M compared to D3NM. Pilot immunohistochemical (IHC) study of PRDX3, CNDP2, SIPA1L2 and CNTN3 expression in 13 full-face formalin-fixed paraffin-embedded tissues of patients that did (mUM) and 13 that did not develop metastasis (nmUM) showed a trend toward higher expression of PRDX3 in mUM compared to nmUM (p: 0.061). Expression of CNDP2, SIPA1L2 and CNTN3 were not significant (p: 0.752, p: 0.094 and p: 0.099 respectively). IHC of PRDX3 in tissue microarray samples of 55 mUM and 37 nmUM tumours showed statistically significant difference in expression between mUM and nmUM (p: 0.001). Significant difference in survival was found based on high and low expression of PRDX3 (67.61 vs. 130.64 months respectively, p: 0.013). In conclusion, differential proteomic analysis of primary UM tissues from patients with and without metastasis has identified PRDX3 to be associated with metastasis and poor survival.

# Acknowledgement

This thesis would not have been possible without the help and support of numerous people to whom I'm eternally grateful. I would like to thank my supervisors Professor Susan Kennedy, Professor Martin Clynes, Professor Conor Murphy and most importantly, Dr Paula Meleady. Their vast knowledge and experience in the field enabled me to stay in the right course of direction, both from a research and career perspective. Their continual support, advice and patience throughout this process will never be forgotten. I would also like to thank them for giving me the opportunity to realise the importance of being a clinician with an active role in the scientific community. I would like to thank the Royal Victoria Eye and Ear Hospital and Eithne Walls Research Foundation for giving me the opportunity to undertake this research and funding the project. Without their tireless fundraising efforts, I wouldn't have had the opportunity to undertake this project.

To the staff and researchers at the National Institute of Cellular Biotechnology, I would like to thank you all for what has been a memorable and truly enriching experience. I would like to thank Dr Annette Linge and Dr Deirdre Flynn for introducing, teaching and assisting me with the technical aspects of proteomic analysis, and Mr Michael Henry for his expertise in mass spectrometry. I would also like to thank Dr Anne-Marie Larkin who was involved in a large part of this project. Without her expert advice on immunohistochemistry, this research would not have been possible. Finally, I'd like to thank Dr Padraig Doolan and Dr Colin Clarke, whose bioinformatics expertise is second to none.

I would like to thank Prof Susan Kennedy and the National Ophthalmic Laboratory in the Royal Victoria Eye and Ear Hospital for providing access to a vast archive of tissues used for this research. I'd also like to thank the staff at the

hospital laboratory, Mr Damien Tiernan, Ms Fionualla McAree and Ms Alison Davis for their assistance in obtaining tissues and immunohistochemical slides. Finally, I'd like to thank my wife for her continual support and patience. Without her endless love, patience and sacrifice, I would not have been able to complete this research. I would like to thank her for always supporting me, giving me perspective, providing motivation and inspiration to complete this thesis.

**This thesis is dedicated to my wife Rachael,**

**daughter Edith, son Theodore,**

**and my mother Pushpa**

# List of outputs

## I. Publications

1. Proteomics in Uveal Melanoma. Ramasamy P et al. Exp Eye Res. 2014 Jan;118:1-12. doi: 10.1016/j.exer.2013.09.005. Epub 2013 Sep 19. Review

## II. Presentations

1. Irish College of Ophthalmologists Annual Conference, Dublin. May 2012. *Proteomics in Uveal Melanoma*
2. Biotechnology in Action, Dublin City University. September 2012. *Label-free Proteomic Analysis of Uveal Melanoma Validates This Novel Technology (poster)*
3. European Association for Vision and Eye Research, Nice. October 2012. *Proteomic Analysis of Uveal Melanoma*
4. RCSI Research Day, Dublin. March 2013. *Label-free Proteomic Analysis of Uveal Melanoma Identifies Novel Proteins Associated with Metastasis and Death*
5. New England Ophthalmological Society, Boston. May 2013. *Label-free Proteomic Analysis of Metastatic versus Non-metastatic Primary Uveal Melanoma (poster)*
6. Irish College of Ophthalmologists conference, Killarney. May 2013. *Bioinformatic Re-analysis of Gene Expression Microarray Data of Uveal Melanoma (poster)*
7. Association for Research in Vision and Ophthalmology, Florida. May 2014. *Proteomics in Uveal Melanoma Identifies Novel Proteins Associated with Metastatic Disease*

## III. Awards

1. Barbara Knox Medal for best oral presentation, Irish College of Ophthalmologists Annual Conference, Dublin. May 2012.
2. Best paper in oncology section, European Association for Vision and Eye Research, Nice. October 2012.

3. Postgraduate Scholar's Prize for best presentation, RCSI Research Day, Dublin. March 2013.
4. International travel grant award, Association for Research in Vision and Ophthalmology, Florida. May 2014.

# 1. Introduction

## 1.1. Introduction to Uveal Melanoma

Uveal melanoma (UM) is the most common primary intraocular malignancy in adults. The overall incidence is approximately 5 to 7 cases per million per year, and climbs to more than 20 cases per million per year by the age of 70 (1,2). It is more common in the Caucasian population, especially those with blue/grey iris. The survival rates at 5, 10 and 15 years are 65%, 50% and 45% respectively (2–4). Ninety-two percent of cases of UM arise in the choroid while the remainder arise in the iris and ciliary body (Figure 1). Choroidal melanomas have the worst prognosis, while iris melanomas have the most favourable. The latter may be due to earlier presentation, as iris melanomas may be detected by the patient externally. Unfortunately, choroidal melanomas are usually detected late, when the patient is symptomatic with decreased visual acuity. This may be due to the involvement of the macula, or when complicated by secondary retinal detachment. There are several treatment options available for uveal melanoma. These include eye-preserving plaque radiation brachytherapy for choroidal tumours measuring less than 10mm in height and 20mm in basal diameter and proton beam therapy for tumours that are small and inaccessible due to its posterior location. However, the vast majority of patients require enucleation due to large tumour size at presentation (Figure 2).

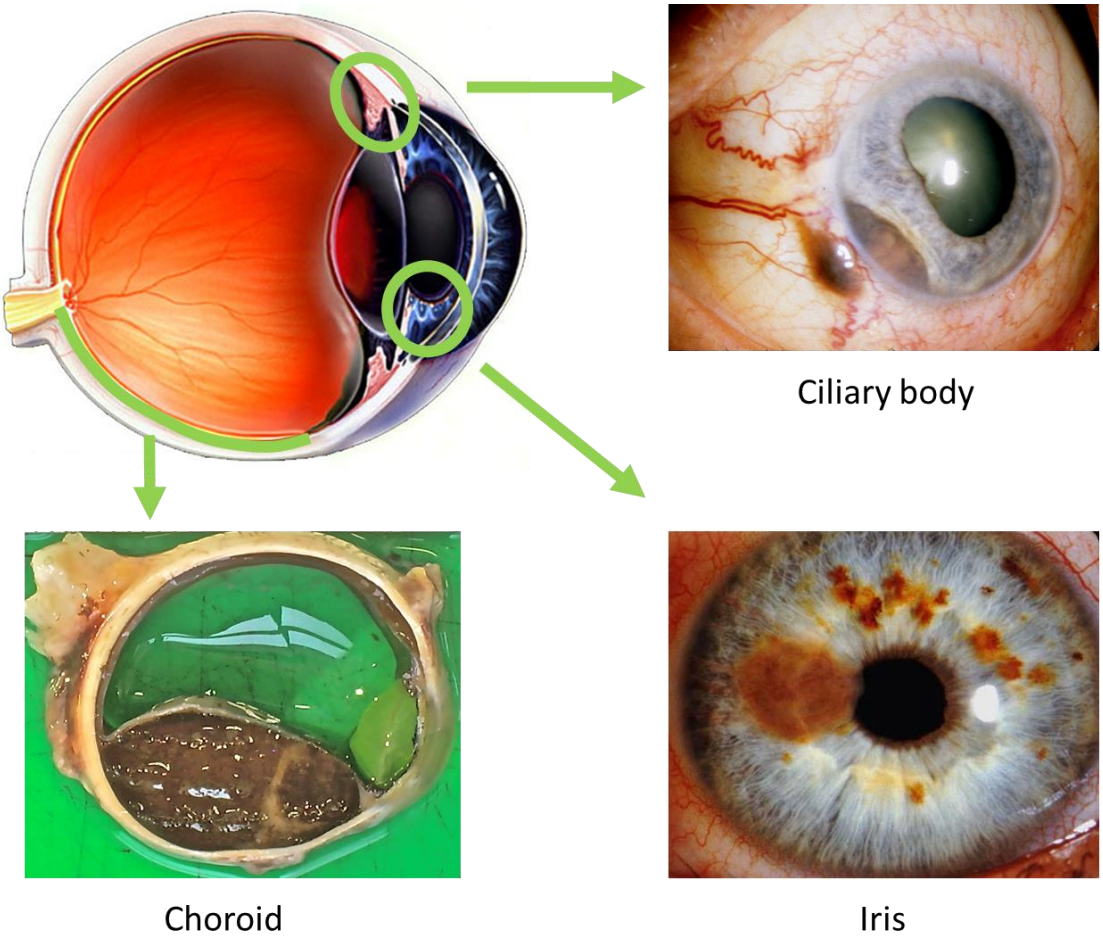


Figure 1: Uveal melanoma may arise anywhere along the uveal tract; choroid (92%), ciliary body (5%) and iris (3%).

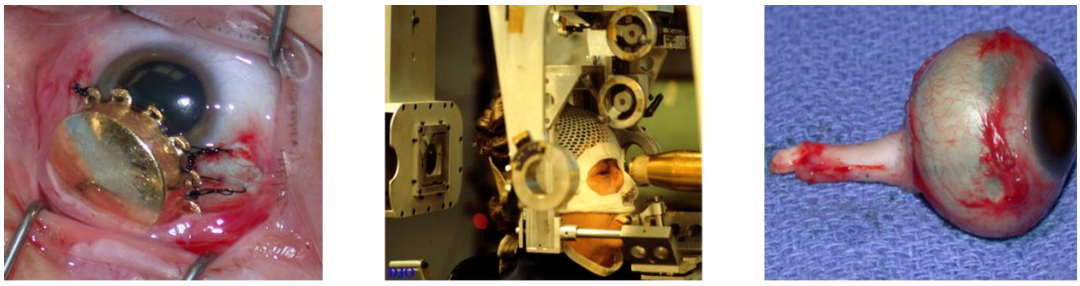


Figure 2: Treatment options for uveal melanoma; (a) plaque radiation brachytherapy for choroidal tumours measuring less than 10mm in height and 20mm in basal diameter; (b) proton beam therapy for tumours that are small and inaccessible due to its posterior location; (c) enucleation for large tumours.

Uveal melanoma is associated with the development of metastasis in about 50% of cases, and 40% of patients with UM die of metastatic disease despite successful treatment of the primary tumour (5,6). Metastatic spread occurs haematogenously, predominantly to the liver in up to 90% of patients with metastatic disease (7). Other potential sites include lung, bone and skin, but these are rare in the absence of liver metastasis (8). The occurrence of metastasis is primarily detected after disease-free intervals following local treatment, sometimes after more than a decade. This suggests the presence of occult micrometastatic disease at the time of the diagnosis and treatment of the primary eye tumour (9). When liver metastasis is diagnosed, treatment options are limited and survival is short, averaging 5-8 months (10). Despite progress in early diagnosis and treatment of primary UM, mortality rates have remained similar over the last 25 years (11,12). This is due to the lack of effective biomarkers to identify early metastasis and therapeutic targets for metastatic uveal melanoma.

There are several prognostic factors which include clinical, histopathologic and cytogenetic factors, the latter being the most accurate and reliable. Until recently, cell type was the most used prognostic indicator as epithelioid and mixed (consisting of both epithelioid and spindle) tumours are more aggressive than spindle cell type. Recent advances in molecular genetics have increased our knowledge on the cytogenetic properties of uveal melanoma. Studies have shown that UM tumours are characterized by non-random alterations in chromosomes 1, 3, 6, and 8 (13). Tumours with loss of chromosome 3 are associated with poor prognosis (14). Approximately 70% of patients with monosomy 3 in the primary tumour died of metastases within 4 years after the initial diagnosis, while tumours with normal chromosome 3 status rarely give rise to metastatic disease (14). Monosomy 3 and trisomy 8, partial duplication of 8q, or iso-chromosome 8q are the most frequent karyotypic abnormalities present in approximately 50% of cases (13). Cytogenetic studies have revealed that deletion or loss of heterozygosity of chromosome 3 and gain of chromosome 8 correlates with an increased risk of metastasis (15,16). Chromosome 8 abnormalities are

also associated with large tumour size and aggressive histology (15). In addition, loss of 1p is an independent prognostic factor for increased risk of metastasis (17,18). Amplification of 6p is found in approximately 25% of tumours (19,20). Chromosome 6p gains are mutually exclusive with monosomy 3 and rarely develop metastasis (20).

A number of gene-expression profiling studies have revealed that primary UM clusters in two different classes; class 1 tumours that are associated with a good prognosis and class 2 tumours with a high metastatic risk (21,22). The most common known oncogenic mutations occur in GNAQ or GNA11 which are found in about 85% of all primary UM, irrespective of tumour class or stage (23,24). These mutations may represent an early event that leads to the development of UM. Further downstream, mutations in BAP1 gene located in chromosome 3, were found to occur almost exclusively in metastasizing class 2 tumours (25). Either BAP1 mutation or loss of chromosome 3 can occur first, but both events appear to be necessary for the tumour to metastasise (26). More recently, mutations in splicing factor SF3B1 were found to be associated with a better prognosis (27). Individuals with SF3B1-mutant tumours tended to have a lower metastasis rate than those with tumours with wild-type SF3B1. SF3B1 and BAP1 mutations were almost mutually exclusive, suggesting that they may represent alternative pathways in tumour progression (27).

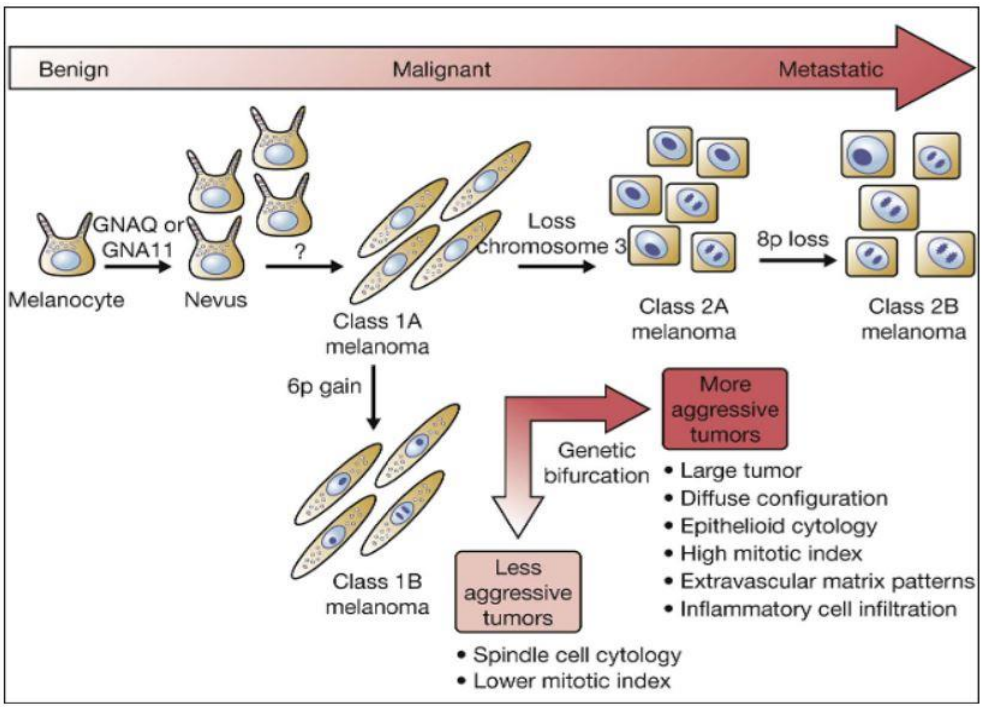


Figure 3: Schematic representation of the transformation of melanocytes to naevus, melanoma and ultimately metastatic phenotype. GNAQ/GNA11 mutation represents an initial event that triggers transformation of melanocytes. Class 1 tumours are characterised by chromosome 3 disomy and low risk for metastasis. Loss of chromosome 3 leads to class 2 tumours with high risk for metastasis. Adopted from Retina, 5$^{th}$ Edition, S Ryan 2013 (28).

Recently, Laurent at al (29) performed gene expression profiling of 28 primary UM tumours from patients who developed metastasis within 3 years compared to 35 primary tumours from patients who did not develop metastasis within 3 years or metastasised after 3 years. Protein tyrosine phosphatase type IV A member 3 (PTP4A3) was found to be associated with metastasis in UM. Overexpression of PTP4A3 in uveal melanoma cell line was found to significantly increase invasion and migration *in vitro*. However, this study has an inherent limitation as UM may metastasise after a disease-free interval of more than a decade. Thus, a direct comparison of the expression profile of metastatic versus non-metastatic primary UM tissue was not determined since tumours from patients who metastasised after 3 years were included with UM tumours from patients who did not metastasise.

## 1.2. Biology of Uveal Melanoma

Uveal melanocytes, like their epidermal counterpart, are derived from pluripotent neural crest cells that migrate out of the neural crest and populate the uveal tract. However, uveal melanocytes appear to have a distinct developmental lineage compared to epidermal melanocytes. Compared to epidermal melanocytes, dermal and uveal melanocytes were shown to be less dependent on KIT signalling and highly dependent on endothelin-3 (ET3) and hepatocyte growth factor (HGF) signalling (30). ET3 mediates its signalling through α g-proteins GNAQ and GNA11 via the endothelin B receptor. In mouse models, mutations in GNAQ and GNA11 were shown to result in dermal melanocytosis and hyperpigmentation (31). Although, the uveal tract was not investigated in this study, these findings are consistent with the suggestion that the ET3/endothelin B receptor/GNAQ or GNA11 pathway is an important developmental pathway for dermal (and likely uveal) melanocytes, distinct from the developmental pathways that result in epidermal melanocytes (32). Uveal melanoma tumours seem to have aberrations in these same pathways that are crucial to uveal melanocyte development.

Constitutive activation of the RAS-RAF-MEK-ERK (extracellular signal-regulated kinase) or mitogen-activated protein kinase (MAPK) pathway plays a crucial role in uveal melanoma development (33,34). G proteins are a family of heterotrimeric protein complex that are coupled to the 7-transmembrane spanning cell surface receptors. Ligand binding to and activating these receptors catalyses the exchange of GDP for GTP bound to the inactive G protein alpha subunit resulting in a conformational change and the subsequent dissociation of the Gα from the Gβγ subunits. These 2 subunits are capable of regulating various second messengers. GNAQ has an intrinsic GTPase domain at the C terminus which causes the hydrolysis of GTP to GDP and the Gα-GDP re-associates with Gβγ subunits. The activated Gα subunit mediates its activity through stimulation of phospholipase C-β (PLC β), which catalyses PIP2 to IP3 and DAG. DAG goes on

to activate protein kinase C (PKC), which activates ras. Ras activates Raf, which subsequently activates MAP/ERK (extracellular signal-regulated kinase) kinase (MEK). MEK phosphorylates and activates ERK, which dimerises and translocates to the nucleus, where it mediates cell proliferation, survival, differentiation, and apoptosis. Phosphorylated ERK also activates mTOR, which stimulates cell proliferation through translational control of cell-cycle progression regulators.

GNAQ or GNA11 mutations are found in about 85-91% of all UM and represents the most common oncogenic mutation (23,24,35). The mutations are mutually exclusive and occur in exon 4 (R183) or exon 5 (Q209) in GNAQ or GNA11. It is not associated with tumour class, stage or clinicopathological parameters and therefore, indicates an early event in the disease pathogenesis (23). Unlike cutaneous melanoma, genetic mutations in BRAF or NRAS are rare in UM, suggesting that activation of MAPK occurs through a mechanism different to cutaneous melanoma (34,36). It has been shown that mutations in the Gqα subunits GNAQ or GNA11 are responsible or the constitutive activation of the MAPK pathway in the development of UM. Mutant GNAQ/GNA11 are affected at the intrinsic GTPase domain where hydrolysis of GTP to GDP and the Gα-GDP re-association with Gβγ subunits is defective. Thus, this leads to the constitutive Gα activation and downstream signalling of the MAPK pathway.

*In vitro*, exogenous expression of mutant GNAQ increased MAPK phosphorylation, whereas knockdown of GNAQ in UM cell lines with mutant GNAQ diminished MAPK phosphorylation, decreased pERK expression with subsequent reduction in growth and increased apoptosis (24,37–39). More recently, it was also shown that the activation of protein kinase C (PKC) pathway is as a consequence of GNAQ/GNA11 mutation, with downstream activation of the MAPK pathway. Two different protein kinase C (PKC) inhibitors, AEB071 and enzastaurin, were shown to independently increase the accumulation of $p27^{Kip1}$, while decreasing the expression of cyclin D1 in three GNAQ-mutated cell lines, leading to G1 cell-cycle arrest (40,41). Several studies have demonstrated that G1 arrest induced by MEK inhibitors is mediated via inhibition of ERK1/2,

characterized by decreased expression of cyclin D1 and accumulation of $p27^{Kip1}$ (42–44). The PKC inhibitors also demonstrated antiproliferative effects on these cell lines, suggesting that the suppression of Erk1/2 phosphorylation may be critical to inhibit proliferation through altering the expression of p27, cyclin D1, Bcl-2 and survivin. In mouse models, treatment with PKC inhibitor significantly slowed tumour growth but did not induce tumour shrinkage. When combined with MEK inhibition, sustained synergistic MAPK pathway inhibition was observed, leading to tumour regression (45). This indicates protein kinase C (PKC) is a target of GNAQ/GNA11 signalling that ultimately leads to ERK1/2 (MAPK3/MAPK1) activation.

The PI3K/AKT signalling pathway has also been implicated in UM. PI3K is activated by G-protein–coupled receptors and by receptor tyrosine kinases. Once activated, PI3K catalyses the conversion of PIP2 to PIP3. AKT activation is initiated by translocation to the plasma membrane mediated by activated PIP3. Once phosphorylated and activated, AKT phosphorylates many other proteins, including the downstream effector mTOR and regulates a wide range of cellular processes involved in protein synthesis, metabolism, cell survival, proliferation, angiogenesis and migration (46,47). Cellular levels of PIP3 are regulated by the opposing activity of PTEN. PTEN, an important tumour suppressor, antagonizes PI3K activity by converting it back to PIP2 and thus, decreases AKT activation.

In a study of 75 UM tumours, loss of heterozygosity of the PTEN locus was found in 76% of tumours and actual mutations within the PTEN coding region was observed in 11% of tumours. Furthermore, downregulation of PTEN expression in aggressive compared with less aggressive tumours was shown immunohistochemically (48). Patients with a total loss of PTEN had a median survival of 60 months compared with more than 120 months for patients with normal or nearly normal PTEN expression (48). Immunohistochemical expression of phosphorylated AKT has also been associated with negative prognostic indicators in UM (49). Several UM cell lines with chromosomal deletions leading to loss of expression of PTEN, show PI3K activation, representing one mechanism

of this pathway activation (48,50,51). However, the effect of activated GNAQ or GNA11 on signalling through the PI3K/AKT pathway appears to be cell-type specific, and has not been determined in uveal melanoma (52,53). An *in vitro* study found that inhibition of MEK, and therefore MAPK signalling results in the reciprocal activation of AKT activity in uveal melanoma cell lines, regardless of GNAQ/11 mutant status (54). MEK inhibition alone caused cell cycle arrest and reduced growth in most UM cells, but only modest apoptosis was observed. Similarly, PI3K inhibition alone caused cell cycle arrest and reduced growth, but was insufficient to induce apoptosis. However, the combination of MEK and PI3K inhibition resulted in a strong induction of apoptotic death. Proteomic network analysis revealed a homeostatic relationship between the MEK/MAPK and PI3K/AKT pathways in uveal melanoma cells. Inhibition of MEK resulted in a relative increase in AKT phosphorylation, whereas, an increase in the phosphorylation of MAPK was observed after inhibition of PI3K. Khalili et al conclude that the PI3K/AKT pathway is stimulated independent of GNAQ/GNA11 mutation status, and a combination of MEK and PI3K inhibitor was more effective at inducing cell death (54). A more recent study showed that PI3K-α inhibitor (BYL719) enhanced the effect of PKC inhibitor (AEB071) in GNAQ/GNA11 mutant cell lines (55). AEB071 treatment inhibited growth and reduced ERK1/2 but persistent AKT activation was observed. BYL719 had minimal anti-proliferative activity in all uveal melanoma cell lines, and inhibited phosphorylation of AKT in most cell lines. Combination treatment showed synergistic inhibition of cell proliferation and apoptotic cell death *in vitro*. Similarly, *in vivo* studies showed reduced xenograft tumour in a GNAQ mutant model. This suggests that the PI3K/AKT pathway is activated and plays a critical role in UM development.

KIT, a member of the PDGFR family of kinases, is a receptor tyrosine kinase that is activated by binding of stem cell-derived factor (SCF) and plays an essential role in the regulation of various cellular processes including cell survival and proliferation, stem cell maintenance, and in melanogenesis (56). KIT activates the AKT signalling pathway by phosphorylating PI3K and also transmits

signals via GRB2 and activation of RAS, RAF1 and the MAPK pathway (56). Mouriaux et al showed KIT expression in normal choroidal melanocytes and activation by SCF stimulated proliferation (57). In normal uveal melanocytes, stimulation with SCF resulted in activation of both ERK1/2 and AKT but in a KIT-expressing UM cell line, stimulation led to MAPK pathway activation only (58). Immunohistochemical expression of KIT was positive in 62.7-78.2% of primary UM tissue and treatment with a KIT inhibitor led to significant decrease in proliferation, invasion and cell death in UM cell lines (58,59). An *in vitro* study found constitutive ERK1/2 activation that enabled UM cell proliferation and transformation in a KIT dependant manner. Inhibition of UM proliferation was observed when depleted of SCF/KIT, but not AKT, suggesting that the proliferative effects of the SCF/KIT autocrine loop in uveal melanoma likely funnel primarily through the MAPK pathway (60). However, activation-related mutations of KIT have not been found (57,61).

The MET proto-oncogene encodes a receptor tyrosine kinase that modulates diverse biological functions such as cell motility, proliferation, survival and is known to be upregulated in multiple cancers (62–65). Hepatocyte growth factor (HGF) binding to MET receptor leads to activation and initiation of downstream signalling mediated by GRB2, PI3K, RAS, and SRC (65). Given the preferential dissemination of UM cells to the liver, HGF and MET have been investigated in several studies. High immunohistochemical expression of HGF and MET in primary UM tissues have been reported (66–68). Mallikarjuna et al found a significant association between high MET expression and death due to uveal melanoma. Interestingly, the 6 tumours with liver metastasis showed higher expression of MET and were negative for HGF, suggesting a possible mechanism of ligand-independent MET activation (69). The activation of PI3K/AKT pathway induced by the HGF/MET was shown to attenuate cell-cell adhesion by downregulation of cell adhesion molecules E-cadherin and beta-catenin, promoting the enhanced motility and migration of uveal melanoma cells (70,71). On HGF stimulation, receptor MET translocated to the nucleus in a ligand-dependent manner, suggesting that MET may modulate the expression of genes

involved in UM cell migration (70). Conversely, downregulation of MET expression decreased proliferation and migration by inhibiting AKT phosphorylation (67,72). However, no activating mutations of MET in primary tumours and cell lines have been found, suggesting that MET activation in is most likely through indirect gene activation rather than copy number alteration or mutation involving the MET gene (67).

Similar to HGF, insulin-like growth factor 1 (IGF-1) is mainly produced by the liver. IGF-1 binds to IGF-1R and activates the intrinsic receptor tyrosine kinase activity and phosphorylates insulin receptor substrate (IRS). IRS, a major effector of insulin signalling in the liver, stimulates the phosphorylation of AKT via PI3K and MAPK to modulate cell proliferation, survival, migration as well as tumour invasiveness (73–75). IGF-1R has been shown to be expressed in primary UM tissues (66,68,76). In multivariate analysis, a significant association between high IGF-1R expression and melanoma-specific mortality was shown (68,76). Treatment of UM cell lines with picropodophyllin (PPP), a specific inhibitor of IGF-1R, decreased IGF-1R expression, phosphorylation, decreased downstream MAPK and PI3K signalling. This led to a decrease in growth and inhibited cell adhesion, migration and invasion. Furthermore, PPP significantly delayed establishment of uveal melanoma tumours, caused tumour regression and reduced the incidence of liver metastasis in mice (77,78).

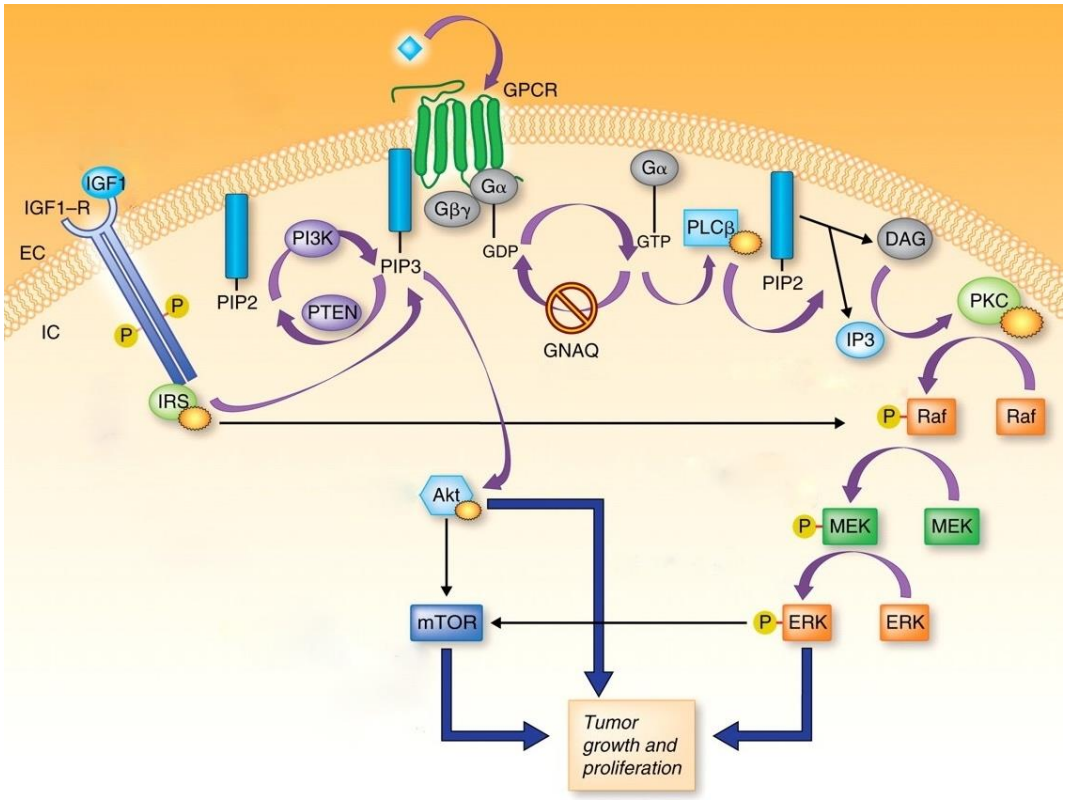


Figure 4: Major signalling pathways in uveal melanoma. The MAPK, P13K (phosphatidylinositol-3-kinase), mTOR, and IGF-1R pathways intersect significantly in uveal melanoma pathogenesis. Stimulation of GPCR (G-protein–coupled receptor) results in replacement of GDP for GTP on the Gα subunit. Gα-GTP is the active form and mediates activation of PLCβ, which promotes cleavage of PIP2 [phosphatidylinositol (4,5)-bisphosphate] to inosol triphosphate (IP3) and diacyl glycerol (DAG). DAG goes on to activate PKC, which stimulates the MAPK signalling pathway. MAPK signalling leads to tumour growth and proliferation. The GNAQ mutation inactivates the intrinsic phosphatase of the Gα protein, thus preventing hydrolysis of GTP to GDP and enabling constitutive downstream MAPK signalling. PI3K mediates phosphorylation of PIP2 to PIP3 [phosphatidylinositol (3,4,5)-trisphosphate], and PTEN (phosphatase and tensin homolog) antagonises this process. PIP3 activates AKT, which promotes tumour growth and proliferation. Both ERK and AKT also activate the mTOR-signalling pathway, which also mediates tumour growth and proliferation. IGF-1 simulation of IGF-1R leads to dimerisation and autophosphorylation of the receptor, resulting in recruitment and activation of IRS, which can then activate both the PI3K and MAPK pathways. Modified from (79)

As monosomy 3 tumours are associated with metastasis and poor prognosis, the remaining chromosome 3 genes likely contains mutations on potential tumour suppressor genes that can lead to an aggressive phenotype. Harbour et al conducted exome sequencing of monosomy 3 UM samples found that BRCA1-associated protein 1 (BAP1) had mutations on 3p21.1 in 85% of class 2 aggressive UM and almost never in class 1 tumours (25). Microarray gene expression profiling of 92.1 UM cells transfected with control versus BAP1 siRNA showed a shift in the expression profile towards class 2 signature in BAP1 depleted cells compared to control cells (25). Interestingly, BAP1 depletion caused an increase in mRNA levels of the proto-oncogene KIT, which are highly expressed in class 2 tumours. Furthermore, RNAi-mediated knock down of BAP1 in 92.1 UM cells, which did not contain a detectable BAP1 mutation, recapitulated many characteristics of the de-differentiated class 2 UM phenotype (80). Either BAP1 mutation or loss of chromosome 3 can occur first, but both events appear to be necessary for the tumour to metastasise (26). It is localised to chromosome 3p21.31-p21.2, a region previously noted by Trolet et al to be deleted in UM (81). It encodes a deubiquitinating enzyme that interacts with the breast cancer susceptibility gene (BRCA1) and BRCA1-associated RING domain protein 1 (BARD1) to form a tumour suppressor heterodimeric complex (29). It possesses a large C-terminal domain which is predicted to coordinate the selective association with potential substrates or regulatory components (82). Functionally, BAP1 enzyme removes ubiquitin molecules from specific proteins to regulate their function. For example, BAP1 removes ubiquitin molecules from histone H2A, which causes changes in the expression of specific genes that are regulated by this histone (83). It also modulates the assembly of multiprotein complexes containing numerous transcription factors and cofactors, and activates transcription in an enzymatic-activity–dependent manner, thereby regulating the expression of a variety of genes involved in various cellular processes (84). BAP1 has been implicated in several types of cancer such as lung, breast, and renal cell carcinoma (85–90). Germline BAP1 mutations have been described in families with a high risk for hereditary cancer and a novel ‘BAP1 cancer syndrome’ that includes UM, cutaneous melanoma and melanocytic

neoplasm, lung adenocarcinoma, meningioma and malignant mesothelioma, has been described (91–95). In HeLa and other cell lines, BAP1 depletion altered the expression of genes that were key mediators of cell-cycle progression, DNA replication and repair, cell metabolism, survival, and apoptosis (84). *In vivo*, expression of wild-type BAP1 was shown to significantly decrease tumourigenicity of a human non-small cell lung cancer cell line in nude mice. Conversely, expression of mutant BAP1 that lacks either deubiquitinating activity or nuclear localization did not suppress tumourigenicity, implying that both deubiquinating activity and nuclear localization are necessary for the tumour-suppressive activity (96). Depsipeptide, a histone deacetylase (HDAC) inhibitor was shown to inhibit proliferation and growth by increasing expression of Fas and FasL in 3 UM cell lines derived from primary tumour and 2 cell lines derived from liver metastasis. Depsipeptide induced gene upregulation of both Fas and FasL in these cells, and an increase in activated caspase-3, apoptosis and cell-cycle arrest was observed in treated cells compared to non-treated cells (97). Landreville et al showed that HDAC inhibitors induced morphologic differentiation, cell-cycle exit, and a shift to a differentiated, melanocytic gene expression profile in cultured UM cells. Furthermore, it was also shown to inhibit growth of UM tumours *in vivo* (98). Although BAP1 may function as a tumour suppressor in UM, the manner in which mutations/loss of this gene plays a role in the development of metastatic disease is not yet understood.

More recently, mutations in splicing factor SF3B1 were found to be associated with a better prognosis (27). Mutations in SF3B1 are single nucleotide point mutations predominantly occurring at arginine-625 and involve only 1 allele. Individuals with SF3B1-mutant tumours tended to have a lower metastasis rate than those with tumours with wild-type SF3B1. SF3B1 encodes a component of the spliceosome and is involved in splicing pre-mRNA. Mutations were associated with differential alternative splicing of protein coding genes. However, it is not clear how this mutation is involved in UM (99). SF3B1 and BAP1 mutations were almost mutually exclusive but occur with equal frequency in GNAQ versus GNA11 mutations, suggesting that they may represent

alternative pathways in tumour progression (27). Another study confirmed this finding, along with the identification of mutations in eukaryotic translation initiation factor 1A, X-linked (EIF1AX) in 24% of uveal melanomas, which were also associated with good prognosis (100). EIF1AX mutations were also found to be mutually exclusive with SF3B1and BAP1 mutations (100). EIF1AX encodes a protein involved in protein translation and biosynthesis but its function in UM is still unclear. Mutations in EIF1AX are non-truncating and heterozygous, which are characteristics usually associated with dominantly acting oncogenes (101). In UM cells with EIF1AX mutations, only mutant mRNA transcripts were expressed, suggesting that the wild-type copy of EIF1AX is epigenetically inactivated, in which case EIF1AX mutations might behave in a recessive fashion (100,101). As these mutations are mutually exclusive, it suggests that the genes have an overlapping function in a common pathway, such that mutation of one gene relieves the selective pressure to mutate the other (102).

## 1.3. Treatment of metastatic disease

Although difficult, successful treatment of the primary ocular tumour is usually achieved in all patients. These include eye-preserving plaque radiation brachytherapy for choroidal tumours measuring less than 10mm in height and 20mm in basal diameter and proton beam therapy for tumours that are small and inaccessible due to its posterior location. The vast majority of patients require enucleation due to large tumour size at presentation. However, the most challenging aspect in the management of UM patients is the treatment of metastatic disease. *In vitro*, numerous laboratory studies have demonstrated favourable or successful therapeutic response by targeting signalling pathways that are known to be involved in the pathogenesis of UM. However, clinical trials utilising these therapeutic agents have shown poor response to treatment. Despite progress in early diagnosis and treatment of primary UM, mortality rates have remained similar over the last 25 years (11,12). Treatment of metastatic disease includes locoregional therapies and systemic chemotherapeutic agents.

### 1.3.1 Surgical resection

In a retrospective study over a 16-year period, surgical resection of liver metastases almost doubled survival time, with complete resection increasing median overall survival from 14 months to 27 months (103). Development of liver metastasis > 24 months after diagnosis of UM, completeness of surgical resection, number of metastases resected of ≤ 4 and absence of miliary disease were associated with improved survival (103). Similarly, another study demonstrated a 3.7 fold increase in survival time of patients who had surgical resection compared to those that did not, with complete microscopic resection almost doubling the survival time compared to incomplete resection (104). Survival of patients with ≤ 5 metastatic lesions were 3.1 times longer than those with ≥ 6 lesions (104). A recent meta-analysis of 22 studies (579 patients) found a median disease-free survival of 8 to 23 months, and median overall survival of 14

to 41 months (105). Conversely, the median survival of non-operated patients ranged from 4 to 12 months (105). These studies demonstrate that only a small subset of patients would benefit from surgical resection of liver metastases. However, liver metastases are usually detected when the disease is disseminated, with multiple lesions involving both lobes. Thus, resection of metastatic lesions is not feasible in most patients.

### 1.3.2 Isolated hepatic perfusion (IHP)

IHP allows delivery of high doses of cytotoxic agents while minimising systemic toxicity. Alexander et al (106) investigated the treatment of unresectable UM liver metastases with 60-minute IHP using melphalan (11 patients) and melphalan with TNF (11 patients). There were 2 (9.5%) complete responses and 11 (52%) partial responses. The median duration of response was 9 months and was significantly longer in patients who received melphalan with TNF compared to melphalan alone (14 vs. 6 months respectively). The overall median survival was 11 months, with one treatment mortality. In a subsequent study by Alexander et al (107), 29 patients with unresectable UM liver metastases were treated with 60-minute IHP using melphalan. There were 3 (10%) complete responses and 15 (52%) partial responses with an overall survival of 12.1 months. Noter et al (108) evaluated 8 patients with UM liver metastases with 60-minute high-dose melphalan IHP. Four patients (50%) responded to treatment (partial/complete) with median overall survival of 9.9 months. Similar results were found by another study of 8 patients, where 3 demonstrated partial response to treatment with an overall survival of 11 months (109). In a recent retrospective study of 34 patients who underwent IHP with melphalan, overall response in 23 patients (68%) was seen, with complete response observed in 4 patients (12%). Time to progression was 7 months and the median overall survival was 24 months. When compared to a control group consisting of the longest surviving UM patients with liver metastases not treated with IHP, a significant survival advantage of 14 months was found (110).

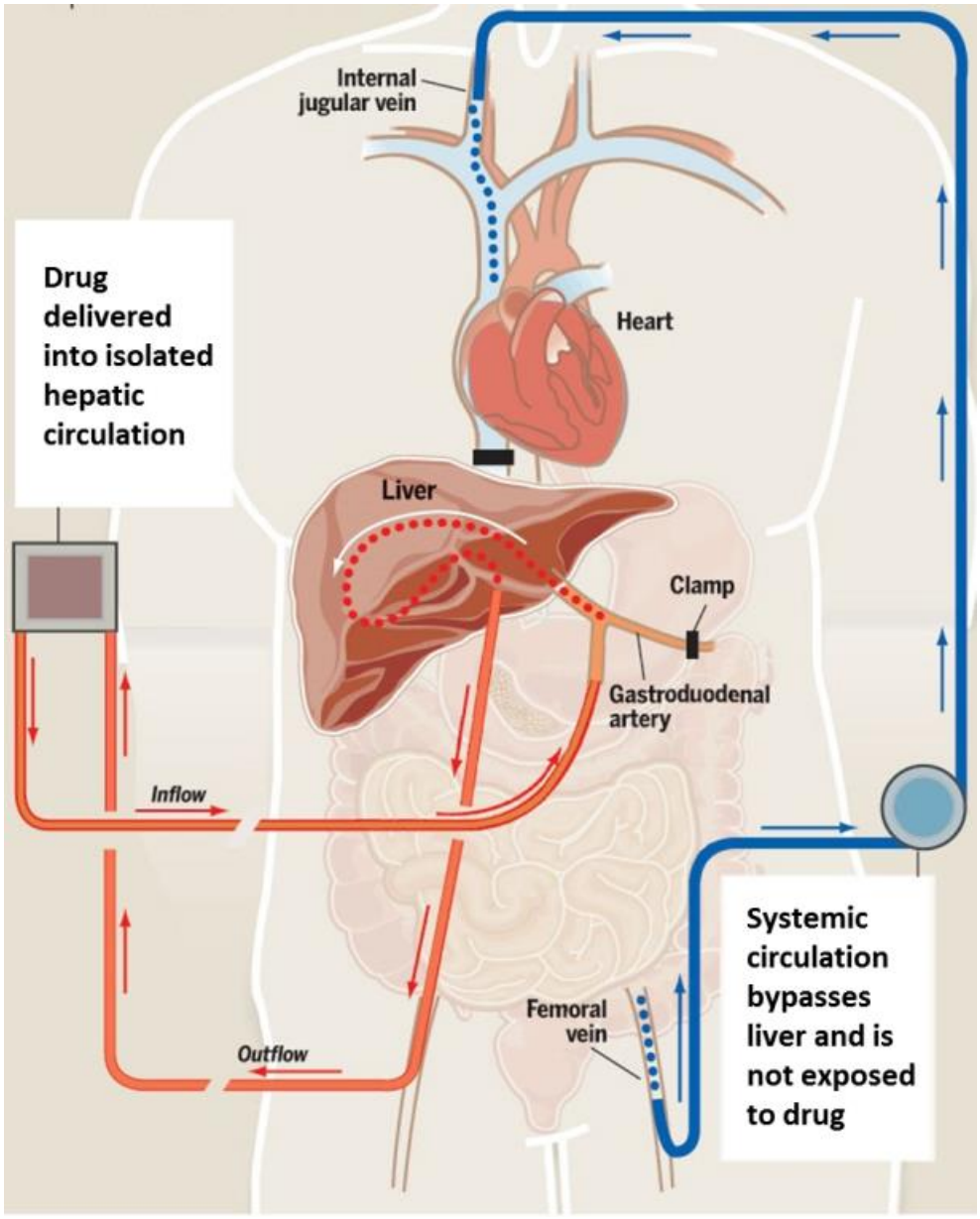


Figure 5: Illustration of the isolated hepatic perfusion (IHP) circuit. It is an invasive surgical procedure that involves laparotomy to isolate the hepatic circulation. The arterial inflow is via the gastroduodenal artery and venous outflow is collected from a cannula positioned in an isolated segment of retrohepatic vena cava. The inflow and outflow cannula are connected to a perfusion circuit. On the patient's left is the venovenous bypass circuit that shunts inferior vena cava blood flow from the femoral vein back to the systemic circulation via the internal jugular vein, thereby avoiding exposure to chemotherapeutic agents. Image modified from media.jsonline.com/images (111)

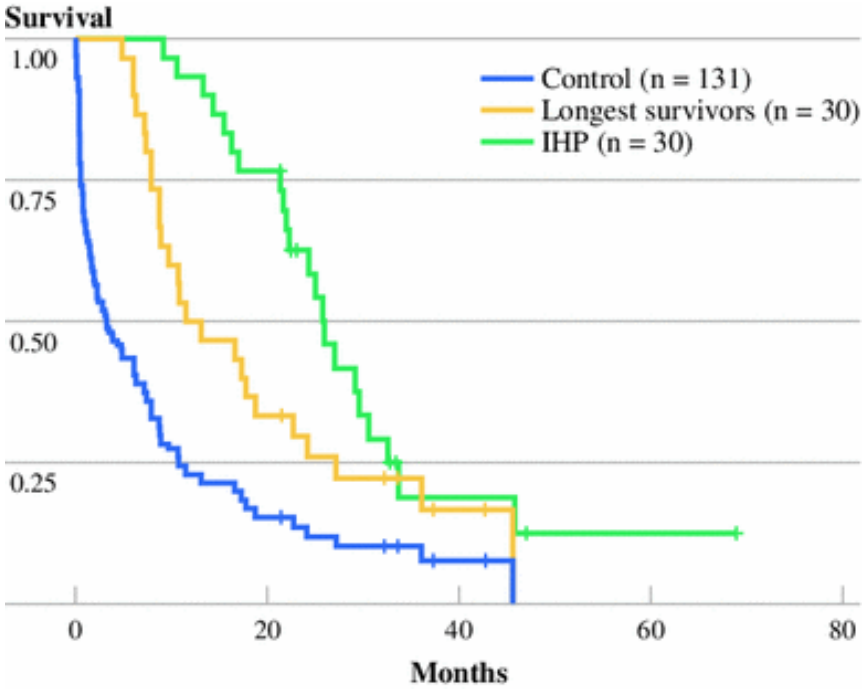


Figure 6: Survival curves showing significantly longer survival of patients treated with IHP (melphalan) compared to all controls and with the 30 longest surviving controls (110).

### 1.3.3. Hepatic intra-arterial chemotherapy (HIA)

HIA is a treatment modality that involves direct delivery of chemotherapeutic agent into the hepatic arterial circulation via a surgically placed hepatic artery catheter. This enables maximum local cytotoxic drug exposure with rapid systemic clearance. It also allows multiple, and outpatient-based administration of treatment once the catheter is in place. In a pilot study of HIA fotemustine in 7 patients, 2 demonstrated partial response while 3 had stable disease and the remaining 2 patients progressed (112). Leyvraz et al demonstrated an objective response in 12 of 30 patients who received HIA fotemustine, with median duration of response of 11 months and median overall survival of 14 months (113). In a larger study of 101 patients, the authors demonstrated an overall response rate of 36% with a median overall survival of 15 months and a 2-year survival rate of 29% (114). Interestingly, Leyvraz et al also found that 22 high-risk patients (without metastasis) treated with 6-month

course of adjuvant HIA fotemustine (four weekly doses of 100 mg/$m^2$, and after a 5-week rest, repeated every 3 weeks) demonstrated longer median overall survival of 1.6 years compared to randomly selected matched control group (from institutional database). The 5-year survival rate for treated patients was 75% compared to 56% for the non-treated group, but this was not significant (115). Melichar et al showed partial response of liver metastasis to hepatic arterial infusion of cisplatin, vinblastine and dacarbazine (116). Two patients had an objective response, 4 patients had stable disease and 4 patients had progressive disease. Patients who responded to treatment or who stabilised survived for over a year while those with progressive disease died within 1 year.

### 1.3.4. Immunoembolisation

Instead of chemotherapeutic agents, immunoembolisation utilises immunologic stimulants such as granulocyte macrophage colony-stimulating factor (GM-CSF). This stimulates recruitment of antigen-presenting cells such as macrophages and dendritic cells, and enhances elimination of tumour cells thereby potentially creating an in-situ tumour vaccine (117). In a phase I trial, Sato et al (118) investigated immunoembolisation in 34 patients with liver metastases. Two patients had a complete response and 8 patients had a partial response and 10 had stable disease. The median overall survival was 14.4 months and survival rate at 1 and 2 years were 62% and 26% respectively. In a subsequent study (119), the authors found that patients treated with high-dose (≥1500μg) GM-CSF had longer progression-free survival of 12.4 months compared to 5.6 months in patients receiving low-dose immunoembolisation (≤1000μg). Patients treated with high-dose immunoembolisation also demonstrated a longer median overall survival than patients treated by TACE with BCNU (20.4 vs 9.8 months). A further randomised phase II study using embolisation with or without GM-CSF in 52 patients showed longer median overall survival in patients treated with GM-CSF compared to those who we not (21.5 vs. 17.2 months respectively). Interestingly, immunoembolisation was shown to only benefit patients with larger volume of metastases (20-50%) where

median overall survival was 18.2 months compared to 16 months. In patients with tumour volume of <20%, immunoembolisation led to shorter time to progression in liver metastases of 3.7 months compared to7.2 months in patients treated without GM-CSF, suggesting an ambivalence biological effect of GM-CSF (120).

### 1.3.5. Transcatheter arterial chemoembolization (TACE)

TACE is an interventional radiological procedure that combines infusion of chemotherapeutic agents into the hepatic artery with simultaneous blockage of the tumour arterial supply. In a phase II trial using 1,3-bis(2-chloroethyl)-1-nitrosourea (BCNU) (121), median survival was 5.2 months (range: 0.1 to 27.6 months). Eighteen of 24 patients enrolled in this study showed response to treatment (1 complete response; 4 partial response; 13 stable disease). The median survival in patients with complete/partial response and stable disease was 21.9 months and 8.7 months respectively (range 7.4-27.6 months and 2.9-14.4 months respectively). In patients who progressed, median survival was 3.3 months. Vogl et al (122) demonstrated mean overall survival of 21 months in 8 of 12 patients who responded to TACE using mitomycin C and mean overall survival of 16.5 months in non-responders. The authors suggest that repeated TACE treatment is a palliative option for patients with multiple liver metastases. In another study using either fotemustine and/or cisplatin, 14 of 25 patients showed stable disease for at least 2 months. The median progression-free survival was 3 months (range: 2-4 months) and the median overall survival was 6 months (range: 5-7 months). It was also found that patients with lactate dehydrogenase levels of less than twice the upper limit of normal showed clinically detectable response to treatment (123). In 14 patients treated with cisplatin and/or carboplatin, 8 patients (57%) achieved partial response, 4 had stable disease and 2 patients progressed. Median survival after was 14.5 months in patients who responded compared to 10 months in those that did not respond (124). In a phase II trial (125), 10 patients were treated with drug-eluting beads preloaded with irinotecan. Of these, 6 patients had a major response of

reduction in tumour size of 80-90% and four patients had a tumour reduction of 60-70% following transarterial chemoembolization. The median overall survival time was 6.5 months (range: 4 to 9 months). Similarly, Venturini et al report a response rate of 80% in 5 patients treated with irinotecan drug-eluting beads (126). In a recent retrospective study of 21 patients treated with fotemustine chemoembolization (127), an overall response rate of 43% was found with partial response was seen in 3 patients (14%). Six patients had stable disease and 12 patients demonstrated progression (29% and 57% respectively).

Figure 7: Hepatic angiogram showing lack of filling of the right hepatic artery (white arrow) following administration of contrast agent, indicating successful embolisation by Transarterial Chemoembolisation (TACE). (128)

### 1.3.6. Adjuvant treatment

There are very few studies of adjuvant treatment in metastatic uveal melanoma. In a recent study to evaluate the efficacy of IFN-α-2a in high-risk patients, 121 patients underwent a 2-year adjuvant IFN-α-2a therapy within 3 years of radiation or enucleation of the primary tumour. A series of historical controls frequency-matched (2:1) to IFN-α-2a treated patients on age, tumour size, gender and survival time between primary therapy and initiation of IFN therapy were selected for comparison. No significant difference in survival between the 2 groups was observed (129). Salmon et al found that adjuvant intra-arterial fotemustine and/or DTIC-platinum following surgical resection of liver metastases in 61 patients did not show a significant survival advantage (130). In a more recent study, 22 high-risk patients (without metastasis) treated with adjuvant hepatic intra-arterial fotemustine after proton beam irradiation of the primary ocular tumour showed a survival benefit compared to randomly selected controls. The 5-year survival rate for treated patients was 75% compared to 56% for the non-treated group, but this was not significant (115).

### 1.3.7. Systemic therapy

Systemic chemotherapy has been the subject of significant research prior to the emergence of other targeted therapies. A meta-analysis of 40 systemic chemotherapeutic studies (131) consisting of 841 patients with metastatic uveal melanoma showed an overall response rate of 4.6%. In 55% of those studies, no response was observed. Median overall survival was reported in 65% of those studies and ranged from 5.2 months in pre-treated, predominantly end-stage patients (132) to 19.0 months in selected first-line patients (133). Progression-free survival (PFS) was reported in 52.5% of studies and ranged from 1.8 to 7.1 months.

Studies using single alkylating agents such as dacarbazine (134), treosulfan (135) and temozolomide (136) have been disappointing, with overall response rate of between 0-8% and overall survival of 6.7-8.7 months. Similarly, older generation immunomodulators such as thalidomide (137) and lenalidomide (138) have been disappointing with no response shown. Treatment with mitotic inhibitors such as DHA-paclitaxel in 22 patients showed partial response in 1 patient (139) while a pilot study using vincristine in 4 patients showed complete response of lung metastasis in 1 patient (140). The safety and efficacy of vincristine is currently being investigated in 50 patients with metastatic UM (NCT00506142). A retrospective study by Spagnolo et al (141) analysed 25 consecutive metastatic UM patients (with and without liver disease) treated with intravenous fotemustine as first-line treatment. Two patients showed partial response while 9 had stable disease with an overall response rate of 8.3% and disease control rate of 44%. The median survival was 13.9 months, and the 1-year survival rate was 60%. In a recent and only randomised phase III trial comparing intravenous and HIA fotemustine in 171 patients, Leyvras et al report similar results between the two treatment groups, with no significant difference or improvement in overall survival (142). In another phase II study, Schmidt-Hieber et al concluded that bendamustine was ineffective in metastatic UM with no response observed in any of the 11 patients (143).

The combination of gemcitabine and treosulfan has been investigated in 6 phase I and II studies. A pilot study by Pfohler et al in 2003 demonstrated an excellent overall response of 28.6% of the 14 patients evaluated, with an overall survival of 15.3 months and progression free survival of 7.1 months (144). However, subsequent studies have failed to replicate these results, with 5 studies reporting an overall response of 0-4.2%, overall survival of 7.5-13.3 months and progression free survival of 2.5-6.8 months (135,145–148). In a randomised control phase II study, Schmittel et al compared gemcitabine and treosulfan combination therapy to treosulfan alone and did not find any significant difference between these regimens (135). In another study by the same author, the combination of cisplatin, gemcitabine and treosulfan triple

therapy was compared to gemcitabine and treosulfan dual therapy (148). Similarly, no significant difference was found.

The immunomodulatory effects of interferon alpha-2b, in combination with other chemotherapeutic agents were investigated in several studies. In 2003, the combination therapy BOLD/INFα-2b (bleomycin, vincristine, lomustine, dacarbazine and INFα-2b) was investigated in a multicentre study (149) after 2 prior phase II studies demonstrated an overall response of 15-20% (150,151). However, no response was observed in any of the 24 patients evaluated. A pilot study of 6 patients investigating the use of thalidomide/INF-α2b therapy did not show any response (152) while 1 patient (8%) responded to a combination of fotemustine/INF-α2b/interleukin-2 investigated in 25 patients (153).

### 1.3.8. Systemic targeted therapies

The most common known oncogenic mutations occur in GNAQ or GNA11 which are found in about 85% of all primary UM, irrespective of tumour class or stage (23,24). These mutations may represent an early event that leads to the development of UM. GNAQ/GNA11 signalling leads to downstream activation protein kinase C and the MEK/MAPK and PI3K/AKT pathways (45,79). Furthermore, the MEK/MAPK and PI3K/AKT pathways are highly activated in UM (33,34,154,155). Further downstream, mutations in BAP1 gene located in chromosome 3, were found to occur almost exclusively in metastasizing class 2 tumours (25). BAP1 loss causes increased histone H2A ubiquitination in melanoma cells and melanocytes (156). Either BAP1 mutation or loss of chromosome 3 can occur first, but both events appear to be necessary for the tumour to metastasise (26).

Drugs targeting the MEK/MAPK/ERK kinase pathways have been investigated. In a phase I study of 16 patients treated with trametinib, no response was observed (157) while selumetinib treatment in 7 patients was also disappointing (158). However, compared with temozolomide, selumetinib was

recently shown to extended progression-free survival by nearly 9 weeks(159). Imatinib is a tyrosine kinase inhibitor that targets the PI3K/AKT pathways and platelet-derived growth factor (PDGF) receptors. However, 2 phase II studies of 19 patients failed to demonstrate any response to imatinib (160,161), while a recent study by Nathan et al (162) showed an overall response rate of 8% (2 partial response out of 25 patients studied). Landreville et al showed that histone deacetylase (HDAC) inhibitors induced morphologic differentiation of UM cells to melanocytes, suggesting therapeutic potential for inducing differentiation and prolong dormancy of micrometastatic disease in UM (98). Depsipeptide, a HDAC inhibitor was shown to inhibit proliferation and growth by increasing expression of Fas and FasL in 3 UM cell lines derived from primary tumour and 2 cell lines derived from liver metastasis. Depsipeptide induced gene upregulation of both Fas and FasL in these cells, and an increase in activated caspase-3, apoptosis and cell-cycle arrest was observed in treated cells compared to non-treated cells (97). Currently, a phase II clinical trial of the HDAC inhibitor vorinostat is underway and is estimated to be completed in June 2015 (clinical trial number: NCT01587352).

*In vitro* studies have shown that UM cells produce vascular endothelial growth factor to stimulate and maintain angiogenesis (163,164). Increased levels of VEGF was also found in the aqueous and vitreous humour in patients with UM (165,166). Furthermore, elevated serum VEGF was shown to correlate with number and location of micrometastases in a murine model of uveal melanoma (167). In contrast, a recent study demonstrated a paradoxical stimulatory effect of the anti-VEGF drug bevacizumab when given as an intraocular injection in murine UM model (168). Phase II studies of bevacizumab/INF-α2b (169) and bevacizumab/temozolomide (170) found no response to either combination regimens. Similarly, Tarhini et al found no observable response to the anti-VEGF drug aflibercept (133).

Sunitinib and sorafenib are tyrosine kinase inhibitors that specifically target VEGF and PDGF receptors. In a pilot study investigating sunitinib as monotherapy in 18 patients, Mahipal et al found an overall response rate of 5%. Three patients had stable disease for over 12 months after failed previous treatments (171). However, a randomised phase II trial comparing dacarbazine and sunitinib as first line treatment in 74 patients found no significant difference in treatment response or survival (134). Sorafenib has never been investigated as a single-agent treatment regime. Kaempgen et al demonstrated an outstanding overall response of 42% (3 of 7 patients studied) in patients treated with fotemustine and sorafenib (172). However, triple combination treatment of carboplatin/paclitaxel/sorafenib in 24 patients showed no response to this regimen. Currently, a randomised, placebo-controlled phase II study is underway to investigate the safety and efficacy sorafenib in metastatic uveal melanoma (clinical trial number: NCT01377025).

Ipilimumab was recently reported to be the first agent to show a survival benefit in cutaneous melanoma (173). It is a monoclonal antibody against CTLA-4. CTLA-4 inhibits cancer cell death by inactivating cytotoxic T lymphocytes. Ipilimumab binds to the inactivating CTLA-4 receptor on APC and inactivates this inhibitory mechanism and allows cytotoxic T lymphocyte-mediated cell destruction. In a recent trial in 5 patients with advanced UM, 2 patients remained stable for 11-15 months before progressing while 3 patients did not respond to treatment, giving an overall survival of 10.3 months (174). In a large study of 82 pre-treated metastatic UM patients, Maio et al demonstrated an overall response rate of 5% and a 29% disease stabilisation with 12 month survival rate of 31% (175). In 22 patients, Kelderman et al reported a similar overall response rate of 4.5% and 12 month survival rate of 27% (132), while Khan et al also reported a response rate of 5% in a study of 20 patients (176). In a retrospective study of 39 patients, ipilimumab treatment had a response rate and stabilisation rate of 2.6% and 46% respectively at 12 weeks, and 2.6% and 28.2% respectively at 23 weeks (177).

Table 1: Summary of 40 studies of systemic chemotherapy in metastatic uveal melanoma. PR, partial response; CR, complete response; ORR, overall response rate; PFS, progression-free survival (months); OS, overall survival (months); IV, intravenous; HIA, hepatic intra-arterial; EAP, expanded access program.

| **Author** | **Year** | **Drug** | **Study design** | **n** | **First line** | **Non-first line** | **Mean age** | **PR/CR** | **ORR (%)** | **PFS** | **OS** |
|---|---|---|---|---|---|---|---|---|---|---|---|
| Flaherty (178) | 1998 | Diverse chemotherapies | Retrospective | 64 | unk | unk | 59 | 3/1 | 9 | unk | 5.2 |
| Tarhini (133) | 2011 | Aflibercept | Phase II | 9 | 10 | 0 | 57 | 0/0 | 0 | 5.7 | 19 |
| Schmidt-Hieber (143) | 2004 | Bendamustine | Phase II | 11 | 0 | 11 | 61 | 0/0 | 0 | unk | unk |
| Guenterberg (169) | 2011 | Bevacizumab/INF-α2b | Phase II | 5 | 4 | 1 | 64 | 0/0 | 0 | 4.5 | 10.8 |
| Piperno-Neumann (170) | 2013 | Bevacizumab/temozolomide | Phase II | 35 | 35 | 0 | 55 | 0/0 | 0 | 3 | 12 |
| Nathan (150) | 1997 | BOLD/INFα-2b | Phase II | 20 | 20 | 0 | 62 | 4/0 | 20 | unk | unk |

| Author | Year | Drug | Study design | n | First line | Non-first line | Mean age | PR/CR | ORR (%) | PFS | OS |
|---|---|---|---|---|---|---|---|---|---|---|---|
| Pyrhonen (151) | 2002 | BOLD/INF-α2b | Phase II | 22 | 18 | 4 | 60 | 0/3 | 15 | 4.4 | 12.3 |
| Kivela (149) | 2003 | BOLD/INF-α2b | Phase II | 24 | 24 | 0 | 61 | 0/0 | 0 | 1.9 | 10.6 |
| Bhatia (179) | 2012 | Carboplatin/paclitaxel/sorafenib | Phase II | 24 | 20 | 4 | 61 | 0/0 | 0 | 4 | 11 |
| Schmittel (148) | 2005 | Cisplatin/gemcitabine/treosulfan | Phase II | 17 | 19 | 0 | 60 | 0/0 | 0 | 3 | 7.7 |
| | | Gemcitabine/treosulfan | Phase II | 33 | 28 | 5 | 62 | 1/0 | 3 | 2.5 | 7.5 |
| Atzpodien (180) | 2008 | Cisplatin (IV/HIA)/gemcitabine/treosulfan | Pilot | 12 | 1 | 11 | 62 | 0/0 | 0 | unk | 6 |
| O'Neill (181) | 2006 | Dacarbacine/treosulfan | Phase II | 14 | 15 | 0 | 64 | 0/0 | 0 | 3 | 7.5 |
| Homsi (139) | 2010 | DHA-paclitaxel | Phase II | 22 | 11 | 11 | 56 | 1/0 | 4.6 | 3 | 9.8 |
| Leyvraz (142) | 2012 | Fotemustine | Phase III | 83 | 83 | 0 | 59 | 2/unk | 2.4 | 3.7 | unk |
| Spagnolo (141) | 2013 | Fotemustine | Retrospective | 24 | 24 | 0 | 62 | 2/0 | 8.3 | unk | 13.9 |

| Author | Year | Drug | Study design | n | First line | Non-first line | Mean age | PR/CR | ORR (%) | PFS | OS |
|---|---|---|---|---|---|---|---|---|---|---|---|
| Becker (153) | 2002 | fotemustine/INF-α2b/IL-2 | Phase II | 25 | unk | unk | 56 | 1/1 | 8 | unk | 15 |
| Kaempgen (172) | 2012 | Fotemustine/sorafenib | Case series | 7 | unk | unk | unk | 3/0 | 42 | unk | unk |
| Pfohler (144) | 2003 | Gemcitabine/treosulfan | Pilot | 14 | 13 | 1 | 63 | 3/1 | 28.6 | 7.1 | 15.3 |
| Keilholz (145) | 2004 | Gemcitabine/treosulfan | Phase I | 33 | 28 | 5 | 62 | 1/0 | 3 | unk | unk |
| Terheyden (146) | 2004 | Gemcitabine/treosulfan | Phase II | 20 | 8 | 14 | 62 | 0/0 | 0 | unk | 11.6 |
| Corrie (147) | 2005 | Gemcitabine/treosulfan | Phase I | 5 | 4 | 1 | 50 | 0/0 | 0 | 6.8 | 13.3 |
| Hofmann (161) | 2008 | Imatinib | Phase II | 9 | 9 | 3 | 63 | 0/0 | 0 | unk | 6.9 |
| Penel (160) | 2008 | Imatinib | Phase II | 10 | 6 | 7 | 58 | 0/0 | 0 | unk | 10.8 |
| Nathan (162) | 2012 | Imatinib | Phase II | 25 | 24 | 13 | 63 | 2/0 | 8 | 3 | 7.4 |
| Khan (176) | 2012 | Ipilimumab | Retrospective | 20 | 0 | 20 | 61 | 1/0 | 5 | unk | unk |
| Danielli (182) | 2012 | Ipilimumab | EAP | 9 | 0 | 13 | 57 | 0/0 | 0 | Unk | 6 |

| Author | Year | Drug | Study design | n | First line | Non-first line | Mean age | PR/CR | ORR (%) | PFS | OS |
|---|---|---|---|---|---|---|---|---|---|---|---|
| Khattak (174) | 2013 | Ipilimumab | EAP | 5 | 0 | 5 | 42 | 0/0 | 0 | unk | 10.3 |
| Kelderman (132) | 2013 | Ipilimumab | EAP | 22 | 0 | 22 | 54 | 1/0 | 4.5 | 2.9 | 5.2 |
| Maio (175) | 2013 | Ipilimumab | EAP | 82 | 0 | 82 | 62 | 4/0 | 5 | 3.6 | 6 |
| Zeldis (138) | 2009 | Lenalidomide | Phase II | 16 | unk | unk | 53 | 0/0 | 0 | unk | unk |
| Bedikian (140) | 2008 | Liposomal vincristine | Pilot | 4 | unk | unk | 56 | 0/1 | 25 | unk | unk |
| Ellerhorst (183) | 2002 | Nitro-camptothecin | Phase II | 14 | 0 | 14 | 59 | 0/0 | 0 | unk | unk |
| Kirkwood (158) | 2011 | Selumetinib | Phase II | 7 | 20 | 0 | 57 | 0/0 | 0 | unk | unk |
| Mahipal (171) | 2012 | Sunitinib | Pilot | 18 | 3 | 17 | 69 | 1/0 | 5 | 4.2 | 8.2 |
| Bedikian (136) | 2003 | Temozolomide | Phase II | 14 | 9 | 5 | 53 | 0/0 | 0 | 1.8 | 6.7 |
| Reiriz (137) | 2004 | Thalidomide | Phase II | 5 | 0 | 5 | 59 | 0/0 | 0 | unk | unk |

| Author | Year | Drug | Study design | n | First line | Non-first line | Mean age | PR/CR | ORR (%) | PFS | OS |
|---|---|---|---|---|---|---|---|---|---|---|---|
| Solti (152) | 2007 | Thalidomide/INF-α2b | Pilot | 6 | 0 | 6 | 59 | 0/0 | 0 | 3.6 | 9 |
| Falchook (157) | 2012 | Trametinib | Phase I | 16 | 1 | 15 | 53 | 0/0 | 0 | 1.8 | unk |
| Schmittel (135) | 2006 | Gemcitabine/treosulfan | Phase II, randomised | 24 | 15 | 9 | 63 | 0/1 | 4.2 | 3 | unk |
| | | Treosulfan | | 24 | 17 | 7 | 58 | 0/0 | 0 | 2 | unk |
| Sacco (134) | 2013 | Dacarbazine | Phase II, randomised | 37 | 37 | 0 | unk | 3/unk | 8 | 3.9 | 8.7 |
| | | Sunitinib | | 37 | 37 | 0 | unk | 0/0 | 0 | 2.8 | 6.4 |

## 1.4. Proteomics

Gene expression profiling/transcriptomic studies identify an intermediate carrier (mRNA) of the genetic information between the genome and proteome. However, genetic and transcriptomic studies alone are not sufficient to fully understand the molecular basis for the association between these cytogenetic alterations and aggressive phenotype, with several investigators reporting a poor correlation between mRNA and protein abundance (184,185). This is due to the fact that a single gene can encode for more than one mRNA species through differential splicing, and proteins can undergo as many as 200 post-translational modifications (186). The regulatory role of micro-RNAs in gene expression at the post-transcriptional level adds to the limitations of genetic studies (187). While genomics is significantly improving our understanding of the molecular basis of this disease, identifying targets suitable for treatment is difficult. Pharmacologic targeting of genetic mutations is complex and challenging. Direct inhibition of mutant GNAQ or GNA11 may prove difficult because these mutations abrogate the intrinsic GTPase activity that would normally allow these proteins to return to their GDP-bound, inactive state (26). Loss of BAP1 also poses a difficult therapeutic challenge, as it is seems to represent a classic loss of a tumour suppressor, and direct therapies would require the reinitiation of function (188). Proteomics delineates the functional units of a cell, proteins and their intricate interaction network and signalling pathways for the underlying disease (189). Proteomic studies have been successfully used to identify several protein alterations in tumour cells, leading to biomarker discoveries (190–193). Progress has been made in several areas of cancer research using proteomics technology, including breast (194), lung (195), oral (196), and colorectal cancers (197).

### 1.4.1. Current proteomic technologies and overview

Proteomics seeks to study the total proteins expressed in any given system, whether by abundance, activity, structure, state of post-translational or other modification, or how these proteins interact with each other in networks or complexes (198). Proteomics workflow involves 2 stages: separation of the biological protein sample to increase visualisation and resolution (gel-based or gel-free) and identification of peptide fragments/proteins using mass spectrometry. These data are then analysed using bioanalytical softwares and databases to identify novel targets for further validatory studies. Proteomics techniques can be broadly divided into top-down or bottom-up strategies. Top-down strategy analyses the proteome at the intact level, thereby retaining the biochemical properties and post-translational modifications of proteins. In contrast, bottom-up strategy involves enzymatic cleavage of complex protein samples, relying on modern chromatography and electrophoretic strategies to simplify the peptide fragment populations (199,200). Thus, bottom-up proteomics usually involves heavy use and reliance on high speed tandem mass spectrometry instruments and high throughput database searches to relate mass spectra to peptide sequences, then peptides to their parent protein (201). Figure 8 illustrates the basic proteomic workflows using both gel-based (i.e. 2D gels) and gel-free/LC-MS based approaches.

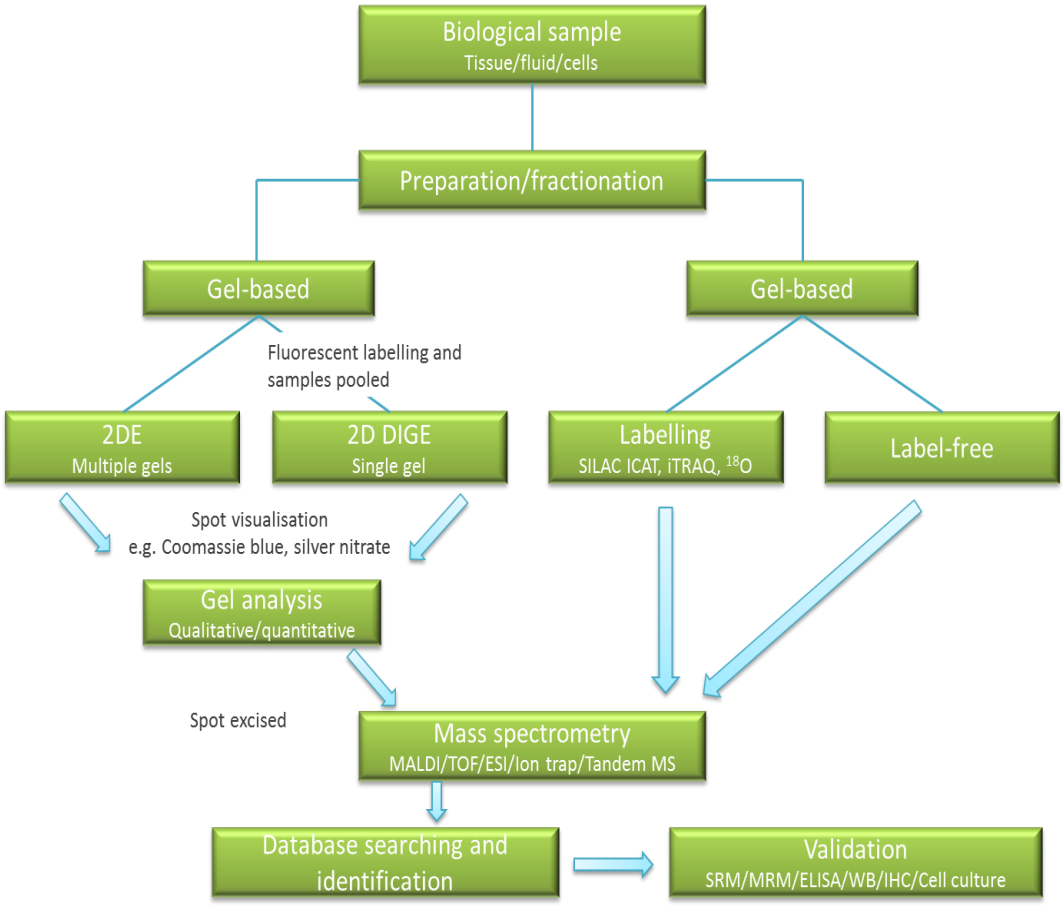


Figure 8: Basic proteomic workflows using both gel-based (i.e. 2D gels) and gel-free/LC-MS based approaches. 2DE=2-Dimensional Electrophoresis. 2D DIGE=2-Dimensional Difference Gel Electrophoresis. SILAC= Stable Isotope Labeling by/with Amino acids in Cell culture. ICAT=Isotope-Coded Affinity Tag. iTRAQ=Isobaric Tag for Relative and Absolute Quantitation. MALDI=Matrix-Assisted Laser Desorption/Ionization. TOF=Time-of-flight. ESI=Electrospray Ionization. SRM=Selected Reaction Monitoring. MRM=Multiple Reaction Monitoring. ELISA=Enzyme-Linked Immunosorbent Assay. WB=Western Blot. IHC=Immunohistochemistry

### 1.4.2. 2D PAGE and Mass Spectrometry

Conventionally, proteomic profiling usually involves separating the complex biological protein mixture using two-dimensional gel electrophoresis (2-DE) prior to their analysis and identification by the mass spectrometer. This process enables assessment of relative protein levels by comparing protein samples from two disease groups. Protein molecules are first separated in one direction based on its isoelectric point (pI), usually using immobilized pH gradient (IPG) strips. The IPG strip is then loaded at the top of a second gel where proteins are separated in a second direction based on its mass (Da). For visualisation, the gel is stained using a number of different techniques, such as Colloidal Coomassie blue, zinc imidazol, and silver nitrate/diamine (Ag) stains for the visible range, and fluorescence staining, such as Spyro Ruby for the nonvisible range (202). The resultant gel is analysed using 2D gel analysis software which compares the stained protein spots' patterns and detects protein changes, both qualitative (presence/absence) and quantitative (spot intensities). Protein spots of interest are then excised from the gel for identification using mass spectrometry (MS).

To overcome the challenges of gel-to-gel variability, reproducibility and to increase reliability of protein quantification, two-dimensional difference gel electrophoresis (2D-DIGE) was developed (203). This method utilizes two (e.g. healthy and disease) samples that are differentially labelled with fluorescent dyes. Subsequently, the two samples are resolved simultaneously within the same gel and compared to a master gel of a pool of both samples. Using differential analysis software, statistically significant proteins spots that are differentially expressed can be determined and processed for mass spectrometry.

Advances in mass spectrometry technologies have increased the reliability, reproducibility and efficiency of proteomic studies. Ionisation techniques such as electrospray ionization (ESI) and matrix-assisted laser desorption/ionization (MALDI) are now the most commonly used methods (204,205) and are regarded as the key to success of MS in life science research (198). These soft ionization techniques are able to ionize large and polar molecules without physically destroying them. Since ESI utilises a liquid solvent, it can be coupled with liquid chromatography for additional sample separation. The evolution of combined quadrupole-time of flight (Q-TOF) mass analysers offer higher sensitivity, improved resolution and mass accuracy. More recently, mass analysers such as the quadrupole and Fourier transformation ion traps offer a superior mass resolution of >100,000 and mass accuracy of <1ppm (206).

The strengths of MS are not only based on its ability to resolve ppm, but also its ability to perform tandem mass spectrometry. MS/MS fragment information is significantly more discriminating in terms of specificity and identification accuracy than MS alone (207). Once a peptide sequence is determined, it is fragmented to generate partial amino acid sequence for further MS (MS/MS). Tandem mass spectrometers contain two mass analysers (tandem in space) or perform the experiment sequentially inside the same mass analyser (tandem in time). There are many different methods that are employed for peptide fragmentation, such as collision induced dissociation (CID), surface induced dissociation (SID), electron capture dissociation (ECD) and electron transfer dissociation (ETD) amongst many others. The most commonly used fragmentation methods in proteomics are CID and ETD (208).

### 1.4.3. Gel –free Quantitative proteomics

As biomarker discovery requires accurate measurements of quantitative difference between diseased and healthy biological analytes, quantitative proteomics has seen a rapid evolution in the last decade. Essentially, two methods are employed in quantitative proteomics; incorporation of metabolic or isobaric label or label-free analysis of MS/MS spectra. As the former implies, proteins/peptides from different analytes are labelled using various technologies such as metabolic labelling (e.g. SILAC) or chemical labelling (e.g. ICAT, iTRAQ, AQUA peptides, $18O^2$). Quantitation is then determined based on the mass increase provided by the labels and the relative signal intensities between the labelled and unlabelled analytes.

#### 1.4.3.1. Stable Isotope Labelling by Amino acids in Cell culture (SILAC)

In cell line models, Stable Isotope Labelling by Amino acids in Cell culture (SILAC) is one of the most popular methods used in quantitative proteomics. Cells are cultured in growth media containing amino acids with isotopes such as $^{15}N$ or $^{13}C$, thus incorporating these heavy elements into the cell. Near complete incorporation of labels typically occurs after five to 10 doubling of cells grown in SILAC media (209). Proteins/peptides from the “heavy” and “light” cells are then distinguished by MS and quantified. Metabolic labelling is regarded as one the most accurate techniques as it reflects the immediate metabolic state of the cell (210).

In contrast to metabolic labelling, chemical labelling relies on biochemical reactions to label protein/peptide samples. Technologies such as isotope-coded affinity tags (ICAT) modify cysteine residues in peptides and link them to a biotin tag that contains either a heavy or light isotopic variant. Two separate samples of

interest are tagged with the light and heavy isotopes, pooled (allowing comparison e.g. between healthy vs. disease samples) and digested. The labelled and unlabelled peptides are then isolated with the aid of the biotin tags using affinity chromatography, followed by quantification by MS.

#### 1.4.3.2. Isobaric Tag for Relative and Absolute Quantification (iTRAQ)

Similar to ICAT, iTRAQ labelling also enables parallel identification and quantification. After labelling, samples are pooled and fractionated using LC. For quantification, these technologies utilise the MS/MS information rather than MS alone. In a single MS mode, the same peptides with different labels are identical in mass. However, in MS/MS mode, where the peptides are fragmented, each tag generates a unique reporter ion. The reporter ions can be used to relatively quantify the peptides and the proteins from which they originated with simultaneous identification based on the associated sequence information (211). The tagging reagents are available in up to eight isotope-coded variants (8-plex), all with an identical molar mass (isobaric) allowing simultaneous profiling and comparison of up to 8 different samples in a single run.

#### 1.4.3.3. Absolute QUAntification of proteins (AQUA)

Another method, known as synthetic spiking or absolute quantification of proteins or AQUA (212), involves introducing a synthetic standard peptide of known concentration to analytes. Quantitation is performed by comparing the mass shift produced by the standard peptides and sample peptides. These peptides can also be synthesized with covalent attachments to mimic protein post-translational modifications such as phosphorylation, methylation, and acetylation (206). However, AQUA is not usually suitable for global discovery proteomics due to the complexity and high cost associated with producing large

numbers of synthetic peptides (213). To address these limitations, a de novo gene design (QconCAT) was developed using Escherichia coli, in which artificial "signature peptides" are expressed at a much reduced cost. As signature peptides are introduced early in the workflow, potential bias is reduced, and accuracy and sample coverage is increased. Despite these, the narrow detection range of mass spectrometers causes difficulties in determining the amount of standard peptides to be used without overshooting the detection range.

#### 1.4.3.4. $^{18}$O labelling

An inexpensive and relatively simple method of isotopic quantitation is by $^{18}$O labelling. During or following protein digestion, the C-termini of peptides are labelled with two $^{18}$O isotopes. The resulting mass shift between "heavy' and "light' proteins can be used for identification, characterization and quantitation (214). Since $^{18}$O labels are stable at low pH but can be lost at high pH values, this type of label is suitable for the mild acidic conditions typically utilized for ESI- and MALDI-MS (206). However, good levels of incorporation are usually difficult to achieve, complicating interpretation and quantification (215). Furthermore, this method limits throughput as it only allows for simultaneous comparison of 2 analytes.

### 1.4.4. Quantitative Label-free proteomics

Despite the strengths of chemical and metabolic labelling technologies, achieving complete proteome coverage is difficult and challenging. In contrast to labelling technologies, label-free proteomics utilises the technological advancements made in both mass spectrometry and bioinformatics capabilities. Without artificially labelling analytes, sample handling and potential contaminants are reduced. Thus, sample bias are minimised and throughput is significantly increased. The basic principle of this technology is based on direct

comparison of MS signal intensities between different analytes. However, it is more sensitive to technical deviations between LC/MS runs as information is compared between different measurements (216). Significant advances in liquid chromatography, mass spectrometry and bioinformatic software algorithms have increased the reliability, reproducibility and accuracy of label-free proteomics.

Samples containing the digested peptide complex are separated on a liquid chromatography column. After elution from the column, analytes are continuously injected into the mass spectrometer. Stacking individual MS runs yields a multidimensional dataset or map, from which quantification can be determined. The bioinformatic analysis of label-free data consists of two main steps; raw MS data signal processing, and quantification. Signal processing steps comprise data reduction procedures such as removal of baseline signal, noise, and centroiding. The raw MS data are processed in order to eliminate baseline signals and high-frequency noise attributed to the detector, solvents, buffers and contaminants. MS data that have been adjusted for baseline and noise signals are then subjected to centroiding and charge estimation. For most MS data, the intensity of a centroided peak is determined using the peak volume, which corresponds directly to the ion count while for high-resolution spectra, the height of the peak is used. To interpret the MS data for quantification, two different techniques are employed; spectral counting and peptide ion intensity counting. The intensity-based measures avoid stochastic effects in ion sampling and are therefore slightly more accurate, and they potentially provide higher reproducibility while spectral counting is easy to implement and fast (216). Figure 9 illustrates the principles of quantitative label-free proteomic methods.

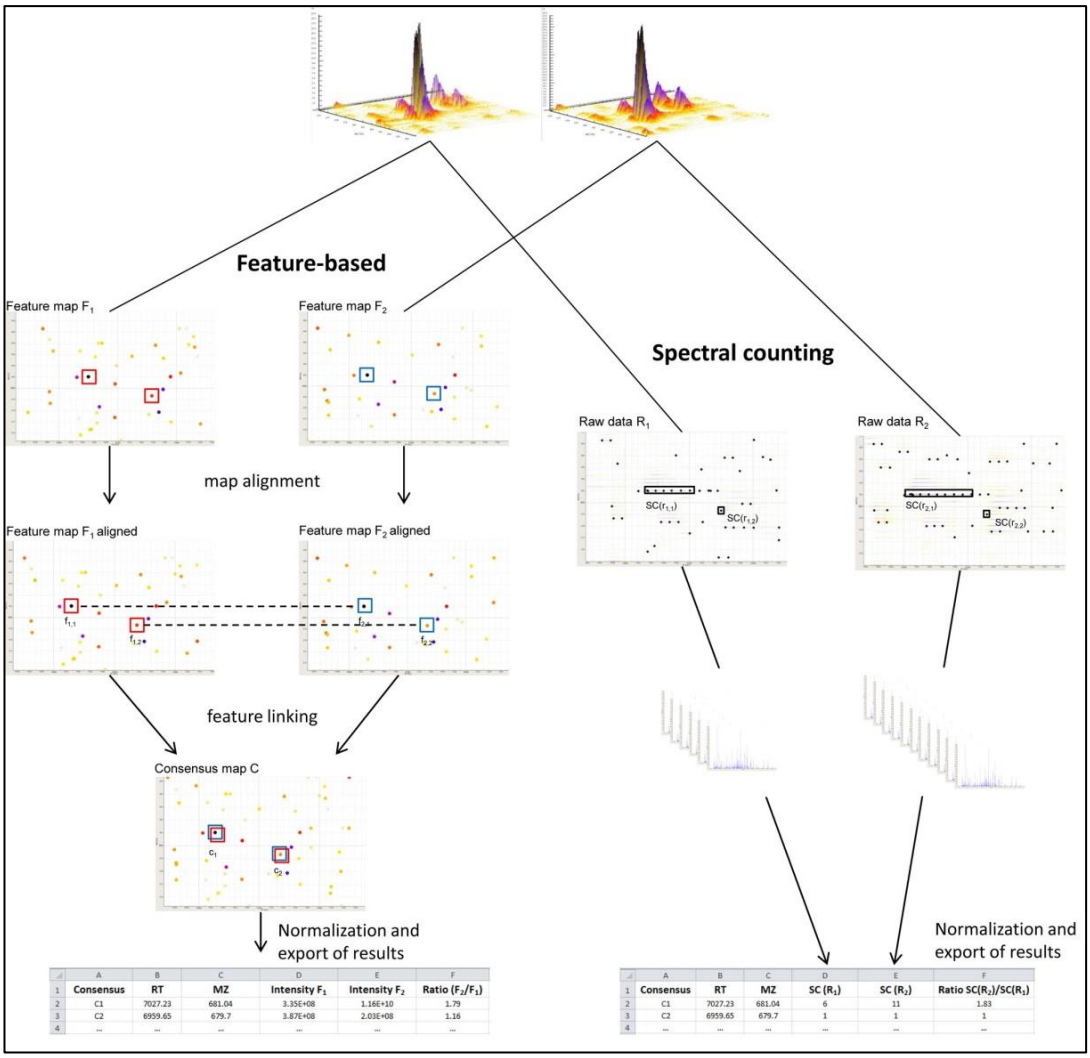


Figure 9: Quantification methods employed in label-free proteomics. The sample cohort that can be analysed via label-free proteomics is not limited in size. Each sample is processed separately through the sample preparation and data acquisition pipeline. For data analysis, the data from the different LC-MS runs are combined. Adopted from Nahnsen et al (216)

Spectral counting depends on high-throughput data acquisition for both identification and quantitation. The simple rational is that the more of a protein there is in a sample, the higher the number of tandem mass spectra the mass spectrometer will acquire for this protein (206). The number of mass spectra for a specific protein is determined and quantitation is derived by comparing it to the protein's abundance. MS runs from multiple analytes can be compared to determine relative abundance and differential quantification of proteins. As this

method relies on simple counting of acquired spectra rather than measuring physical data, the spectral counting method is controversial (217). Furthermore, as the peak is being sampled more than once, the identification dynamic range is limited, and low-level ions may be missed in preference to the higher intensity ions, limiting the application of spectral counting to moderately to highly abundant proteins, or to proteins whose abundance varies significantly between the samples (218) However, it has been further developed and is widely used (219). Modified spectral counting that take into account aspects influencing the number of spectral counts, like physicochemical properties of peptides as well as the lengths of the corresponding proteins, may be employed (220). These approaches are known as absolute protein expression (APEX) (221) and normalised spectral abundance factor (NSAF) (222,223). More recently, normalised spectral index (SIN) which combines peptide count, spectral count and fragmentation intensity was shown to eliminate variances between replicate measurements, increase reproducibility and reliable quantification (224). Spectral counting approaches are also strongly influenced by the acquisition methods, in particular those which are normally optimized to limit the number of MS/MS events for an individual peptide, such as the dynamic exclusion parameters and the exclusion width (218). Spectral total ion chromatogram (TIC) generates more tryptic peptide and takes the average of the total ion count for a protein for quantification, thereby eliminating bias towards larger and more abundant proteins (225). It also expands the dynamic range of quantification compared to basic spectral counting methods (225).

In peptide ion intensity counting, individual analytes are subjected to LC-MS. Central to this are bioanalytical softwares that process complex raw LC-MS data for quantification. This includes signal processing (discussed above), feature detection, alignment of retention times, normalisation of MS intensities, peak picking and quantification. Advances in high-resolution mass spectrometers have made signal processing and peak picking simpler than lower resolution instruments (216). Peptides are eluted over time from the LC column, ionised and are injected into the mass spectrometer. Measurements are taken in

regular, short intervals thereby sampling the amount of the eluting ion over time, resulting in an elution profile. Each peptide of a particular charge and mass generates a mono-isotopic mass peak based on its atomic composition. Extracted across a time domain, the intensity of the peak is visualised in an extracted ion chromatogram (XIC), which is used to integrate the LC elution peak of the compound of interest. The area under the curve (AUC) of extracted peptide ions intensities at a specific retention time in an LC-MS run is correlated linearly with the protein abundance, which makes their measurement feasible for quantification (226,227). Under well-standardised LC-MS conditions, the AUC of features of interest can compared with those of other analytes to produce relative quantification. To achieve this, the map of peptide ion features from individual LC-MS runs are aligned using software algorithms. This is done based on the assumption that the chromatographic elution time of a peptide, as well as its ionisation behaviour, stays relatively constant between measurements and that the measured mass-to-charge ratio does not differ (216). Whereas the differences in the mass-to-charge ratio are rather marginal, the shifts in retention time can become very large and frequently show some nonlinearity (216). Once aligned, systematic biases in the measured intensities are adjusted (intensity normalisation) to account for variability in intensity signals from errors in experimentation, sample preparation, chromatography and mass spectrometry (228). Accurate map alignment is important for quantification using peptide ion intensity counting, while in spectral counting the identification of the peptide can be used to assign corresponding quantities across maps. Recent and continued improvements made in bioinformatic softwares and algorithms have enabled accurate and reproducible map alignments and intensity normalisation across multiple LC-MS runs, and has improved the ability to process peptides shared amongst proteins and minimise false discovery rates (229–231). Peptide ion intensity counting also relies on obtaining a highly reproducible LC profile to maximise mass resolution, accuracy and proteome coverage (198). The LC retention time in has to be managed closely, either by the incorporation of retention time markers or using software algorithms to realign and optimise the chromatographic profiles of peptides (206). Improvements

made in LC systems, such as the nanoflow-LC reduces misalignment and ensures good reproducibility in elution.

### 1.4.5. Selected Reaction Monitoring (SRM)/Multiple Reaction Monitoring (MRM)

Once an interesting protein biomarker has been identified, several methods may be employed for validation. Typically, antibody-based techniques are utilised such as ELISA. However, these methods are costly and usually take a long time to be developed and optimised. As an alternative, targeted proteomic technologies have been developed (selected reaction monitoring, SRM and multiple reaction monitoring, MRM). These MS-based technologies are highly sensitive, specific and high throughput, making it attractive in many systems biological applications that require the repeated measurement of a predefined set of proteins (232). In the SRM/MRM technique, a triple quadrupole mass spectrometer is used to assay the presence target peptides by focusing the first quadrupole on one particular peptide of interest followed by fragmentation of this peptide inside the second quadrupole and collection of one (SRM) or a few (MRM) particular fragment ions in the third quadrupole (206). As specific proteins of interest are preselected for analysis, only ions of interest are monitored and recorded. By rejecting all other ions entering the mass spectrometer, this mode of operation translates into an increased sensitivity by one or two orders of magnitude compared with conventional “full MS-scan” techniques (233). This also allows the detection of low-abundance in high complex mixtures (234,235). The sensitivity of MRM is also considerably increased when used in combination with stable isotope standards and capture by antipeptide antibodies (SISCAPA), a method for enriching target peptides using antipeptide antibodies (236).

## 1.5. Proteomics in uveal melanoma

A number of proteomic studies have been carried out to date, investigating the biology of the metastatic phenotype of uveal melanoma. A summary of these studies is outlined in Table 2. The majority of these studies have used cultured cell line models (237–242). More recently proteomic studies on tissue from uveal melanoma patients has been carried out; one study compared the proteome of monosomy 3 to disomy 3 tumours (243) while a second study from our group compared primary tumours from patients who developed metastatic disease compared to primary tissue from patients who did not develop metastatic disease (244).

Table 2: Summary of proteomic studies in uveal melanoma

| **Studies** | **Study type** | **Principal findings** |
|---|---|---|
| Pardo et al., 2005 (239) | Global proteome of UM cell line | 683 proteins, 96% of which were novel in UM |
| Pardo et al., 2006 (238) | Differential proteomics of UM cell lines | Upregulation of DJ-1, HMG-1 and MUC18 in aggressive UM |
| Pardo et al., 2007 (237) | Global secretome of 5 UM cell lines | Cathepsin D, gp100 and syntenin-1 |
| Zuidervaart et al., 2006 (242) | Differential proteomics of UM cell lines derived from primary and metastatic tumours | Upregulation of HSP-27, αB-crystallin and cofilin in metastatic cell line |
| Coupland et al., 2010 (243) | Differential proteomics of primary tissues | Downregulation of HSP-27 in monosomy 3 UM tumours |
| Linge et al., 2012 (244) | Differential proteomics of primary tissues | Upregulation of FABP3 and TPI1 in aggressive primary UM tumours |
| Wang et al., 2013 (240) | Differential proteomics of irradiated UM cell line | Downregulation of S100A11, PHB1, PHB2,TPI1 and upregulation of HSP-27 in irradiated cells. |
| Yan et al., 2013 (241) | Differential proteomics of irradiated UM cell line | Downregulation of PKFM and upregulation LDHB in irradiated cells. |

### 1.5.1. Cell line studies

In 2005, Pardo et al (239) published the first proteomic study in uveal melanoma. They analysed the global proteome of a primary UM cell culture (UM-A). Ninety-six percent of the proteins have never been reported in UM before. Sixty-nine proteins (18%) identified have been previously described as cancer related. The majority were involved in invasion and metastasis (33%), such as melanoma-associated antigen MUC 18. It has been implicated in facilitating melanoma cells to interact with cellular elements of the vascular system, enhancing haematogenous spread. Albelda et al suggested that it may play a major role in metastasis by not only mediating melanoma cell-cell interactions, but also melanoma-endothelial cell adhesion (245). Other proteins were involved in drug resistance (10%), cell division and proliferation (14%) and oncogenes (6%). Eleven percent (11%) of the proteins were heat shock proteins (HSPs) and chaperones (11%). HSPs will be discussed in tissue studies, where it was identified in a differential proteomic tissue study by Coupland et al (243).

In a follow-up study (238), differential proteomic analysis of UM primary cell culture (UM-A < 7) and the resulting cell line (UM-A > 7) was analysed. UM-A < 7 showed a low degree of metastatic potential compared to cell lines derived after passage 7 (UM-A > 7). New nuclear proteins were identified in UM-A > 7, such BRCA-1, proteins associated with myc, and gene expression regulating protein HMG-1. The latter has been reported to play a role in the transcription of many genes involved at different steps in the metastatic cascade and has been linked with cancer in human and animal models (246). Other proteins that were only present in UM-A > 7 cell lines include HSP60β and cell adhesion protein MUC18. The expression of HMG-1 and MUC18 were determined in UM-A and other UM cell cultures (UW-1, SP6.5, OCM-1, 92.1 and normal melanocytes). HMG-1 was found to be higher in the invasive UM-A cell line (UM-A > 7) than in primary culture (UM-A < 7). It was also overexpressed in all other cell lines assayed. However, a clear correlation between HMG-1 expression and invasion

potential was not found. As for MUC18, low levels were identified in UM-A < 7, UM-1 and 92.1. It was overexpressed in UM-A > 7, OCM-1 and SP6.5 while in normal melanocytes, it was absent. There was a positive correlation between MUC18 expression in UM cultures and invasion potential. However, no significant correlation was found in one cell line (92.1), suggesting that more than one molecular event may govern invasion (238).

The authors also studied DJ-1, a novel oncogene identified in the first proteomic study. It was expressed in all cell lines and found in the culture media. As expected, it was absent in normal melanocyte cell line or culture media. Malignant cells have been described to secrete DJ-1 and it plays a role in tumourigenesis in breast cancer, non-small cell lung carcinoma and prostate cancer (247,248). Kim et al identified DJ-1 as a negative regulator of the tumour suppressor PTEN, promoting cell survival in primary breast and lung cancer patients (249). A recent study suggested serum DJ-1 level as a potential biomarker for the diagnosis and prognosis prediction of patients with pancreatic cancer (250). Recently, it was shown that elevated DJ-1 was found to be significantly associated with risk factors for malignant transformation of choroidal naevus, namely nevus thickness greater than 1.5 mm, diameter larger than 8 mm, and presence of acoustic hollowness on ultrasonography (251). This interesting finding, coupled with the identification of DJ-1 in UM tissue by our group (244) warrants further investigation into the potential role serum DJ-1 may play in tumourigenesis and monitoring of patients at risk for malignancy.

In a subsequent study (237), media containing proteins secreted from the UM cell lines (UM-A, UW-1, OCM-1, SP5.6, and 92.1) during the incubation period were subjected to 2-DE proteomic analysis. Twenty-three secreted proteins were common in all 5 cell lines' media. These included cathepsin D, melanocyte protein Pmel (gp100) and mda-9/syntenin 1, amongst many others. Correlation between cathepsin D tissue concentration and tumour aggressiveness has been found in lung cancer and cutaneous melanoma (252,253). Gp 100 is normally expressed at low levels in quiescent adult

melanocytes but overexpressed by proliferating neonatal melanocytes and during tumour growth (237). Gp 100 expression in uveal melanoma has been identified in numerous studies (254–257). Proteomic analysis of 11 UM patients' serum (without metastasis) and 8 healthy subjects' serum found higher levels of cathepsin D and gp100 in UM patients' serum compared to those of healthy subjects. Mda-9/syntenin 1 was not detected in either group of serum samples. However, the authors did not determine the expression of this protein in serum of patients that developed metastatic disease, given the role it plays in the development of metastasis.

Several studies demonstrate the role of mda-9/syntenin in promoting metastasis in both uveal (258) and cutaneous melanoma (259,260). High expression of mda-9/syntenin 1 has been found in advanced metastatic cutaneous melanoma compared to benign naevi and primary cutaneous melanoma (261). Mda-9/syntenin, through interaction with c-Src/FAK, activates the p38 MAPK/NFkB pathway with subsequent induction of genes involved in migration and invasion (262). The Raf kinase inhibitor RKIP was shown to inhibit mda-9/syntenin-mediated metastasis in cutaneous melanoma, by inhibiting cell invasion, anchorage-independent growth and in-vivo dissemination of tumour cells (263). In UM, high levels of syntenin protein expression in primary tumour was found to be significantly associated with earlier metastatic progression and correlated with metastatic risk as strongly as monosomy 3. Furthermore, UM liver metastases also showed higher syntenin expression compared to primary tumours (258). The authors also demonstrated that inhibition of syntenin expression reduces the activation of FAK, Src and AKT. Src has been shown to be an upstream tyrosine kinase for ERK1/2 activation in primary UM (264). Similarly, MAPK pathway has been implicated in uveal melanoma (33,34,154).Dasatinib, a Src family kinase inhibitor, was recently shown to inhibit MAPK and induce growth arrest in monosomy 3 UM cell cultures (265). Taken together, mda-9/syntenin may be critical in metastatic formation and dissemination in UM, and warrants further investigation as a therapeutic agent in this disease.

Zuidervaart et al (242) found 24 differentially expressed proteins between primary and metastatic uveal melanoma in three cell lines. One cell line was derived from primary uveal melanoma (Mel 270) and two were derived from liver metastases from the same primary tumour (Omm 1.3 and Omm 1.5). By studying cell lines derived from the same patient, they hypothesized that differential protein expression between the three cell lines may identify proteins related to tumour progression and metastatic growth. Of those that are upregulated in metastatic cell lines, HSP-27 and αB-crystallin are proteins that are fundamentally involved in cellular defence against various stimuli and stress. HSP-27 was also identified by (243) in primary UM tissue, with high HSP-27 indicating a favourable prognosis. This supports the different roles HSP-27 may play in primary and metastatic tumours (discussed in Tissue studies, section 1.5.2 below). Another protein, phosphorylated inactive cofilin was also upregulated in metastatic cell lines. PAK1, a cofilin-inactivating enzyme that leads to stimulation of cell spreading activities (266), has been associated with an increased invasive potential in uveal melanoma (267). Promotion of cell motility and stabilization of cell shape may be enhanced during acquisition of the metastatic phenotype by phosphorylation of cofilin and could therefore be of great importance for the metastatic potential of uveal melanoma cells (242). Another proteomic study supports this finding, indicating that phosphorylation of cofilin, together with HSP-27, is altered in response to angiogenesis inhibitors, affecting the endothelial cell cytoskeleton to prevent endothelial migration (268).

More recently, Wang et al (240) studied 92.1 UM cell line 15 and 48 hours post X-ray radiation to identify proteins associated with cell cycle arrest. At 15 hours post radiation, 290 proteins were found to be down-regulated by more than two-fold, while 86 were up-regulated by more than two-fold. At 48 hours post radiation, 97 were down-regulated while 78 were up-regulated by more than two-fold. Proteins that were downregulated in both groups were predominantly associated with cell death and apoptosis, suggesting an important role in cell cycle suspension. Of these, S100A11 belongs to the S100 protein family and is involved in regulation of cell cycle progression and differentiation. It

has also been shown to be overexpressed in many other types of cancers, such as prostate (269), bladder (270), colorectal (271) and breast cancer (272), Elevated serum S100β was shown to predict the development of hepatic metastasis in UM, suggesting its potential use in monitoring patients at risk for metastasis (273,274). Prohibitins PHB1 and PHB2 are mitochondrial proteins that have a wide range of cellular functions including cell death and senescence (275). They have also been shown to play an important role in cancer cell proliferation, propagation, adhesion and survival (276). High expression of PHB1 was found in other types of malignancies such as lung (277), breast (278), prostate (279) and gastric cancer (280,281). In a previous study by the same group, 92.1 cells were found to exhibit senescence-like phenotype when cell cycle suspension was induced after 3 days of X-ray irradiation (282). Since significantly lower levels of PHB1 and PHB2 were found by Wang et al, this strongly suggests that irradiation-induced decrease in expression of these proteins may play a role in cell cycle suspension, and subsequently senescence of 92.1 cells. Interestingly, this study also identified TPI1 and HSP-27, both of which were identified by recent UM tissue studies by Linge et al and Coupland et al respectively.

Similarly, Yan et al (241) analysed the proteome of 92.1 UM cell line 15 hours post irradiation. Lactate dehydrogenase B (LDHB) showed the highest fold-change in irradiated cells. In contrast to Wang et al, the authors validated their findings by immunoblotting. LDHB is involved in glycolysis and is also released in response to tissue injury, necrosis or apoptosis (283). Elevated serum levels were found to correlate with the clinical stage of non-small cell lung cancer (284). LDHB promoter hypermethylation occurred at a higher frequency in prostate cancer compared to benign prostate tissues, leading to loss of LDHB expression in cancer tissues. Similarly, LDHB expression was higher in normal prostate tissues compared to prostate cancer, and was absent in secondary metastatic tissues (285). This supports the high expression of LDHB found in irradiated 92.1 cell line, suggesting that an increase in LDHB level may be related to a halt in growth and progression of UM. PFKM (phosphofructokinase, muscle) is also a glycolytic enzyme, but was found to be downregulated in irradiated 92.1 cells.

Tumour cells demonstrate high metabolic rate to support rapid growth and turnover rate. In a metabolomics study, significantly elevated activating phosphorylation levels of phosphofructokinase and pyruvate kinase in lung tumours confirmed hyperactive glycolysis (286). Activation of PFKM is regulated by the bifunctional enzyme 6-phosphofructo-2-kinase/fructose-2,6-bisphosphatase (PFKFB), which in turn is regulated by protein kinases such as AKT and MAPK (287). It has been shown that the MEK/MAPK and PI3K/AKT pathways are highly activated in UM (33,34,154,155). In an on-going phase II study, the MEK inhibitor selumetinib extended progression-free survival by nearly 9 weeks and reduced tumour size by 50% in patients with UM (288). Taken together, this downregulation of PFKM may reflect a shift in the energy demand of tumour cells post radiation, possibly via the inhibition of MAPK and AKT pathways. The proteins identified by (240) and (241) in irradiated UM cells warrants further investigation in order to understand the molecular characteristics of UM cells that undergo cell-cycle suspension. Identification of other interacting proteins and therapeutic targets may provide novel, medical treatment strategies for primary UM thereby reducing the need for radiation therapy and its associated side-effects to surrounding ocular structures.

### 1.5.2. Tissue studies

Coupland et al (243) performed proteomic analysis of primary uveal melanoma tissue, the first study to do so. They determined differential protein expression between four monosomy 3 and three disomy 3 tumours using 2-DE analysis. Differentially expressed proteins of statistical significance were HSP-27 and vimentin. HSP-27 was downregulated in monosomy 3 tumours while the latter was upregulated. The expression of these two proteins were examined in 41 formalin-fixed paraffin-embedded tissue slides by immunohistochemistry. Twenty of these were monosomy 3 tumours, while 21 were disomy 3. Expression of HSP-27 was found to be significantly lower in monosomy 3 uveal melanoma when compared with disomy 3 tumours. No statistical significance was found in the expression of vimentin.

A follow-up study (289) analysed the immunohistochemical expression of HSP-27 on 99 formalin-fixed paraffin embedded tumour samples. The possibility of using HSP-27 expression score to predict monosomy 3 was also assessed. Samples were selected based on their chromosome 3 status; 49 disomy 3 and 50 monosomy 3 tumours were analysed. Monosomy 3 tumours were found to have a significantly lower HSP-27 expression compared to disomy 3 tumours, demonstrating a significant negative correlation between reduced HSP-27 expression and a predicted survival of < 8 years. However, HSP-27 score alone did not predict monosomy 3 with high-enough specificity. When using a model incorporating other clinicopathological factors such as largest tumour diameter, presence of closed extravascular loops and cell type, monosomy 3 was predicted with greater accuracy (sensitivity 78% and specificity 72%).

HSP-27 is a cytoplasmic protein involved in the inhibition of cell proteolysis and protein conformation stabilisation (290,291). It is overexpressed in a variety of cancer cells and is associated with a poor prognosis in gastric, prostate, and node-negative breast carcinoma (292–294). In contrast, high levels

of HSP-27 expression indicate a good prognosis in non–small-cell lung carcinomas and ovarian carcinomas (295,296). This suggests that HSP-27 may play different roles in different tissues or that there are other elements present in some malignancies that can override or bypass any effects HSP-27 may have (297). Of interest, HSP-27 overexpression has been shown to inhibit cell proliferation and reduce cell invasiveness in one human cutaneous melanoma cell line (298). From this, it was postulated that underexpression of HSP-27 in melanoma cells results in increased tumour cell motility and invasiveness.

More recently, our group (244) performed 2D-DIGE proteomic analysis comparing 9 primary UM tumour samples from patients who developed metastatic disease versus 16 primary UM tumour samples from patients who did not develop metastatic disease, with a minimum of 7 years follow-up. Nine proteins were upregulated in primary UM tissue that developed metastasis. These were disulphide-isomerase A3 precursor (PDIA3), selenium-binding protein 1 (SELENBP1), alpha-enolase, F-actin capping protein subunit alpha-1 (CAPZA1), endoplasmic reticulum protein ERp29 precursor, triosephosphate isomerase (TPI1), protein DJ-1 (PARK7), and fatty acid-binding protein, heart-type (FABP3). The 5 proteins that showed decreased expression in primary UM tissue that developed metastasis were eukaryotic translation initiation factor 2 subunit 1, proteasome subunit alpha type 3, 40S ribosomal protein SA, tubulin beta chain and tubulin alpha-1B chain. Follow-up immunohistochemical study was performed to determine the expression of FABP3, TPI1, CAPZA1, PDIA3, SELENBP1 and PARK7 on 8 formalin-fixed paraffin-embedded (FFPE) primary UM tissue from patients who developed metastasis and 8 FFPE primary UM tissue from patients who did not develop metastasis. Of these, increased expression levels of FABP3 and TPI1 correlated with the 2D DIGE results. Further validation by siRNA knockdown of these 2 proteins in one primary UM cell line (92.1) showed significant reduction in invasion and migration.

FABPs are expressed in a variety of tissues, playing role in fatty acid metabolism (299) and are suggested to be involved in a number of biological processes such as cell differentiation, cell growth, and apoptosis (300). One proteomics study showed a heterogeneous but unique FABP expression pattern in the different subtypes of renal cell carcinoma, suggesting its use for classification of this disease (299). Expression of FABP was significantly high in an aggressive small cell lung cancer cell line, suggesting that it may influence mitosis and cell growth (301). Another proteomic study identified FABP as a biomarker to predict gefininib treatment response in patients with lung adenocarcinoma (302). FABP was also shown to be expressed in human gastric carcinoma, and was associated with disease progression, tumour aggressiveness and poor patient survival (303). In contrast, ectopic expression of FABP3 in breast cancer cells was shown to reduce tumourigenicity in nude mice (304). This suggests a complex relationship between FABP and cancer. TPI1 is an enzyme that's critical in glycolysis and gluconeogenesis (305) and a high rate of glycolysis is required to support tumour growth (306). Functional inactivation of TPI induced apoptosis in cervical cancer cells (307). It has also been shown to be involved in the aggressiveness of breast cancer (308). Other proteomic studies found it to be significantly increased in lung cancer tissue (309), cell lines and patients' plasma (310), and in prostate cancer (311), suggesting its use as a serum biomarker. Interestingly, TPI1 was also shown to be expressed in uveal melanoma primary cell cultures by Pardo et al in the first proteomic study in UM.

## 1.6. Deficiencies in current knowledge of the molecular biology of metastatic disease

Progress made in molecular genetics has led to significant improvement in prognostic stratification of patients into high-risk and low-risk for developing metastatic disease. This has enabled closer surveillance of patients at-risk for metastasis, and earlier detection and treatment of metastatic disease. It has also increased the understanding of the triggering events that lead to the development of UM. However, very little is known about the molecular biology of the development of metastasis, and pathways involved in this fatal disease. Proteomic studies of malignancies have yielded information about tumour biology and led to the discovery of many biomarkers. However, this technique has not been used to study UM as extensively as other cancers. While numerous genomic studies have led to the identification of novel genes involved in the developmental biology and prognostic classification of patients, there is a distinct lack of effective therapeutic targets for these patients. Although only a few proteomic studies have been carried out so far, the results are very encouraging. Many of these proteins have not been described in the biology of UM before. Novel proteins involved in cell growth, proliferation, adhesion and metastasis have been identified. Most studies have been performed using cell lines, with only 2 studies using primary UM tissue. These studies were predominantly performed using the older 2-DE method. However, recent advances in proteomic technologies provide the opportunity for high-throughput quantitative studies to be performed using various biological material such as the primary tumour and metastatic tissue, vitreous, and serum. This would be an important step towards the identification of effective biomarkers and therapeutic targets for personalised medicine in uveal melanoma.

## 1.7. Objectives

To identify differentially expressed proteins and genes between primary UM tissue from patients who developed metastatic disease, versus primary UM tissue from patients who did not develop metastasis.

This will be achieved as follows;

1. Quantitative Label-free LC-MS proteomic profiling to identify differentially expressed proteins between primary UM tissue from patients who developed metastatic disease, versus primary UM tissue from patients who did not develop metastasis

2. Bioinformatic reanalysis of publically available gene expression microarray datasets of monosomy 3 tumours that developed metastatic disease versus disomy 3 tumours that did not develop metastatic disease

3. Immunohistochemical validation of targets of interest from objective 1 and 2 using formalin-fixed paraffin-embedded tissues and tissue microarrays of primary uveal melanoma tissue from patients who did and did not develop metastatic disease

# 2. Materials and methods

## 2.1. Uveal melanoma tissue label-free LC-MS

### 2.1.1. Sample collection, consent and ethics

Sixteen fresh frozen primary UM tissue specimens from patients with a minimum clinical follow-up of 7 years were used for label-free proteomic analysis. Of these, 8 patients subsequently developed metastasis while 8 patients did not. Tissue specimens were accessioned from the National Ophthalmic Laboratory, Royal Victoria Eye and Ear Hospital, Dublin. Fresh uveal melanoma samples were obtained from patients who had enucleation and stored at -80°C. Samples were also formalin-fixed and paraffin-embedded and cut in 4-µm sections for morphological assessment by immunohistochemistry. Cytogenetic analysis of chromosome 3 status was performed using fluorescent in situ hybridisation (FISH) by the Merseyside and Cheshire Genetics Laboratory, Crown St., Liverpool, UK. A number of the patients have since died as samples were collected between 1994 and 2003. As per the recommended guidelines of the Irish Council for Bioethics: "Human Biological Material: Recommendations for the collection, use and storage in research 2005"- chapter 3, pg 52, there is a waiver to consent (312). Ethical approval was obtained from the Research and Ethics Committee of the Royal Victoria Eye and Ear Hospital, Dublin (Title: Proteomic analysis of tissue samples from uveal melanoma patients; expiry date: 25 July 2014; reference number: 250711SK; principal investigator: Professor Susan Kennedy).

Prospectively, matched clinical samples were collected after obtaining informed consent from patients. These include the enucleated eye, vitreous fluid and patient serum for future biomarker studies. The project was funded by the Royal Victoria Eye and Ear Research Foundation. The research adhered to tenets of the Declaration of Helsinki.

### 2.1.2. Sample preparation and mass spectrometry

Fresh frozen uveal melanoma tissue specimens were removed from -80°C and allowed to thaw at room temperature. To homogenise the tissue sample, a small piece of tumour was added to Sample Grinding Kit (GE Healthcare, Little Chalfont, Buckinghamshire, UK) with 300 µL of 2D lysis buffer containing 7 M urea, 2 M thiourea, 4% (wt/vol) CHAPS, 40 mM dithiothreitol (DTT), and 0.5% immobilized pH gradient (IPG) buffer pH 3 to 11 (GE Healthcare) as per the manufacturer's recommendation. The sample was grinded with the grinding kit pestle for approximately 3 minutes at room temperature. Insoluble material was removed by centrifugation at 14,000 rpm for 5 minutes at room temperature, and supernatants were stored at -80°C until required. This sample prep was carried out by Dr Annett Linge and Deirdre O'Flynn. The samples used for this label-free proteomic analysis were a subset of samples that were used in a previous 2D-DIGE proteomic study (244)

For label-free proteomic analysis, stored samples were removed from -80°C and allowed to thaw at room temperature. To remove interefering detergents from the 2D lysis buffer in order to make the samples compatible for use by LC-MS, sample clean-up was performed using ReadyPrep 2D-clean-up kit as per manufacturer's instructions (Bio-Rad, Hemel-Hempstead, Hertfordshire, UK). 300 µL of precipitating agent 1 was added to 100 µg of protein sample in 100 µL and mixed well by vortexing. After incubating on ice for 15 minutes, 300 µL of precipitating agent 2 was added and mixed. The sample was centrifuged at 14,000 rpm for 5 minutes and the supernatant discarded. 40 µL of wash reagent 1 was added on top of the protein pellet and centrifuged at 14,000 rpm for 5 minutes. The supernatant was removed and 25 µL of ultrapure water was added to the pellet and mixed. 1 mL of wash reagent 2 (prechilled at -20°C for 1 hour) and 5 µL of wash 2 additive was added. The sample was mixed by vortexing for 1 minute. The mixture was incubated at -20°C for 30 minutes. During this incubation period, the sample was mixed by vortexing for 30 seconds every 10

minutes. Samples were centrifuged at 14,000 rpm for 5 minutes and the supernatant discarded. The resultant white pellet was air-dried at room temperature until translucent but for no more than 5 minutes. Protein pellets were resuspended in label-free solubilisation buffer, consisting of 6 M urea, 2 M thiourea and 10 mM Tris, pH 8.0 in LC-MS grade water. Protein suspensions were vortexed, sonicated and centrifuged to ensure pellets were fully resuspended. Protein concentrations were determined using the thiourea-compatible Quick Start Bradford Protein Assay Kit (Bio-Rad Laboratories Inc., Hercules, CA). For label-free MS analysis, volumes were kept to a minimum and initially equalized using label-free solubilisation buffer. Samples were reduced for 30 min with 10 mM DTT and alkylated for 20 minutes in the dark with 25 mM iodoacetamide in 50 mM ammonium bicarbonate. Initial proteolytic digestion was carried out with sequencing grade Lys-C at a ratio of 1:100 (protease/protein) for 4 h at 37ºC. The samples were subsequently diluted with 4 times the initial sample volume in 50 mM ammonium bicarbonate. A second digestion step was performed with sequencing grade trypsin at a ratio of 1:25 (protease/protein) overnight at 37$^{o}$C. Trifluoroacetic acid was added to a final concentration of 0.5% and incubated at room temperature for 5 minutes. The digest was snap-frozen in dry ice and stored at -20$^{o}$C until MS analysis. (Annett Linge, Deirde O'Fylnn)

Nano LC–MS/MS analysis was carried out using an Ultimate 3000 nanoLC system (Dionex) coupled to a hybrid linear ion trap/Orbitrap mass spectrometer (LTQ Orbitrap XL; Thermo Fisher Scientific). Five microlitres of digest were loaded onto a C18 trap column (C18 PepMap, 300 µm ID×5 mm, 5 µm particle size, 100 Å pore size; Dionex) and desalted for 10 min using a flow rate of 25 µL/min in 0.1% trifluoroacetic acid. The trap column was then switched online with the analytical column (PepMap C18, 75 µm ID×250 mm, 3 µm particle and 100 Å pore size; Dionex) and peptides were eluted with the following binary gradients of solvent A and B: 0–25% solvent B in 120 min and 25–50% solvent B in a further 60 min, where solvent A consisted of 2% acetonitrile (ACN) and 0.1% formic acid in water and solvent B consisted of 80% ACN and 0.08% formic acid in LC-MS grade water. Column flow rate was set to 350 nL/min. Data were acquired with

Xcalibur software, version 2.0.7 (Thermo Fisher Scientific). The mass spectrometer was operated in data-dependent mode and externally calibrated. Survey MS scans were acquired in the Orbitrap in the 300–2000 m/z range with the resolution set to a value of 60,000 at m/z 400. Up to seven of the most intense ions (1+, 2+ and 3+) per scan were CID fragmented in the linear ion trap. A dynamic exclusion window was applied within 40 s. All tandem mass spectra were collected using normalised collision energy of 35%, an isolation window of 3 m/z, and one microscan. All samples were set up and run by LC-MS by Mr Michael Henry, DCU.

### 2.1.3. Progenesis label-free LC-MS bioinformatic analysis

The acquired spectra for all 16 samples (Thermo raw files) were loaded to Progenesis label-free LC–MS software version 3.1 (NonLinear Dynamics, Newcastle upon Tyne, UK) for analysis. The software processes the raw data in two steps. Firstly each sample run was subjected to alignment which involved aligning the data based on the LC retention time of each sample; this allows for any drift in retention time giving an adjusted retention time for all runs in the analysis. The sample run with the most number of features (i.e. peptide ions) was selected as the reference run (run NM5), to which retention time of all of the other runs were aligned and peak intensities were normalised. This was done by manually reviewing each run, and aligning as many vectors as possible. Samples M1-8 were assigned to "metastatic" group, while samples NM1-8 were assigned to "non-metastatic" group.

Prior to exporting the MS/MS output files to MASCOT (www.matrixscience.com) for protein identification, a number of criteria were used to filter the data. These are (i) mass peak features with charge states from +1, +2 and +3 (ii) greater than 3 isotopes per peptide and (iii) peptide features with ANOVA p-value < 0.01 between experimental groups. All MS/MS spectra were exported from Progenesis software as a MASCOT generic file (mgf) and used for peptide identification with MASCOT (version 2.2) searched against the UniProtKB–SwissProt database (taxonomy: Homo sapiens, downloaded 1$^{st}$ October 2012). The search parameters used were as follows: (i) peptide mass tolerance set to 10 ppm (ii) MS/MS mass tolerance set at 0.5 Da (iii) up to two missed cleavages were allowed (iv) carbamidomethylation set as a fixed modification (v) methionine oxidation and deamination set as a variable modification. Only peptides with ion scores of 30 and above were considered and re-imported back into Progenesis LC–MS software for further analysis.

The Progenesis peptide quantification algorithm calculates peptide abundance as the sum of the peak areas within its isotope boundaries. Each abundance value is then transformed to a normalised abundance value by applying a global scaling factor. Normalization corrects for factors resulting from experimental variation and was automatically calculated over all features in all samples. It results in a unique factor for each sample that corrects all features in the sample in a similar way for experimental variation. Protein abundance was calculated as the sum of the abundances of all peptide ions which have been identified as coming from the same protein.

Proteins with 1 matched peptide and proteins with peptide conflicts were excluded to remove false positive identifications. For validation studies, a number of criteria were applied to assign a protein as significant; proteins with ≥ 3 peptides matched, and an ANOVA p-value between experimental groups of ≤ 0.05. The distribution of protein abundance for each statistically significant protein was reviewed to identify proteins that demonstrated good separation between the M and NM disease groups. Enrichment analysis of proteins with $p \leq 0.05$ and ≥ 2 peptides matched against GO (gene ontology) was conducted using the DAVID interface (http://david.abcc.ncifcrf.gov/) (313,314) to determine if any biological processes were overrepresented. Proteins were also analysed using the PANTHER Database (Protein ANalysis THrough Evolutionary Relationships, http://www.pantherdb.org/) (315–317) for protein categorization according to biological process, molecular function, protein class and PANTHER pathway.

## 2.2. Bioinformatic reanalysis of gene expression microarray data

Laurent et al (29) compared 28 tumours from patients who developed metastasis within 3 years vs. 35 from patients who did not develop metastasis/metastasised after 3 years. They identified high expression of PTP4A3 gene in high risk UM. Gene expression microarray and comparative genomic hybridization microarray data published by Laurent et al was obtained from GEO database (http://www.ncbi.nlm.nih.gov/geo/), under accession number GSE22138. This dataset was reanalysed to remove confounding clinical samples and samples with poor quality control. From 63 samples present in the original study, samples with chromosome 3 monosomy but without metastasis, and samples with chromosome 3 disomy with metastasis were excluded. Samples with other potential confounding factors were also excluded; tumours with extrascleral extension/no extrascleral extension information and tumours anterior to the equator (e.g. ciliary body tumours) were excluded. Quality control of the microarray data was conducted using hierarchical cluster analysis and principal component analysis. In total, 11 monosomy three tumours with metastasis and 9 disomy three tumours without metastasis were selected for transcriptomic analysis. Genes were considered to be differentially expressed upon observation of a fold change ≥ 1.3 and a P-value < 0.05 (Padraig Doolan). Enrichment analysis of genes with $p \leq 0.05$ and ≥ 2 peptides matched against GO (gene ontology) was conducted using the DAVID interface (http://david.abcc.ncifcrf.gov/) (313,314) to determine if any biological processes were overrepresented. Genes were also analysed using the PANTHER Database (Protein ANalysis THrough Evolutionary Relationships, http://www.pantherdb.org/) (315–317) for gene categorization according to biological process, molecular function, gene class and PANTHER pathway.

## 2.3. Immunohistochemistry

### 2.3.1. Preparation of full-face uveal melanoma section tissue slides

A total of 13 patients who developed metastasis and 13 patients who did not develop metastasis were identified and selected for pilot immunohistochemical studies. These samples were accessioned from the National Ophthalmic Laboratory, Royal Victoria Eye and Ear Hospital, Dublin. Immediately after enucleation, the globe is fixed in 10% neutral buffered formalin for 24 to 48 hours. Tissue block(s) of approximately 5 to 10mm thickness are selected and placed in numbered processing/embedding cassettes. The tissue cassettes are dehydrated in graded alcohols cleared in Xylene and saturated with paraffin wax according to the overnight process of the Sakura VIP automatic Tissue Processor. The tissue sections are then embedded in solid paraffin wax utilising the Tissue Tek Embedding Station. After removing the blocks from the embedding moulds the paraffin blocks are trimmed, cut at 4µm on the Microm HME 325 Microtome and floated out on deionised water at a temperature of 59 °C. The paraffin sections are then mounted on VWR SuperFrost Plus slides appropriately labelled with the specimen identification number and dried in a 37 °C incubator overnight followed by two hours at 60 °C in an oven chamber to maximise tissue adhesion to the slides. (Damien Tiernan)

### 2.3.2. Preparation of uveal melanoma tissue microarray slides

Details of archived tissue in the National Ophthalmic Laboratory, Royal Victoria Eye and Ear Hospital Dublin were reviewed. To identify UM tissues with suitable clinical follow-up information (metastatised/non-metastatised information, survival, date of death from metastatic disease) for TMA

construction, patients' clinical notes were reviewed. Further information was obtained by contacting patients' primary care physicians and the National Cancer Registry Ireland (www.ncri.ie). A total of 92 UM patients were identified as suitable for further study and tumours selected for TMA construction. Of these, 55 tumours were from patients who developed metastasis while 37 were from patients who did not. Tissue blocks were retrieved from the archive (National Ophthalmic Laboratory, Royal Victoria Eye and Ear Hospital Dublin, 1966-2009) and a fresh full face 5 µm haematoxylin and eosin stain (H&E) section was cut and reviewed under the light microscope. The area of interest was identified and marked on the glass slide so that the corresponding area on the tissue block can be sampled. A smaller diameter tissue arrayer needle (0.4 mm) was used to extract the paraffin core from the recipient block in order to create the space for the core from the donor UM block. A larger diameter tissue arrayer needle (0.6 mm) was used to extract the tissue core from the donor UM block. Both needled were positioned with the aid of micrometers for accuracy of placement. An adjustable depth stop was used to enable a constant depth of hole to be created in the recipient block. The hole in the recipient block was created, and the donor core extracted and inserted into the recipient block with the help of the steel stylet. After the recipient hole is filled, the needles are moved along the x axis to the right using the micrometer. This is repeated until the designed plan of microarray map is achieved. Throughout the whole process, both the block of origin and the TMA position of each individual core were carefully documented to ensure that the tissue microarray corresponded accurately with the pre-designed microarray map. Once completed, the blocks were placed upside down onto a glass slide and into an oven at 40°C overnight to facilitate bonding of the donor cores with the paraffin wax of the recipient blocks. The following morning, the glass slide attached to the TMA block was used to level the TMA block surface by gently pushing the cores into the block if necessary. After cooling, the TMA block was cut into 4µm sections using a microtome, and placed onto VWR SuperFrost Plus glass slides. To achieve maximal concordance with the results from full tissue sections, four cores per tumour were used. Two cores of control

tissue were placed at the top-right of each TMA to aid in orientation of tumour tissues. (Damien Tiernan, Fionnuala McAree)

### 2.3.3. Immunohistochemical staining of uveal melanoma slides

All immunohistochemical staining was performed using the DAKO Autostainer (Dako). Dewaxing and antigen retrieval was done in the PT Link system (Dako) using Target retrieval solution (Dako, Glostrup, Denmark) pH 9 for PRDX3, SIPA1L2, and CNTN3 for 20 minutes at 97°C. For CNDP2, a longer duration of 40 minutes at 97°C was done. After heating the slides at 97°C for the duration mentioned above, it was allowed to cool down to 65°C. The slides were then immersed in 1X wash buffer (Dako). On the autostainer, slides were blocked for 10 minutes with 200 µL of HRP Block (Dako). The slides were washed with 1X wash buffer and 200 µL of antibody solution added to the slides for 30 minutes for PRDX3 (GeneTex, Inc., Irvine, California [GTX111887]; dilution 1:400 vol/vol for full face UM section slides and 1:430 vol/vol for TMA slides), CNTN3 (Atlas Antibodies, Stockholm, Sweden [HPA003341]; dilution 1:30 vol/vol for full face UM section slides) and SIPA1L2 (Atlas Antibodies, Stockholm, Sweden [HPA024181]; dilution 1: 35 vol/vol for full face UM section slides. For CNDP2, an incubation time of 40 minutes was used (GeneTex, Inc., Irvine, California [GTX116375]; dilution 1:50 vol/vol for full face UM section slides). Antibodies were diluted using rabbit polyclonal antibodies in Dako REAL Antibody Diluent. Slides were washed again with 1X wash buffer and then incubated with 200 µL REAL EnVision (Dako) for 30 minutes. Slides were washed again with 1X wash buffer and then stained with 200 µL 3-amino-9-ethylcarbazole (AEC) substrate chromogen (Dako) for 5 minutes and this was repeated once more. All slides were counterstained with haematoxylin (Dako) for 5 minutes and rinsed with deionised water, followed by wash buffer. Once staining was completed, each slide was mounted with a coverslip using Faramount mounting solution (Dako).

Negative control slides were incubated with Dako REAL Antibody Diluent only; the primary antibody was omitted.

The immunohistochemical staining for the selected proteins were assessed by two observers who were blinded to all clinicopathologic and cytogenetic details including metastatic/non-metastatic information (Pathma Ramasamy, Anne-Marie Larkin)). A scoring system similar to the one first described by Remmele and Stegner (318), and adapted by Coupland et al (243) was used. The full face UM section slides were scored based on intensity of staining (A) and percentage of tumour cells that stained (B). Intensity was graded as 0 for no staining, 1+ for weak, 2+ for moderate and 3+ for strong staining. A percentage score was assigned as follows: 1 (0-49%), 2 (50-74%), 3 (75-89%) and 4 (90-100%). A total score was obtained by multiplying (A) and (B). Thus, a minimum score of 0 and a maximum score of 12 was obtained. The TMA slides were scored based on staining only, as all cases demonstrated 100% staining given the small tumour core size. The staining intensities observed in TMA tumours were either negative, weak or strong. Each tumour had 4 representative cores, and each core was assigned a score of 0-2. No staining was scored as 0, weak staining as 1 and strong staining as 2. A total score for each patient was obtained by adding the scores of all 4 cores. Thus, a minimum score of 0 and a maximum score of 8 was obtained. The total score was divided into 2 categories: 0-3 as low expression and 4-8 as high expression. In order for a patient to be categorised as “low expression”, a minimum of at least 1 core per patient would be required to demonstrate negative staining. The minimum staining for a patient to be categorised as “high expression” requires all 4 cores to demonstrate weak staining, 1 strong with 2 weak staining or 2 strong with 2 negative staining tumour cores. Thus, tumours with heterogenous PRDX3 staining in 4 cores would be classified as low or high based on the presence or absence of negative staining. Using this method, 4 weak staining cores would be appropriately categorised as a positive result.

All data were processed in SPSS for statistical analyses (version 22.0; SPSS Science, Chicago, IL, USA). The data analysed were ordinal, and thus, nonparametric analyses were conducted. The Fisher's exact test (two-tailed), Pearson correlation and Spearman correlation was used to assess the association between clinical, histopathological and cytogenetic factors with immunohistochemical expression score. Differences of immunohistochemical expression score between samples of patients that developed and those that did not develop metastasis were examined by Mann-Whitney U test. Kaplan-Meier survival curves were produced for metastatic/non-metastatic information and PRDX3 expression based on immunohistochemical analysis in tissue microarray.

# 3. Results

## 3.1. Uveal melanoma tissue label-free proteomics

To identify differentially expressed proteins between primary UM tissue from patients who developed metastatic disease versus primary UM tissue from patients who did not develop metastatic disease, quantitative label-free LC-MS proteomic profiling was performed. Sixteen fresh frozen primary UM tissue specimens from patients with a minimum clinical follow-up of 7 years were used. Of these, 8 patients subsequently developed metastasis (M) while 8 patients did not (NM). The clinical and histopathological characteristics of these samples are detailed in Table 3.

### 3.1.1. Label-free LC-MS analysis

All samples were prepped (Annett Linge, Deirde O'Fylnn), and run as 5 hour gradients by LC-MS (Michael Henry). The resultant LC-MS files were analysed using Progenesis software to look for differentially expressed proteins between experimental groups. Several criteria were applied to MS/MS data for identification; (i) mass peak features with charge states from +1, +2 and +3 (ii) ≤ 3 isotopes per peptide and (iii) peptide features with ANOVA p-value < 0.01 between experimental groups. A total of 1316 features matched these criteria and were identified with MASCOT (version 2.2) searched against the UniProtKB–SwissProt database (taxonomy: Homo sapiens, downloaded 1$^{st}$ October 2012). Proteins with peptide conflicts and those with 1 peptide matched were excluded to reduce possible false positive results. A number of criteria were applied to assign a protein as significant; an ANOVA between experimental groups of ≤0.05, proteins with ≥3 peptides matched. No fold change cut off was applied.

Table 3: Clinical and histopathological details of 16 fresh-frozen uveal melanoma tissue samples used for quantitative label-free LC-MS proteomic analysis.

| Sample | Sex | Age at diagnosis (years) | Metastatic sites | Survival after diagnosis (years) | Ciliary body involvement | Extraocular extension | Cell type | LTD (mm) | Chr. 3 |
|---|---|---|---|---|---|---|---|---|---|
| 1 | F | 40 | Liver, lung | 2 | Y | N | S | 18 | NA |
| 2 | F | 49 | Kidney | NA | N | N | S | 12 | Monosomy |
| 3 | M | 71 | Liver | 7 | Y | Y | E | 20 | Monosomy |
| 4 | F | 58 | Liver | 5 | Y | N | M | 15 | Monosomy |
| 5 | M | 71 | Lung | 2 | N | N | M | 11 | Monosomy |
| 6 | F | 69 | Liver | 11 | N | N | S | 12 | Monosomy |
| 7 | F | 51 | Liver | 1 | N | N | E | 15 | Monosomy |
| 8 | M | 64 | Lung | 10 | Y | N | M | 10 | Disomy |
| 9 | F | 76 | N | [redacted] | N | N | M | 8 | Disomy |
| 10 | F | 46 | N | [redacted] | N | N | E | 23 | Disomy |
| 11 | F | 74 | N | [redacted] | N | N | M | 14 | NA |
| 12 | M | 68 | N | [redacted] | Y | N | S | 20 | Disomy |
| 13 | F | 52 | N | [redacted] | N | Y | M | 10 | Disomy |
| 14 | F | 75 | N | [redacted] | N | N | S | 22 | Disomy |
| 15 | F | 42 | N | [redacted] | N | N | S | 17 | Disomy |
| 16 | M | 50 | N | [redacted] | N | N | M | 17 | Disomy |

N, no; Y, yes; S, spindle cells; E, epitheloid cells; M, mixed cells; LTD, largest tumour diameter; NA, not available.

In total, 216 differentially expressed proteins were identified which had an ANOVA $p \leq 0.05$ between the two patient groups (supplementary data appendix I, ). Of these, 106 and 110 proteins were differentially upregulated and downregulated, respectively, in primary UM samples that metastasised (M) compared to those that did not (NM). There were 122 proteins with 1 peptide, 44 with 2 peptides and 50 proteins with 3 or more peptides assigned (Table 4).

Table 4: Eight fresh frozen primary UM tissue specimens from patients who developed metastasis versus 8 fresh frozen primary UM tissue specimens from patients who did not develop metastasis, with a minimum clinical follow-up of 7 years were subjected to quantitative label-free LC-MS proteomic profiling. Table 4 shows proteins identified with MASCOT with mass peak features with charge states from +1 to +3, greater than 3 isotopes per peptide and peptide features with ANOVA p-value < 0.01 between experimental groups.

| | **Number of proteins** |
|---|---|
| **$p \leq 0.05$** | 216 |
| **1 peptide** | 122 |
| **2 peptides** | 44 |
| **3 or more peptides** | 50 |

Of the 50 proteins with $\leq 0.05$ and $\geq 3$ peptides assigned, 29 were upregulated in primary UM tissue of patients that metastasised (M), while 21 proteins were downregulated in M (Table 5 and Table 6 respectively). The feature data and peptide measurements are detailed in supplementary data appendix I ( and ). Complete protein information including peptide count, confidence score, p value, fold change, normalised abundance, raw abundance and spectral counts are provided in supplementary data appendix I (). The distribution of protein abundance for each sample was reviewed to identify proteins that demonstrated

good separation between the M and NM disease groups. Of the 50 proteins, 7 showed good separation between the two disease groups. Six were upregulated in M and 1 was downregulated. Upregulated proteins in M are elongation factor 1-gamma (EF1G), thioredoxin-dependent peroxide reductase (PRDX3), importin subunit beta-1 (IMB1), rab GDP dissociation inhibitor beta (GDIB), heterogeneous nuclear ribonucleoprotein K (HNRPK) and glucose-6-phosphate isomerase (G6PI). Cytosolic non-specific dipeptidase (CNDP2) was downregulated in M. The fold change, p value, and number of peptides assigned to these proteins are outlined in Table 7. For each of the 7 protein, the standardised normalised abundance in samples 1-16 are shown in Figure 10.

Table 5: Details of 29 differentially upregulated proteins in 8 primary uveal melanoma tissues of patients who metastasised (M) compared to 8 primary uveal melanoma tissues without metastasis (NM), with $p \leq 0.05$, and $\geq 3$ peptides assigned to each protein. Proteins are presented from lowest to highest p value.

| Protein Accession | Anova (p) | Fold | Peptides matched | Ion score | Description |
|---|---|---|---|---|---|
| P26641 EF1G | 0.000387 | 2.02 | 3 | 142.69 | Elongation factor 1-gamma |
| P06733 ENOA | 0.000726 | 1.68 | 10 | 662.16 | Alpha-enolase |
| P15531 NDKA | 0.000947 | 1.89 | 5 | 235.99 | Nucleoside diphosphate kinase A |
| P30048 PRDX3 | 0.00218 | 1.58 | 4 | 273.05 | Thioredoxin-dependent peroxide reductase, mitochondrial |
| P55072 TERA | 0.00262 | 1.45 | 4 | 301.59 | Transitional endoplasmic reticulum ATPase |
| P11142 HSP7C | 0.00268 | 1.54 | 5 | 306.74 | Heat shock cognate 71 kDa protein |
| Q14974 IMB1 | 0.00292 | 1.47 | 4 | 271.69 | Importin subunit beta-1 |
| P50395 GDIB | 0.00314 | 1.61 | 5 | 280.72 | Rab GDP dissociation inhibitor beta |

| Protein Accession | Anova (p) | Fold | Peptides matched | Ion score | Description |
|---|---|---|---|---|---|
| P60709 ACTB | 0.00512 | 3.54 | 5 | 259.7 | Actin, cytoplasmic 1 |
| P61978 HNRPK | 0.00617 | 1.56 | 3 | 189.73 | Heterogeneous nuclear ribonucleoprotein K |
| P43320 CRBB2 | 0.00619 | 42.66 | 3 | 168.38 | Beta-crystallin B2 |
| P60174 TPIS | 0.00664 | 1.79 | 8 | 523.06 | Triosephosphate isomerase |
| P11021 GRP78 | 0.00779 | 1.45 | 6 | 488.32 | 78 kDa glucose-regulated protein |
| P62937 PPIA | 0.0084 | 1.33 | 3 | 169.95 | Peptidyl-prolyl cis-trans isomerase A |
| P10721 KIT | 0.00874 | 4.85 | 6 | 273.77 | Mast/stem cell growth factor receptor |
| P02768 ALBU | 0.01 | 2.66 | 4 | 292.09 | Serum albumin |
| P35749 MYH11 | 0.02 | 9.99 | 5 | 262.63 | Myosin-11 |
| P06865 HEXA | 0.02 | 3.04 | 7 | 484.38 | Beta-hexosaminidase subunit alpha |

| Protein Accession | Anova (p) | Fold | Peptides matched | Ion score | Description |
|---|---|---|---|---|---|
| P62140 PP1B | 0.02 | 2.04 | 3 | 128 | Serine/threonine-protein phosphatase PP1-beta catalytic subunit |
| P08670 VIME | 0.02 | 1.98 | 23 | 1409.7 | Vimentin |
| P16615 AT2A2 | 0.02 | 1.76 | 6 | 342.56 | Sarcoplasmic/endoplasmic reticulum calcium ATPase 2 |
| P06744 G6PI | 0.02 | 1.54 | 5 | 461.9 | Glucose-6-phosphate isomerase |
| P08758 ANXA5 | 0.03 | 3.98 | 3 | 172.89 | Annexin A5 |
| P36957 ODO2 | 0.03 | 1.99 | 3 | 128.45 | Dihydrolipoyllysine-residue succinyltransferase component of 2-oxoglutarate dehydrogenase complex, mitochondrial |
| P13639 EF2 | 0.03 | 1.8 | 5 | 228.5 | Elongation factor 2 |
| P19338 NUCL | 0.03 | 1.75 | 10 | 726.89 | Nucleolin |
| P11940 PABP1 | 0.03 | 1.37 | 3 | 167.51 | Polyadenylate-binding protein 1 |

| Protein Accession | Anova (p) | Fold | Peptides matched | Ion score | Description |
|---|---|---|---|---|---|
| P05413 FABPH | 0.04 | 2.46 | 4 | 289.17 | Fatty acid-binding protein, heart |
| P07686 HEXB | 0.04 | 2.39 | 6 | 413.84 | Beta-hexosaminidase subunit beta |

Table 6: Details of 21 differentially downregulated proteins in 8 primary uveal melanoma tissues of patients who metastasised (M) compared to 8 primary uveal melanoma tissues without metastasis (NM), with $p \leq 0.05$, and $\geq 3$ peptides assigned to each protein. Proteins are presented from lowest to highest p value.

| Protein Accession | Anova (p) | Fold | Peptides matched | Ion score | Description |
|---|---|---|---|---|---|
| Q96KP4 CNDP2 | 0.00132 | 1.75 | 6 | 304.06 | Cytosolic non-specific dipeptidase |
| Q13813 SPTA2 | 0.00187 | 2.3 | 8 | 352.15 | Spectrin alpha chain, brain |
| P15428 PGDH | 0.00446 | 38.81 | 4 | 234 | 15-hydroxyprostaglandin dehydrogenase [NAD+] |
| Q9UNF0 PACN2 | 0.00619 | 3.53 | 3 | 104.12 | Protein kinase C and casein kinase substrate in neurons protein 2 |
| Q8WUM4 PDC6I | 0.00761 | 2.27 | 4 | 247.14 | Programmed cell death 6-interacting protein |
| Q9NQ79 CRAC1 | 0.02 | 1.97 | 3 | 116.9 | Cartilage acidic protein 1 |
| P29401 TKT | 0.02 | 3.43 | 5 | 257.21 | Transketolase |
| P02511 CRYAB | 0.02 | 4.27 | 3 | 179.54 | Alpha-crystallin B chain |

| Protein Accession | Anova (p) | Fold | Peptides matched | Ion score | Description |
|---|---|---|---|---|---|
| P31937 3HIDH | 0.03 | 1.46 | 4 | 344.15 | 3-hydroxyisobutyrate dehydrogenase, mitochondrial |
| Q9BZQ8 NIBAN | 0.03 | 1.66 | 5 | 314.36 | Protein Niban |
| P05023 AT1A1 | 0.03 | 1.81 | 3 | 178.83 | Sodium/potassium-transporting ATPase subunit alpha-1 |
| Q99536 VAT1 | 0.03 | 2.09 | 4 | 170.67 | Synaptic vesicle membrane protein VAT-1 homolog |
| P61313 RL15 | 0.03 | 4.63 | 3 | 129.17 | 60S ribosomal protein L15 |
| P01009 A1AT | 0.04 | 1.99 | 4 | 204.7 | Alpha-1-antitrypsin |
| P27816 MAP4 | 0.04 | 2.33 | 14 | 730.03 | Microtubule-associated protein 4 |
| Q03252 LMNB2 | 0.04 | 2.36 | 3 | 136.84 | Lamin-B2 |
| P08107 HSP71 | 0.04 | 3.16 | 3 | 189.72 | Heat shock 70 kDa protein 1A/1B |
| P02649 APOE | 0.04 | 5.82 | 10 | 594.63 | Apolipoprotein E |

| Protein Accession | Anova (p) | Fold | Peptides matched | Ion score | Description |
|---|---|---|---|---|---|
| P04350 TBB4 | 0.05 | 1.41 | 8 | 706.15 | Tubulin beta-4 chain |
| P04792 HSPB1 | 0.05 | 1.56 | 6 | 464.12 | Heat shock protein beta-1 |
| P11216 PYGB | 0.05 | 1.95 | 11 | 678.11 | Glycogen phosphorylase, brain form |

Table 7: Details of 7 proteins with $p \leq 0.05$, $\geq 3$ peptides assigned to each protein and showing good separation between primary uveal melanoma tissue of patients who metastasised (M) compared to those that did not metastasise (NM). A positive fold change value represents the differential upregulation of a protein in M versus NM, while a negative fold change value represents downregulation in M compared to NM. Proteins are presented from lowest to highest p value.

| Protein Accession | Anova (p) | Fold | Peptides matched | Ion score | Description |
|---|---|---|---|---|---|
| P26641 EF1G | 0.000387 | 2.02 | 3 | 142.69 | Elongation factor 1-gamma |
| Q96KP4 CNDP2 | 0.00132 | –1.75 | 6 | 304.06 | Cytosolic non-specific dipeptidase |
| P30048 PRDX3 | 0.00218 | 1.58 | 4 | 273.05 | Thioredoxin-dependent peroxide reductase, mitochondrial |
| Q14974 IMB1 | 0.00292 | 1.47 | 4 | 271.69 | Importin subunit beta-1 |
| P50395 GDIB | 0.00314 | 1.61 | 5 | 280.72 | Rab GDP dissociation inhibitor beta |
| P61978 HNRPK | 0.00617 | 1.56 | 3 | 189.73 | Heterogeneous nuclear ribonucleoprotein K |
| P06744 G6PI | 0.02 | 1.54 | 5 | 461.9 | Glucose-6-phosphate isomerase |

(i) Elongation factor 1-gamma, EF1G

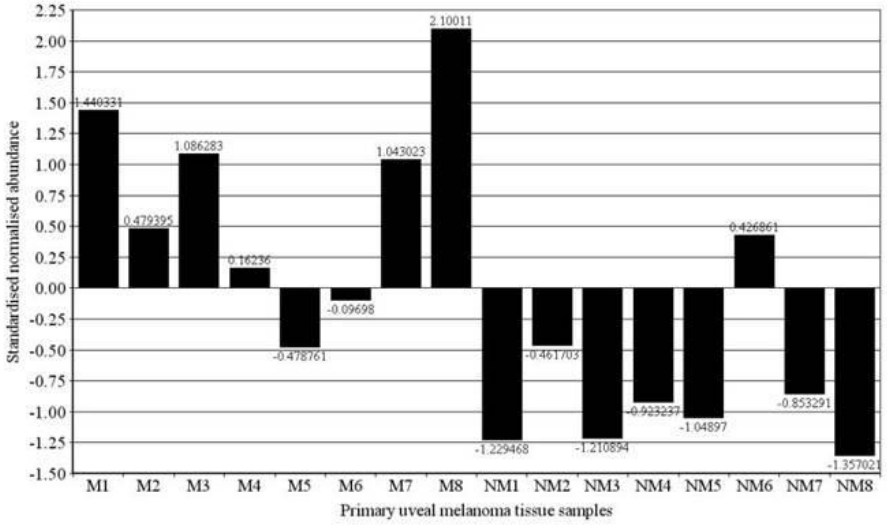


(ii) Cytosolic non-specific dipeptidase 2, CNDP2

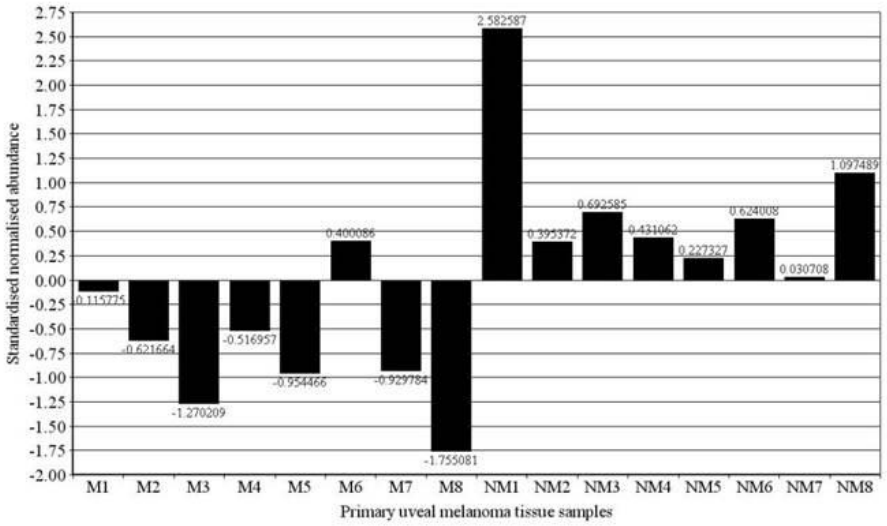


(iii) Thioredoxin-dependent peroxidase reductase, PRDX3

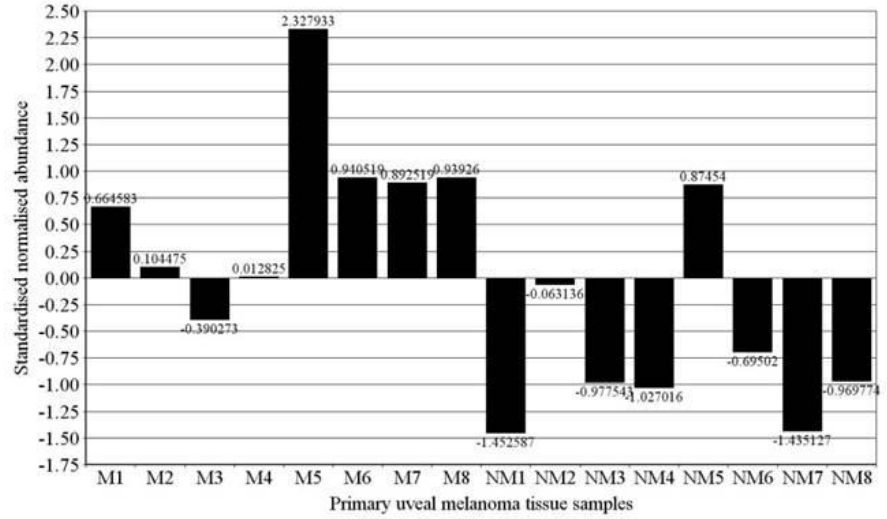

(iv) Importin subunit beta-1, IMB1

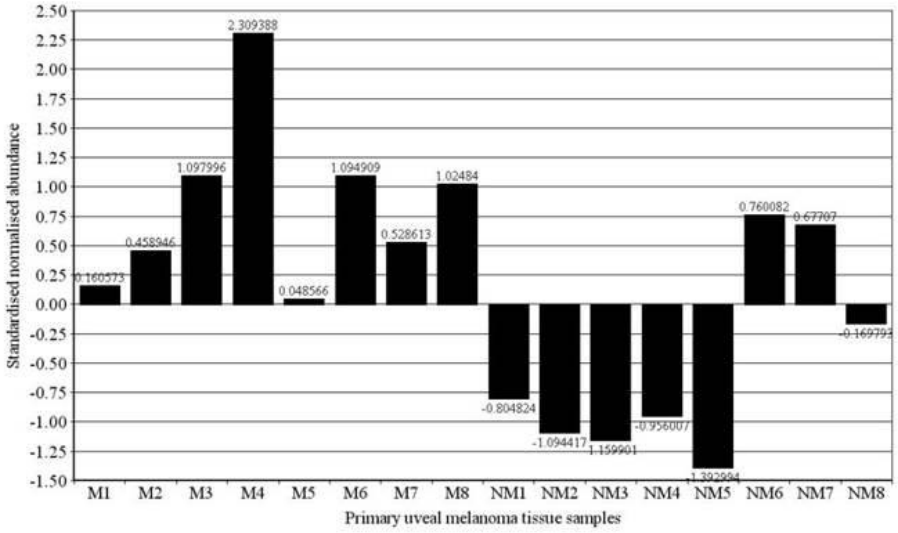


(v) Rab GDP dissociation inhibitor beta, GDIB

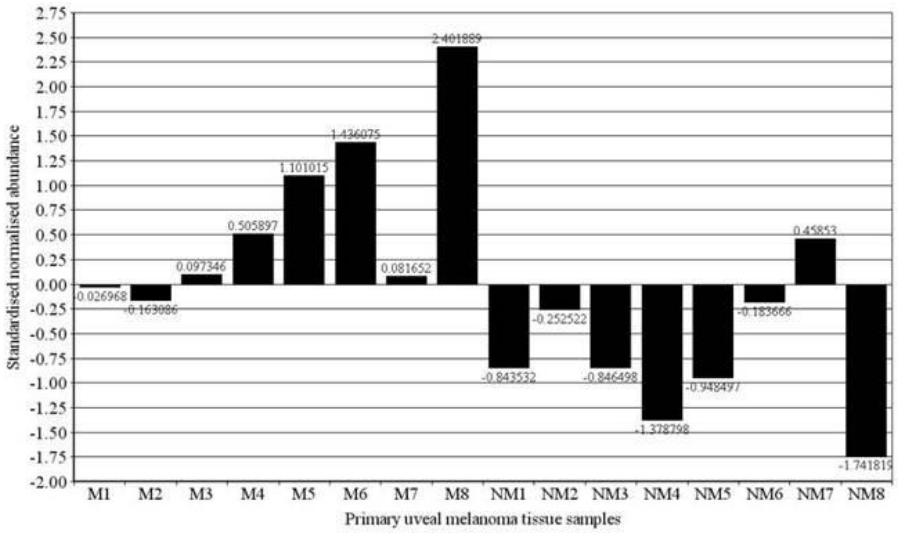


(vi) Heterogeneous nuclear ribonucleoprotein K, HNRPK

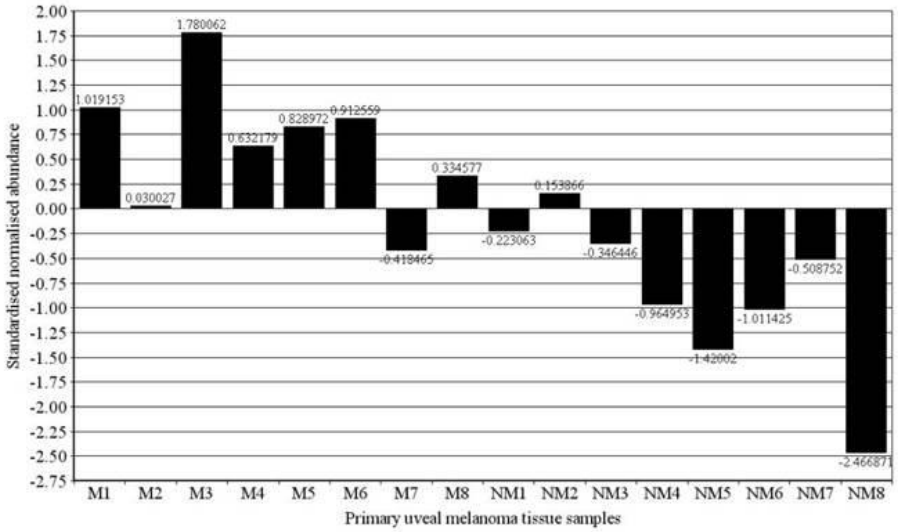

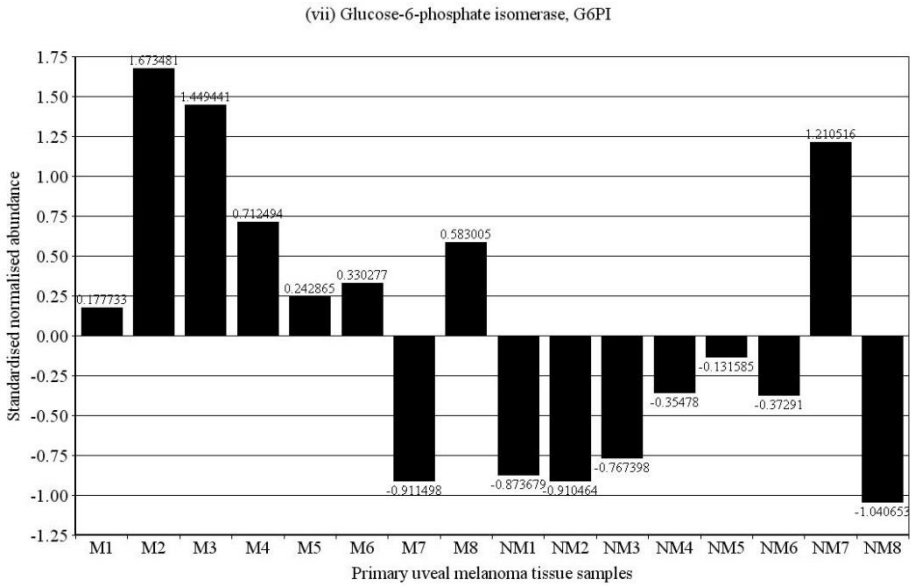


Figure 10: LC-MS/MS label-free results showing expression levels of 7 proteins with good separation of abundance between the 2 disease groups: (i) elongation factor 1-gamma, 2.02 fold upregulated in metastatic group, p: 0.000387 (ii) cytosolic non-specific dipeptidase, 1.75 fold downregulated in metastatic group, p: 0.00132 (iii) thioredoxin-dependent peroxide reductase, 1.58 fold upregulated in metastatic group, p: 0.00218 (iv) importin subunit beta-1, 1.47 fold upregulated in metastatic group, p: 0.00292 (v) rab GDP dissociation inhibitor beta, 1.61 fold upregulated in metastatic group, p: 0.00314 (vi) heterogeneous nuclear ribonucleoprotein K, 1.56 fold upregulated in metastatic group, p: 0.00617 (vii) Glucose-6-phosphate isomerase, 1.54 fold upregulated in metastatic group, p: 0.02 in eight primary UM tissues from patients who developed metastasis and eight primary UM tissues from patients who did not develop metastasis. The graph shows average normalised abundance volumes of the identified proteins from LC-MS/MS analysis of each sample (adapted from output from Progenesis LC-MS analysis software). The horizontal axis represents the individual biological replicates from the 8 patients who developed metastatic disease (M1-M8) and the eight patients who did not develop metastatic disease (NM1-NM8). The vertical axis represents normalised abundance volumes (log).

For these 7 proteins, the standardised normalised abundances (SNA) in individual samples were reviewed to identify proteins that demonstrated the best separation between M and NM disease groups. Outliers are samples with differential expression of standardised normalised protein abundance that were in the opposite trend compared to other samples within the sample group of M or NM. EF1G and GDIB had 3 samples that were outliers. The remaining proteins had 2 samples that were outliers except CNDP2, which only had 1 outlying sample. EEF1G was differentially upregulated by 2.02 fold in M. The outlying samples were M5 and M6, where the standardised normalised abundances (SNA) were differentially downregulated while that of sample NM6 was upregulated. GDIB was differentially upregulated by 1.61 fold in M. Samples M1 and M2 were outliers where the SNA were differentially downregulated while the SNA of sample NM7 was upregulated. EEF1G and GDIB were not considered for further follow-up based on the presence of 3 outliers. G6PI was upregulated by 1.54 fold in M and had 2 samples that were outliers. These are M7, where its expression was differentially downregulated more than all NM samples except NM8. Sample NM7 was also an outlier, where its expression was differentially upregulated with only two other M samples demonstrating higher expression. Thus, G6PI was excluded from further follow-up due to the significant outliers. IMB1 was differentially upregulated by 1.47 fold in M. No outlying samples were present in M, but 2 outliers were found in NM. These were samples NM6 and NM7, both of which demonstrated higher differential upregulation than 4 of 8 primary UM samples from patient with metastatic disease. For this reason, IMB1 was not considered for further validation. HNRPK was upregulated by 1.56 fold in M with 2 outlying samples. In sample M7, the differential expression level of HNRPK was found to be lower than three NM samples, while that of NM2 was differentially upregulated higher than 2 primary UM samples of patients who subsequently developed metastatic disease. PRDX3 was upregulated by 1.58 fold in M, with 2 samples that were outliers. In sample M3, PRDX3 was differentially downregulated lower than two NM samples while in sample NM5, it was differentially upregulated higher than 4 M samples. Both HNRPK and PRDX3 demonstrated similar number and patterns of outliers. Based on stronger statistical strength, PRDX3 was selected for validation studies (p: 0.00218

vs. p: 0.00617 for PRDX3 and HNRPK, respectively). Furthermore, PRDX3 had 4 assigned peptides, compared to 3 peptides matched to HNRPK. CNDP2 was the only protein that was differentially downregulated in M compared to NM, which also demonstrated good separation between the two groups of samples. It was downregulated by 1.75 fold in M and had the most number of peptides assigned to it (6 peptides). Furthermore, only 1 outlying sample was present (M6). For these reasons, CNDP2 was chosen for validation studies by immunohistochemistry.

### 3.1.2. Gene ontology analysis of uveal melanoma tissue label-free LC-MS results

Gene ontology (GO) enrichment analysis of 50 differentially expressed proteins with $p \leq 0.05$ and ≥ 3 peptides matched was conducted using the DAVID interface (313,314) to determine if any biological processes were overrepresented. Due the small number of proteins with ≥ 3 peptides matched, no significant results were found. For all subsequent GO analysis, 94 proteins with ≥ 2 peptides matched with $p \leq 0.05$ were included; 49 were upregulated and 45 were downregulated in primary UM tissues that developed metastatic disease compared to those that did not. Table 8 shows the enriched GO biological processes for proteins with a Benjamani Hochberg adjusted p of ≤ 0.05.

Table 8: List of Gene Ontology enriched biological processes of 94 differentially expressed proteins identified by quantitative label-free LC-MS profiling, with ≥ 2 peptides assigned and ANOVA $p \leq 0.05$ between experimental groups, of 8 primary uveal melanoma tissue of patients who developed metastatic disease and 8 primary tissues of patients who did not develop metastatic disease. Data presented in this table are those with Benjamani Hochberg adjusted $p \leq 0.05$, in ascending order.

| Biological process | Count | % of proteins | p value | Benjamini Hochberg adjusted p value | Proteins |
|---|---|---|---|---|---|
| GO:0006006~glucose metabolic process | 11 | 11.702 | 6.03E-08 | 7.90E-05 | TPI, CRYAB, 3HIDH, PPP1CB, PGAM1, PGM2, ENOA, G6PI, PKM2, PYGL, PYGB |
| GO:0005996~monosaccharide metabolic process | 12 | 12.765 | 2.16E-07 | 1.41E-04 | TPI, CRYAB, 3HIDH, PPP1CB, PGAM1, PGM2, ENOA, G6PI, PKM2, PYGL, HEXB |

| Biological process | Count | % of proteins | p value | Benjamini Hochberg adjusted p value | Proteins |
|---|---|---|---|---|---|
| GO:0019318~hexose metabolic process | 11 | 11.702 | 5.05E-07 | 2.20E-04 | TPI, CRYAB, 3HIDH, PPP1CB, PGAM1, PGM2, ENOA, G6PI, PKM2, PYGL, PYGB |
| GO:0016052~carbohydrate catabolic process | 9 | 9.5744 | 5.64E-07 | 1.84E-04 | TPI, 3HIDH, PGAM1, ENOA, PYGB, G6PI, PKM2, PYGL, HEXB |
| GO:0044275~cellular carbohydrate catabolic process | 8 | 8.5106 | 1.37E-06 | 3.58E-04 | TPI, 3HIDH, PGAM1, ENOA, PYGB, G6PI, PKM2, PYGL |
| GO:0043069~negative regulation of programmed cell death | 13 | 13.829 | 3.84E-06 | 8.37E-04 | PRDX3, SYUA, APOH, ALBU, NDKA, KIT, HSP71, CRYAB, APOE, HSPD1, GRP78, ANXA5, HSP27 |
| GO:0010033~response to organic substance | 18 | 19.148 | 3.84E-06 | 7.17E-04 | SYUA, SORBS1, COL1A1, HSP72, MGP, NDKA, HSP7C, HSP71, FABP3, CRYAB, APOE, GNB2, HSPD1, PRDX3, SERPINA1, ANXA5, HSP27, TERA |
| GO:0060548~negative regulation of cell death | 13 | 13.829 | 3.95E-06 | 6.46E-04 | PRDX3, SYUA, APOH, ALBU, NDKA, KIT, HSP71, CRYAB, APOE, HSPD1, GRP78, ANXA5, HSP27 |
| GO:0006091~generation of precursor metabolites and energy | 12 | 12.765 | 6.25E-06 | 9.09E-04 | TPI, PP1B, PGAM1, SYUA, ENOA, PYGB, G6PI, PKM2, ODO2, PYGL, CISY, NNTM |

| Biological process | Count | % of proteins | p value | Benjamini Hochberg adjusted p value | Proteins |
|---|---|---|---|---|---|
| GO:0043066~negative regulation of apoptosis | 12 | 12.765 | 1.99E-05 | 0.002595 | PRDX3, SYUA, APOH, ALBU, NDKA, HSP71, CRYAB, APOE, HSPD1, GRP78, ANXA5, HSP27 |
| GO:0006007~glucose catabolic process | 6 | 6.3829 | 3.83E-05 | 0.004549 | TPI, 3HIDH, PGAM1, ENOA, G6PI, PKM2 |
| GO:0010035~response to inorganic substance | 9 | 9.5744 | 5.99E-05 | 0.006512 | APOE, CRYAB, SYUA, PRDX3, COL1A1, SERPINA1, MGP, ACTB, IMPA1 |
| GO:0019320~hexose catabolic process | 6 | 6.3829 | 8.88E-05 | 0.008900 | TPI, 3HIDH, PGAM1, ENOA, G6PI, PKM2 |
| GO:0046365~monosaccharide catabolic process | 6 | 6.3829 | 1.02E-04 | 0.009473 | TPI, 3HIDH, PGAM1, ENOA, G6PI, PKM2 |
| GO:0006986~response to unfolded protein | 6 | 6.3829 | 1.02E-04 | 0.009473 | HSP7C, HSP71, HSPD1, HSP72, TERA, HSP27 |
| GO:0046164~alcohol catabolic process | 6 | 6.3829 | 1.90E-04 | 0.016468 | TPI, 3HIDH, PGAM1, ENOA, G6PI, PKM2 |
| GO:0006096~glycolysis | 5 | 5.3191 | 2.52E-04 | 0.020372 | TPI, PGAM1, ENOA, G6PI, PKM2 |
| GO:0015980~energy derivation by oxidation of organic compounds | 7 | 7.4468 | 3.69E-04 | 0.027995 | PPP1CB, SYUA, PYGB, ODO2, PYGL, CISY, NNTM |
| GO:0051789~response to protein stimulus | 6 | 6.3829 | 6.91E-04 | 0.048995 | HSP7C, HSP71, HSPD1, HSP72, TERA, HSP27 |

As shown in Figure 11, the majority of proteins are involved in carbohydrate catabolic and metabolic processes, and negative regulation of apoptosis.

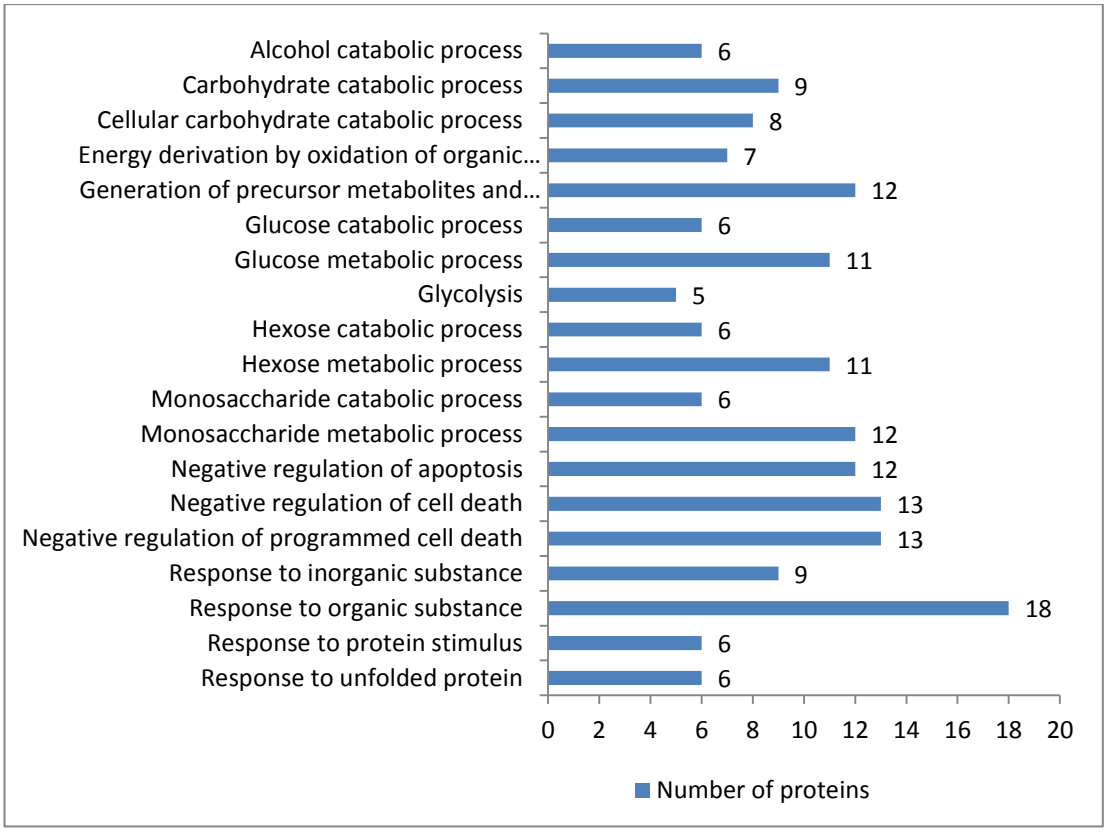


Figure 11: Graphical representation of statistically significant (Benjamani Hochberg adjusted $p \leq 0.05$) Gene Ontology enriched biological processes of 94 differentially expressed proteins identified by quantitative label-free LC-MS profiling, with ≥ 2 peptides assigned and ANOVA $p \leq 0.05$ between experimental groups, of 8 primary uveal melanoma tissue of patients who developed metastatic disease and 8 primary tissues of patients who did not develop metastatic disease.

Proteins in each disease group of primary UM tissue that and did not develop metastatic disease were also analysed and compared directly using the PANTHER Database (http://www.pantherdb.org/) (315–317), for protein categorization according to biological process, molecular function, protein class and PANTHER pathway. Figure 12 shows the biological processes of proteins that were upregulated in primary UM tissues of patients who did (M) and did not develop

metastatic disease (NM). A similar number of proteins in most biological process were observed. A higher number of proteins involved in metabolic process (32 vs. 28) and biological regulation (9 vs. 6), and a lower number of proteins involved in biological adhesion (0 vs. 5), multicellular organismal process (3 vs. 8) and response to stimulus (4 vs. 8) were found in M compared to NM.

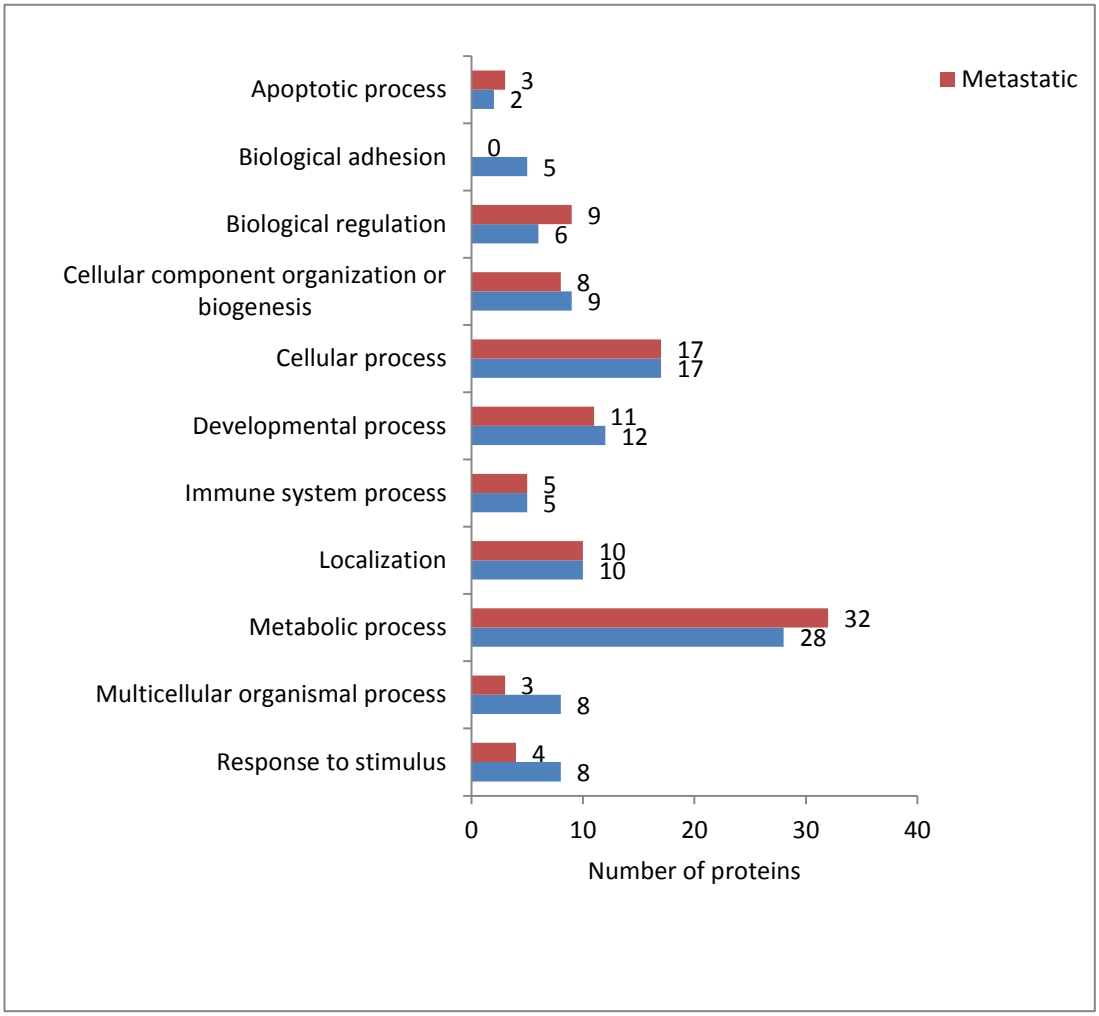


Figure 12: Graphical representation of biologic processes of 49 vs. 45 proteins that were upregulated in 8 primary UM tissue of patients that developed metastasis and 8 primary UM tissue of patients that did not develop metastatic disease, respectively. A total of 94 differentially expressed proteins were identified by quantitative label-free LC-MS profiling, with ≥ 2 peptides assigned and ANOVA $p \leq 0.05$ between experimental groups.

Table 9 shows statistically significant biological process enrichment based on differential protein expression levels in M compared to NM. Processes involving adhesion and skeletal system development were found to be significantly lower while those involving cytokinesis and mitosis were higher in M compared to NM.

Table 9: Statistically significant biological process enrichment based on differential protein expression levels in 8 primary UM tissue from patients who developed metastatic disease (M) compared to 8 primary UM tissue from patients who did not metastasise. A total of 94 differentially expressed proteins were identified by quantitative label-free LC-MS profiling, with ≥ 2 peptides assigned and ANOVA $p \leq 0.05$ between experimental groups. ↑ and ↓ indicate increased and decreased expression in M.

| **Biological Process** | **Number of proteins** | **Expression in "M"** | **P value** |
|---|---|---|---|
| Cell adhesion | 5 | ↓ | 0.0124 |
| Biological adhesion | 5 | ↓ | 0.0124 |
| Cell-cell adhesion | 3 | ↓ | 0.0161 |
| Cytokinesis | 2 | ↑ | 0.0256 |
| Skeletal system development | 2 | ↓ | 0.0292 |
| Mitosis | 4 | ↑ | 0.0389 |

Figure 13 shows the molecular function of proteins that were upregulated in M and NM. A higher number of proteins with binding (15 vs. 11) and catalytic activity (26 vs. 16), and lower number of proteins with structural molecule (8 vs. 12) and receptor activity (0 vs. 5) were found M compared to NM. Based on differential protein expression levels, receptor activity was significantly enriched in NM compared to M (p: 0.0124). The difference in other categories was not significant.

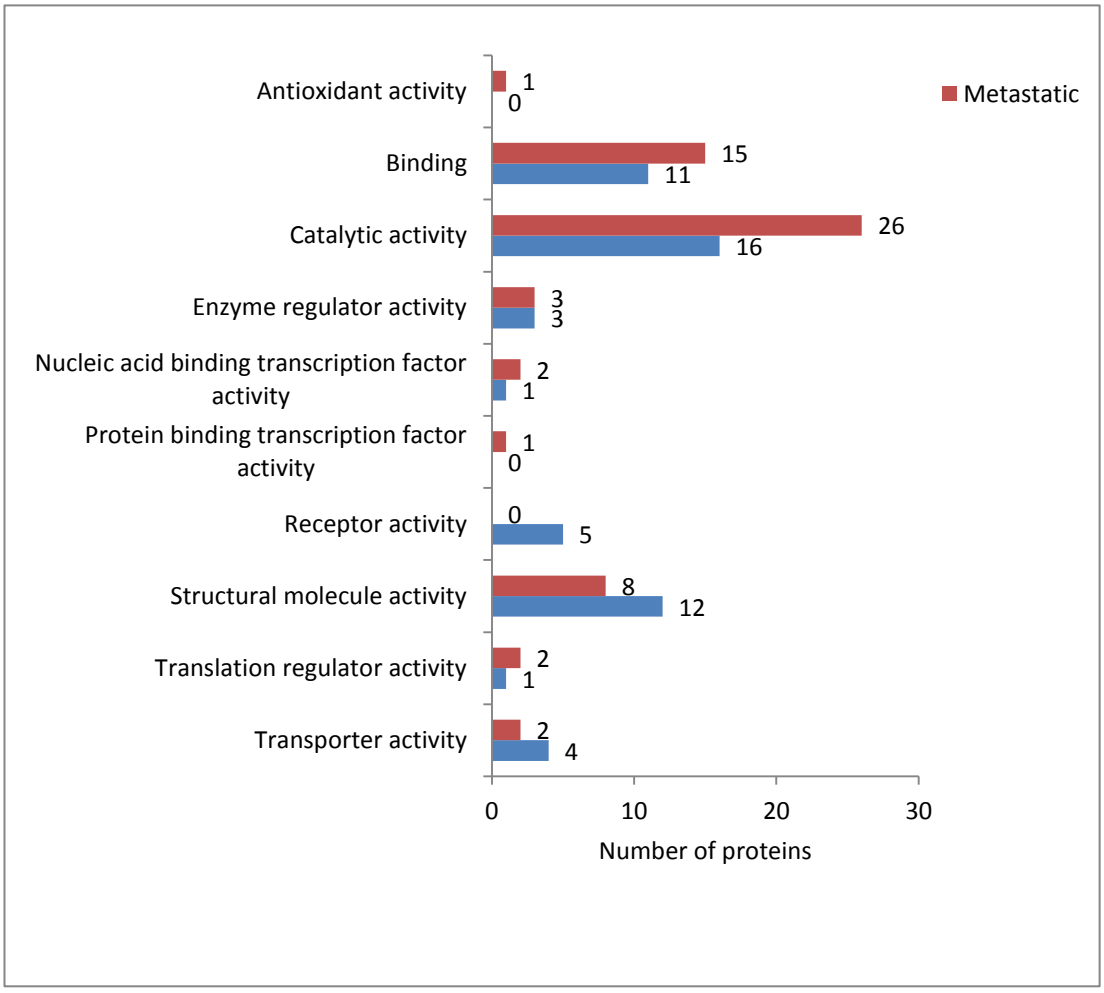


Figure 13: Graphical representation of molecular function of 49 vs. 45 proteins that were upregulated in 8 primary UM tissue of patients that developed metastasis (M) and 8 primary UM tissue of patients that did not develop metastatic disease (NM), respectively. A total of 94 differentially expressed proteins were identified by quantitative label-free LC-MS profiling, with ≥ 2 peptides assigned and ANOVA $p \leq 0.05$ between experimental groups. Based on differential protein expression levels, receptor activity was significantly enriched in NM compared to M (p: 0.0124).

Figure 14 shows proteins in PANTHER pathways that were upregulated in M and NM. A higher number of proteins involved in FAS signalling (2 vs. 0), glycolysis (5 vs. 0), nicotinic acetylcholine receptor signalling (2 vs. 0) and pyruvate metabolism (2 vs. 0), and lower number of proteins involved in gonadotropin releasing hormone receptor pathway (1 vs. 3), heterotrimeric Gi-α and Gs-α G-protein signaling pathway (0 vs. 3) and integrin signalling pathway (1 vs. 3) were found in M compared to NM. Based on differential protein expression levels, nicotinic acetylcholine receptor signalling pathway was significantly enriched in M compared to NM (p: 0.0256) while the difference in other pathways were not significant.

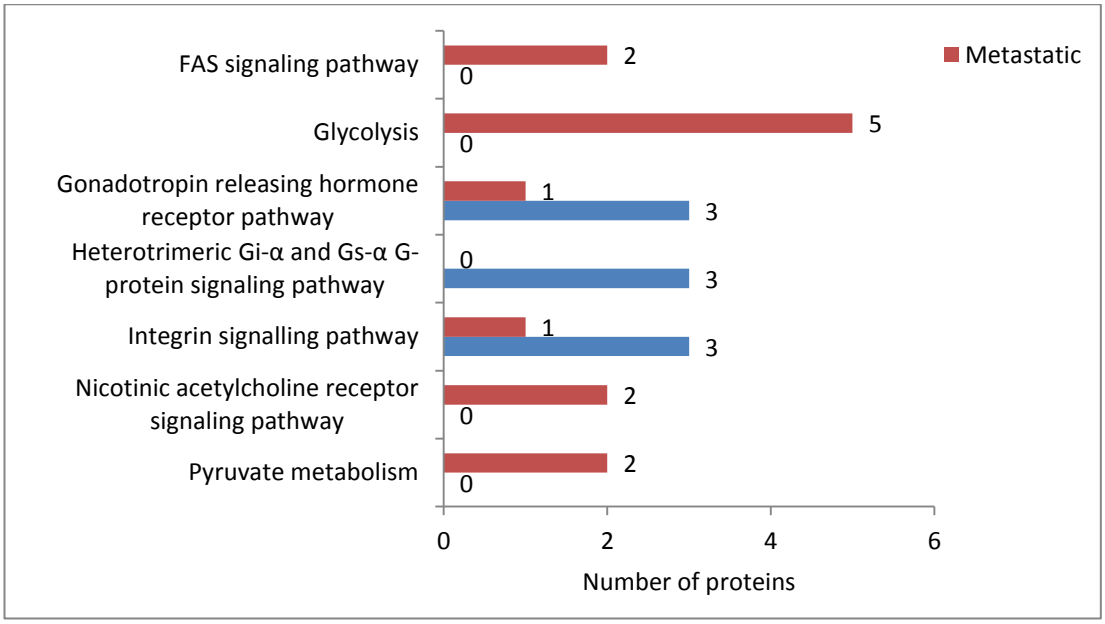


Figure 14: Graphical representation of proteins in PANTHER pathways that were upregulated in 8 primary UM tissue of patients that developed metastasis (M) and 8 primary UM tissue of patients that did not develop metastatic disease (NM), respectively. A total of 94 differentially expressed proteins were identified by quantitative label-free LC-MS profiling, with ≥ 2 peptides assigned and ANOVA $p \leq 0.05$ between experimental groups. Based on differential protein expression levels, nicotinic acetylcholine receptor signalling pathway was significantly enriched in M compared to NM (p: 0.0256). Due to large number of pathways, only those that showed a difference of more than 1 protein between disease groups are shown.

Figure 15 shows protein classes that were upregulated in M and NM. A higher number of isomerases (7 vs. 0), nucleic acid binding proteins (7 vs. 3), phosphatases (2 vs. 0), transfer/carrier proteins (3 vs. 1) and transferases (6 vs. 3) were found in M compared to NM. In NM, cell adhesion molecules (3 vs. 0), chaperones (7 vs. 4), defence/immunity proteins (2 vs. 0), extracellular matrix proteins (5 vs. 0), membrane traffic proteins (5 vs. 1), oxireductases (5 vs. 3), proteases (2 vs. 0), and receptor proteins were found to be higher than in M. Based on differential protein expression levels, extracellular matrix and receptor proteins were significantly enriched in NM compared to M (p: 0.0113 and 0.0124 respectively). A complete list of GO molecular function, GO biological process, PANTHER protein class and pathway can be found in supplementary data appendix I ().

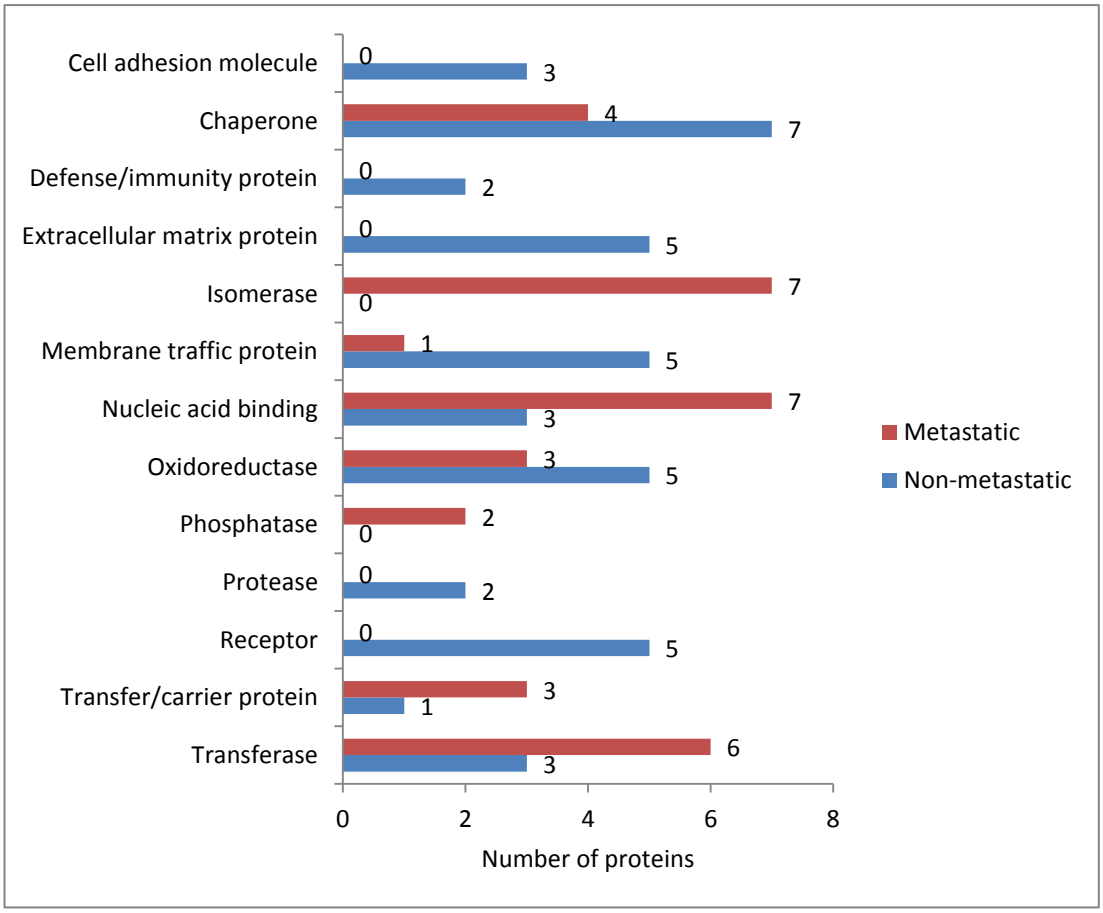


Figure 15: Graphical representation of protein class of 49 vs. 45 proteins that were upregulated in 8 primary UM tissue of patients that developed metastasis (M) and 8 primary UM tissue of patients that did not develop metastatic disease (NM),

respectively. A total of 94 differentially expressed proteins were identified by quantitative label-free LC-MS profiling, with ≥ 2 peptides assigned and ANOVA $p \leq 0.05$ between experimental groups. Based on differential protein expression levels, extracellular matrix and receptor proteins were significantly enriched in NM compared to M (p: 0.0113 and 0.0124 respectively). Due to large number of protein classes, only those that showed a difference of more than 1 protein between disease groups are shown.

## 3.2. Bioinformatic reanalysis of gene expression microarray data

To identify differentially expressed genes between primary UM tissue from patients who developed metastatic disease, versus primary UM tissue from patients who did not develop metastatic disease, bioinformatic reanalysis of publically available gene expression microarray datasets of monosomy 3 tumours that developed metastatic disease versus disomy 3 tumours that did not develop metastatic disease was performed. Laurent et al (29) compared 28 uveal melanomas from patients who developed liver metastases within three years of enucleation with 35 tumours from patients without metastases or who developed metastases more than 3 years after enucleation. However, it is not uncommon for UM patients to develop metastatic disease after 3 years. In order to eliminate this bias and obtain a more direct comparison, we studied monosomy 3 tumours that metastasised (M3M) versus disomy 3 tumours that did not metastasise (D3NM).

### 3.2.1. Gene expression microarray analysis

Comparative genomic hybridization microarray data published by Laurent et al was obtained from GEO database (http://www.ncbi.nlm.nih.gov/geo/), under accession number GSE22138. This dataset was reanalysed to remove confounding clinical samples and samples with poor quality control (Padraig Doolan). From 63 samples present in the original study, samples with chromosome 3 monosomy but without metastasis (n=10), and samples with chromosome 3 disomy with metastasis (n=4) were excluded. Tumours with partial monosomy 3 (n=5) and without chromosome 3 status (n= 8) were also excluded. Samples with other potential confounding factors were also excluded; tumours with extrascleral extension (n=2), no extrascleral extension information (n=2) and tumours anterior to the equator (e.g. ciliary body tumours, n=2). Quality control of the microarray

data was conducted using hierarchical cluster analysis and principal component analysis. Ten samples with poor quality control were excluded based on hierarchical cluster analysis (Figure 16, n=9) and principal component analysis (Figure 17, n=1). Figure 17 shows principal component analysis of 22 M3M and 14 D3NM tumours, and illustrates samples that were excluded from further analysis. In total, 43 samples were excluded from further analysis (table 10).

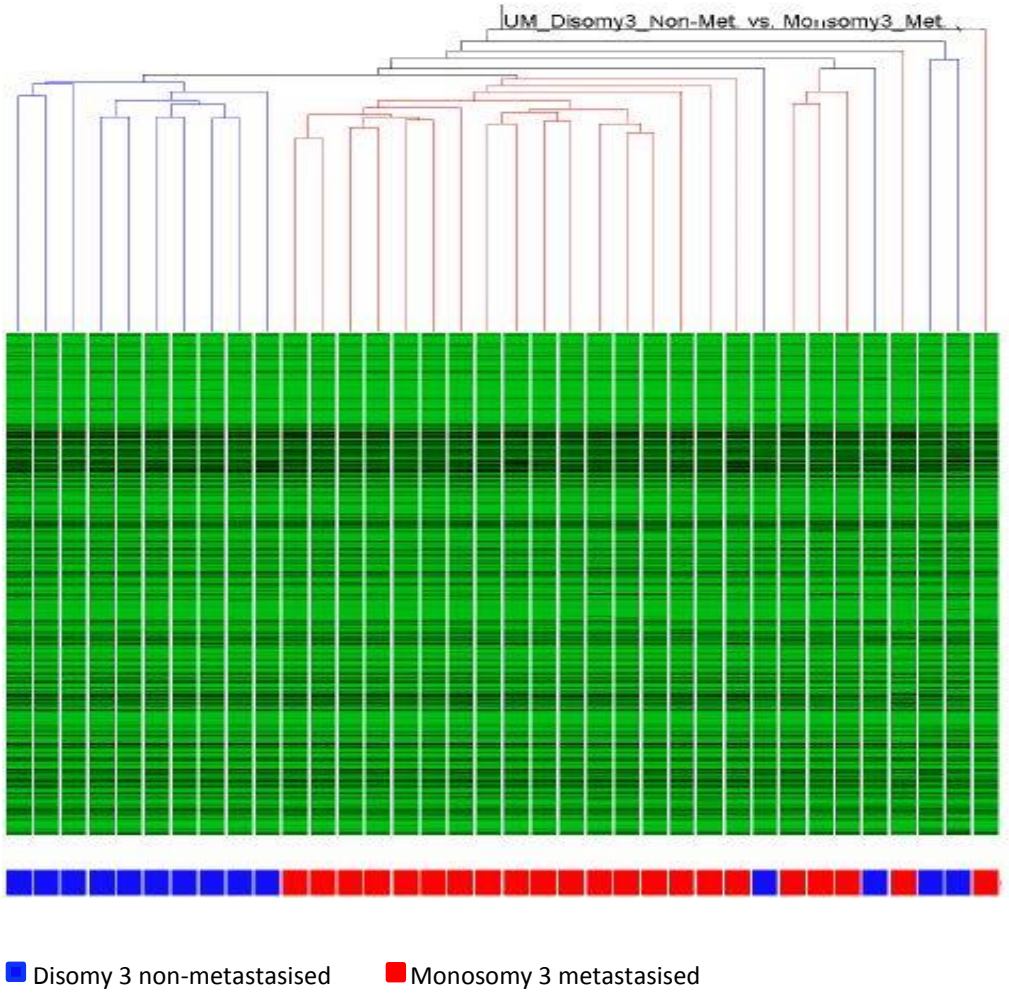


Figure 16: Hierarchical cluster analysis (Pearson correlation coefficient) of 36 samples following exclusion of monosomy 3 tumours that did not metastasise, disomy 3 tumours that metastasised and tumours with unknown or partial monosomy 3. Nine outlying samples were excluded from further analysis.

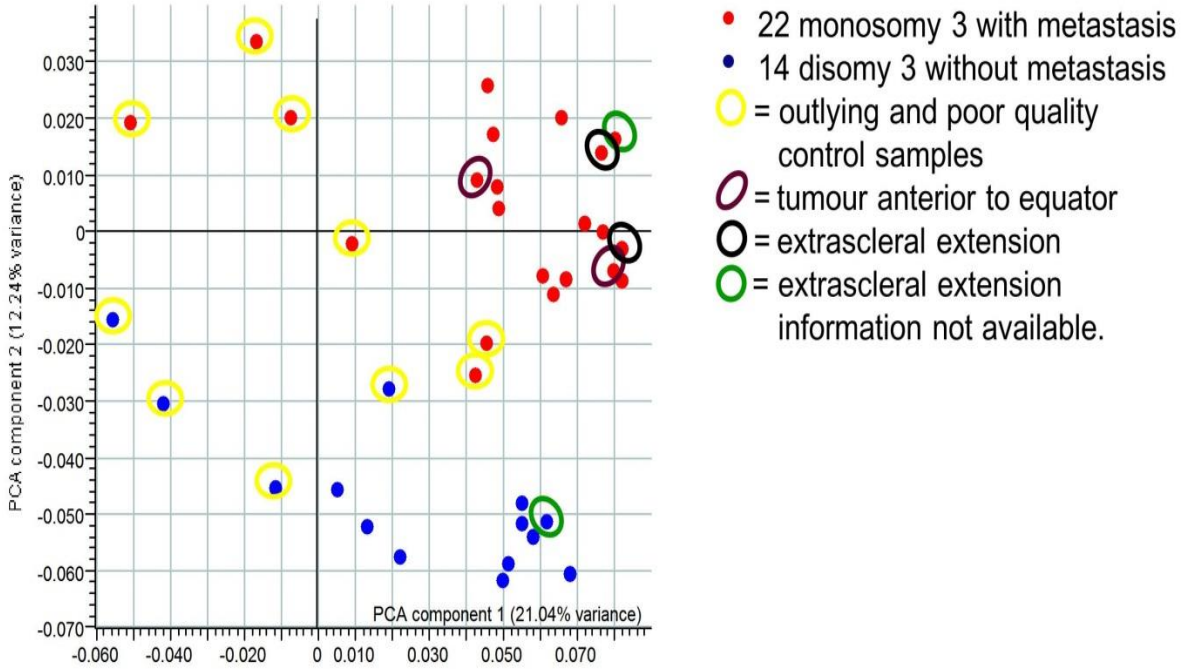


Figure 17: Principal component analysis showing distribution of 36 samples following exclusion of monosomy 3 tumours that did not metastasise, disomy 3 tumours that metastasised and tumours with unknown or partial monosomy 3. Circled samples were excluded from further analysis for reasons illustrated above.

Table 10: Samples that were excluded prior to transcriptomic analysis

| **Exclusion criteria** | **Number of samples** |
|---|---|
| Monosomy 3 non-metastasised | 10 |
| Disomy 3 metastasised | 4 |
| Partial monosomy 3 | 5 |
| Chromosome 3 status unknown | 8 |
| Extrascleral extension | 2 |
| Extrascleral extension unknown | 2 |
| Tumours anterior to equator | 2 |
| Poor quality control | 10 |
| Total number of samples excluded | 43 |

Eleven M3M and 9 D3NM samples were selected for transcriptomic analysis. Figure 18 and Figure 19 show hierarchical cluster analysis and principal component analysis of these samples, respectively.

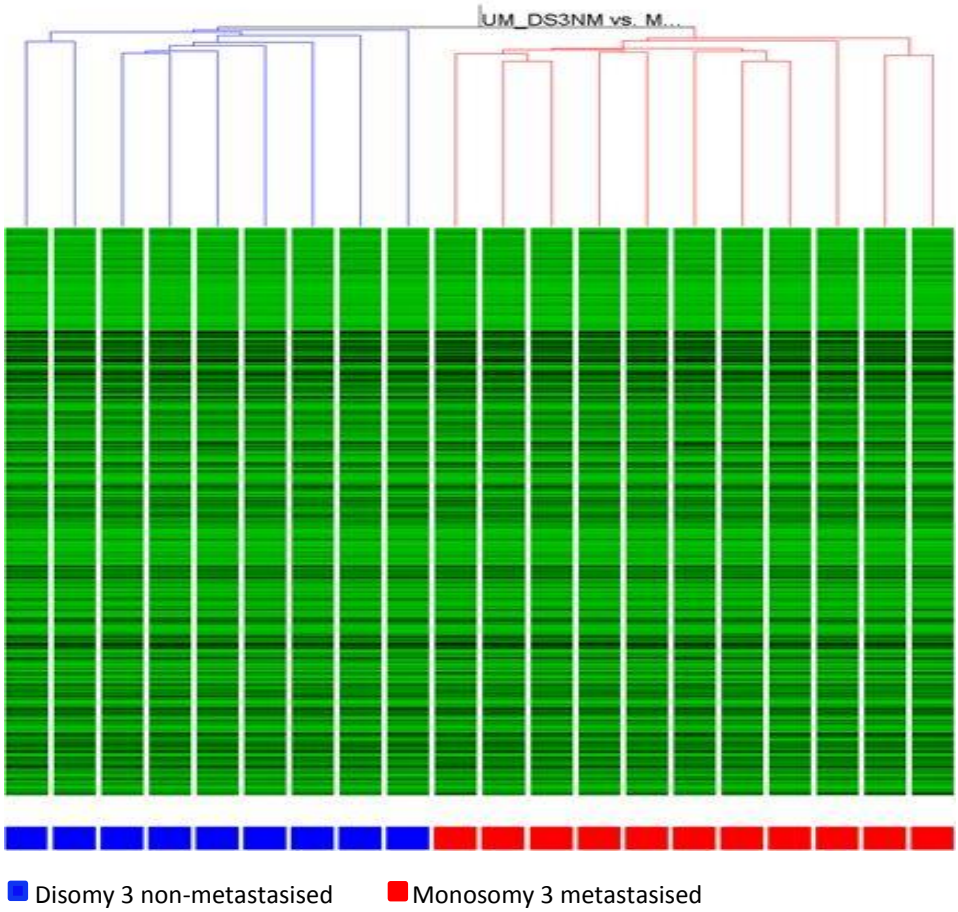


Figure 18: Hierarchical cluster analysis (Spearman correlation coefficient) of 20 samples following exclusion of monosomy 3 tumours that did not metastasise, disomy 3 tumours that metastasised, tumours with unknown chromosome 3 status or partial monosomy 3, tumours anterior to the equator of the globe and tumours with extrascleral extension or without extrascleral information.

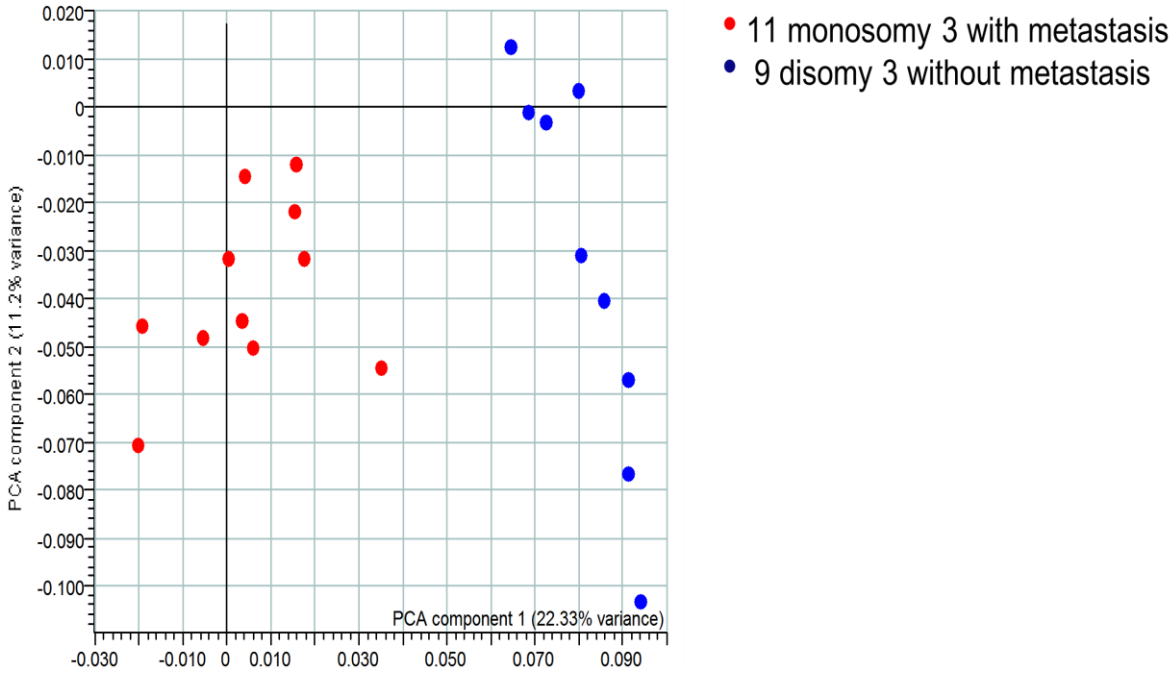


Figure 19: Principal component analysis of 20 samples following exclusion of monosomy 3 tumours that did not metastasise, disomy 3 tumours that metastasised, tumours with unknown chromosome 3 status or partial monosomy 3, tumours anterior to the equator of the globe and tumours with extrascleral extension or without extrascleral information, showing good distribution within each disease group and good separation between both disease groups.

Clinicopathologic details of samples that were analysed for differential gene expression are outlined in Table 11. In total, 449 genes were differentially expressed with a fold change ≥ 1.3 and P-value < 0.05. Of these, 246 genes were upregulated in the M3M group, while 203 were downregulated. A full list of these genes can be found in supplementary data appendix II ( and ). Six upregulated and 6 downregulated genes were considered for further follow-up based on p value, biological function and involvement in other diseases. SIPA1L2, CELF2, BCAT1, SDC2, WARS, and THBS2 are genes upregulated in M3M, while CNTN3, SORBS2, MEGF10, CHL1, DLC1, and PPP1R3C are downregulated genes that were considered (Table 12). Of these, SIPA1L2 (1.516 fold upregulated in M3M, p: 0.00107) and CNTN3 (3.068 fold downregulated in M3M, p: 0.000807) were chosen for further

validation by immunohistochemistry on FFPE UM sections. The former was selected for validation based on its novelty, as little is known about SIPA1L2, while CNTN3 was chosen primarily due to its localisation to chromosome 3, which has significant prognostic implication in UM. Other genes that have been described by in other studies have also been found, validating our results. Onken et al (319) described a 12-gene signature that accurately classifies patients to class 1 low-risk for metastasis and class 2 high-risk for metastasis. Of the 12 genes, 8 were identified in this study (HTR2B, FXR1, ID2, LMCD1, MTUS1, RAB31, ROBO1, and SATB1) with identical up/downregulation pattern. Mutations in BAP1 gene located in chromosome 3 occurs almost exclusively in metastasizing class 2 tumours (25), which was also found to be downregulated in M3M tumours in our study. Specifically, Laurent et al's principal finding of high expression of PTP4A3 in metastasising tumours was also found, ensuring internal validation of our analysis.

Table 11: Clinicopathologic details of 20 tumours that were analysed for differential gene expression. Eleven monosomy three tumours that metastasised versus 9 disomy three tumours that did not metastasise were compared. M3: monosomy 3; D3: disomy 3; NA: not available. (29)

| Sample | Ch 3 status | Meta-stasis | Age | Gender | Tumour location | Diameter (mm) | Tumour cell type | Retinal detach-ment | Extrascleral extension | Survival after diagnosis |
|---|---|---|---|---|---|---|---|---|---|---|
| GSM550663 | M3 | Y | 54.41 | F | on equator | 10 | epithelioid | Y | N | 0.13 |
| GSM550671 | M3 | Y | 56.33 | M | posterior to equator | NA | epithelioid | Y | N | 7.33 |
| GSM550638 | M3 | Y | 51.61 | F | on equator | 12 | epithelioid | N | N | 21.78 |
| GSM550668 | M3 | Y | 48.46 | M | on equator | 12 | NA | Y | N | 14.95 |
| GSM550630 | M3 | Y | 59.1 | M | on equator | 20.9 | epithelioid | Y | N | 6.14 |
| GSM550662 | M3 | Y | 62.88 | M | on equator | NA | epithelioid | N | N | 12.88 |
| GSM550673 | M3 | Y | 69.05 | M | posterior to equator | NA | epithelioid | NA | N | 8.34 |
| GSM550679 | M3 | Y | 50.17 | M | on equator | 19.6 | epithelioid | Y | N | 17.61 |
| GSM550633 | M3 | Y | 70.09 | M | on equator | 13 | mixed | Y | N | 7.92 |

| | | | | | | | | | | |
|---|---|---|---|---|---|---|---|---|---|---|
| GSM550682 | M3 | Y | 64.55 | M | on equator | 10 | mixed | Y | N | 14.85 |
| GSM550670 | M3 | Y | 62.12 | M | posterior to equator | NA | mixed | Y | N | 18.89 |
| GSM550628 | D3 | N | 50.64 | F | on equator | NA | mixed | Y | N | |
| GSM550674 | D3 | N | 50.17 | M | on equator | 10 | epithelioid | Y | N | |
| GSM550644 | D3 | N | 47.62 | F | on equator | 17 | mixed | Y | N | |
| GSM550629 | D3 | N | 38.67 | M | on equator | 11 | NA | Y | N | |
| GSM550680 | D3 | N | 66.26 | M | on equator | 15 | epithelioid | NA | N | |
| GSM550656 | D3 | N | 57.69 | M | posterior to equator | 16 | NA | Y | N | |
| GSM550675 | D3 | N | 56.25 | F | on equator | 15 | epithelioid | Y | N | |
| GSM550654 | D3 | N | 40.31 | M | on equator | 18 | NA | Y | N | |
| GSM550640 | D3 | N | 51.95 | F | on equator | 23 | mixed | N | N | |

Table 12: Statistically significant genes that were considered for validation by immunohistochemistry. Elevan monosomy 3 tumours with metastasis (M3M) and 9 disomy 3 tumours without metastasis (D3NM) were analysed for differential gene expression. A positive fold change represents upregulation while a negative fold change represents downregulation in M3M compared to D3NM. SIPA1L2 and CNTN3 were chosen for validation by immunohistochemistry.

| Gene ID | Gene name | Fold change | P value |
|---|---|---|---|
| **Genes upregulated in monosomy 3 metastasised tumours** | | | |
| CELF2 | Elav-like family member 2 | 1.987 | 0.0000188 |
| WARS | Tryptophanyl-tRNA synthetase | 1.39 | 0.0001440 |
| SDC2 | Syndecan 2 | 1.848 | 0.0003480 |
| THBS2 | Thrombospondin 2 | 2.033 | 0.0008640 |
| SIPA1L2 | Signal-induced proliferation-associated 1 like 2 | 1.516 | 0.0010700 |
| BCAT1 | Branched chain aminotransferase 1, cytosolic | 1.674 | 0.0070600 |
| **Genes downregulated in monosomy 3 metastasised tumours** | | | |
| MEGF10 | Multiple Epidermal Growth Factor 10 | -3.472 | 0.0000084 |
| DLC1 | Deleted in liver cancer 1 | -2.137 | 0.0000142 |
| CHL1 | Cell adhesion molecule with homology to L1CAM | -2.924 | 0.0000643 |
| PPP1R3C | Protein phosphatase 1, regulatory (inhibitor) subunit 3C | -1.376 | 0.0001640 |
| SORBS2 | Arg/Abl-interacting protein ArgBP2 | -2.545 | 0.0001810 |
| CNTN3 | Contactin 3 (plasmacytoma associated) | -3.067 | 0.0008070 |

### 3.2.2. Gene ontology analysis

Gene ontology (GO) enrichment analysis of 449 differentially expressed genes with $p \leq 0.05$ and fold change of $\geq 1.3$ was conducted using the DAVID interface (313,314) to determine if any biological processes were overrepresented. Of these, 246 genes were upregulated and 203 genes were downregulated in monosomy 3 tumours that developed metastatic disease (M3M) compared to disomy 3 tumours that did not develop metastasis (D3NM). Table 13 shows the enriched GO biological processes for genes with a Benjamani Hochberg adjusted p of $\leq 0.05$. A complete list of GO molecular function, GO biological process, PANTHER class and pathway can be found in supplementary data appendix II ()

Table 13: List of Gene Ontology enriched biological processes of 449 differentially expressed genes with $p \leq 0.05$ and fold change of $\geq 1.3$ between experimental groups of 11 monosomy 3 tumours that developed metastatic disease compared to 9 disomy 3 tumours that did not develop metastatic disease. Data presented in this table are those with Benjamani Hochberg adjusted $p \leq 0.05$, in ascending order.

| Biological process | Count | % of genes | p value | Benjamini Hochberg adjusted p value | Proteins |
|---|---|---|---|---|---|
| GO:0042127~regulation of cell proliferation | 42 | 9.41704 | 8.45E-06 | 0.006136 | DLC1, NBN, FGFR3, NDN, ERBB3, PPARG, PTGS1, PRRX1, BAP1, ZEB1, JAG1, CXADR, IL12RB2, WARS, AZGP1, EDNRB, ALDH1A2, CDCA7, ANG, RARB, IL13RA1, AKIRIN2, SYK, TCIRG1, PRKCA, PTPRC, ADAM10, LYN, STAT1, FOXP1, CLEC11A, KDR, CDC25B, CDKN1A, CTH, ID2, CCND2, JUN, GDF11, ADAMTS1, KLF4, NFIB |
| GO:0010033~response to organic substance | 40 | 8.96861 | 5.88E-06 | 0.006398 | ME1, ADCY1, ADCY2, DERL1, ERBB3, PPARG, PTGS1, PRKDC, C1S, TIMP3, B2M, IL12RB2, CD48, TNFRSF1A, FOS, ALDH1A2, GSTM3, PLIN2, BCHE, ANG, CASP8, FAS, DDAH2, AKIRIN2, PRKCA, ADAM10, LYN, SOCS2, PDE3A, STAT1, CDKN1A, ID2, CCND2, FYN, SQLE, JUN, RYR1, IGFBP2, TJP2, ABCC5 |

| Biological process | Count | % of genes | p value | Benjamini Hochberg adjusted p value | Proteins |
|---|---|---|---|---|---|
| GO:0006955~immune response | 39 | 8.744395 | 5.14E-06 | 0.011171 | NBN, CADM1, ENPP2, PPARG, TLR1, PRKDC, HFE, C1R, ZEB1, C1S, C1QC, B2M, RNF125, AZGP1, TNFRSF1A, TAP1, HLA-DRB4, FAS, MR1, C2, HLA-DOA, SPON2, APLN, AKIRIN2, PTPRC, LYN, C4A, PTGER4, C4B, CTSS, GEM, PRKCD, TRIM22, FOXP1, CCL18, PSMB9, HLA-F, IGSF6, CD209 |
| GO:0002252~immune effector process | 14 | 3.139013 | 3.46E-05 | 0.014992 | PTPRC, NBN, CADM1, LYN, C4A, C4B, PRKDC, C1R, C1S, C1QC, PRKCD, FOXP1, C2, FAS |
| GO:0002449~lymphocyte mediated immunity | 10 | 2.242152 | 6.35E-05 | 0.017182 | NBN, CADM1, C4A, C4B, C1R, C1S, FAS, C2, C1QC, PRKCD |
| GO:0007507~heart development | 18 | 4.035874 | 3.32E-05 | 0.01795 | DLC1, ERBB3, PDLIM3, PRKDC, CXADR, FOXP1, GJC1, ALDH1A2, CHD7, ID2, PLN, CASP8, FOXC1, ADAMTS1, RARB, BCOR, HTR2B, COL11A1 |
| GO:0019724~B cell mediated immunity | 9 | 2.017937 | 7.58E-05 | 0.018221 | NBN, C4A, C4B, C1R, C1S, FAS, C2, C1QC, PRKCD |

| Biological process | Count | % of genes | p value | Benjamini Hochberg adjusted p value | Proteins |
|---|---|---|---|---|---|
| GO:0002443~leukocyte mediated immunity | 11 | 2.466368 | 6.02E-05 | 0.018603 | NBN, CADM1, C4A, LYN, C4B, C1R, C1S, FAS, C2, C1QC, PRKCD |
| GO:0048002~antigen processing and presentation of peptide antigen | 7 | 1.569507 | 5.88E-05 | 0.021173 | CD209, HFE, MR1, HLA-DOA, TAPBPL, B2M, HLA-F |
| GO:0002250~adaptive immune response | 10 | 2.242152 | 1.35E-04 | 0.029027 | NBN, CADM1, C4A, C4B, C1R, C1S, FAS, C2, C1QC, PRKCD |
| GO:0002460~adaptive immune response based on somatic recombination of immune receptors | 10 | 2.242152 | 1.35E-04 | 0.029027 | NBN, CADM1, C4A, C4B, C1R, C1S, FAS, C2, C1QC, PRKCD |
| GO:0019882~antigen processing and presentation | 10 | 2.242152 | 2.41E-04 | 0.046663 | AZGP1, CD209, HLA-DRB4, HFE, MR1, HLA-DOA, TAPBPL, PSMB9, B2M, HLA-F |

As shown in Figure 20, enrichment analysis identified 9.42% of the differentially regulated genes to be involved in regulation of cell proliferation, while biological processes involving immune response were also significantly enriched.

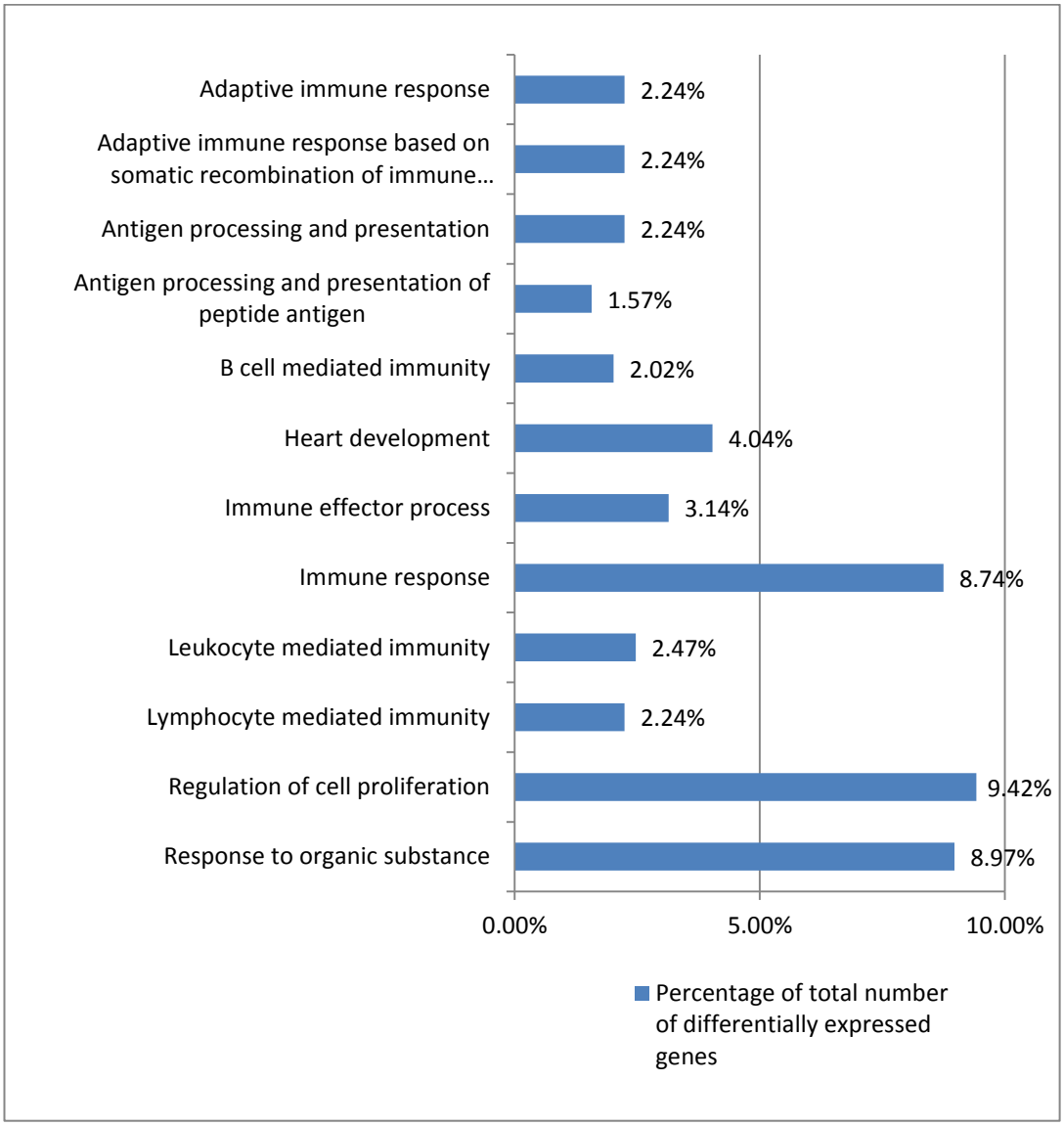


Figure 20: Graphical representation of statistically significant (Benjamani Hochberg adjusted $p \leq 0.05$) Gene Ontology enriched biological processes of 449 differentially expressed genes with $p \leq 0.05$ and fold change of $\geq 1.3$ between experimental groups of 11 monosomy 3 tumours that developed metastatic disease compared to 9 disomy 3 tumours that did not develop metastatic disease.

Differentially expressed genes in each disease group of monosomy 3 tumours that developed metastatic disease and disomy 3 tumours that did not develop metastatic disease were also analysed and compared directly using the PANTHER Database (http://www.pantherdb.org/) (315–317), for gene categorization according to biological process, molecular function, gene class and PANTHER pathway. Figure 21 shows the biological processes of genes that were upregulated in M3M and D3NM. A similar number of genes involved in apoptosis, biological regulation and cellular process and localisation were found in both groups. A higher number of genes involved in response to stimulus (15.4% vs. 9.4%) and immune system process (15.4% vs. 0%) were found in M3M compared to D3NM. Within these categories, statistically significant enrichment of processes involving complement activation (p: 0.003) and immune response (p: 0.044) were found based on the level of differential expression of genes in M3M compared to D3NM. Significant enrichment of phagocytosis was also found (p: 0.035). A lower number of genes involving metabolic process (45.4% vs. 51.3%), biological adhesion (7.9% vs. 11.1%) and developmental process (17.1% vs. 26.1%) were found M3M compared to D3NM. Within developmental process, significant enrichment of angiogenesis (p: 0.001), nervous system development (p: 0.001) and ectoderm development ( p: 0.024) were found based on the level of differential expression of these genes in D3NM compared to M3M. The difference in other categories was not significant.

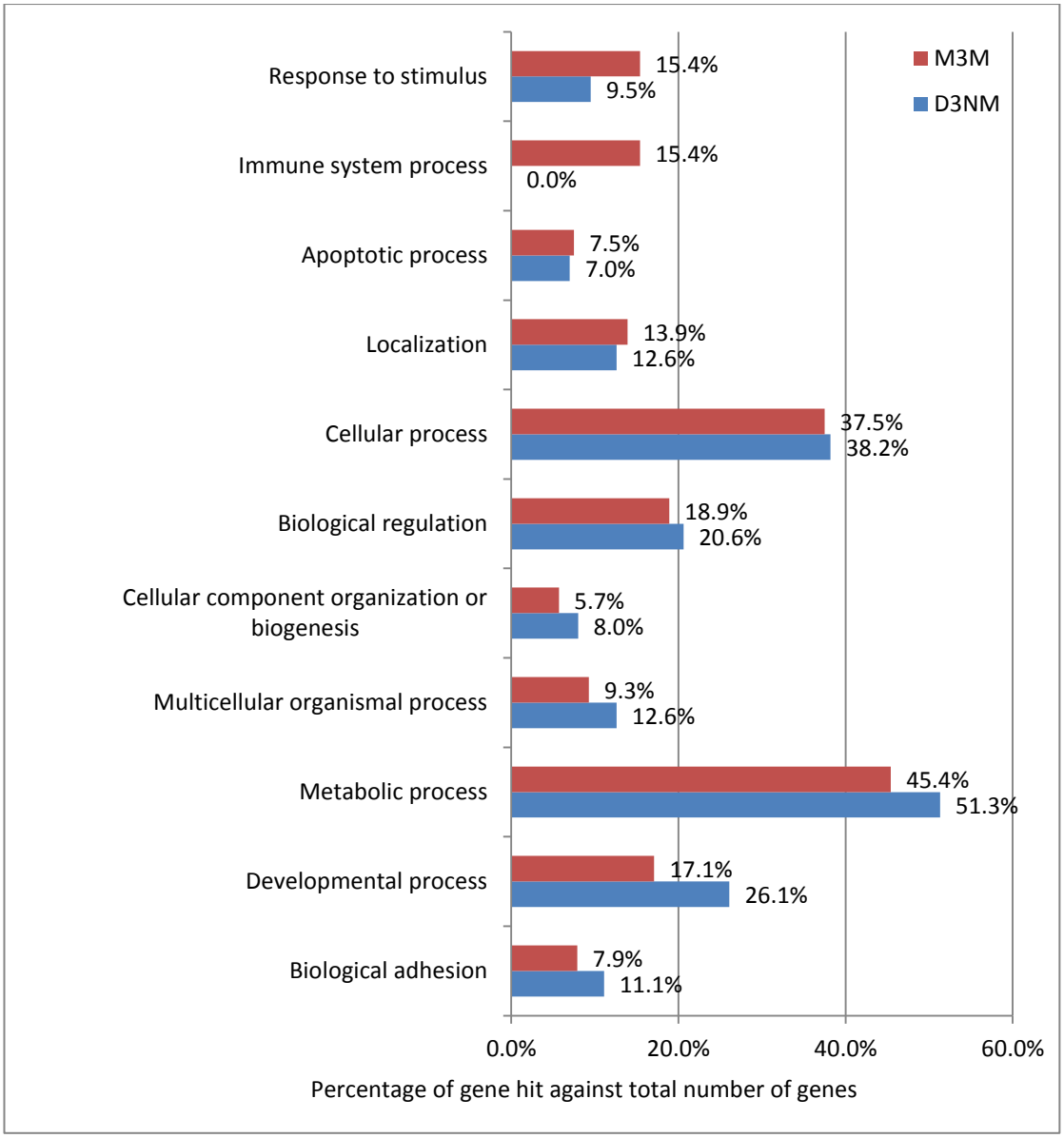


Figure 21: Graphical representation of biologic processes of genes that were upregulated in 11 monosomy 3 tumours that developed metastatic disease (M3M, 246 genes) and 9 in disomy 3 tumours that did not develop metastatic disease (D3NM, 203 genes). Based on differential gene expression level, processes involving immune system (p: 0.044) and response to stimulus (p: 0.031) were significantly enriched in M3M while developmental process (p: 0.001) was significantly enriched in D3NM.

Table 14 shows statistically significant biological process enrichment based on differential gene expression level in M3M compared to D3NM. Differential expression of genes in processes involving immune response and localisation were significantly higher in M3M while that of genes involved in angiogenesis, nervous system and ectoderm development were lower in M3M.

Table 14: Statistically significant biological process enrichment based the level of differential expression of genes in 11 monosomy 3 tumours that that developed metastasis (M3M) compared to 9 disomy 3 tumours that did not develop metastasis (D3NM). ↑ and ↓ indicate increased and decreased expression in M3M.

| **Biological Process** | **Number of genes** | **Expression in "M3M"** | **P value** |
|---|---|---|---|
| Nervous system development | 32 | ↓ | 0.001 |
| Angiogenesis | 12 | ↓ | 0.001 |
| Complement activation | 6 | ↑ | 0.003 |
| Ectoderm development | 32 | ↓ | 0.024 |
| Phagocytosis | 4 | ↑ | 0.035 |
| Immune response | 26 | ↑ | 0.044 |

Figure 22 shows the molecular function of genes that were upregulated in M3M and D3NM. Overall, a similar number of genes in each category were found. A higher number of genes with enzyme regulator (10% vs. 7.5%) and catalytic activity (34.3% vs. 31.7%) were found in M3M compared to D3NM. Lower number of genes with structural molecule (3.9% vs. 9%), receptor (10.4% vs. 12.6%) and binding activity (28.6% vs. 35.7%) were found M3M compared to D3NM. Based on the level of differential gene expression, only binding activity was significantly enriched in D3NM compared to M3M (n=3, p: 0.011). The difference in other categories was not significant.

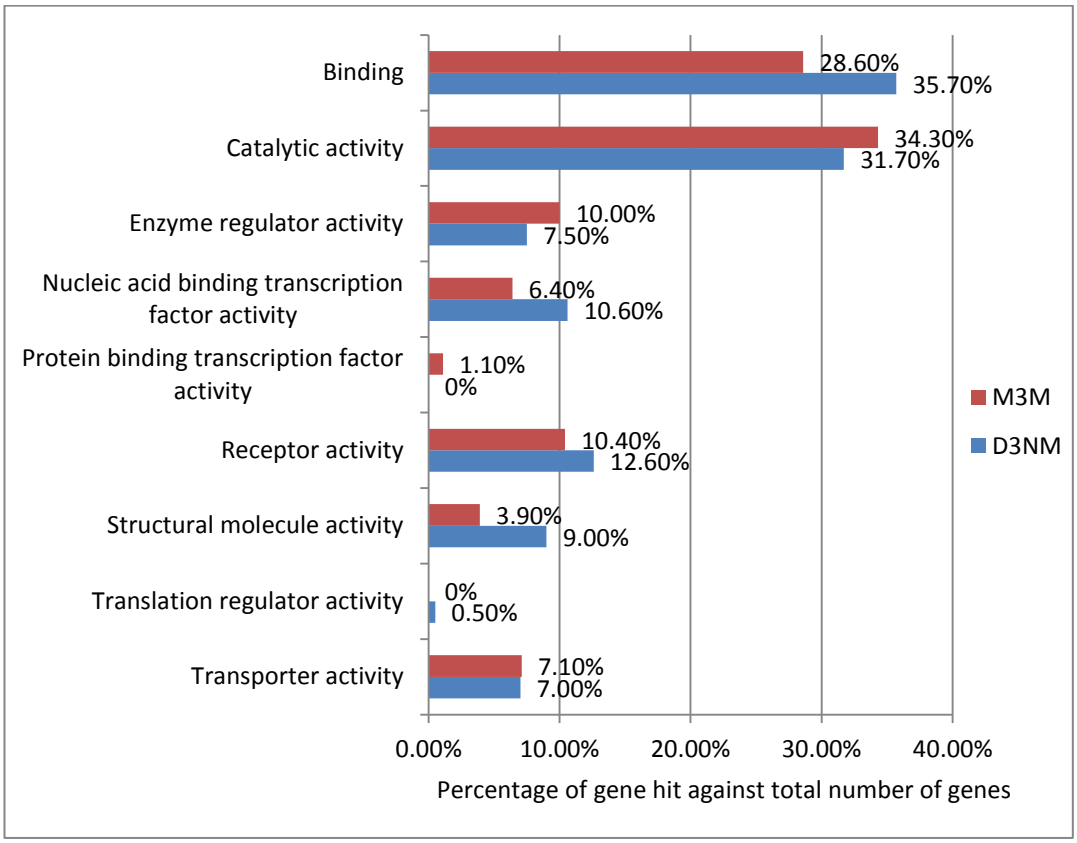


Figure 22: Graphical representation of molecular function of genes that were upregulated in 11 monosomy 3 tumours that developed metastatic disease (M3M, 246 genes) and in 9 disomy 3 tumours that did not develop metastatic disease (D3NM, 203 genes). A higher number of genes with enzyme regulator and catalytic activity were found in M3M compared to D3NM while lower number of genes with structural molecule, receptor and binding activity were found M3M compared to D3NM. Based on the level of differential gene expression, binding activity was significantly enriched in D3NM compared to M3M (p: 0.011).

Figure 23 shows genes in PANTHER pathways that were upregulated in M3M and D3NM. A similar number of genes in both disease groups were found in most pathway categories. Compared to D3NM, higher number of genes involved in apoptosis signalling (1.8% vs. 1%), p53 pathway (1.1% vs. 0%), inflammation mediated by chemokine and cytokine signalling pathway (2.1% vs. 1%), heterotrimetric G-protein (2.5% vs. 0.5%) and PDGF signalling (2.5% vs. 1.5%) pathways were found in M3M but these were not significantly enriched based on differential gene expression levels. A lower number of genes involved in Wnt signalling (1.4% vs. 2.5%) and cadherin signalling (0.4% vs. 3.5%) pathway was found in M3M compared to D3NM. Significant enrichment of the latter was found based on the level of differential gene expression (p: 0.014).

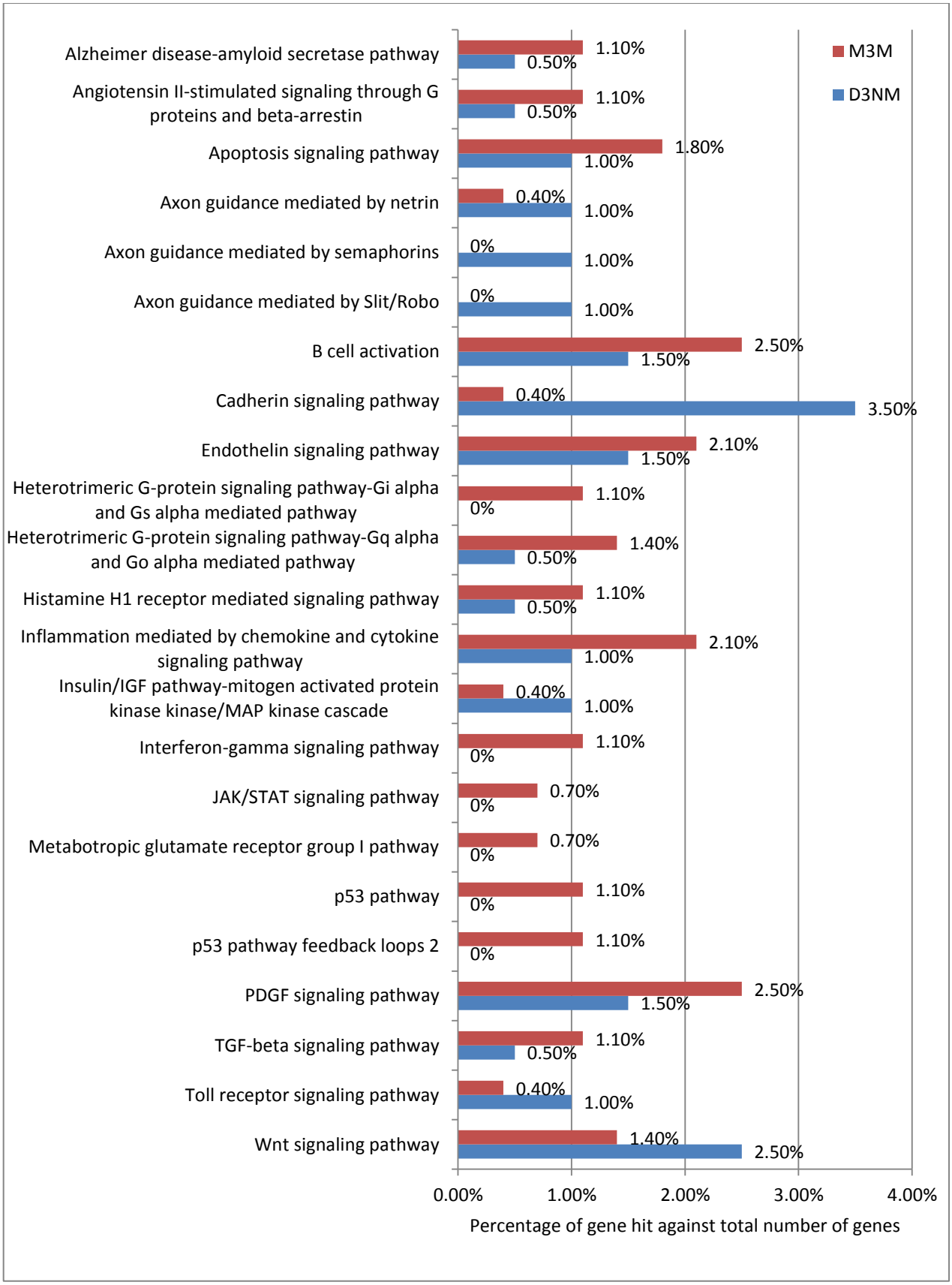
M3M
D3NM
Alzheimer disease-amyloid secretase pathway
1.10%
0.50%
Angiotensin II-stimulated signaling through G proteins and beta-arrestin
1.10%
0.50%
Apoptosis signaling pathway
1.80%
1.00%
Axon guidance mediated by netrin
0.40%
1.00%
Axon guidance mediated by semaphorins
0%
1.00%
Axon guidance mediated by Slit/Robo
0%
1.00%
B cell activation
2.50%
1.50%
Cadherin signaling pathway
0.40%
3.50%
Endothelin signaling pathway
2.10%
1.50%
Heterotrimeric G-protein signaling pathway-Gi alpha and Gs alpha mediated pathway
1.10%
0%
Heterotrimeric G-protein signaling pathway-Gq alpha and Go alpha mediated pathway
1.40%
0.50%
Histamine H1 receptor mediated signaling pathway
1.10%
0.50%
Inflammation mediated by chemokine and cytokine signaling pathway
2.10%
1.00%
Insulin/IGF pathway-mitogen activated protein kinase kinase/MAP kinase cascade
0.40%
1.00%
Interferon-gamma signaling pathway
1.10%
0%
JAK/STAT signaling pathway
0.70%
0%
Metabotropic glutamate receptor group I pathway
0.70%
0%
p53 pathway
1.10%
0%
p53 pathway feedback loops 2
1.10%
0%
PDGF signaling pathway
2.50%
1.50%
TGF-beta signaling pathway
1.10%
0.50%
Toll receptor signaling pathway
0.40%
1.00%
Wnt signaling pathway
1.40%
2.50%
0.00%
1.00%
2.00%
3.00%
4.00%
Percentage of gene hit against total number of genes

Figure 23 shown above: Graphical representation of genes in PANTHER pathways that were upregulated in 11 monosomy 3 tumours that developed metastatic disease (M3M, 246 genes) and in 9 disomy 3 tumours that did not develop metastatic disease (D3NM, 203 genes). Higher number of genes involved in apoptosis signalling, p53 pathway, inflammation mediated by chemokine and cytokine signalling pathway, heterotrimetric G-protein and PDGF signalling pathways were found in M3M, while a lower number of genes involved in Wnt signalling (1.4% vs. 2.5%) and cadherin signalling (0.4% vs. 3.5%) pathway was found in M3M compared to D3NM. Based on differential gene expression level, significant enrichment of cadherin signalling pathway was found (p: 0.014). Due the high number of pathways identified with the total number of differentially expressed genes, those with less than 0.5% difference between M3M and D3NM are not shown.

Figure 24 shows gene classes that were upregulated in M3M and D3NM. A higher number of genes associated with calcium binding proteins (3.2% vs. 2.5%), chaperones (2.5% vs. 0%), defence/immunity protein (6.8% vs. 4%), enzyme modulator (10.7% vs. 9%), ligase (3.2% vs. 2.5%), and signalling molecules (6.4% vs. 5.5%) were found in M3M. Compared to D3NM, a lower number of cell adhesion molecules (2.5% vs. 6%), cytoskeletal protein (3.2% vs. 6%), extracellular matrix protein (2.5% vs. 5%), hydrolase (10.7% vs. 12.6%), membrane traffic protein (0.7% vs. 2%), nucleic acid binding (9.3% vs. 13.1%), oxidoreductase (3.2% vs. 5%), phosphatase (2.1% vs. 4%), receptor (10.4% vs. 12.6%), structural protein (0% vs. 2%), transcription factor (6.8% vs. 11.1%), and transfer/carrier protein (3.2% vs. 4.5%) were found in M3M. A similar number of genes in classes such as cell junction protein, isomerase, kinase, lyase, protease, surfactant, transferase, transmembrane receptor regulatory/adaptor protein and transporter proteins were found in both M3M and D3NM.

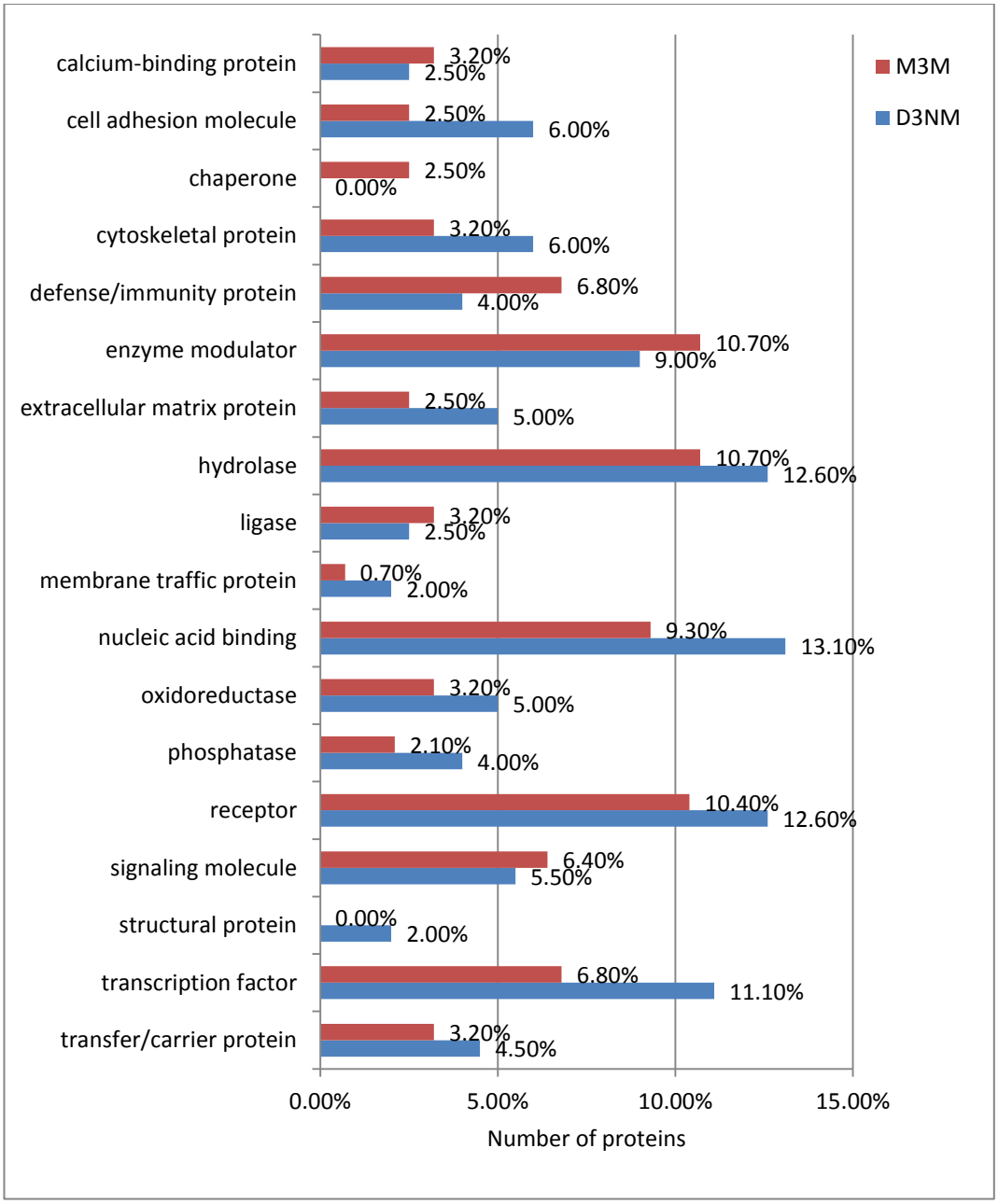


Figure 24: Graphical representation showing gene class that were upregulated in 11 monosomy 3 tumours that developed metastatic disease (M3M, 246 genes) and in 9 disomy 3 tumours that did not develop metastatic disease (D3NM, 203 genes). Based on differential gene expression level, significant enrichment of gene classes associated with cell adhesion molecule (p: 0.041), defence/immunity protein (p: 0.003), cytoskeletal protein (p: 0.03) and transcription factor (p: 0.01) were found. Due the high number of gene classes present within the total number of differentially expressed genes, those with less than 0.5% difference between M3M and D3NM are not shown.

Based on differential gene expression levels, significant enrichment in several gene classes were found. Compared to M3M, significant enrichment of cell adhesion molecule, cytoskeletal protein, membrane traffic protein, structural protein and transcription factor were found in D3NM. These are outlined in Table 15.

Table 15: Statistically significant gene class enrichment based the level of differential expression of genes in 11 monosomy 3 tumours that developed metastasis (M3M, 246 genes) compared to 9 disomy 3 tumours that did not develop metastasis (D3NM, 203 genes). ↑ and ↓ indicate increased and decreased expression in M3M.

| **Gene class** | **Number of genes** | **Expression in "M3M"** | **P value** |
|---|---|---|---|
| Cell adhesion molecule | 19 | ↓ | 0.041 |
| Cytoskeletal protein | 12 | ↓ | 0.029 |
| Defence/immunity protein | 6 | ↑ | 0.029 |
| Membrane traffic protein | 6 | ↓ | 0.023 |
| Structural protein | 4 | ↓ | 0.037 |
| Transcription factor | 11 | ↓ | 0.015 |

## 3.3. Validation of selected targets by immunohistochemistry

In label-free LC-MS proteomic analysis of 8 primary UM tissue from patients who developed metastatic disease versus 8 from patients who did not develop metastatic disease, thioredoxin-dependant peroxidase reductase (PRDX3) was upregulated by 1.58 fold (p: 0.002) and cytosolic non-specific dipeptidase (CNDP2) was downregulated by 1.75 fold (p: 0.001) in primary UM tissues from patients that developed metastasis compared to those that did not. These targets demonstrated the most distinguishable difference of protein abundance in individual samples between the two disease groups (Figure 10).

In the bioinformatic reanalysis of gene expression microarray data of monosomy 3 tumours with metastasis versus disomy 3 tumours that did not develop metastatic disease, signal-induced proliferation-associated 1-like protein 2 (SIPA1L2) was upregulated by 1.516 fold (p: 0.00107) and contactin 3 (CNTN3) was downregulated by 3.068 fold (p: 0.000807) in monosomy 3 tumours that developed metastasis compared to disomy 3 tumours that did not metastasise. These targets were selected based on high statistical significance of differential expression, fold change and biological function.

To determine the expression of these proteins in UM tissues, a total of 26 full face UM tumour sections of 13 patients that developed metastasis (mUM) versus 13 that did not develop metastasis (nmUM) were used for immunohistochemistry for PRDX3, CNDP2, SIPA1L2 and CNTN3. Based on this pilot study, PRDX3 was selected for immunohistochemical validation in a larger cohort of 92 primary UM tissue microarray samples of 55 tumours that developed metastasis and 37 that did not develop metastasis. The immunohistochemical staining for the selected proteins were assessed by two observers who were blinded to all clinicopathologic and cytogenetic details including metastatic/non-metastatic information (Pathma Ramasamy, Anne-

Marie Larkin). A scoring system similar to the one first described by Remmele and Stegner (318), and adapted by Coupland et al (243) was used. The full face UM section slides were scored based on intensity of staining (A) and percentage of tumour cells that stained (B). Intensity was graded as 0 for no staining, 1+ for weak, 2+ for moderate and 3+ for strong staining. A percentage score was assigned as follows: 1 (0-49%), 2 (50-74%), 3 (75-89%) and 4 (90-100%). A total score was obtained by multiplying (A) and (B). Thus, a minimum score of 0 and a maximum score of 12 was obtained.

### 3.3.1. Demographics and clinicopathologic details of primary uveal melanoma tissues

The demographics, clinicopathologic and cytogenetic details of 26 full face tumour sections of 13 patients that developed metastasis (mUM) versus 13 that did not develop metastasis (nmUM) are outlined in Table 17. Patients who metastasised were diagnosed with UM between 1994-2010. Patients without metastasis were diagnosed with UM between 1994-2006 and were metastasis-free for a period of 7-19 years (up to 2013). There were 11 males and 15 females. The mean age of diagnosis is 59.04 years (range: 35-88, SD: 13.75). Nine patients (69.2%) developed metastases to the liver, 2 to the lung, 1 to the kidney and 1 to both liver and skin. The mean survival for patients who developed metastases is 41 months (range: 4-142, SD: 41.35). In total, 6 (23.1%) patients also had ciliary body involvement. Of those, 5 patients developed metastatic disease (4 developed liver metastasis and 1 developed lung metastasis). In total, 10 patients (38.5%) had epithelioid cell type; 7 of those (70%) had metastatic disease. There were ten patients (38.5%) with mixed (spindle and epithelioid cell types) cell type; 4 developed metastasis and 6 did not. Six patients (23%) had spindle cell type tumours; 2 developed metastasis and 4 did not. The majority of tumours (16 patients, 61.5%) did not exhibit extrascleral extension, one tumour that developed metastasis demonstrated extrascleral extension while this

information was unavailable for 9 tumours. Twenty tumours had largest tumour dimension (LTD) information available. The mean LTD was 13.5 mm (range: 8-20, SD: 4.55). There was no tumour size information available for 6 tumours. Five tumours (25%) were classified as small (<10mm), 9 (45%) were medium (10-15mm), and 6 (30%) were large (>15mm). One out of 5 small tumours, 5 out of 9 medium tumours and 4 out of 6 large tumours developed metastasis. All 13 UM tumours of patients that developed metastasis demonstrated chromosome 3 monosomy. There were no monosomy 3 tumours in the non-metastasised group. Of the 13 UM tumours of patients that did not develop metastasis, 7 (53.8%) were disomy 3 tumours, 2 (15.4%) were trisomy 3 while chromosome 3 information was not available for 4 (30.8%) tumours. A summary of demographics, clinical, histopathologic and cytogenetic details of 26 patient tumours analysed are outlined in table 16.

Table 16: Demographics, clinical, histopathologic and cytogenetic details of 26 uveal melanoma patient tumours analysed for immunohistochemical expression of thioredoxin-dependant peroxidase reductase 3 (PRDX3), cytosolic non-specific dipeptidase (CNDP2), contactin 3 (CNTN3) and signal-induced proliferation-associated 1-like protein 2 (SIPA1L2). NA: not available

| | **Metastasis (mUM)** | **No metastasis (nmUM)** | **Total** |
|---|---|---|---|
| **Mean age of diagnosis (years)** | 60.46 (SD: 15.04)<br>Range: 36 - 88 | 57.62 (SD: 12.78)<br>Range: 35 - 77 | 59.04 (SD 13.75)<br>Range 35 - 88 |
| **Dead** | 13 (100%) | 0 | 13/26 (50%) |
| **Mean survival (months)** | 41.0 (SD: 41.35)<br>Range: 4 - 142 | | |
| **Male** | 3 (23.1%) | 8 (61.5%) | 11 (42%) |
| **Female** | 10 (76.9%) | 5 (38.5%) | 15 (57.7%) |
| **Metastasis/No metastasis** | 13 (50%) | 13 (50%) | 26 (100%) |

| | Metastasis (mUM) | No metastasis (nmUM) | Total |
|---|---|---|---|
| **Liver** | 9 (69.2%) | - | - |
| **Lung** | 2 (15.4%) | - | - |
| **Kidney** | 1 (7.7%) | - | - |
| **Kidney and skin** | 1 (7.7%) | - | - |
| **Ciliary body involvement** | 5 (38.4%) | 1 (7.7%) | 6/26 (23.1%) |
| **Extrascleral extension** | | | 26 |
| **No** | 9 (69.2%) | 7 (53.9%) | 16 (61.5%) |
| **Yes** | 1 (7.7%) | 0 | 1 (3.8%) |
| **NA** | 3 (23.1%) | 6 (46.1%) | 9 (34.6%) |
| **Cell types** | | | 26 |
| **Spindle** | 2 (15.3%) | 4 (30.8%) | 6 (23.1%) |
| **Epithelioid** | 7 (53.9%) | 3 (23.1%) | 10 (38.5%) |
| **Mixed** | 4 (30.8%) | 6 (46.1%) | 10 (38.5%) |
| **Tumour size** | | | 26 |
| **Small (< 10mm)** | 1 (7.7%) | 4 (30.8%) | 5 (19.2%) |
| **Medium (10-15mm)** | 5 (38.4%) | 4 (30.8%) | 9 (34.6%) |
| **Large (> 15mm)** | 4 (30.8%) | 2 (15.3%) | 6 (23.1%) |
| **NA** | 3 (23.1%) | 3 (23.1%) | 6 (23.1%) |
| **Chromosome 3 status** | | | 17/92 (18.5%) |
| **Monosomy 3** | 13 (100%) | 0 | 13 (50%) |
| **Disomy 3** | 0 | 7 (53.8%) | 7 (26.9%) |
| **Trisomy** | 0 | 2 (15.4%) | 2 (7.7%) |
| **NA** | 0 | 4 (30.8%) | 4 (15.4%) |

Table 17: Clinical, histopathologic and cytogenetic details of full uveal melanoma sections used for immunohistochemistry

| Sample | Sex | Age at diagnosis (years) | Metastatic sites | Survival after diagnosis (months) | Ciliary body involvement | Extrascleral extension | Cell type | LTD | Chr. 3 |
|---|---|---|---|---|---|---|---|---|---|
| 1 | F | 58 | Liver | 62 | Y | NA | M | NA | Monosomy |
| 2 | F | 39 | Kidney | 142 | N | N | S | Medium | Monosomy |
| 3 | F | 88 | Liver | 5 | N | N | M | NA | Monosomy |
| 4 | M | 71 | Lung | 26 | N | N | M | Medium | Monosomy |
| 5 | F | 50 | Liver, skin | 64 | N | NA | S | Small | Monosomy |
| 6 | M | 54 | Liver | 18 | Y | N | M | Large | Monosomy |
| 7 | F | 58 | Liver | 52 | N | N | E | Large | Monosomy |
| 8 | F | 51 | Liver | 8 | N | N | E | Medium | Monosomy |
| 9 | F | 73 | Liver | 4 | Y | N | E | Medium | Monosomy |
| 10 | M | 72 | Liver | 92 | N | Y | E | Large | Monosomy |
| 11 | F | 76 | Liver | 10 | Y | NA | E | NA | Monosomy |

| Sample | Sex | Age at diagnosis (years) | Metastatic sites | Survival after diagnosis (months) | Ciliary body involvement | Extrascleral extension | Cell type | LTD | Chr. 3 |
|---|---|---|---|---|---|---|---|---|---|
| 12 | F | 36 | Lung | 7 | Y | N | E | Large | Monosomy |
| 13 | F | 60 | Liver | 43 | N | N | E | Medium | Monosomy |
| 14 | M | 51 | None | NA | N | N | S | Small | NA |
| 15 | F | 43 | None | NA | N | N | S | Small | Normal |
| 16 | M | 68 | None | NA | N | N | E | Medium | Trisomy |
| 17 | F | 64 | None | NA | N | N | E | Medium | Normal |
| 18 | M | 69 | None | NA | Y | N | S | Large | Normal |
| 19 | F | 77 | None | NA | N | NA | M | NA | Normal |
| 20 | F | 53 | None | NA | N | NA | M | NA | Normal |
| 21 | F | 56 | None | NA | N | N | E | Large | Normal |
| 22 | M | 74 | None | NA | N | NA | M | Small | NA |

| Sample | Sex | Age at diagnosis (years) | Metastatic sites | Survival after diagnosis (months) | Ciliary body involvement | Extrascleral extension | Cell type | LTD | Chr. 3 |
|---|---|---|---|---|---|---|---|---|---|
| 23 | M | 54 | None | NA | N | NA | M | Medium | Trisomy |
| 24 | M | 43 | None | NA | N | NA | M | NA | NA |
| 25 | M | 35 | None | NA | N | N | M | Medium | Normal |
| 26 | M | 62 | None | NA | N | NA | S | Small | NA |

N, no; Y, yes; S, spindle cells; E, epithelioid cells; M, mixed cells; LTD, largest tumour diameter; NA, not available.

For the larger tissue microarray study, 92 tumour samples were used for PRDX3 immunohistochemistry. Each UM tumour sample was represented by 4 tissue cores in the TMA slides. The full demographics, clinicopathologic and cytogenetic details of these patients are outlined in supplementary data appendix III (). There were 55 tumours (59.8%) from patients that developed metastatic disease, while 37 (40.2%) were from patients that did not develop metastasis. Patients who metastasised were diagnosed with UM between 1994-2010. The majority of patients without metastasis (31/37, 83.8%) were diagnosed with UM between 1994-2006 and were metastasis-free for a period of 7-19 years (up to 2013). There were 2 patients diagnosed in 2007 with monosomy 3 tumours that are metastasis-free for at least 6 years, and one patient diagnosed in 2009 with monosomy 3 tumour is metastasis-free for at least 4 years. A further 3 patients with disomy 3 tumours that are metastasis-free for at least 4 years were also included. Forty-nine (53.3%) were males and 43 (46.7%) were females. The mean age of diagnosis is 59.77 years (SD 14.82, range 24.75-93.75). Twenty-nine patients developed metastasis to the liver (52.7%), 3 to the lung (5.5%), 2 to the brain (3.6%), 2 to the spine (3.6%) while 6 patients developed multiple metastases including the liver (10.9%). Metastatic site information was not available for 13 patients (23.6%). Fifty-four patients have died from metastasis (1 patient still alive with liver metastasis diagnosed in 2013). Twenty three (62.2%) patients without metastasis are still alive while 14 (37.8%) have died of causes unrelated to UM. Fourteen tumours (15.2%) also involved the ciliary body and 11 (78.7%) of these developed metastasis. Forty-seven tumours were of mixed cell type (51.1%), 31 were spindle (33.8%) and 13 (14.1%) were epithelioid. The majority of tumours (n=78, 84.8%) did not exhibit extrascleral extension, 7 tumours (7.6%) had extrascleral extension and this information was not available for 7 cases. Twelve tumours (13%) were classified as small (<10mm), 23 (25%) were medium (10-15mm), 46 (50%) were large (>15mm) while this information was unavailable for 11 cases (12%). Chromosome 3 information was available for 17 tumours; 10 were monosomy 3 and 7 were disomy 3 (58.8% and 41.2% respectively). In patients with monosomy 3 tumours, 6 (60%) developed metastasis. The remaining 4 patients with monosomy 3 tumours, diagnosed

between 2005 and 2009, are metastasis-free while all 7 patients with disomy 3 tumours did not develop metastasis. The demographics, clinical, histopathologic and cytogenetic details of 92 patient tumours analysed are outlined in Table 18.

Table 18: Demographics, clinical, histopathologic and cytogenetic details of 92 uveal melanoma patient tumours analysed for immunohistochemical expression of thioredoxin-dependant peroxidase reductase 3 (PRDX3) using tissue microarray. NA: not available

| | **Metastasis** | **No metastasis** | **Total** |
|---|---|---|---|
| **Mean age of diagnosis (years)** | 61.81 (SD: 14.6)<br>Range: 31.25 - 93.75 | 56.76 (SD: 14.84)<br>Range: 24.75 - 85.0 | 59.77 (SD 14.82)<br>Range: 24.75-93.75 |
| **Dead** | 54/55 (98.2%) | 14/37 (37.8%)* | 68/92 (73.9%) |
| **Mean survival (months)** | 64.04 (SD: 77.84)<br>Range: 3 - 427 | 189.07 (SD: 53.73)<br>Range: 96 - 328 | 89.78 (SD: 89.15)<br>Range: 3 - 427 |
| **Male** | 30 (61.2%) | 19 (38.8) | 49 (53.3%) |
| **Female** | 25 (58.1%) | 18 (41.9%) | 43 (46.7%) |
| **Metastasis/No metastasis** | 55 (59.8%) | 37 (40.2%) | 92 (100%) |
| **Liver** | 29 (52.7%) | - | - |
| **Lung** | 3 (5.5%) | - | - |
| **Brain** | 2 (3.6%) | - | - |
| **Spine** | 2 (3.6%) | - | - |
| **Multiple** | 6 (10.9%) | - | - |
| **Site NA** | 13 (23.6%) | - | - |
| **Ciliary body involvement** | 11 (78.7%) | 3 (21.3%) | 14 (15.2%) |
| **Extrascleral extension** | | | 92 |
| **No** | 45 (57.7%) | 33 (42.3%) | 78 (84.8%) |
| **Yes** | 6 (85.7%) | 1 (14.3%) | 7 (7.6%) |
| **NA** | 4 (57.1%) | 3 (42.9%) | 7 (7.6%) |
| **Cell types** | | | 92 |
| **Spindle** | 16 (51.6%) | 15 (48.4%) | 31 (33.7%) |
| **Epithelioid** | 10 (76.9%) | 3 (23.1%) | 13 (14.1%) |
| **Mixed** | 28 (59.6%) | 19 (40.4%) | 47 (51.1%) |
| **NA** | 1 (100%) | 0 | 1 (0.1%) |

| | Metastasis | No metastasis | Total |
|---|---|---|---|
| **Tumour size** | | | 92 |
| **Small (< 10mm)** | 3 (33.3%) | 9 (66.7%) | 12 (13%) |
| **Medium (10-15mm)** | 13 (56.5%) | 10 (43.5%) | 23 (25%) |
| **Large (> 15mm)** | 32 (69.6%) | 14 (30.4%) | 46 (50%) |
| **NA** | 7 (63.6%) | 4 (36.4%) | 11 (12%) |
| **Chromosome 3 status** | | | 17/92 (18.5%) |
| **Monosomy 3** | 6 (60%) | 4 (40%) | 10 (58.8%) |
| **Disomy 3** | 0 | 7 (100%) | 7 (41.2%) |
| **NA** | 49 (65.3%) | 26 (34.7%) | 75 (81.5%) |

*Cause of death unrelated to uveal melanoma

### 3.3.2. Pilot immunohistochemistry study in full face uveal melanoma tissue sections

To determine the expression of selected target proteins in UM tissues, a total of 26 full face UM tumour sections of 13 patients that developed metastasis (mUM) versus 13 that did not develop metastasis (nmUM) were used for immunohistochemistry for PRDX3, CNDP2, SIPA1L2 and CNTN3. Based on this, further validation of the most promising target was carried out in a larger cohort of 147 UM tissue microarray samples.

#### 3.3.2.1. Thioredoxin-dependent peroxidase reductase (PRDX3)

In LC-MS/MS label-free analysis, PRDX3 was upregulated by 1.58 fold (p: 0.002) in primary UM tissues from patients that developed metastasis compared to those that did not. To determine the expression of PRDX3 in primary UM tissues, immunohistochemical staining of PRDX3 was performed on 13 primary UM tumours of patients that developed metastatic disease (mUM) and 13 primary UM tumours of patients that did not develop metastasis (nmUM). The demographics and clinicopathologic details of these samples are outlined in Table 17. Staining of PRDX3 in UM tissues was cytoplasmic with no nuclear staining.

In mUM, the mean score was 8.3 (median: 8, range: 4-12, SD: 2.43). There were no tumours that showed negative (0) or weak staining (1+). Ten (76.9%) tumours showed moderate (2+) staining that ranged from 50-100% and 3 tumours (23.1%) showed strong staining (3+) throughout the tumour. Tumours that showed strong staining in mUM were from patients that developed metastasis and died within 10 months of diagnosis.

In nmUM, the mean score was 5.85 (median: 4, range: 2-12, SD 3.6). There were no tumours that showed negative staining. Four (30.8%) tumours showed weak staining ranging between 40-80%, 5 (38.4%) showed moderate staining ranging between 40-100% and 4 showed strong staining ranging between 50-100% staining of tissues. Representative immunohistochemical expression of PRDX3 in UM tissues are shown in Figure 25.

A trend towards higher expression score in mUM compared to nmUM was observed, but it was not statistically significant (Mann-Whitney U test, p: 0.061). No significant difference was seen when comparing the intensity of staining between mUM and nmUM (p: 0.435, Mann-Whitney U test). However, a significant difference between percentage of tumour cells staining was seen (p: 0.011, Mann-Whitney U test). A summary of the expression of PRDX3 in all 26 UM tissues are shown in Table 19.

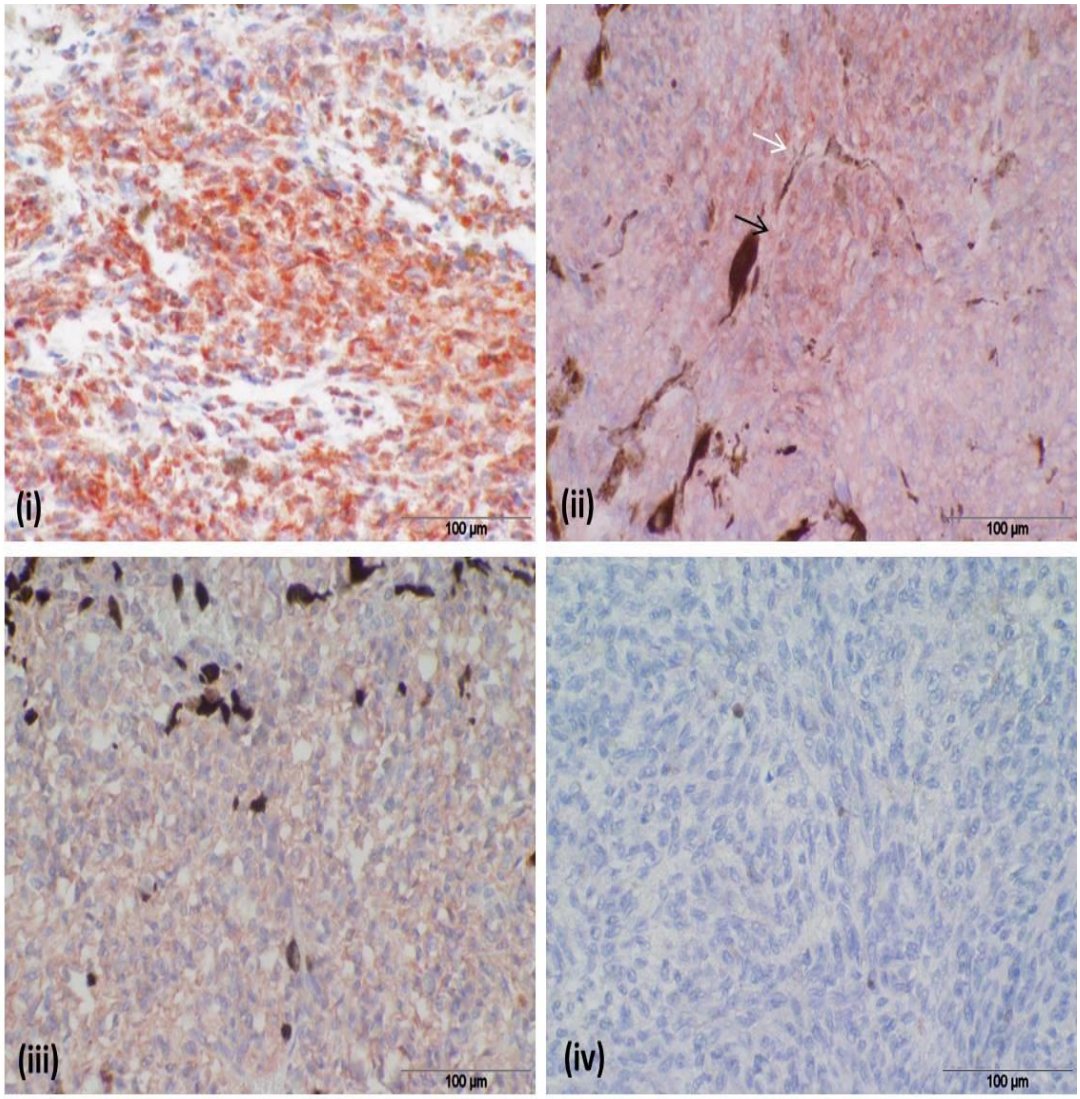


Figure 25: Representative immunohistochemical slides of thioredoxin-dependant peroxidase reductase 3 (PRDX3) expression in uveal melanoma tissues, showing different intensities of cytoplasmic staining. (i) Strong staining in sample 9 mUM; (ii) Moderate staining in areas (white arrow) and scattered areas of melanin (black arrow) in sample 18 nmUM; (iii) Weak staining and scattered areas of dense melanin in sample 15 nmUM; (iv) Negative control showing no staining. LC-MS proteomic profiling of primary UM tissues identified upregulation of PRDX3 in tissues of patients who developed metastasis compared to those who did not develop metastasis. Immunohistochemical expression in 13 primary UM tissues of patients who developed metastasis (mUM) and 13 patients who did not develop metastasis (nmUM) showed a trend toward higher expression score in mUM (p: 0.061, Mann-Whitney U test). Magnification X 400, scale bar=100µm

Table 19: Summary of results of thioredoxin-dependant peroxidase reductase 3 (PRDX3) immunohistochemistry in 13 primary UM tissues of patients who developed metastasis (mUM) and 13 patients who did not develop metastasis (nmUM). LC-MS proteomic profiling of 16 primary UM tissues identified upregulation of PRDX3 (1.58 fold, p: 0.002) in tissues of patients who developed metastasis (n=8) compared to those who did not develop metastasis (n=8). *Significant difference in percentage of tumour cells staining

| | | **Metastasis (n=13)** | **No metastasis (n=13)** |
|---|---|---|---|
| **Overall staining score (0-12)** | | Mean: 8.3, SD: 2.43<br>Median: 8, Range: 4-12 | Mean: 5.85, SD: 3.6<br>Median: 4, Range: 2-12 |
| **Difference in scores, p** | | 0.061† | |
| **Staining** | **Weak intensity** | 0 | 4 |
| | **Percentage staining range** | - | 60-80% |
| | **Moderate intensity** | 10 | 5 |
| | **Percentage staining range** | 50-100% | 40-100% |
| | **Strong intensity** | 3 | 4 |
| | **Percentage staining range** | 100% | 50-100% |
| **Difference in staining intensity, p** | | 0.435† | |
| **Difference in staining percentage, p** | | 0.011†* | |

†Mann Whitney U

No significant correlation between PRDX3 score and survival in patients with metastatic disease was found (p: 0.502, Spearman correlation). Higher expression of PRDX3 significantly correlated with monosomy 3 tumours compared to disomy/trisomy 3 (p: 0.014, Spearman correlation). No significant correlation between PRDX3 score and cell type was found (p: 0.693, Spearman correlation). Furthermore, no significant correlation between PRDX3 score and tumour size was identified (p: 0.462, Spearman Correlation). Higher PRDX3 score was seen in tumours with ciliary body involvement, but this was not statistically significant (p: 0.059, Spearman correlation). No significance between PRDX3 score and extrascleral extension was found (p: 0.684, Spearman correlation). These results are summarised in table 20.

Table 20: Correlation between thioredoxin-dependant peroxidase reductase 3 (PRDX3) immunohistochemistry score in 13 primary UM tissues of patients who developed metastasis (mUM) and 13 patients who did not develop metastasis (nmUM), and clinicopathological parameters. All p values were derived from Spearman correlation. *Statistically significant correlation between higher PRDX3 score and aggressive monosomy 3 tumours was found.

| | **PRDX3 expression score (p value)** |
|---|---|
| **Survival** | 0.502 |
| **Chromosome 3 status** | 0.014* |
| **Cell type** | 0.693 |
| **Tumour size** | 0.462 |
| **Ciliary body involvement** | 0.059 |
| **Extrascleral extension** | 0.684 |

#### 3.3.2.2. Cytosolic non-specific dipeptidase 2 (CNDP2)

In LC-MS/MS label-free analysis, CNDP2 was downregulated by 1.75 fold (p: 0.001) in primary UM tissues from patients that developed metastasis compared to those that did not. Immunohistochemical staining of CNDP2 was performed on 13 primary UM tumours of patients that developed metastatic disease (mUM) and 13 primary UM tumours of patients that did not develop metastasis (nmUM). The demographics and clinicopathologic details of these samples are outlined in Table 17. Despite using a higher concentration of CNDP2 antibody, the overall staining intensity in UM tissues was less than that of PRDX3, and was cytoplasmic with no nuclear staining.

In mUM, the mean score was 5.31 (median: 4, range: 0-12, SD: 3.04). One tumour showed negative staining while 4 tumours (30.8%) showed weak (1+) staining that ranged between 90-100% of the tumours. Six tumours (46.2%) showed moderate (2+) staining that ranged from 50-100% while 2 tumours (15.4%) showed strong staining (3+) between 40-100% of tumour tissue.

In nmUM, the mean score was 6.08 (median: 4, range: 2-12, SD 3.73). There were no tumours that showed negative staining. Five tumours (38.5%) showed weak staining ranging between 50-90%, 2 (15.4%) showed moderate staining ranging between 60-90% and 6 showed strong staining ranging between 30-90% staining of tumour tissues. Representative immunohistochemical expression of CNDP2 in UM tissues are shown in Figure 26.

No clear trend towards lower expression score in mUM compared to nmUM was observed (p: 0.752, Mann-Whitney U test). No significant difference was seen when comparing the intensity or percentage of staining between mUM and nmUM (p: 0.318 and p: 0.113 respectively, Mann-Whitney U). Summary of the expression of CNDP2 in 26 UM tissues are shown in Table 21.

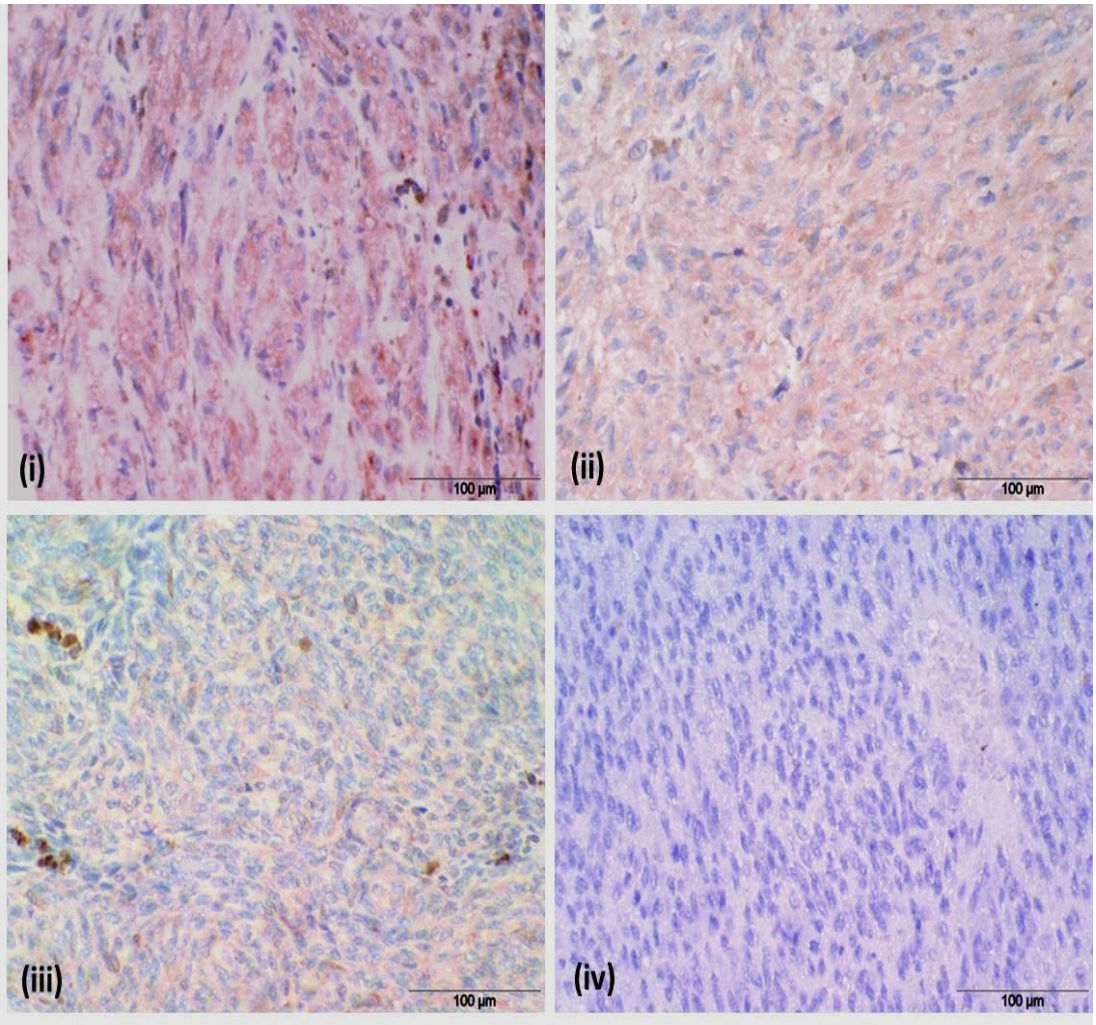


Figure 26: Representative immunohistochemical slides of cytosolic non-specific dipeptidase (CNDP2) expression in uveal melanoma tissues, showing different intensities of cytoplasmic staining. Relative to other targets, the overall staining intensity of CNDP2 was less, and was graded accordingly. (i) Strong staining in sample 21 nmUM; (ii) Moderate staining in sample 3 mUM; (iii) Weak staining and scattered areas of melanin in sample 11 mUM; (iv) Negative control showing no staining. LC-MS proteomic profiling of primary UM tissues identified downregulation of CNDP2 in tissues of patients who developed metastasis compared to those who did not develop metastasis. Immunohistochemical expression in 13 primary UM tissues of patients who developed metastasis (mUM) and 13 patients who did not develop metastasis (nmUM) did not show a significant difference in expression score between the two groups (p: 0.752, Mann-Whitney U test). Magnification X 400, scale bar =100 µm

Table 21: Summary of results of cytosolic nonspecific dipeptidase reductase (CNDP2) immunohistochemistry in 13 primary UM tissues of patients who developed metastasis (mUM) and 13 patients who did not develop metastasis (nmUM). LC-MS proteomic profiling of 16 primary UM tissues identified downregulation of CNDP2 (1.75 fold, p: 0.001) in tissues of patients who developed metastasis (n=8) compared to those who did not (n=8).

| | | **Metastasis (n=13)** | **No metastasis (n=13)** |
|---|---|---|---|
| **Overall staining score (0-12)** | | Mean: 5.31, SD: 3.04<br>Median: 4, Range: 0-12 | Mean: 6.08, SD: 3.73<br>Median: 4, Range: 2-12 |
| **Difference in scores, p** | | 0.752† | |
| **Staining** | **Negative** | 1 | - |
| | **Percentage staining range** | 100% | - |
| | **Weak intensity** | 4 | 5 |
| | **Percentage staining range** | 90-100% | 50-90% |
| | **Moderate intensity** | 6 | 2 |
| | **Percentage staining range** | 50-100% | 60-90% |
| | **Strong intensity** | 2 | 6 |
| | **Percentage staining range** | 40-100% | 30-90% |
| **Difference in staining intensity, p** | | 0.318† | |
| **Difference in staining percentage, p** | | 0.113† | |

†Mann Whitney U

No significant correlation between CNDP2 score and survival in patients with metastatic disease was found (p: 0.323, Spearman correlation). Higher expression of CNDP2 significantly correlated with disomy/trisomy 3 tumours compared to monosomy 3 (p: 0.045, Spearman correlation). No significant correlation between CNDP2 score and cell type was found (p: 0.563, Spearman correlation). Furthermore, no significant correlation between CNDP2 score and tumour size, ciliary body involvement or extrascleral extension was identified (p: 0.831, p: 0.336 and p: 0.753 respectively, Spearman Correlation). These results are summarised in table 22.

Table 22: Correlation between cytosolic nonspecific dipeptidase reductase (CNDP2) immunohistochemistry score in 13 primary UM tissues of patients who developed metastasis (mUM) and 13 patients who did not develop metastasis (nmUM), and clinicopathological parameters. All p values were derived from Spearman correlation.. *Statistically significant correlation between higher CNDP2 score and non-aggressive disomy/trisomy 3 tumours was found.

| | **CNDP2 expression score, p value** |
|---|---|
| **Survival** | 0.323 |
| **Chromosome 3 status** | 0.045* |
| **Cell type** | 0.563 |
| **Tumour size** | 0.831 |
| **Ciliary body involvement** | 0.336 |
| **Extrascleral extension** | 0.753 |

#### 3.3.2.3. Contactin 3 (CNTN3)

In the bioinformatic reanalysis of gene expression microarray data of monosomy 3 tumours with metastasis (M3M) versus disomy 3 tumours without metastasis (D3NM), CNTN3 was downregulated by 3.07 fold (p: 0.0008) in M3M compared to D3NM. Immunohistochemical staining of CNTN3 was performed on 13 primary UM tumours of patients that developed metastatic disease (mUM) and 13 primary UM tumours of patients that did not develop metastasis (nmUM). The demographics and clinicopathologic details of these samples are outlined in Table 17. Staining of CNTN3 in UM tissues was cytoplasmic with no nuclear staining.

In mUM, the mean score was 2.54 (median: 1, range: 0-12, SD: 3.71). Six tumours (46.2%) showed negative staining while 3 tumours (23.1%) showed weak (1+) staining that ranged between 30-100% of the tumours. Three tumours (23.1%) showed moderate (2+) staining that ranged from 20-100% while 1 tumours (7.7%) showed strong staining (3+) between 40-100% of tumour tissue.

In nmUM, the mean score was 3.31 (median: 4, range: 1-8, SD: 2.10). There were no tumours that showed negative staining. Eight tumours (61.5%) showed weak staining ranging between 20-90% and 5 (38.5%) showed moderate staining ranging between 20-90%. No tumours demonstrated strong staining. Representative immunohistochemical expression of CNTN3 in UM tissues are shown in Figure 27.

A trend towards lower expression score in mUM compared to nmUM was observed but it was not statistically significant (p: 0.099, Mann-Whitney U test). No significant difference was seen when comparing the intensity or percentage of staining between mUM and nmUM (p: 0.127 and p: 0.154 respectively, Mann-Whitney U test). A summary of the expression of CNTN3 in all 26 UM tissues are shown in table 23.

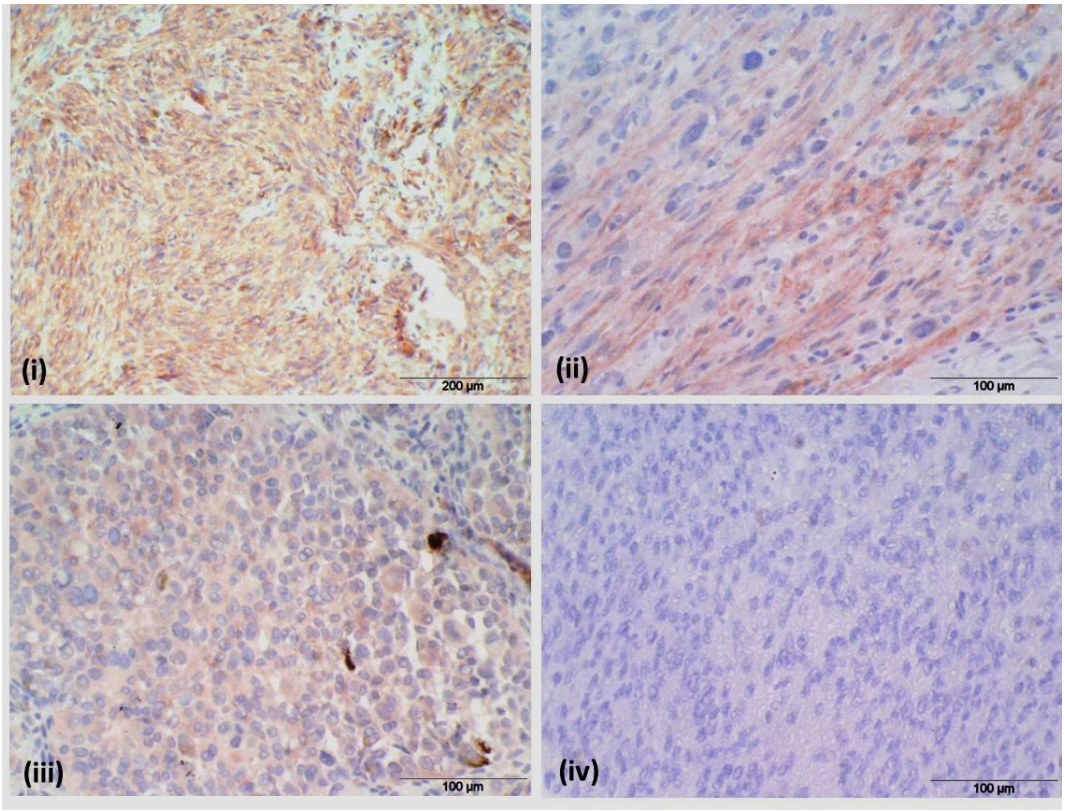


Figure 27: Representative immunohistochemical slides of contactin 3 (CNTN3) expression in uveal melanoma tissues, showing different intensities of cytoplasmic staining. (i) Strong staining in sample 12 mUM; (ii) Moderate staining in sample 23 nmUM; (iii) Weak staining in sample 25 nmUM; (iv) no staining in sample 1 mUM. Similarly, negative controls showed no staining. Bioinformatic reanalysis of gene expression microarray data showed downregulation of CNTN3 in 11 monosomy 3 tumours that developed metastasis compared to 9 disomy 3 tumours without metastasis. Immunohistochemical expression in 13 primary UM tissues of patients who developed metastasis (mUM) and 13 patients who did not develop metastasis (nmUM) showed a trend towards lower expression score in mUM compared to nmUM (p: 0.099, Mann-Whitney U test).
i: magnification X 200, scale bar = 200 µm
ii-iv: magnification X 400, scale bar = 100 µm

Table 23: Summary of results of contactin 3 (CNTN3) immunohistochemistry in 13 primary UM tissues of patients who developed metastasis (mUM) and 13 patients who did not develop metastasis (nmUM). Bioinformatic reanalysis of gene expression microarray data showed downregulation of CNTN3 (3.07 fold, p: 0.0008) in 11 monosomy 3 tumours that developed metastasis compared to 9 disomy 3 tumours without metastasis.

| | | **Metastasis (n=13)** | **No metastasis (n=13)** |
|---|---|---|---|
| **Overall staining score (0-12)** | | Mean: 2.54, SD: 3.71<br>Median: 1, Range: 0-12 | Mean: 3.31, SD: 2.10<br>Median: 4, Range: 1-8 |
| **Difference in scores, p** | | 0.099† | |
| **Staining** | **Negative** | 6 | - |
| | **Percentage staining range** | 100% | - |
| | **Weak intensity** | 3 | 8 |
| | **Percentage staining range** | 30-100% | 20-100% |
| | **Moderate intensity** | 3 | 5 |
| | **Percentage staining range** | 20-100% | 20-90% |
| | **Strong intensity** | 1 | - |
| | **Percentage staining range** | 100% | - |
| **Difference in staining intensity, p** | | 0.127† | |
| **Difference in staining percentage, p** | | 0.154† | |

†Mann Whitney U

No significant correlation between CNTN3 score and survival in patients with metastatic disease was found (p: 0.728, Spearman correlation). CNTN3 score showed no significant correlation with chromosome 3 status or cell type (p: 0.157 and p: 0.176 respectively, Spearman correlation). Furthermore, no significant correlation between CNTN3 score and tumour size, ciliary body involvement or extrascleral extension was identified (p: 0.133, p: 0.856 and p: 0.218 respectively, Spearman Correlation). These results are summarised in table 24.

Table 24: Correlation between contaction 3 (CNTN3) immunohistochemistry score in 13 primary UM tissues of patients who developed metastasis (mUM) and 13 patients who did not develop metastasis (nmUM), and clinicopathological parameters. All p values were derived from Spearman correlation.

| | **CNTN3 expression score, p value** |
|---|---|
| **Survival** | 0.728 |
| **Chromosome 3 status** | 0.157 |
| **Cell type** | 0.176 |
| **Tumour size** | 0.133 |
| **Ciliary body involvement** | 0.856 |
| **Extrascleral extension** | 0.218 |

#### 3.3.2.4. Signal-induced proliferation-associated 1 like 2 (SIPA1L2)

In the bioinformatic reanalysis of gene expression microarray data of monosomy 3 tumours with metastasis versus disomy 3 tumours without metastasis, SIPA1L2 was upregulated by 1.52 fold (p: 0.001) in M3M compared to D3NM. Immunohistochemical staining of SIPA1L2 was performed on 13 primary UM tumours of patients that developed metastatic disease (mUM) and 13 primary UM tumours of patients that did not develop metastasis (nmUM). The demographics and clinicopathologic details of these samples are outlined in Table 17. Staining of SIPA1L2 in UM tissues was cytoplasmic with no nuclear staining. Overall, the staining intensity was relatively weak compared to other targets, with no sample demonstrating strong staining intensity.

In mUM, the mean score was 2.85 (median: 4, range: 0-4, SD: 1.72). Three tumours (23.1%) showed negative staining while 8 tumours (61.5%) showed weak (1+) staining that ranged between 75-100% of the tumours. Two tumours (15.4%) showed moderate (2+) staining that ranged from 20-50% while no tumours showed strong staining (3+).

In nmUM, the mean score was 1.62 (median: 1, range: 0-6, SD: 1.98). Six tumours (46.2%) showed negative staining and 6 tumours (46.2%) showed weak staining ranging between 40-100%. One showed moderate staining in 75% of tumour tissue. No tumours showed strong staining. Representative SIPA1L2 immunohistochemical expression in UM tissues are shown in Figure 28.

A trend towards higher expression score in mUM compared to nmUM was observed but it was not statistically significant (p: 0.094, Mann-Whitney U test). No significant difference was seen when comparing the intensity or percentage of staining between mUM and nmUM (p: 0.218 and p: 0.055

respectively, Mann-Whitney U test). A summary of the expression of SIPA1L2 in all 26 UM tissues are shown in table 25.

Table 25: Summary of results of signal-induced proliferation-associated 1-like protein 2 (SIPA1L2) immunohistochemistry in 13 primary UM tissues of patients who developed metastasis (mUM) and 13 patients who did not develop metastasis (nmUM). Bioinformatic reanalysis of gene expression microarray data showed upregulation of SIPA1L2 (1.52 fold p: 0.001) in 11 monosomy 3 tumours that developed metastasis compared to 9 disomy 3 tumours without metastasis.

| | | **Metastasis (n=13)** | **No metastasis (n=13)** |
|---|---|---|---|
| **Overall staining score (0-12)** | | Mean: 2.85, SD: 1.72<br>Median: 4, Range: 0-4 | Mean: 1.62, SD: 1.98<br>Median: 1, Range: 0-6 |
| **Difference in scores, p** | | 0.094† | |
| **Staining** | **Negative** | 3 | 6 |
| | **Percentage staining range** | 100% | 100% |
| | **Weak intensity** | 8 | 6 |
| | **Percentage staining range** | 75-100% | 40-100% |
| | **Moderate intensity** | 2 | 1 |
| | **Percentage staining range** | 20-50% | 75% |
| | **Strong intensity** | - | - |
| | **Percentage staining range** | - | - |

| | |
|---|---|
| **Difference in staining intensity, p** | 0.218[†] |
| **Difference in staining percentage, p** | 0.055[†] |

[†]Mann Whitney U

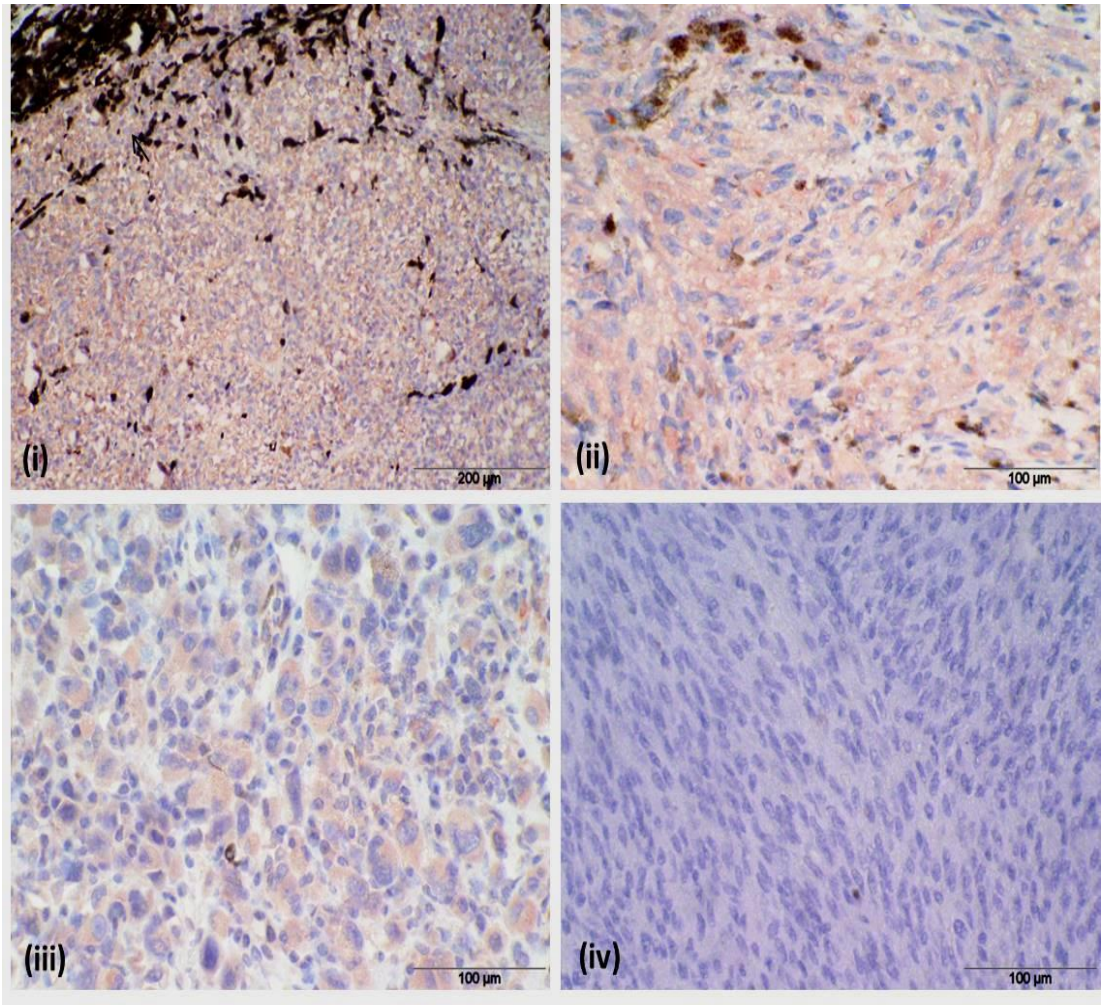


Figure 28: Representative immunohistochemical slides of signal-induced proliferation-associated 1 like 2 (SIPA1L2) expression in uveal melanoma tissues, showing different intensities of cytoplasmic staining. (i) Moderate staining and scattered areas of melanin (black arrow) in sample 4 mUM; (ii) Moderate staining in sample 10 mUM; (iii) Weak staining in sample 19 nmUM; (iv) No staining in sample 14 mUM. Similarly, negative control showed no staining. Bioinformatic reanalysis of gene expression microarray data showed upregulation of SIPA1L2 in patients with 11 monosomy 3 tumours that developed metastasis compared to 9 disomy 3 tumours without metastasis. Immunohistochemical expression in 13 primary UM tissues of patients who developed metastasis (mUM) and 13 patients who did not develop metastasis (nmUM) showed a trend towards higher expression score in mUM compared to nmUM (p: 0.094, Mann-Whitney U test).
i: magnification X 200, scale bar = 200 µm
ii-iv: magnification X 400, scale bar = 100 µm

No significant correlation between SIPA1L2 score and survival in patients with metastatic disease was found (p: 0.055, Spearman correlation). SIPA1L2 score showed no significant correlation with chromosome 3 status or cell type (p: 0.202 and p: 0.071 respectively, Spearman correlation). Furthermore, no significant correlation between SIPA1L2 score and tumour size, ciliary body involvement or extrascleral extension was identified (p: 0.249, p: 0.779 and p: 0.678 respectively, Spearman Correlation). These results are summarised in table 26.

Table 26: Correlation between signal-induced proliferation-associated 1-like protein 2 (SIPA1L2) immunohistochemistry score in 13 primary UM tissues of patients who developed metastasis (mUM) and 13 patients who did not develop metastasis (nmUM), and clinicopathological parameters. All p values were derived from Spearman correlation.

| | **SIPA1L2 score, p** |
|---|---|
| **Survival** | 0.055 |
| **Chromosome 3 status** | 0.202 |
| **Cell type** | 0.071 |
| **Tumour size** | 0.249 |
| **Ciliary body involvement** | 0.779 |
| **Extrascleral extension** | 0.678 |

### 3.3.3. Immunohistochemical validation of thioredoxin-dependant peroxidase reductase (PRDX3) in larger tissue microarray study

In the pilot immunohistochemical study of 26 samples, a trend toward higher expression of PRDX3 in primary UM samples that developed metastasis was found. Compared to all other targets, PRDX3 also demonstrated the most significant difference in expression in primary UM tissues of patients that developed metastasis versus those that did not (p: 0.061). Thus, PRDX3 was chosen for further validation in a larger cohort of 92 primary UM tissue microarray samples of 55 tumours that developed metastasis and 37 that did not develop metastasis.

The TMA slides were scored based on staining only, as all tumours demonstrated homogenous staining given the small core size. The staining intensities observed in TMA tumours were either negative, weak or strong. Each tumour had 4 representative cores, and each core was assigned a score of 0-2. No staining was scored as 0, weak staining as 1 and strong staining as 2. A total score for each patient was obtained by adding the scores of all 4 cores. Thus, a minimum score of 0 and a maximum score of 8 was obtained. The total score was divided into 2 categories: 0-3 as low expression and 4-8 as high expression. In order for a patient to be categorised as “low expression”, a minimum of at least 1 core per patient would be required to demonstrate negative staining. The minimum staining for a patient to be categorised as “high expression” requires all 4 cores to demonstrate weak staining, 1 strong with 2 weak staining or 2 strong with 2 negative staining tumour cores. Thus, tumours with heterogenous PRDX3 staining in 4 cores would be classified as low or high based on the presence or absence of negative staining. Using this method, 4 weak staining cores, with a total score of 4 would be appropriately categorised as a positive

result. Figure 29 and 30 demonstrates representative strong positive, weak positive and negative staining in TMA tumour tissues.

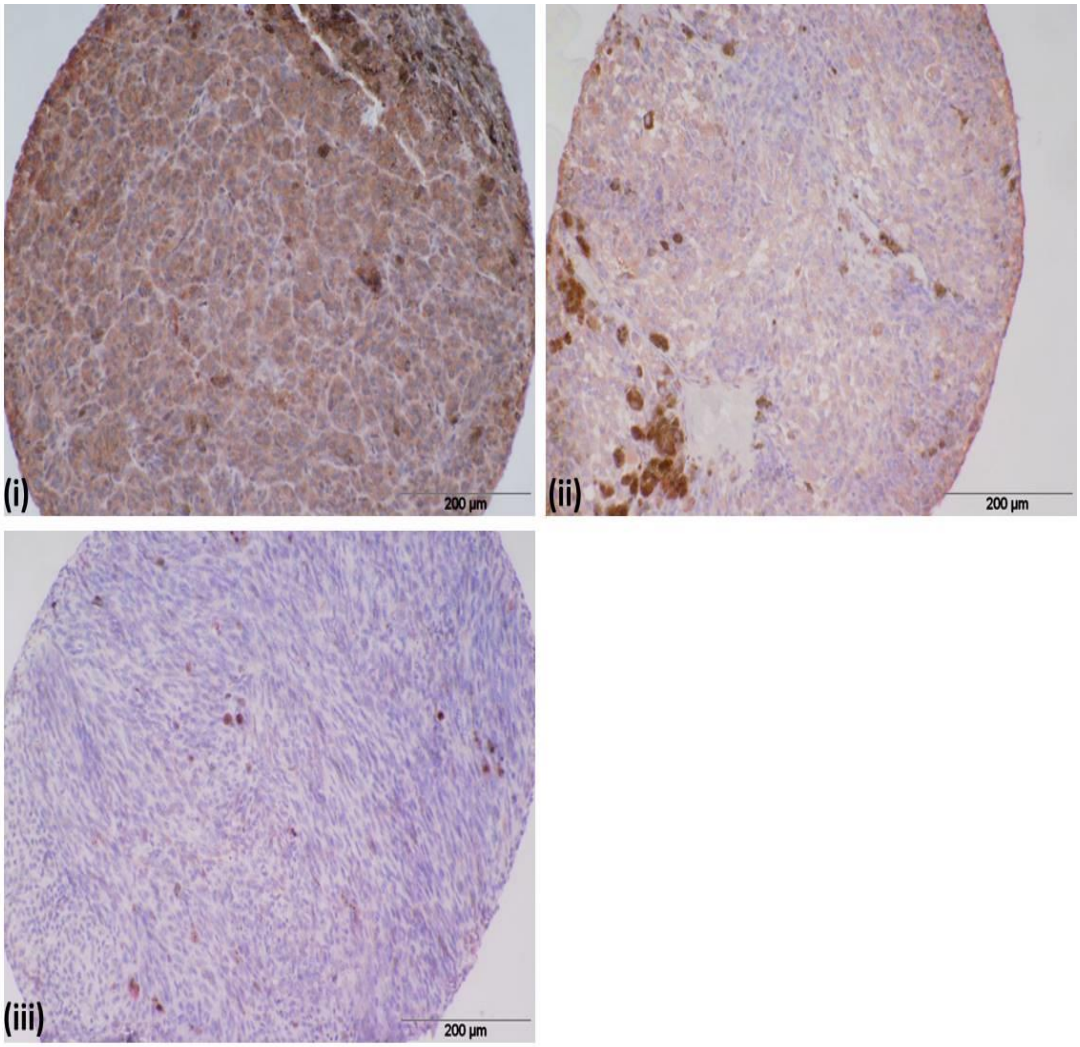


Figure 29: Representative immunohistochemical slides of thioredoxin-dependant peroxidase reductase 3 (PRDX3) expression in uveal melanoma tissue microarray samples showing (i) strong positive cytoplasmic staining (ii) weak positive cytoplasmic staining and (iii) no staining. Quantitative label-free LC-MS proteomic profiling identified upregulation of PRDX3 (1.58 fold, p: 0.00218) in 8 fresh frozen primary UM tissue specimens from patients who developed metastasis compared to 8 fresh frozen primary UM tissue specimens from patients who did not develop metastasis. Magnification X 200, scale bar=200 µm

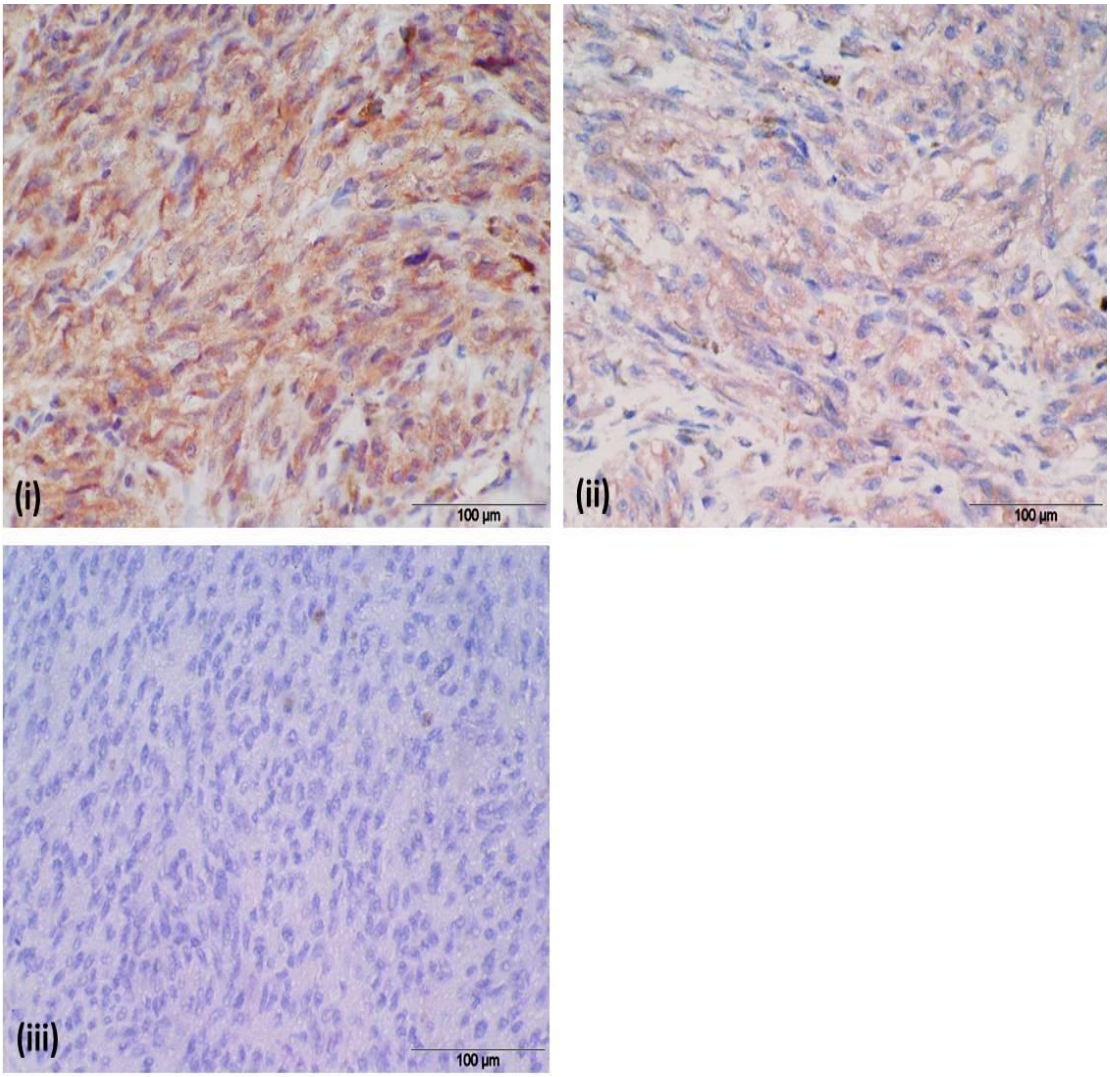


Figure 30: Representative immunohistochemical slides of thioredoxin-dependant peroxidase reductase 3 (PRDX3) expression in uveal melanoma tissue microarray samples, showing (i) strong positive cytoplasmic staining (ii) weak positive cytoplasmic staining and (iii) no staining. Quantitative label-free LC-MS proteomic profiling identified upregulation of PRDX3 (1.58 fold, p: 0.00218) in 8 fresh frozen primary UM tissue specimens from patients who developed metastasis compared to 8 fresh frozen primary UM tissue specimens from patients who did not develop metastasis.

Magnification X 400, scale bar = 100 µm

The majority of tumours demonstrated the same intensity of staining across all 4 cores of tissue [26/37 (70.3%) of tumours without metastasis and 47/55 (85.5%) in tumours with metastasis]. There were a number of tumours that demonstrated different staining intensities in the 4 cores of tissue. In patients without metastasis, 11/37 (29.7%) tumours demonstrated varied staining in the 4 representative cores. Of these, 10 tumours had 3 cores with the same intensity of staining while 1 tumour had 2 cores that stained differently to the other 2. In patients with metastasis, 8/55 (14.5%) tumours demonstrated varied staining in the 4 representative cores. Of these, 6 tumours had 3 cores with the same intensity of staining while 2 tumours had 2 cores that stained differently to the other 2. These are outlined in Table 27. The mean score in the metastasised patients is 6.18 (SD: 2.66, 95% CI: 5.46 – 6.90). The mean score in patient tumours with no metastasis is 4.54 (SD: 3.56, 95% CI: 3.36 – 5.73).

Table 27: Each tumour was represented by 4 tumour cores. The figures show the majority of tumours demonstrated the same intensity of staining in all 4 tumour cores.

| | **Number of cores staining with the same intensity** | | |
|---|---|---|---|
| | **4** | **3** | **2** |
| **No metastasis** | 26/37 (70.3%) | 10/37 (27%) | 1/37 (2.7%) |
| **Metastasis** | 47/55 (85.5%) | 6/55 (10.9%) | 2/55 (3.6%) |

There were 23 and 69 number of patient tumours with a score of 0-3 (categorised as low expression) and 4-8 (categorised as high expression) respectively. Seven and 48 patients who developed metastasis demonstrated low and high expression respectively. Sixteen and 21 patients who did not develop metastasis demonstrated low and high expression respectively (table 28). In the non-metastasised group, 4 of the 21 patient tumours that demonstrated high expression of PRDX3 are monosomy 3 tumours that were diagnosed between 2005-2009 (when chromosome 3 monosomy test was commenced as part of routine clinical practice). Although at the time of this study these patients are metastasis-free, it is highly likely that these patients will develop metastasis based on their cytogenetic risk factor of monosomy 3.

Table 28: Distribution or PRDX3 expression score in primary uveal melanoma tumours with metastasis and without metastasis. Low expression is defined as a combined score of 0-3 and high expression is defined as a combined score of 4-8 for all 4 cores of tumour tissues per patient. Quantitative label-free LC-MS proteomic profiling identified upregulation of PRDX3 (1.58 fold, p: 0.00218) in 8 fresh frozen primary UM tissue specimens from patients who developed metastasis compared to 8 fresh frozen primary UM tissue specimens from patients who did not develop metastasis.

| **PRDX3 expression** | **Metastasised tumours (n=55)** | **Non-metastasised tumours (n=37)** | **Total (n=92)** |
|---|---|---|---|
| **Low Expression** | 7 (12.7%) | 16 (43.2%) | 23 (25%) |
| **High expression** | 48 (87.3%) | 21 (56.8%) | 69 (75%) |

Multivariate studies have demonstrated that tumours consisting of epithelioid and mixed cell types are associated with high risk for metastasis. This was assessed in our population of patients to determine if a similar relationship may be found. Although figure and table 31 demonstrates a shorter survival time in patients with tumours of epithelioid and mixed cell type compared to spindle, there was no significant correlation identified (p: 0.074; n: 65, Pearson Correlation). Furthermore, no correlation was identified between cell type and metastasis (p: 0.561; n: 91, Pearson Correlation). This was further analysed to determine if patients with epithelioid and mixed cell type demonstrated higher rate of metastasis. After grouping these two cell types together, no significant difference in the rate of metastasis was identified compared to spindle cell type (p: 0.368, Fisher's Exact). No significant correlation was found between PRDX3 expression and cell type (p: 0.797, n: 91, Spearman Correlation). Conventionally, large tumour size is associated with high risk for metastasis. A positive correlation was identified between tumour size and the presence of metastasis (p: 0.01, n: 81, Spearman Correlation). However, no significant correlation was found between PRDX3 expression and tumour size (p: 0.313, n: 81, Spearman Correlation). No significant correlation was found between tumour size and cell type (p: 0.159, n: 80, Spearman Correlation). Furthermore, no significant difference between the frequency of metastasis and extrascleral extension was found (p: 0.147, Pearson Chi-square; p: 0.234, Fisher's Exact).

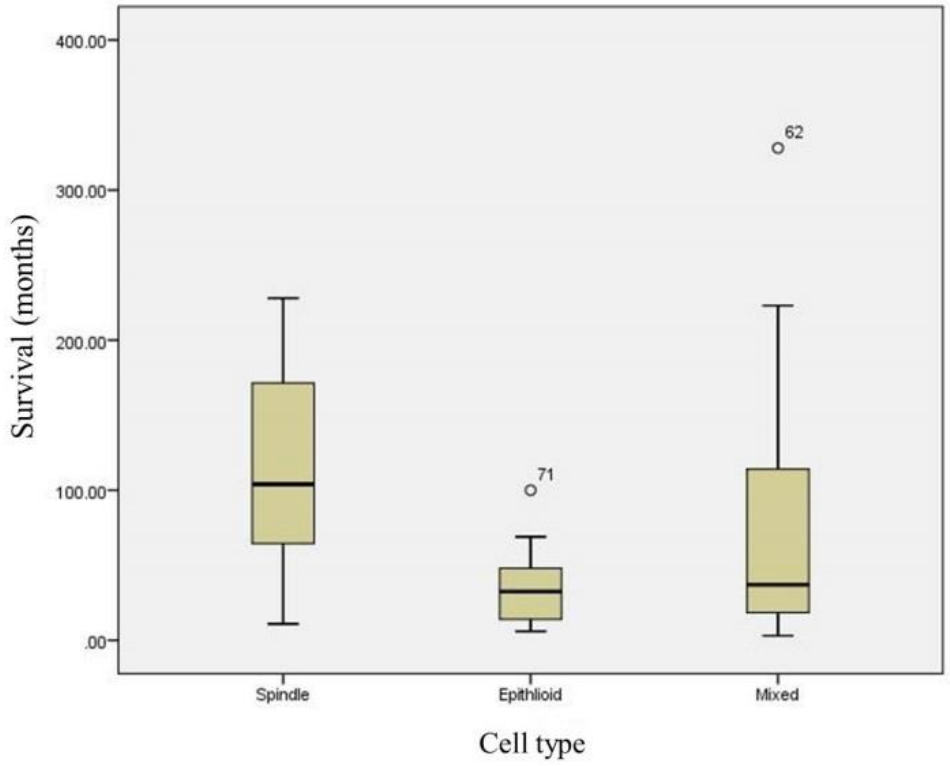


Figure and table 31: Box plot demonstrating relationship between cell type and survival. There was no significant correlation between cell type and survival (p: 0.074, Pearson Correlation). All data in the table are represented as months.

| | Cell type | | |
|---|---|---|---|
| | **Spindle** | **Epithelioid** | **Mixed** |
| **Mean** | 116.15 | 38.2 | 74.11 |
| **Median** | 104 | 32.5 | 37 |
| **Standard deviation** | 69.8 | 28.78 | 78.32 |
| **95% CI** | 83.48 - 148.82 | 17.61 - 58.79 | 47.21 - 101.02 |
| **Minimum** | 11 | 6 | 3 |
| **Maximum** | 228 | 100 | 328 |
| **Interquartile range** | 112.5 | 39.5 | 115 |

Currently, chromosome 3 monosomy is one of the most widely used prognostic markers for metastatic risk. In this study, a significant correlation was demonstrated between chromosome 3 status and the presence of metastasis (p: 0.008, n: 17, Spearman Correlation). A significant difference in the frequency of metastasis was identified based on chromosome 3 status (p: 0.034, n: 17 Fishers Exact). However, no association between cell type, tumour size and chromosome 3 status was found (p: 0.339 n: 17, and p: 0.549, n: 16 respectively, Spearman Correlation). As only 5/17 patients with chromosome 3 status available (all monosomy 3 tumours) have died, survival analysis for chromosome 3 was not possible. It was not possible to determine if PRDX3 expression was associated with chromosome 3 status, as all 17 tumours with chromosome 3 information available (10 monosomy and 7 disomy 3 tumours) demonstrated high expression of PRDX3.

A statistically significant difference of PRDX3 expression was observed in patients that did and did not develop metastasis (p: 0.001, Mann-Whitney U, Table 29). A significant positive correlation between high PRDX3 expression and metastasis was also observed (p: 0.001, correlation coefficient: 0.346, n: 92 Spearman correlation). Furthermore, a significant negative correlation between PRDX3 staining score and expression with survival was found (p: 0.005, correlation coefficient: -0.343, n: 66 and p: 0.017, correlation coefficient: -0.294, n: 66 respectively, Spearman correlation).

Table 29: Test statistics showing the statistically significant difference of PRDX3 expression in patients that did or did not develop metastasis. A total of 92 patients were studied; 55 with metastasis and 37 without metastasis. *p < 0.05

| Test statistics | PRDX3 expression |
|---|---|
| **Mann-Whitney U** | 707 |
| **Wilcoxon W** | 1410 |
| **Z** | -3.296 |
| **Asymp. Sig. (2-tailed)** | 0.001* |

Kaplan-Meier survival analysis was performed to demonstrate the significant impact of metastasis on patient survival. In patients with metastasis, 2 samples were excluded from analysis (sample 60 and 65). These patients lived for 35.6 and 27.75 years after enucleation, respectively. Information such as date of metastasis and location were unavailable for these patients. As described by Harbour et al, low-risk class 1 patients can be further subdivided to 1a and 1b (315–317). Class Ib is associated with a low risk of late onset metastasis. These 2 patients were significant outliers and were excluded from subsequent survival analyses.

The details and distribution of survival rates in patients with and without metastasis are outlined in figure 32. The mean survival for patients who developed metastases is 51.88 months (SD: 46.32, 95% CI: 38.99 – 64.78). The mean survival for patients who did not develop metastasis is 189.07 months (SE: 53.73, 95% CI: 158.05 – 220.09). Figure 33 shows the Kaplan-Meier survival analysis for patients with and without metastasis (p: 0.000).

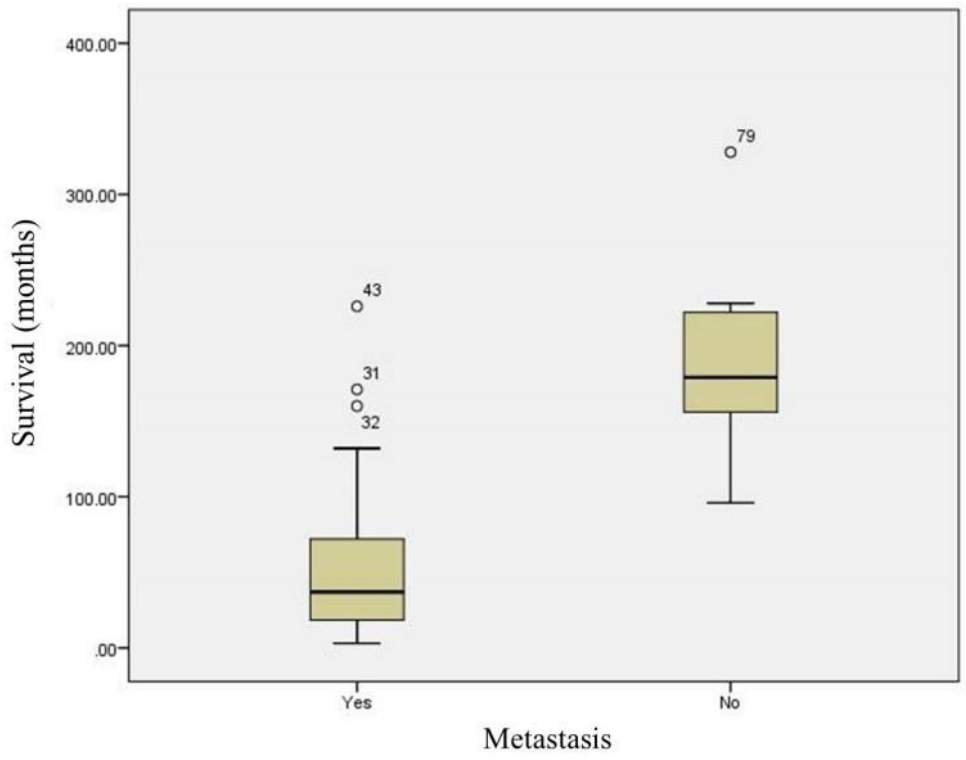


Figure 32: Box plot demonstrating the distribution of survival months in patients with and without metastasis. The table shows the details of survival of these patients. The data are presented in months.

| | Metastasis | |
|---|---|---|
| | **Yes n=52** | **No n=14** |
| **Mean** | 51.89 | 189.07 |
| **Median** | 37 | 179 |
| **Standard deviation** | 46.32 | 53.73 |
| **95% CI** | 38.99 – 64.78 | 158.05 – 220.09 |
| **Minimum** | 3 | 96 |
| **Maximum** | 226 | 328 |
| **Interquartile range** | 54.25 | 67.25 |

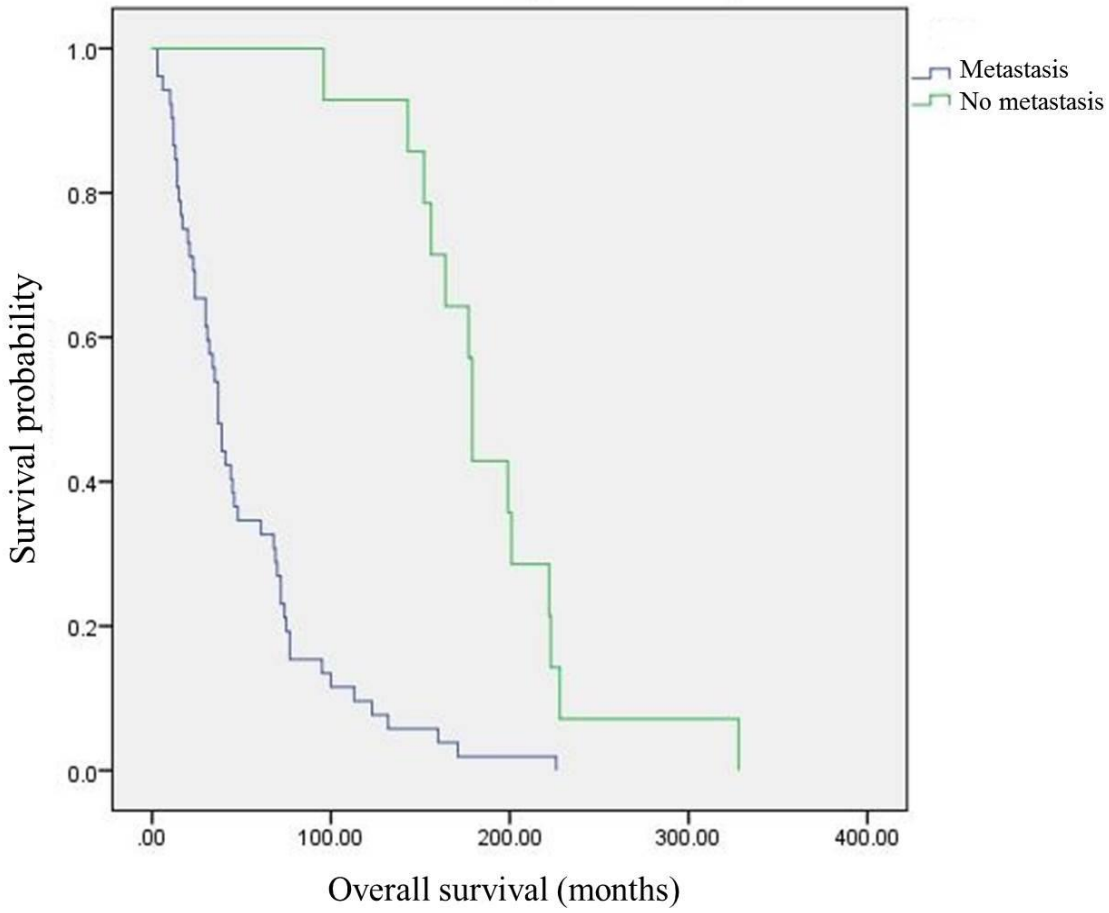


Figure 33: Kaplan-Meier survival analysis showing significant correlation between metastasis and death in 52 patients that developed metastasis compared to 14 patients that did not develop metastasis. The mean survival for patients with and without metastasis is 51.89 and 189.07 months respectively.

Survival analysis was performed to determine if PRDX expression was significantly associated with overall survival. In the 66 patients that have died, 14 demonstrated low expression while 52 demonstrated high expression (21.2% and 78.8% respectively). The mean, standard error and 95% confidence interval for survival time for low and high expression of PRDX3 is outlined in table 30. A statistically significant difference in overall survival was observed between tumours that demonstrated low and high expression of PRDX3 (p: 0.013, Mantel-Cox log-rank; p: 0.026, Wilcoxon-Breslow; p: 0.017, Tarone-Ware). Kaplan-Meier analysis demonstrated a significant negative correlation between PRDX3 expression and survival (Figure 34).

Table 30: Survival rates of patients with tumours that demonstrated low and high expression of PRDX3. A statistically significant difference in survival rate was observed between tumours that demonstrated low and high expression (p: 0.013, Mantel-Cox log-rank; p: 0.026, Wilcoxon-Breslow; p: 0.017, Tarone-Ware)

| **PRDX3 expression** | **Survival (months)** | | |
|---|---|---|---|
| | **Mean** | **Standard error** | **95% confidence interval** |
| **Low (n=14)** | 130.64 | 24.77 | 82.14 – 179.14 |
| **High (n=52)** | 67.61 | 8.67 | 50.63 – 84.61 |
| **Overall (n=66)** | 80.99 | 9.09 | 63.17-98.80 |

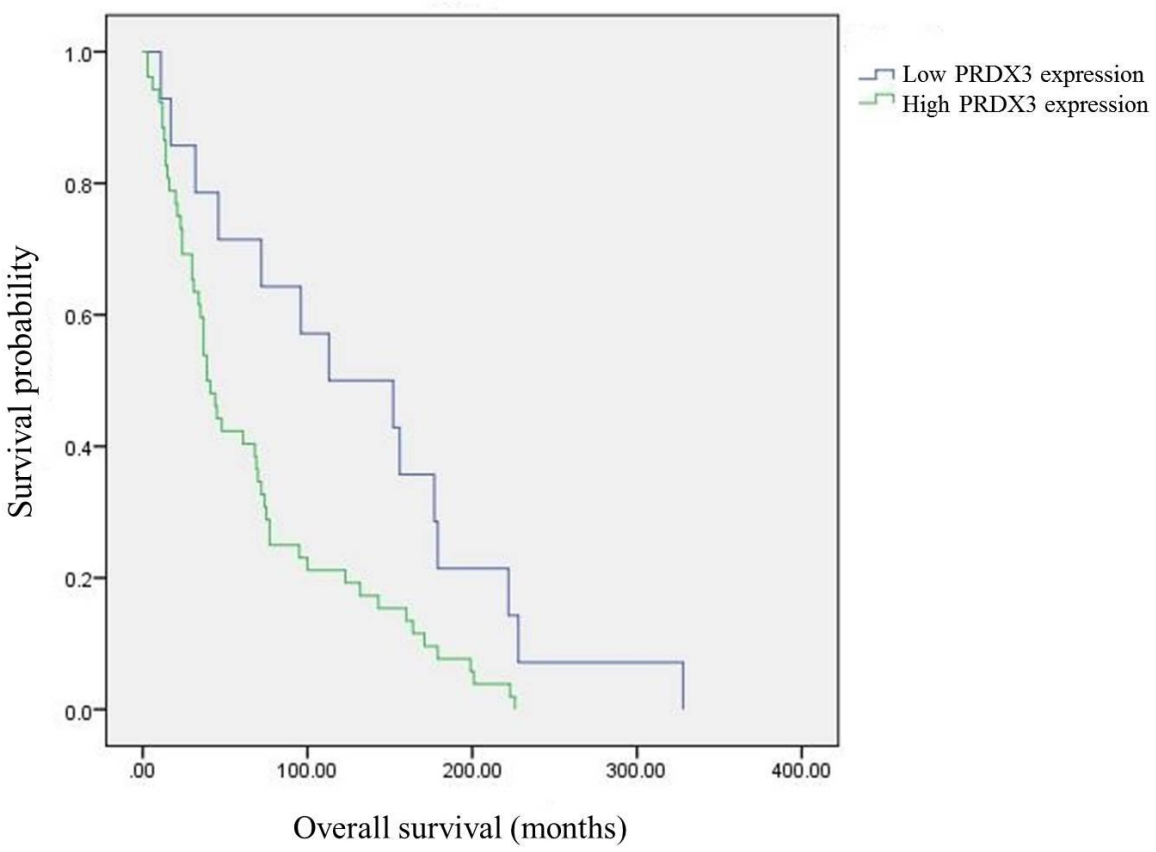


Figure 34: Kaplan-Meier survival analysis showing a significant negative correlation between PRDX3 expression and survival in 52 patients that demonstrated high expression compared to 14 patients that demonstrated low expression. The mean survival for patients with low and high PRDX3 expression is 130.64 and 67.61 months respectively. (p: 0.013, Mantel-Cox log-rank; p: 0.026, Wilcoxon-Breslow; p: 0.017, Tarone-Ware)

Table 31: Summary of association between PRDX3 expression and clinicopathological parameters.

| | **PRDX3 expression score, p value** |
|---|---|
| **Metastasis** | 0.001[†], 0.001* |
| **Survival** | 0.017*, 0.013[§] |
| **Cell type** | 0.797* |
| **Tumour size** | 0.313* |

†Mann Whitney U
*Spearman Correlation
[§] Mantel-Cox

# 4. Discussion

Uveal melanoma is the most common primary intraocular malignancy in adults. It is associated with the development of metastatic disease in about 50% of patients, and 40% of patients with UM die of metastatic disease despite successful treatment of the primary tumour (5,6). Progress made in molecular genetics has led to significant improvement in prognostic stratification of patients into low-risk and high-risk for developing metastatic disease (21,22). This has enabled closer surveillance of patients at-risk for metastasis, and earlier detection and treatment of metastatic disease. It has also increased the understanding of the events that trigger the development of UM. However, very little is known about the molecular biology of the development of metastatic disease. Effective treatment strategies for metastatic disease remain elusive and survival rates are poor. Only a few proteomic studies of uveal melanoma have been carried out to date. Most of these studies have been performed using cell lines, with only 2 studies using primary UM tissue. Using recent advances in proteomic technologies, quantitative label-free LC-MS proteomic profiling was performed to identify differentially expressed proteins between primary UM tissue from patients who developed metastatic disease, versus primary UM tissue from patients who did not develop metastasis. Furthermore, bioinformatic reanalysis of publically available gene expression microarray datasets of monosomy 3 tumours that developed metastatic disease versus disomy 3 tumours that did not develop metastatic disease was also carried out to identify differentially expressed genes.

## 4.1. Quantitative label-free LC-MS proteomic analysis

To identify differentially expressed proteins, 8 fresh-frozen primary UM tissues from patients that developed metastatic disease (M) and 8 from patients that did not develop metastasis (NM), with a minimum follow-up of 7 years, were subjected to quantitative label-free LC-MS proteomic analysis.

Gene ontology (GO) enrichment analysis of 94 proteins with $p \leq 0.05$ and ≥ 2 peptides matched using the DAVID interface showed significant enrichment of proteins involved in negative regulation of apoptosis and in carbohydrate metabolic and catabolic processes. Furthermore, in primary UM tissues that developed metastasis (M), processes involving metabolism, mitosis and biological regulation were higher than that in primary UM tissues that did not metastasise (NM) while processes involving cell-to-cell and biological adhesion were lower in M compared to NM. PANTHER pathway categorisation showed a higher number of proteins involved in glycolysis and pyruvate metabolism in M compared to NM. Lower number of proteins involved in gonadotropin releasing hormone receptor pathway, heterotrimeric Gi-α and Gs-α G-protein signalling pathway and integrin signalling pathway were found in M compared to NM.

### 4.1.1. Proteins associated with apoptosis and proliferation

In 2000, Hanahan and Weinberg defined resistance to apoptosis as one of the hallmarks of cancer (320). This concept has been established by several studies over the last two decades, where suppression of apoptosis has been shown to enable progression to high-grade malignancy and resistance to therapy (321–323). Tumour cells evolve various strategies to circumvent apoptosis. In UM, alterations in p53, BCL-2 and PTEN downregulation have been shown to enhance resistance to apoptosis (324). In this study, PRDX3, HSP27 and KIT, along with proteins HSP71, HSPD1, NDKA, ANXA5, SYUA, APOH, ALBU, CRYAB, APOE and GRP78 were associated with negative regulation of apoptosis. PRDX3 and its

involvement in apoptosis will be discussed later. Heat shock protein-27 (HSP27) was found to be upregulated by 1.56 fold (p: 0.05) in M compared to NM. This is in agreement with another UM tissue proteomic study by Coupland et al (243) where higher HSP27 expression was associated with a favourable prognosis. Monosomy 3 tumours were found to have a significantly lower HSP-27 expression compared to disomy 3 tumours, demonstrating a significant negative correlation between reduced HSP-27 expression and a predicted survival of < 8 years (289).

HSP-27 is a cytoplasmic protein involved in the inhibition of cell proteolysis and protein conformation stabilisation (290,291). It is overexpressed in a variety of cancer cells and is associated with a poor prognosis in gastric, prostate, and node-negative breast carcinoma (292–294). In contrast, high levels of HSP-27 expression indicate a good prognosis in non–small-cell lung carcinomas and ovarian carcinomas (295,296). This suggests that HSP-27 may play different roles in different tissues or that there are other elements present in some malignancies that can override or bypass any effects HSP-27 may have (297). Of interest, HSP-27 overexpression has been shown to inhibit cell proliferation and reduce cell invasiveness in one human cutaneous melanoma cell line (298). From this, it was postulated that underexpression of HSP-27 in melanoma cells results in increased tumour cell motility and invasiveness. HSP27 was also identified in another proteomic study by Wang et al (240). A UM cell line was analysed 15 and 48 hours post X-ray radiation to identify proteins associated with cell cycle arrest. It was found to be nearly 3 fold higher 48 hours post radiation, suggesting a role in growth arrest and cellular senescence.

Mast/stem cell growth factor receptor (KIT) was also identified in this study, where it was 4.85 fold upregulated (p: 0.008) in M compared to NM. KIT, a member of the PDGFR family of kinases, is a receptor tyrosine kinase that is activated by binding of stem cell-derived factor (SCF) and plays an essential role in the regulation of various cellular processes including cell survival and proliferation, stem cell maintenance, and in melanogenesis (56). KIT activates the

AKT signalling pathway by phosphorylating PI3K and also transmits signals via GRB2 and activation of RAS, RAF1 and the MAPK pathway (56). Mouriaux et al showed KIT expression in normal choroidal melanocytes and activation by SCF stimulated proliferation (57). In normal uveal melanocytes, stimulation with SCF resulted in activation of both ERK1/2 and AKT but in a KIT-expressing UM cell line, stimulation led to MAPK pathway activation only (58). Immunohistochemical expression of KIT was positive in 62.7-78.2% of primary UM tissue and treatment with KIT inhibitor led to significant decrease in proliferation, invasion and cell death in UM cell lines (58,59). An *in vitro* study found constitutive ERK1/2 activation that enabled UM cell proliferation and transformation in a KIT dependant manner. Inhibition of UM proliferation was observed when depleted of SCF/KIT, but not AKT, suggesting that the proliferative effects of the SCF/KIT autocrine loop in uveal melanoma likely funnel primarily through the MAPK pathway (60). However, activation-related mutations of KIT have not been found (57,61).

DJ-1, an oncogene identified by Pardo et al (239) in the first proteomic study of uveal melanoma, was found to be upregulated by 2.15 fold (p: 0.009) in M compared to NM. It was expressed *in vitro* and found in the culture media but was absent in normal melanocyte cell line or culture media (239). Importantly, DJ-1 functions as a redox-sensitive chaperone and as a sensor against oxidative stress (325). It may act as an atypical peroxiredoxin-like peroxidase that scavenges $H_2O_2$ and protect cells against $H_2O_2$-mediated cell death (325). Furthermore, it is required for correct mitochondrial morphology and for autophagy of dysfunctional mitochondria(325). Malignant cells have been described to secrete DJ-1 and it plays a role in tumourigenesis in breast cancer, non-small cell lung carcinoma and prostate cancer (247,248). Kim et al identified DJ-1 as a negative regulator of the tumour suppressor PTEN, promoting cell survival in primary breast and lung cancer patients (249). A recent study suggested serum DJ-1 level as a potential biomarker for the diagnosis and prognosis prediction of patients with pancreatic cancer (250). Recently, it was shown that elevated DJ-1 was found to be significantly associated with risk

factors for malignant transformation of choroidal naevus, namely nevus thickness greater than 1.5 mm, diameter larger than 8 mm, and presence of acoustic hollowness on ultrasonography (251). This interesting finding, coupled with the identification of DJ-1 in UM tissue in this label-free proteomic study, warrants further investigation into the potential role serum DJ-1 may play in tumourigenesis and monitoring of patients at risk for malignancy.

In PANTHER analysis, lower number of proteins involved in gonadotropin releasing hormone (GnRH) receptor pathway (GnRHR) were found in M compared to NM. Four proteins were associated with this pathway; integrin β1 (ITGB1, downregulated in M), heat shock 70 kDa protein 1A (HSPA1A, downregulated in M), guanine nucleotide-binding protein G(I)/G(S)/G(T) subunit beta-2 (GNB2, downregulated in M) and Annexin A5 (ANXA5, upregulated in M). In primary ovarian cultures of ovarian carcinomas and tumour biopsies, widespread presence (>80%) of GnRH receptor has been reported, suggesting that alterations of GnRH receptor may be one of the most common abnormalities in human ovarian cancer (326,327). It has been implicated in proliferation, tumour progression and metastatic spread, suggesting a regulatory role in ovarian cancer (328–330). Following silencing of GnRH receptors, Cheung et al recently showed inhibition of adhesion to peritoneal mesothelium of highly malignant ovarian cancer cells *in vitro* (331). *In vivo*, GnRH receptor inhibition decreased the expression of integrin β1, α2 and α5 and P-cadherin, leading to significant attenuation of tumour growth and peritoneal metastasis (331). However, upregulation of proteins involved in the GnRH receptor pathway in UM tissues appear to inhibit metastatic formation, suggesting that this pathway is involved in an alternative manner than that reported by Cheung et al. This is supported by the contrasting findings of other studies that have shown that GnRH and its agonists are effective in controlling tumour growth and invasiveness in endometrial, ovarian and prostate cancer (332–334). GnRH/GnRHR mediated inhibition of tumour invasion and metastatic potential were associated with upregulation of actin cytoskeleton remodelling, mainly through the activation of Rac1 (335,336), as well as by influencing the activity of

cell-cell adhesion molecules and/or the regulation of cell substrate attachment-associated proteins (337,338). In breast cancer, GnRH and its agonists inhibited growth and metastatic capacity both *in vitro* and *in vivo* (332,339–341). Furthermore, its inhibitory effects on breast cancer cell migration has also been established (333,334). The activation of GnRH receptor in a highly invasive breast cancer cell line increased RhoA-GTP levels and stimulated actin remodelling, resulting in increased cell adhesion and loss of migration capacity, suggesting that GnRH may act to reduce the metastatic potential and invasiveness of malignant breast tumour cells (342). GnRH receptor pathway has not been implicated in UM, but the finding of downregulation of this pathway in primary UM that developed metastasis needs to be investigated further.

In PANTHER analysis, lower number of proteins involved in the heterotrimeric Gi-α and Gs-α G-protein signalling pathway were found in M compared to NM. GNB2, PYGL and PYBG were all found to be differentially expressed in NM. Gs and Gi are guanine nucleotide-binding, heterotrimer proteins that regulate the activity of adenylate cyclase, and are responsible for transferring stimulatory and inhibitory signals, respectively, from cell surface receptors to the enzyme catalytic unit (343). Gs-α protein stimulates adenylyl cyclase to produce the second messenger molecule cyclic AMP (cAMP), and the Gi-α proteins have an antagonistic inhibitory function. Thus, these proteins act to regulate and mediate intracellular signal transduction. The Gs-α protein (GNAS) gene has been found to play an important role in promoting tumour cells apoptosis in squamous cell cancer cells (344). In UM, activating mutation of GNAQ or GNA11 mutations are found in about 85-91% of cases and represents the most common oncogenic mutation (23,24,35). The mutations are mutually exclusive and occur in exon 4 (R183) or exon 5 (Q209) in GNAQ or GNA11. It is not associated with tumour class, stage or clinicopathological parameters and therefore, indicates an early event in the disease pathogenesis (23). It has been shown that mutations in the Gqα subunits GNAQ or GNA11 are responsible or the constitutive activation of the MAPK pathway in the development of UM. Mutant GNAQ/GNA11 are affected at the intrinsic GTPase domain where

hydrolysis of GTP to GDP and the Gα-GDP re-association with Gβγ subunits is defective. Thus, this leads to the constitutive Gα activation and downstream signalling of the MAPK pathway. However, mutations in GNAI or GNAS (encoding Gi-α and Gs-α G-protein respectively), or the expression of these G-protein coupled receptors have not been investigated in UM. Interestingly, GnRH antagonists were shown to promote proapoptotic signalling in reproductive tumour cells by activating a Gi-α-coupling state of the GnRH receptor (345). This antiproliferative action occurs through a Gi-α -mediated activation of stress-activated protein kinase pathways, resulting in caspase activation and transmembrane transfer of phosphatidlyserine to the outer membrane envelope. In ovarian and endometrial cancer cells, antiproliferative signal transduction by luteinizing hormone-releasing hormone was found to be mediated by Gi-α, resulting in down-regulation of mitogenic signal transduction and cell proliferation (346). Gs-α mutations have also been shown to be associated with endocrine adenomas (343). More recently, a high throughput analysis found Gs-α R201 mutations in a small subset of pancreatic and ovarian cancers and a significant percentage of breast cancers (347). Furthermore, numerous studies have shown amplification or polymorphisms of GNAS to be associated with increased survival and a predictor of response to treatment in ovarian, bladder, renal, colorectal, breast, oesophageal and non-small cell lung cancer (344,348–352). These studies support the findings of higher expression of proteins involved in the Gi-α and Gs-α G-protein signalling pathway in UM samples of patients who did not develop metastasis. Further investigation of the role of these G-protein coupled receptors in UM may improve insights into the development of metastatic disease, and therapeutic targets.

### 4.1.2. Proteins associated with energy metabolism

A decade later, Hanahan and Weinberg added to the hallmarks of cancer, the ability of neoplastic cells to reprogram and upregulate energy metabolism to sustain cell growth and uncontrolled proliferation (353). In fact, the enhanced metabolism of cancer cells can be visualised in many malignancies using positron emission tomography (PET) with a radiolabeled analog of glucose (18F-fluorodeoxyglucose, FDG) as a reporter. In this study, TPI, PKM2, CRYAB, 3HIDH, PPP1CB, PGAM1, PGM2, ENOA, G6PI, PYGL and HEXB were associated with carbohydrate metabolic and catabolic processes. Triosephosphate isomerase (TPI) was upregulated by 1.79 fold (p: 0.006) in primary UM tissues of patients that developed metastatic disease compared to those that did not. This protein was also identified by a previous 2D-DIGE study by our group, where it was associated with invasion and migration (244). TPI is an enzyme that's critical in glycolysis and gluconeogenesis (305). In cervical cancer cells, functional inactivation of TPI induced apoptosis (307). It has also been shown to be involved in the aggressiveness of breast cancer (308). Other proteomic studies found it to be significantly increased in lung cancer tissue (309), cell lines and patients' plasma (310), and in prostate cancer (311), suggesting its use as a serum biomarker. Interestingly, TPI was also shown to be expressed in uveal melanoma primary cell cultures by Pardo et al (239) in the first proteomic study in UM. Cancer cells use intermediates of carbohydrate metabolism for various biosynthetic pathways, such as those generating nucleosides and amino acids (353,354). Pyruvate kinase isozymes M2 (PKM2) was upregulated by 1.84 fold (p: 0.05) in M compared to NM. PKM2 provides the metabolic advantage that the phosphometabolites upstream of pyruvate accumulate and are then available as precursors for the synthesis of amino acids, nucleic acids, and lipids (355). In proliferating cancer cells, pyruvate metabolism and its intermediates also becomes available for the synthesis of fatty acids, cholesterol, and isoprenoids (33). Thus, the entire metabolism of cancer cells is reprogrammed in a manner

that drives biosynthetic reactions and energy production that are necessary to support tumour growth and proliferation.

Fatty acid binding protein 3 (FABP3) was identified to be upregulated by 2.46 fold (p: 0.04) in M compared to NM. Similar to TPI, this protein was also identified by a previous 2D-DIGE study by our group and was shown to be associated with UM cell invasion and migration (244). FABPs are expressed in a variety of tissues, playing a role in fatty acid metabolism (299) and are suggested to be involved in a number of biological processes such as cell differentiation, cell growth, and apoptosis (300). One proteomics study showed a heterogeneous but unique FABP expression pattern in the different subtypes of renal cell carcinoma, suggesting its use for classification of this disease (299). Expression of FABP was significantly high in an aggressive small cell lung cancer cell line, suggesting that it may influence mitosis and cell growth (301). Another proteomic study identified FABP as a biomarker to predict gefininib treatment response in patients with lung adenocarcinoma (302). FABP was also shown to be expressed in human gastric carcinoma, and was associated with disease progression, tumour aggressiveness and poor patient survival (303). In contrast, ectopic expression of FABP3 in breast cancer cells was shown to reduce tumourigenicity in nude mice (304). This suggests a complex relationship between FABP and cancer.

### 4.1.3. Proteins associated with adhesion and cellular organisation

Neoplastic cells also demonstrate evasion of contact-inhibition that normally supress further proliferation in cells. *In vitro* studies have shown that cell-cell contact in dense populations of normal cells propagated in two-dimensional culture operate to suppress further cell proliferation, yielding confluent cell monolayers (353). This is abolished in various types of cancer cells in culture, suggesting that contact inhibition is an *in vitro* surrogate of a mechanism that operates *in vivo* to ensure normal tissue homeostasis, one that is abrogated during the course of tumourigenesis (353). Adhesion proteins ITGB1, PRELP, TLN1, APOH, COL1A1 and DCN were all downregulated in primary UM tissues that developed metastasis. In PANTHER analysis, a lower number of proteins involved in integrin signalling pathways were found in M compared to NM. Specifically, integrin β1 (ITGB1) was upregulated by 1.68 fold (p: 0.04) in NM. Integrins and its role in tumour cell proliferation, migration, and invasion has been the subject of intense research. Conventionally, increased expression of integrins have been implicated in tumour growth and metastasis (356,357). However, recent studies suggest a crucial, contradictory role of integrins in the regulation of tumour cell survival. Integrins are able to either enhance cell survival or initiate apoptosis depending on environmental cues. While ligated integrins promote cell survival, it is now emerging that unligated integrins promote pro-apoptotic cascades (358,359). In a process called integrin-mediated death (IMD), unligated integrins on adherent cells recruit and activate caspase 8, resulting in apoptotic cell death (358). It was also shown that integrin-mediated metastatic dissemination is achieved by the loss of caspase 8, thereby avoiding IMD (360). This may explain the findings of several studies that showed that the pro-tumourigenic integrin αvβ3 could inhibit tumour progression in mouse models of glioblastoma (361) and cutaneous melanoma (362). Decreased expression of integrin α2β1 was shown to increase tumour dissemination but re-expression reversed some of the malignant properties of breast cancer cells,

suggesting that α2β1 could function as a tumour suppressor (363). In a mouse model of spontaneous pancreatic islet cancer, integrin β1 inhibited tumour cell motility (364). Other studies have shown the ability of integrin α5β1 to inhibit oncogene-induced transformation (365,366). Thus, it is likely that the higher expression of integrin β1 in non-metastatic primary UM tissues represents a pro-apoptotic effect, thereby limiting tumour growth and metastatic dissemination.

EF1G was upregulated by 2.02 fold in M disease group (p: 0.000387). Elongation factor-1 is a GTP-binding protein that plays a role in translation and protein biosynthesis by mediating the transport of aminoacyl-tRNA to 80S ribosome (367,368). It has 4 subunits: α, β, γ, and δ. The γ and β subunit demonstrates strong affinity to leucyl- and histidyl-tRNA synthetases, while glu-proly-, glutaminyl-, alanyl-, aspartyl-, lysyl-, phenylalanyl-, glycyl-, and tryptophanyl-tRNA synthetases show moderate interactions with the α and δ subunits (369). It is a major substrate for phosphorylation by maturation-promoting factor, which regulates entry into the M-phase of the cell cycle (370). Maturation-promoting factor is a protein kinase that consists a cdc2 and cyclin B complex, and its levels peak just before anaphase and then decline rapidly (371). Overexpression of EF1G has been demonstrated in 7 out of 9 pancreatic cancer tissues compared to matched normal tissues from the same patients (372). In oesophageal carcinoma, Mimori et al identified a significant association between overexpression of EF1G mRNA and severe lymph node metastases, suggesting its use as a preoperative biomarker to identify high-risk patients (373). The authors also reported similar overexpression in gastric carcinoma, where EF1G was overexpressed in 22 of 30 tumours compared to normal tissue (374). Furthermore, the expression of EF1G was also observed in gastric, hepatic, ileocecal, duodenal, and colon carcinoma cell lines (374). Frazier and colleagues also demonstrated overexpression of EF1G-hybridizing RNA in 25 of 29 colorectal carcinomas relative to normal adjacent tissue, and in 14 of 25 adenomas (375,376). This is further supported by another study that reported over 2 fold expression of EF1G in colorectal adenocarcinomas compared to normal-appearing more distal mucosa (377).

Vimentin was upregulated by 1.98 fold in M disease group (p: 0.02). It is an intermediate filament protein that plays an important role in maintenance of cell structure and organelle positioning, including mitochondrial morphology (378,379). It is also important for cellular cytoskeleton flexibility and motility (380,381). In prostate cancer, vimentin expression is associated with invasiveness, and contributes to metastatic disease (382–385). Furthermore, vimentin has been shown to be associated with metastatic gastric cancer (386,387), lymph node metastases in oesophageal cancer (388) and metastatic hepatocellular carcinoma (389). In a 2-DE proteomic study, differential upregulation of vimentin was observed in colorectal cancer tissue compared to surrounding normal tissue (390). Similarly, overexpression increased invasion and migration of breast cancer cell lines (391,392). In cutaneous melanoma, a proteomic study demonstrated vimentin overexpression may serve as a diagnostic marker in primary tumours, and as a predictor of hematogenous metastases (393), while other studies also support its overexpression in metastatic melanoma (394–397).

In a recent study by Corbi et al, EF1G was shown to bind to promoter region of the vimentin gene (398). In HeLa cells, EF1G depletion led to mis-localisation of vimentin protein, resulting in a severe compromise of cellular shape and mitochondria localisation (398). EF1G also co-localised in mitochondria and following knockdown, mitochondrial fragmentation and increased cellular superoxide was observed (398). Interestingly, vimentin was identified in the 50 statistically significant proteins in our study (1.98 fold upregulated in M, p: 0.017). Thus, it is likely that upregulation of EF1G in UM upregulates vimentin expression. This, supported by other studies, and may lead to the development of metastases and poor survival. The relationship between EF1G and mitochondrial localisation and maintenance demonstrated by Corbi et al is also an interesting finding. In our study, PRDX3 was upregulated by 1.58 fold in the M group (p: 0.002). PRDX3 is a protein that exclusively localises in mitochondria. It reduces cellular reactive oxidative species such as $H_2O_2$, and may be upregulated as part of the mitochondrial anti-oxidant defence response

in order to protect organelles from oxidative damage and prevent cell death (399). Furthermore, PRDX3 overexpression in prostate cancer confers resistance to $H_2O_2$-induced apoptosis through a failure to activate pro-apoptotic pathways (400). Taken together, EF1G, vimentin and PRDX3 may interact in a synergistic manner to increase UM cell protein synthesis, metabolism, cellular organisation, proliferation and ultimately, metastatic dissemination.

## 4.2. Bioinformatic reanalysis of gene expression microarray data

To identify differentially expressed genes between primary UM tissue from patients who developed metastatic disease, versus primary UM tissue from patients who did not develop metastatic disease, bioinformatic reanalysis of publically available gene expression microarray datasets of monosomy 3 tumours that developed metastatic disease versus disomy 3 tumours that did not develop metastatic disease was performed. Laurent et al (29) compared 28 uveal melanomas from patients who developed liver metastases within three years of enucleation with 35 tumours from patients without metastases or who developed metastases more than 3 years after enucleation. However, it is not uncommon for UM patients to develop metastatic disease after 3 years. In order to eliminate this bias and obtain a more direct comparison, we studied monosomy 3 tumours that metastasised (M3M) versus disomy 3 tumours that did not metastasise (D3NM). After exclusion of 43 samples, 11 M3M and 9 D3NM samples were analysed. In total, 449 genes were differentially expressed with a fold change ≥ 1.3 and P-value < 0.05. Of these, 246 genes were upregulated in the M3M group, while 203 were downregulated. Six upregulated and 6 downregulated genes were considered for further follow-up based on p value, biological function and involvement in other diseases. SIPA1L2, CELF2, WARS, SDC2, THBS2 and BCAT1 are genes upregulated in M3M, while CNTN3, MEGF10, DLC1, CHL1, PPP1R3C, and SORBS2 are downregulated genes that were considered (Table 12). Of these, SIPA1L2 (1.516 fold upregulated in M3M, p: 0.00107) and CNTN3 (3.068 fold downregulated in M3M, p: 0.000807) were chosen for further validation by immunohistochemistry on FFPE UM sections. The former was selected for validation based on its novelty, as little is known about SIPA1L2, while CNTN3 was chosen primarily due to its localisation to chromosome 3, which has significant prognostic implication in UM. Other genes that have been described by in other studies have also been found, validating our results. Onken et al (319) described a 12-gene signature that accurately

classifies patients to class 1 low-risk for metastasis and class 2 high-risk for metastasis. Of the 12 genes, 8 were identified in this study (HTR2B, FXR1, ID2, LMCD1, MTUS1, RAB31, ROBO1, and SATB1) with identical differential expression pattern. Mutations in BAP1 gene located in chromosome 3 occurs almost exclusively in metastasizing class 2 tumours (25), which was also found to be downregulated in M3M tumours in our study. Specifically, Laurent et al's principal finding of high expression of PTP4A3 in metastasising tumours was also found, ensuring internal validation of our analysis.

Gene ontology (GO) enrichment analysis of 449 differentially expressed genes with $p \leq 0.05$ and fold change of $\geq 1.3$ using the DAVID interface showed significant enrichment of genes involved in regulation of proliferation and immune response. These includes BAP1, JUN, DLC1, ADAM10 and WARS. Compared to disomy 3 tumours without metastasis (D3NM), processes involving immune system and response to stimulus were significantly enriched in monosomy 3 tumours that developed metastatic disease (M3M) based on differential gene expression level. Based on molecular function of genes identified, binding activity was also significantly enriched in M3M compared to D3NM. PANTHER pathway categorisation showed significant enrichment of cadherin signalling pathway in D3NM compared to M3M with genes involved in GO biological processes such as cell signalling, proliferation, apoptosis and adhesion. Similarly, significant enrichment of cell adhesion molecules, such as CNTN3, CHL1 and SDC2 were found in D3NM compared to M3M.

Elav-like family member 2 (CELF2) was upregulated by 1.987 fold in M3M (p: 0.0000188). It is located at cytoband 10p13 and encodes for a member of a protein family that regulate pre-mRNA alternative splicing and may also be involved in mRNA editing, and translation (401). In breast cancer cells, CELF2 protein was found to be elevated in response to irradiation and promoted apoptosis. Knockdown of CELF2 expression in irradiated cells inhibited apoptosis, suggesting that CELF2 is a critical regulator of the apoptotic response to genotoxic injury in breast cancer cells (402). A similar relationship was identified

in colon cancer cells and suggests the use of CELF2 as a chemotherapeutic agent, where CELF2 overexpression induced apoptosis by inhibition of prostaglandin E2 via the COX-2 pathway, which is frequently overexpressed in neoplasms. Furthermore, downregulation inhibited radiation-induced apoptosis of colon cancer cells (403). CELF2 expression was also found to be reduced during neoplastic transformation in colon cancer, suggesting that it might play a crucial role in tumour initiation and progression (404). In pancreatic cancer, curcumin was found to inhibit tumour growth through mitotic catastrophe by increasing the expression of CELF2, thereby inhibiting the translation of COX-2 and VEGF mRNA (405). These studies suggest that overexpression of CELF2 has tumour-suppressive properties, and enhances apoptosis of tumour cells. In our study, an opposite relationship was found, where CELF2 was upregulated in aggressive tumours. Burgess and McCannel et al recently performed gene-expression analysis of 3 primary UM cell lines derived from patients who developed liver metastases within 1.5 years (406,407). In agreement to our findings, they identified CELF2 to be significantly upregulated in monosomy 3 tumours. Furthermore, van Gils et al also support this finding, with CELF2 upregulation identified as a classifier gene associated with poor prognosis (408). This suggests that CELF2 may play a role in UM via an alternative, unknown mechanism.

Protein phosphatase 1, regulatory subunit 3C (PPP1R3C) was downregulated by 1.376 fold in M3M (p: 0.000164). It is located at cytoband 10q23 and encodes a regulatory subunit of protein phosphatase-1 (PP1). It interacts with PPP1CC catalytic subunit of PP1 and associates with glycogen by forming complexes with glycogen phosphorylase, glycogen synthase and phosphorylase kinase which is necessary for its regulation of PP1 activity (409,410). PPP1R3C is predominantly involved in glycogen metabolism by activating glycogen synthase, reducing glycogen phosphorylase activity and limiting glycogen breakdown (410). PPP1R3C has been shown to be induced by hypoxia (411,412) and in breast cancer cells, hypoxia-inducible factor was shown to induce PPP1R3C expression to promote glycogen accumulation (413). PPP1R3C mRNA was reduced in a number of cutaneous melanoma cell lines

compared to melanocytes and was correlated with high proportion of promoter methylation (414). PPP1R3C was also found to be methylated in 25% of cutaneous melanoma tumours and in colon cancer cell lines, suggesting its role as a tumour suppressor gene (414). PPP1R3C was also identified as one of top 20 differentially methylated region in prostate cancer (415). Mutation and promoter hypermethylation of this gene with downregulation of expression was also identified in colorectal adenocarcinoma, but this was not observed in normal colonic mucosa (416,417). Although these studies have identified PPP1R3C in cancer, its role has not been studied extensively, and little is known about its functions.

### 4.2.1. Genes associated with apoptosis and proliferation

BRCA1-associated protein 1 (BAP 1) gene was downregulated by 1.34 fold in M3M compared to D3NM (p: 0.026). As monosomy 3 tumours are associated with metastasis and poor prognosis, the remaining chromosome 3 genes likely contain mutations on potential tumour suppressor genes that can lead to an aggressive phenotype. Harbour et al conducted exome sequencing of monosomy 3 UM samples and found that BAP1 had mutations on 3p21.1 in 85% of class 2 aggressive UM and almost never in class 1 tumours (25). Microarray gene expression profiling of 92.1 UM cells transfected with control versus BAP1 siRNA showed a shift in the expression profile towards a class 2 signature in BAP1 depleted cells compared to control cells (25). Interestingly, BAP1 depletion caused an increase in mRNA levels for the proto-oncogene KIT, which is highly expressed in class 2 tumours. Furthermore, RNAi-mediated knock down of BAP1 in 92.1 UM cells, which did not contain a detectable BAP1 mutation, recapitulated many characteristics of the de-differentiated class 2 UM phenotype (80). Either BAP1 mutation or loss of chromosome 3 can occur first, but both events appear to be necessary for the tumour to metastasise (26). It is localised to chromosome 3p21.31-p21.2, a region previously noted by Trolet et al to be deleted in UM (81). It encodes a deubiquitinating enzyme that interacts with the

breast cancer susceptibility gene (BRCA1) and BRCA1-associated RING domain protein 1 (BARD1) to form a tumour suppressor heterodimeric complex (29). It possesses a large C-terminal domain which is predicted to coordinate the selective association with potential substrates or regulatory components (82). Functionally, BAP1 enzyme removes ubiquitin molecules from specific proteins to regulate their function. For example, BAP1 removes ubiquitin molecules from histone H2A, which causes changes in the expression of specific genes that are regulated by this histone (83). It also modulates the assembly of multiprotein complexes containing numerous transcription factors and cofactors, and activates transcription in an enzymatic-activity–dependent manner, thereby regulating the expression of a variety of genes involved in various cellular processes (84). BAP1 has been implicated in several types of cancer such as lung, breast, and renal cell carcinoma (85–90). Germline BAP1 mutations have been described in families with a high risk for hereditary cancer and a novel 'BAP1 cancer syndrome' that includes UM, cutaneous melanoma and melanocytic neoplasm, lung adenocarcinoma, meningioma and malignant mesothelioma, has been described (91–95). In HeLa and other cell lines, BAP1 depletion altered the expression of genes that were key mediators of cell-cycle progression, DNA replication and repair, cell metabolism, survival, and apoptosis (84). *In vivo*, expression of wild-type BAP1 was shown to significantly decrease tumourigenicity of a human non-small cell lung cancer cell line in nude mice. Conversely, expression of mutant BAP1 that lacks either deubiquitinating activity or nuclear localization did not suppress tumourigenicity, implying that both deubiquinating activity and nuclear localization are necessary for the tumour-suppressive activity (96). Depsipeptide, a histone deacetylase HDAC inhibitor was shown to inhibit proliferation and growth by increasing expression of Fas and FasL in 3 UM cell lines derived from primary tumour and 2 cell lines derived from liver metastasis. Depsipeptide induced gene upregulation of both Fas and FasL in these cells, and an increase in activated caspase-3, apoptosis and cell-cycle arrest was observed in treated cells compared to non-treated cells (97). Landreville et al showed that HDAC inhibitors induced morphologic differentiation, cell-cycle exit, and a shift to a differentiated, melanocytic gene expression profile in

cultured UM cells. Furthermore, it was also shown to inhibit growth of UM tumours *in vivo* (98). Although BAP1 may function as a tumour suppressor in UM, the manner in which mutations/loss of this gene plays a role in the development of metastatic disease is not yet understood.

v-jun sarcoma virus 17 oncogene homolog (JUN) was differentially downregulated in M3M by 1.32 fold (p: 0.023). It is located in cytoband 1p32 and interacts directly with specific target DNA sequences to regulate gene expression. It is involved in a number of cell responses, such as cell proliferation and cell death (418). C-Jun and Jun kinase have been implicated in both pro- and antiapoptotic responses in different cells types (419). The most common known oncogenic mutations occur in GNAQ or GNA11, found in about 85% of all primary UM irrespective of tumour class or stage (23,24). Constitutive activation of the RAS/RAF/MEK/ERK pathway plays a crucial role in UM development, likely as a consequence of active mutations in the G-proteins GNAQ and GNA11 (24,34,36,37). In a recent study, microarray analysis of UM cell lines with GNAQ mutations treated with the MEK inhibitor selumetinib was performed to identify gene targets of activated GNAQ (38). The expression of JUN was shown to be induced upon treatment of UM cells with selumetinib while knockdown of c-Jun expression significantly increased the antiproliferative effects in these cell lines, suggesting that c-Jun induction may be involved in mechanisms of resistance to MEK inhibition. In another study, combined inhibition of MEK/MAPK and PI3K/AKT pathways in GNAQ-mutant cells showed significant increase of phosphorylated c-jun (54). Similarly, knockdown of c-jun significantly enhanced the growth-inhibitory effect of MEK and PI3K inhibitors. These studies coupled with our finding of downregulation of JUN in monosomy 3 tumours with metastasis suggest that JUN may play a metastasis-suppressor role in UM.

Deleted in liver cancer, DLC1 was downregulated by 2.137 fold in M3M (p: 0.0000142). It is located in cytoband 8p22 and encodes a GTPase-activating protein (GAP) that acts as a negative regulator of small RhoGTP-binding proteins (420). Aberrant upregulation of Rho proteins plays an important role in

tumourigenesis, progression and metastasis (421). DLC1 has been established as a genuine tumour suppressor gene and is increasingly considered a metastasis suppressor gene (422). It has been shown to regulate and inhibit cell motility, migration (423) and angiogenesis (424). Downregulation of DLC1 has been shown to be critically involved in hepatocellular carcinoma (425–429), breast carcinoma (430–434), lung carcinoma (431,435–437), prostate carcinoma (438–440) and various other malignancies (430,431,441–444) where it has been shown to promote neoplastic transformation, proliferation, invasion, migration, and metastatic dissemination. DLC1 also mediates its tumour suppressive effects via GAP-independent mechanisms. In lung carcinoma cells, Yang et al reported that DLC1 displaced Annexin 2 binding from the pro-inflammatory protein S100A10 (435). The latter is a critical surface receptor for plasminogen, which facilitates tumour invasion. Increased expression of DLC1 inactivated plasminogen and resulted in inhibition of *in vitro* cell migration, invasion, colony formation, and anchorage-independent growth of aggressive lung cancer cells (435). The Rho-GTPase activity is dependent on tensin-1, -2 and -3 binding, which is required to activate and mediate the antioncogenic effects of DLC1 (445,446). Dysregulation of epidermal growth factor receptor (EGFR) plays a critical role in cell growth and migration, and is associated with metastatic formation (447). Tensin-3 was shown regulate DLC1 Rho-GAP activity and inhibit EGFR-mediated cell migration and transformation, suggesting a combined therapeutic approach to target aberrant EGFR expression in cancer (445). Onken et al demonstrated that deletion of 8p12-22 was associated with more rapid onset of metastasis within high-risk class 2 tumours. They identified Leucine zipper tumour suppressor-1 (LZTS1) within this region as a metastasis suppressor gene in functional studies (448). In another study of 86 UM tumours and 66 liver metastases, loss of 8p has also been observed in 46% of primary UM tumours that metastasised, and in only one of the 15 non-metastasising tumours (449). Further, 45% of UM liver metastases also showed deletion of this region. Apart from chromosome 3 status, 8p loss and 8q gain were the main differences between metastasising and non-metastasising tumours. A recent large study of 320 UM tumours by Shields and colleagues showed that even in the presence monosomy 3, 8p loss

significantly increased the risk of metastasis and was found to be an independent predictor or poor metastatic outcome (450). Van Gils et al also identified DLC1 downregulation to be associated with 4-year disease free survival (408). However, DLC1 was not found to be a classifier gene in UM. Although DLC1 has never been studied in UM, our study provides compelling evidence to warrant further investigation into its role in the development of metastatic disease, which may yield novel biomarkers and targets for therapeutic intervention.

A disintegrin and metalloproteinase domain 10 (ADAM10) was found to be differentially upregulated in M3M by 1.72 fold (p: 0.008). This gene is located in cytoband 15q22 and is a cell surface protein with a unique structure possessing both potential adhesion and protease domains. ADAM10 is the principle sheddase for several other molecules associated with cancer proliferation, differentiation, adhesion and migration such as MET, Notch, E-cadherin, CD44 and L1 adhesion molecule (451). In agreement with our findings, the first and only study implicating ADAM10 in promoting UM metastasis and invasiveness was recently reported. Gangemi et al showed high ADAM10 mRNAexpression correlated with metastatic progression where only 37% of patients with high ADAM10 expression were metastasis-free after 6 years, compared to 70% of patients with low ADAM10 expression (452). *In vitro*, UM cells express the active form of ADAM10 which cleave m-Met and promote soluble MET release. As expected, siRNA knockdown of ADAM10 led to reduction of soluble MET levels and significantly inhibited cell invasion (452). Given the preferential dissemination of UM cells to the liver, HGF and MET have been investigated in several studies. High immunohistochemical expression of HGF and MET in primary UM tissues have been reported (66–68). Mallikarjuna et al found a significant association between high MET expression and death due to uveal melanoma. Interestingly, the 6 tumours with liver metastasis showed higher expression of MET and were negative for HGF, suggesting a possible mechanism of ligand-independent MET activation (69). The activation of PI3K/AKT pathway induced by the HGF/MET was shown to attenuate cell-cell adhesion by downregulation of cell adhesion molecules E-cadherin and beta-

catenin, promoting the enhanced motility and migration of uveal melanoma cells (70,71). On HGF stimulation, receptor MET translocated to the nucleus in a ligand-dependent manner, suggesting that MET may modulate the expression of genes involved in UM cell migration (70). Conversely, downregulation of MET expression decreased proliferation and migration by inhibiting AKT phosphorylation (67,72). Taken together, the correlation between ADAM10 expression and MET at mRNA and protein level shown by Gangemi et al, and our findings of differential upregulation of ADAM10 expression in monosomy 3 tumours with metastasis, suggests that both molecules contribute to the development of metastatic disease in UM.

Inhibition of Notch signalling has been shown to inhibit several cancer types, such as lung (453) , pancreatic (454,455) and gastrointestinal cancers (456,457). In UM cells, Asnaghi et al demonstrated suppression of tumour spread and hypoxia-induced invasion by inhibition of Notch signalling *in vitro* (458). Transfection of the Notch ligand Jag2 into UM cells led to a 3 fold increase in growth, motility and invasion, suggesting the involvement of Notch pathway in promoting growth and metastasis (459). Furthermore, direct knockdown and suppression of Notch1 expression in UM cells resulted in significant inhibition of growth (460). When combined with recombinant oncolytic adenovirus H101, which replicates specifically in p53-depleted tumour cells, remarkable tumour growth inhibition and prolonged mouse survival in xenograft mice model was successfully demonstrated, suggesting Notch pathway deregulation in UM (460). Indeed, the expression of Notch receptors, ligands and targets were found in 5 UM cell lines and 30 primary UM tissue samples (461). Constitutively active forms of Notch1 and Notch2 promoted growth of UM cells but pharmacologic blockade using the γ-secretase inhibitor MRK003 suppressed growth and invasion *in vitro* and *in vivo* (461). TIMP3 is an endogenous inhibitor of ADAM, and the activity of ADAM is thought to be upregulated in cancers due to the loss of TIMP3, possibly through its promoter hypermethylation (462). In our analysis, TIMP3 was found to be differentially downregulated by 1.41 fold in monosomy 3 tumours with metastasis (M3M) compared to disomy 3 tumours without

metastasis (D3NM). This is an interesting finding, as van der Velden et al also demonstrated differential downregulation of TIMP3, due to promoter methylation, in metastatic cell lines (derived from liver metastases) compared to primary UM cell lines from the same patient (463).

Tryptophanyl-tRNA synthetase (WARS) was upregulated by 1.39 fold in M3M (p: 0.000144). It is located at cytoband 14q32 and regulates ERK, AKT, and eNOS activation pathways that are associated with angiogenesis, cytoskeletal reorganization and shear stress-responsive gene expression (464,465). Elevated WARS has been shown to be induced by TNF- α, interferon-α and γ, resulting in inhibition of angiogenesis and cell growth (466–469). Specifically in the eye, it is a potent antagonist of VEGF-induced retinal angiogenesis and has been suggested as a potential treatment of neovascular ocular diseases (470). Low immunohistochemical expression of WARS in colorectal carcinoma tissue correlated with increased risk for recurrence and worse survival, likely secondary to its antiangiogenic properties (471). In pancreatic carcinoma cell lines, low expression of WARS with concomitant increase in metastatic potential was shown to be induced by hypoxia (472). Anti-VEGF agents have been shown to suppress *in vitro* growth and *in vivo* hepatic micrometastases in UM (473,474). In our study, WARS was upregulated in aggressive UM by a modest 1.39 fold. Nevertheless, it is likely that the molecular characteristics of upregulated WARS in aggressive UM is independent of its anti-angiogenic properties.

Branched chain aminotransferase 1, cytosolic (BCAT1) is located at cytoband 12p12 and was upregulated by 1.674 fold in M3M (p: 0.0071). It was also identified to be upregulated by McCannel et al in their study of 3 aggressive primary UM cell lines with monosomy 3 loss (407). It is involved in amino acid metabolism and is essential for cell growth (475). BCAT1 is suggested to be involved in proliferation and tumour formation (476). In colorectal cancer, BCAT1 protein expression was significantly higher in advanced primary tumours that metastasised, compared to those that did not. Positive immunohistochemical expression predicted distant metastases and was associated with poor 5 year

survival compared to negative tumours, suggesting its use as a biomarker and therapeutic target (477). BCAT1 gene expression is regulated by MYC (478) and has been shown to be directly targeted by MYC during tumourigenesis (479,480). MYC induced overexpression of BCAT1 gene in nasopharyngeal carcinoma and *in vitro* inhibition of proliferation was observed when BCAT1 expression was suppressed (481,482). It is likely that BCAT1 upregulation in M3M is secondary to MYC expression. The MYC gene is located on chromosome 8q24.21. In UM, amplification of chromosome 8q is strongly associated with metastatic death (483). In our proteomic study, PRDX3 was upregulated in aggressive UM. MYC also directly induces PRDX3 expression which is required for MYC-mediated transformation and maintenance of mitochondrial function (484). The potential significance of MYC in UM is discussed **in** section 4.3.2, page 230.

### 4.2.2. Genes associated with adhesion and cellular organisation

Syndecan 2 (SDC2) was upregulated by 1.848 fold in M3M (p: 0.000348). It is located at cytoband 8q22.1 and functions as an integral membrane protein and participates in cell proliferation, cell migration and cell-matrix interactions via its receptor for extracellular matrix proteins (485). SDC2 also mediates cell binding and signalling (485). It has been shown to interact with syntenin-1, which functions as a cytosolic signal effector downstream from SDC2 to regulate the surface availability of a number of cell adhesion and signalling molecules (486–488). Syntenin-1 was identified by Pardo et al (489) in a proteomic study of 5 UM cell lines' secretome. SDC2 was also identified by van Gils et al as a classifier gene (408). In another study, high levels of syntenin protein expression in primary UM tumour was found to be significantly associated with earlier metastatic progression and correlated with metastatic risk as strongly as monosomy 3 (490). Furthermore, UM liver metastases also showed higher syntenin expression compared to primary tumours (490). The authors also demonstrated that inhibition of syntenin expression reduces the activation of FAK, Src and AKT. Src has been shown to be an upstream tyrosine kinase for ERK1/2 activation in primary UM (264). Similarly, MAPK pathway has been implicated in uveal melanoma (33,34,154).Dasatinib, a Src family kinase inhibitor, was recently shown to inhibit MAPK and induce growth arrest in monosomy 3 UM cell cultures (265). Thus, syndecan 2 and its intrinsic interaction with syntenin-1 may be critical in metastatic formation and dissemination in UM, and warrants further investigation as a therapeutic target.

Cell adhesion molecule with homology to L1CAM, CHL1 was downregulated by 2.924 fold in M3M (p: 0.0000643). It is located in cytoband 3p26 and encodes a member of the L1 gene family of neural cell adhesion molecules (L1CAM). Deregulated expression of L1CAM has been implicated in various cancers such as cutaneous melanoma (491), ovarian (492), prostate (493)

and colon cancer (494). Deletions of chromosome 3p is one of the most common alterations in oesophageal squamous cell carcinoma, and CHL1 deletion was associated with poor prognosis and identified as a putative tumour suppressor gene (495,496). Similarly, CHL1 was also suggested as a tumour suppressor gene in nasopharyngeal carcinoma (497). In breast cancer tissues, CHL1 downregulation was associated with high-grade phenotype while *in vitro* studies showed that overexpression suppressed proliferation and invasion (498). Likewise, knockdown of CHL1 expression increased proliferation and invasion in breast cancer cells (498). In neural progenitor cells (NPCs), CHL1 deficiency enhanced activation of ERK1/2 mitogen-activated protein kinase (MAPK) and stimulated proliferation and differentiation of these cells (499). Downregulation of CHL1 was also observed in several types of cancer (breast, kidney, rectum, colon, thyroid, stomach, skin, small intestine, bladder, vulva and pancreatic cancer), and suggested to act as a tumour suppressor gene (500). However, upregulation of CHL1 was associated with metastatic growth in ovarian, colon and breast cancer (500). This suggests that CHL1 may function as a tumour suppressor gene in several cancers and as an oncogene in others. In cervical cancer cells, Long et al demonstrated that miR-10a regulated CHL1 expression (501). Overexpression of miR-10a negatively regulated CHL1 expression and promoted colony formation, migration and invasion, suggesting that miR-10a/CHL1 mediated metastatic formation. Cell adhesion molecules in UM have been investigated in several studies. Burgess and McCannel et al have also identified CHL1 downregulation in primary UM cell lines derived from aggressive tumours (406,407). Analysis of activated leukocyte cell adhesion molecule (ALCAM) located in chromosome 3q13 did not reveal methylation-mediated silencing of this gene in UM tumour tissues (502). In a more recent study, silencing ALCAM expression reduced invasiveness of a UM cell line *in vitro*. However, ALCAM overexpression did not increase motility or invasion, suggesting that ALCAM's regulation of adherens junctions may differentially enhance or decrease invasiveness, depending on the type of cadherin adhesion complexes present in the primary tumour, and on the cadherin status of the tumour cells themselves (503). Immunohistochemical expression of melanoma

adhesion molecule (MCAM) in primary UM tumours was shown to be associated with metastatic death (504). In another study, intercellular cell adhesion molecule 1 (ICAM1) was an independent risk factor for metastasis within 5 years of diagnosis, while expression of neural cell adhesion molecule (NCAM) and vascular cell adhesion molecule 1 (VCAM1) was not related to metastasis formation (505). Mooy et al, however, demonstrated that NCAM was significantly more expressed in aggressive, rapidly metastasising tumours and in metastatic tissues (506). Interestingly, complete loss of CHL1 expression was shown in monosomy 3 tumours, but not due to allele loss, mutations or epigenetic alteration, suggesting that CHL1 downregulation was mediated by other mechanisms (507). However, functional studies of CHL1 in UM are lacking and its role as a potential tumour suppressor gene in UM needs to be investigated further.

Arg/Abl-interacting protein ArgBP2 (SORBS2) was downregulated by 2.545 fold in M3M (p: 0.000181). It is located in cytoband 4q35 and encodes an adapter protein that plays a role in the assembling of signalling complexes, being a link between ABL kinases and actin cytoskeleton (508). SORBS2, also known as Sorbin and SH3 domain-containing protein 2, has several well-defined structural motifs comprising three Scr homology 3 domains (SH3), a sorbin homology domain (SoHo), proline-rich ligand-binding sites and several serine/threonine phosphorylation sites (509). It also functions as a scaffold protein that regulates the balance between adhesion and motility by coordinating the function of multiple signalling pathways converging on the actin cytoskeleton (509). SORBS2 protein can form complex with ABL1 and CBL, thus promoting ubiquitination and degradation of ABL1 (508). SORBS2γ also functions as an adaptor protein for AKT1 and PAK1 to promote cell survival via AKT1/PAK1 pathway (510). An immunohistochemical study has demonstrated that phosphorylated AKT correlates with poor prognosis in UM (49). Increased PAK1 expression was identified in invasive UM cell lines and knockdown led to a 5-fold decrease in invasive potential, suggesting that it is associated with tumour progression and metastasis (511). Suppression of AKT activation and MET (also implicated in UM)

by natural withanolide withaferin A inhibited cell proliferation, and induced apoptosis in multiple UM cell lines *in vitro* (512). However, whether the AKT/PAK1 pathway plays a role in UM is unknown. In our study, SORBS2 was downregulated in aggressive UM. This suggests that SORBS2 plays a protective role in a manner that is independent of γ-isoform's AKT/PAK binding properties. Interestingly, McCannel et al also identified decreased SORBS2 expression in monosomy 3 tumours (407). Furthermore, van Gils et al identified SORBS2 as a classifier gene in UM, with decreased expression associated with poor prognosis (408). SORBS2 was identified as a tumour suppressor gene in cervical carcinoma. Inducing its expression in cell lines led to significant reduction in proliferation, colony formation and anchorage-dependant growth (513). A truncation in the SORBS2 gene has also been identified in a Burkitt lymphoma cell line (514). SORBS2 expression in the pancreas, which is high in normal tissue, was lost during oncogenic transformation, and its expression was decreased in malignant tumours (515). *In vitro*, expression of SORBS2 inhibited adhesion and migration of cancer cells. When its expression in a highly invasive cell line was restored and injected into mice, the ability to form tumours was reduced, demonstrating anti-tumoural properties. As SORBS2 is involved in the organisation and stabilisation of the actin cytoskeleton, Taieb et al postulated that decreased expression leads to actin disorganization, cell dedifferentiation, and eventually, to abnormal cell migration and invasion (515). Taken together, these findings suggest that downregulation of SORBS2 may increase its metastatic capabilities while its expression may inhibit metastatic formation in UM.

Thrombospondin 2 (THBS2) was upregulated by 2 fold in M3M (p: 0.000864). It is located at cytoband 6q27 and encodes the thrombospondin family of matricellular proteins that mediates cell-to-cell and cell-to-matrix interactions (516). It interacts with matrix metalloproteinase-2 (MMP2) where high expression of THBS2 led to increased cell adhesion and migration (517). In ovarian and colorectal carcinoma, THBS2 was one of 2 genes suggested as a "core metastasis-associated" gene expression signature (518). In lung carcinoma, THBS2 and MMP9 was suggested to play an important role in metastatic

formation (519). Gene expression profiling of prostate cancer versus normal prostate tissue identified THBS2 as one of 28 transcripts significantly associated with recurrence after radical prostatectomy (520). Tumour-derived pancreatic stellate cells are essential cellular components of the pancreatic tumour microenvironment that releases growth factors, proteases, and extracellular matrix proteins to stimulate the spread of pancreatic cancer (521). These cells were shown to express high levels of THBS2 protein to promote and enhance invasion of pancreatic cancer cell lines while the opposite held true, where knockdown of THBS2 expression suppressed invasion of cancer cells (521). In epithelial ovarian tumours, higher expression of THBS2 was shown to correlate with an aggressive phenotype, while its expression was not detected in borderline epithelial tumours (522). In cutaneous melanoma, THBS2 was strongly expressed in melanoma metastases but not in primary tumours (523). Another study however suggests the opposite, where THBS2 was suggested to suppress haematogenous metastasis (524). THBS2 protein has also been shown to inhibit angiogenesis (525,526) and tumour growth *in vivo* (526). It has been shown to be protective in multistep carcinogenesis where THBS2 deficient mice demonstrated dramatically enhanced susceptibility to skin carcinogenesis, accelerated tumour formation and growth (527). In an immunohistochemical study, variable THBS2 expression was detected in UM tumour tissues in approximately 40% of specimens, but was not associated with survival, tumour vascularity or any other histopathological parameters of survival (528). In another UM study, another member of the thrombospondin family, THBS1 was effective in attenuation of tumour growth while THBS1 was decreased in response to the angiogenic switch during progression of uveal melanoma (529). Based on current evidence, high expression of the matricellular THBS2 may be associated with aggressive/metastatic disease in some malignancies, likely by facilitating adhesion and activating cell signalling pathways that regulate motility. Conversely, its protective effect in other tumours may be secondary to its antiangiogenic properties.

Multiple Epidermal Growth Factor 10, MEGF10 was downregulated by 3.47 fold in M3M (p: 0.0000084). It is located at cytoband 5q23 and encodes for membrane receptors that are critical in phagocytosis of apoptotic cells by macrophages (530). It also plays a role in cell adhesion by facilitating mosaic-like adhesion patterns such as those found in retinal neuronal arrangement (531,532). It is essential in the regulation of myogenesis and has been described in a variety of disorders such as congenital myopathy (533), and early onset myopathy, areflexia, respiratory distress and dysphagia (EMARDD) (534,535). MEGF10 has also been shown to suppress proliferation by inhibiting cell motility necessary for cell division (532). MEGF10 was 1 of 25 genes identified in 12 different paediatric cancer tissues compared to normal, suggesting that it may play a significant role in tumourigenesis (536). In acute myeloid leukaemia, MEGF10 it was identified as a marker of favourable outcome (537). Interestingly, MEGF10 was also significantly downregulated in fine-needle aspiration biopsy samples of monosomy 3 UM tumours (407) and in 3 UM cell lines derived from primary UM tumours that metastasised within 1.5 years (406). Our results are in keeping with these studies, and suggests that downregulation of MEGF10 may promote UM metastases by promoting tumour cell motility and proliferation with a concomitant inhibition of apoptosis.

## 4.3. Thioredoxin-dependant peroxidase reductase (PRDX3)

Quantitative LC-MS proteomic analysis of UM tissues identified differential upregulation of PRDX3 by 1.58 fold (p: 0.002) in primary UM tissues from patients that developed metastasis compared to those that did not. Although not statistically significant, immunohistochemical staining of PRDX3 on 13 primary UM tumours of patients that developed metastatic disease (mUM) and 13 primary UM tumours of patients that did not develop metastasis (nmUM) showed a trend towards higher expression in mUM compared to nmUM. All of the tumours in the mUM group demonstrated either moderate or strong staining (76.9% and 23.1%). Interestingly, 3 samples in mUM that showed strong staining throughout the tumour were from patients that died within 10 months after enucleation; 2 with liver metastases died between 4-10 months after enucleation and 1 with lung metastasis died 7 months after enucleation. However, there were also 4 tumours in nmUM that demonstrated strong staining varying from 50% to 100% of tumour tissue. A significant difference between percentage of tumour cells staining in mUM compared to nmUM was observed, but not for intensity of staining. There was a significant correlation between high PRDX3 expression and monosomy 3 tumours. No other significant correlation was found between PRDX3 expression and other histopathologic factors. The lack of meaningful statistically significant results of PRDX3 expression may be explained by the relatively small sample size of 26 tumours.

No significant correlation was found between PRDX3 expression and cell type or tumour size. It was not possible to determine if PRDX3 expression was associated with chromosome 3 status, as all 17 tumours with chromosome 3 information available (10 monosomy and 7 disomy 3 tumours) demonstrated high expression of PRDX3. A statistically significant difference of PRDX3 expression was observed in patients that did and did not develop metastasis. A significant positive correlation between high PRDX3 expression and metastasis

was observed. Likewise, a significant correlation between high PRDX3 expression and shorter survival was found. The difference in overall survival between tumours that demonstrated low and high expression of PRDX, demonstrated by Kaplan-Meier survival curve, was also significant. Incorporation of PRDX3 expression in logistic regression analysis increased the probability of predicting metastasis by 9.8%. Using PRDX3 expression score of low/high, 43.2% of patients with no metastasis and 87.3% of patients with metastasis would be successfully predicted, giving an overall positive predictive percentage of 69.6%. Based on this study population, a patient with high expression of PRDX3 would be 5.22 times more likely to develop metastasis compared to one with low expression.

In this study, 2 members of the PRDX family were identified that were statistically significant; PRDX3 and PRDX4 (1.58 and 2.19 fold upregulated in metastatic primary UM respectively. The PRDX family (I–VI) is critically involved in redox regulation of the cell and protect radical-sensitive enzymes from oxidative damage by a radical-generating system. These isoenzymes are widely distributed subcellularly, in contrast to the most other antioxidant enzymes. PRDXs exert their protective antioxidant role in cells through their peroxidase, whereby hydrogen peroxide, peroxynitrite and a wide range of organic hydroperoxides are reduced and detoxified (538–540). In addition, these proteins are also involved in a range of other cellular roles, including the modulation of cytokine-induced hydrogen peroxide levels, which have been shown to mediate signalling cascades leading to gene expression, cell proliferation, differentiation and apoptosis (538,541,542).

### 4.3.1. PRDX3 inhibits apoptosis via the intrinsic pathway

Normal cellular processes that involve oxygen result in the production of reactive oxygen species (ROS) such as superoxide ($O_2^{\cdot -}$), hydrogen peroxide ($H_2O_2$), and hydroxyl radical ($OH^{\cdot}$). Each of these species has the potential to oxidize macromolecules and thereby to induce mutation of DNA, impairment of protein function, and lipid peroxidation. $O_2^{\cdot -}$ does not readily cross the mitochondrial membrane, given its charged nature. $O2^-$ is catalysed by $Mn^{2+}$ dependent superoxide dismutase (MnSOD) present in mitochondrial matrix (543). This protects mitochondrial function from $O_2$- mediated damage of various enzymes. Although MnSOD relieves mitochondrial oxidative stress caused by $O_2^{\cdot -}$, it generates $H_2O_2$ causing a different type of oxidative stress. Furthermore, $H_2O_2$ is readily converted to the more powerful oxidant $OH^{\cdot}$ via the Fenton reaction. Intracellular $H_2O_2$ is removed mostly by catalase, glutathione peroxidase (GPx), and peroxiredoxin (PRDX). However, the vast majority of mitochondrial $H_2O_2$ is catalysed by PRDX3, with mitochondrial GPx1 accounting for removal of only 15% of $H_2O_2$ (544). Furthermore, PRDX3 is much more abundant in mitochondria than GPx and is therefore a critical regulator of mitochondrial $H_2O_2$ concentration (545). On reaction with $H_2O_2$, the redox-sensitive Cysteine residue of each subunit of the PRDX homodimer is oxidized to Cys-SOH, which then reacts with a neighboring Cys-SH of the other subunit to form an intermolecular disulphide (546). This disulfide is reduced specifically by thioredoxin, not by glutathione or glutaredoxin (546). The reduced form of thioredoxin is then regenerated by thioredoxin reductase at the expense of NADPH .(547–549).

Apoptosis is a genetically determined process of cell self-destruction to eliminate DNA-damaged, superfluous, or unwanted cells. Dysregulation of this normal physiological process may result in uncontrolled cell growth and ultimately, tumour formation and progression. Resistance to apoptosis can also augment the escape of tumour cells from surveillance by the immune system

(550). Apoptosis occurs via two alternative pathways: either through “death receptors” on the cell surface (extrinsic pathway) or through intracellular mitochondria (intrinsic pathway). Mitochondria play a central role in this process by releasing cytochrome c and other proapoptotic proteins that ultimately leads to the formation of an apoptosome and subsequently apoptosis. The mitochondrial production of ROS is also thought to be associated with the activation and propagation of apoptosis (551,552). Indeed, generation of ROS by mitochondria appears to be an early event in apoptotic signalling initiated by TNF-α, ceramide, or glutamate (553–555). Various studies have demonstrated the role of $H_2O_2$ as a second messenger in both extrinsic and intrinsic apoptotic pathway (556–558).

Chang et al recently identified PRDX3, via its effects on $H_2O_2$, to be a critical regulator of apoptotic signalling (545). Depletion of PRDX3 resulted in increased intracellular $H_2O_2$, cytochrome c and other proapoptotic molecules such as caspase 3, sensitising cells to induction of apoptosis by staurosporine or TNF-α (545). Although many proapoptotic stimuli induce the intracellular accumulation of $H_2O_2$, a causal relationship between the mitochondrial generation of $H_2O_2$ and its active participation in apoptosis was shown (545). Therefore, cells that express PRDX, or indeed increased PRDX expression may catalyse the production of TNF/staurosporine-mediated mitochondrial $H_2O_2$ necessary for apoptosis. The increased expression of PRDX3 in primary UM tissues from patients who developed metastasis found in this study indicates its potential role as a suppressor of mitochondria-mediated apoptosis by eliminating $H_2O_2$. Via this mechanism, UM cells expressing high levels of PRDX3 may evade apoptosis, leading to uncontrolled cell proliferation. PRDX3 also protects the mitochondria against $H_2O_2$ and $OH^{\cdot}$ mediated mitochondrial RNA damage. This supports the well-established knowledge that tumour cells exhibit a high metabolic rate to support rapid proliferation and growth.

Overexpression of PRDX3 protects thymoma cells from apoptosis induced by hypoxia, a bolus of peroxide or the anticancer agent imexon (559). In prostate cancer cells, increased mitochondrial ROS was observed secondary to high metabolism (560). In these cells, PRDX3 and PRDX4 may be upregulated as part of their anti-oxidant defence response in order to protect organelles from oxidative damage and prevent cell death (399). Another study also identified PRDX3 overexpression in prostate cancer, where these cells demonstrated resistance to $H_2O_2$-induced apoptosis through a failure to activate pro-apoptotic pathways (400). High expression of PRDX3 in prostate cancer tissues was also shown to be associated with aggressive disease and poor patient outcome (561). PRDX3, along with PRDX4, was also identified in a prostate cancer tissue proteomic study where these proteins were overexpressed and increased proliferation of prostate cancer cell lines (562). An immunohistochemical study identified a positive correlation between PRDX3 expression and proliferation in breast cancer tissues. Silencing PRDX3 gene in breast cancer cell lines also decreased proliferation and induced cell cycle arrest at the S and G2/M phase (563). Another study observed that the overexpression of PRDX I–III in breast cancer could be explained by the antiapoptotic and proliferative effects that these proteins exert (564). Karihtala et al found high expression of PRDX I, III, IV and V in breast carcinoma, suggesting that PRDXs are able to inhibit $H_2O_2$-mediated physiological apoptosis, cause abnormal proliferation, and thereby may lead to tumourigenesis (565). Specifically, they found a correlation between strong PRDX3 expression and poorly differentiated tumours. In lung squamous and adenocarcinoma, upregulation of PRDX1, PRDX3 and TRX was observed and suggested to represent an attempt by tumour cells to adjust to the microenvironment in a manner that is advantageous to survival and proliferation (566). In hepatoma cells, overexpression of PRDX6 conferred resistance to peroxide-induced apoptosis, suggesting that its up-regulation may be a tumour-supportive adaptation in cancerous states (567). Neuroblastoma cells that were depleted of PRDX3, along with PRDX5 were more prone to oxidative damage and apoptosis (568). Taken together, high PRDX3 expression found in aggressive UM may be necessary to inhibit apoptosis, upregulate cell proliferation to provide

growth advantage to the tumours cells. In addition to that, high PRDX3 expression would sustain and support the high metabolic demand of these cells, facilitating propagation and dissemination, ultimately leading to metastasis.

Dioscin is a glucoside saponin which has been shown to possess anti-proliferative properties against a number of human cancer cells such as leukaemia, lung adenocarcinoma and HeLA cells (569–571). A recent study by Wang et al demonstrated that the pro-apoptotic activity of dioscin in oesophageal cancer cell lines was mediated by PRDX1 and PRDX6, via the intrinsic mitochondrial pathway (572). Dioscin led to a decrease in PRDX1 and PRDX6 levels, thereby causing an increase in ROS levels leading to apoptosis. However, overexpression of PRDXs significantly blocked the elevated ROS levels and apoptosis induced by dioscin, suggesting the central importance of PRDXs in the mechanism of action of dioscin in inducing cancer cell apoptosis. The authors suggest that agents which either increase ROS generation or decrease the expression of antioxidant enzymes have the potentiality to target cancer cells with little or no effect on normal cells. This may have significant therapeutic implications in UM. While PRDX3 wasn't identified by Wang et al, the use of this agent to determine its effects in UM cells *in vitro* should be investigated. To support this, Wang et al identified PRDX1 and PRDX6 by comparing dioscin-treated and non-treated cancer cells, to identify differential expression of proteins that may be central to its apoptotic effects. As shown in numerous other studies, a variety of PRDXs have been implicated in different human cancers. As dioscin has been shown to initiate apoptosis via the mitochondrial pathway, the exclusive localisation of PRDX3 within the mitochondria provides further justification to study its effects in UM.

### 4.3.2. MYC activates PRDX3 expression and stimulates proliferation

Deregulated overexpression of MYC, which mimics conditions found in cancer cells, directly induces PRDX3 expression that is required for MYC-mediated transformation and maintenance of mitochondrial function (484). The MYC gene is located on chromosome 8q24.21. In UM, amplification of chromosome 8q is strongly associated with metastatic death (483). Several studies have determined the expression of MYC in UM. MYC was amplified in 5 of 8 hepatic metastatic lesions analysed by FISH (573). Larger tumour size and tumours with monosomy 3 were significantly associated with amplification of MYC (574). High expression of MYC was associated with high proliferative index in UM tissues (575), and high MYC expression, MIB-1 index and large tumour diameter were independent prognostic parameters for poor outcome (576). Conversely, Chana et al demonstrated improved survival in MYC positive tumours (577,578). The authors did however identify a link between MYC overexpression and UM resistance to interferon-α, supporting the concept that MYC downregulation is associated with the cell growth inhibition produced by interferon-α and that resistance is associated with tumour MYC overexpression (579). Recently, gene microarray study of high-grade tumours overexpressing chromosome 8q showed upregulation of Development And Differentiation-Enhancing Factor (DDEF1) also located on chromosome 8q24.21, but not MYC (580). However, the specific functional effects of MYC in UM are yet to be determined. Given that it directly activates PRDX3, future studies to investigate this may yield further insights into the tumour biology and potential therapeutic targets.

Experimental models of MYC-mediated tumourigenesis suggest that established tumours are addicted to MYC and that deregulated expression of MYC result in an addiction not only to MYC but also to nutrients (581). MYC regulates energy metabolism through its direct activation of genes involved in glycolysis, glutamine metabolism and mitochondrial biogenesis (582,583). MYC is also known to induce the production of ROS, possibly through its induction of mitochondrial biogenesis and increased metabolism, causing genomic instability (584–586). In UM, overexpression of MYC may induce sustained oxidative insult on the genome of tumour cells, causing specific chromosomal alterations found in UM, such as loss of heterozygosity/monosomy 3 that ultimately leads to the metastatic phenotype. It may also be hypothesised that once the level of MYC-induced ROS reaches this threshold level, the expression of PRDX3 increases in response to the increased oxidative stress. This would further inhibit apoptosis and protect mitochondria from oxidative damage, enabling normal physiological function to meet the high-energy requirement of UM tumour cells.

This potential MYC-induced changes in aggressive UM provides an opportunity to develop therapeutic targets. In fact, knock-down of MYC in established cancer cell lines inhibited cell proliferation at various stages of the cell cycle, and in some instances induced apoptosis (587–589). Furthermore, expression of a dominant negative inhibitor of MYC heterodimerization *in vivo* resulted in rapid regression of incipient and established lung tumours, suggesting that inhibiting MYC function could be a potential therapeutic strategy (590). Strategies have emerged to inhibit MYC expression, to interrupt MYC-MAX dimerization, to inhibit MYC-MAX DNA binding, and to interfere with key MYC target genes (581). BET bromodomain regulatory proteins recently emerged as potent regulators of MYC expression in different tumour types (581). BRD4, a transcriptional regulator in the BET domain, was shown to bind to the MYC promoter region and play a critical role in MYC expression in human cancer cells. Inhibition of BET BRD4 protein could inhibit *in vivo* tumourigenesis, suggesting that targeting MYC expression is feasible in selected cancers (591,592). Targeting MYC-induced repression of miR-26a in liver cancer animal models resulted in a

remarkable response, suggesting that interfering with MYC regulated microRNAs could be therapeutically feasible (593). Phosphofructokinase, PFKM is another target gene of MYC (594) that may have implications in UM. Although not statistically significant (p=0.06), PFKM was upregulated by 2 fold in metastatic primary UM tissue. Furthermore, a recent proteomic study found downregulation of PFKM in irradiated 92.1 cells, suggesting its role in cell-cycle arrest and tumour senescence (241). Activation of PFK is regulated by the bifunctional enzyme 6-phosphofructo-2-kinase/fructose-2,6-bisphosphatase (PFKFB), which in turn is regulated by protein kinases such as AKT and MAPK (287). It has been shown that the MEK/MAPK and PI3K/AKT pathways are highly activated in UM (33,34,154,155). In a phase II study, the MEK inhibitor selumetinib extended progression-free survival by nearly 9 weeks and reduced tumour size by 50% in patients with UM (288). This downregulation of PFKM may reflect a shift in the energy demand of tumour cells post radiation, possibly via the inhibition of MAPK and AKT pathways. Taken together, the direct inhibition of MYC may be a feasible therapeutic target in UM, and warrants further investigation.

In this study, the significance of high PRDX3 expression in primary UM tissues that developed metastasis and its association with shorter survival may represent a potential involvement of this protein in tumour growth and dissemination. Its role in inhibiting apoptosis and interaction with the MYC and MAPK pathway likely promotes tumour cell survival, proliferation and eventually metastatic formation. Further analysis of the expression, activity level, and function of PRDX3 in UM would be essential for defining the potential role of these proteins as novel biomarkers and therapeutic targets. Such studies could also provide new insights into the role of PRDX3 as a potential biological determinant contributing to the development of metastatic disease.

## 4.4. Cytosolic non-specific dipeptidase (CNDP2)

Quantitative LC-MS proteomic analysis of UM tissues identified CNDP2 as being was downregulated by 1.75 fold (p: 0.001) in primary UM tissues from patients that developed metastasis compared to those that did not. Immunohistochemical staining of CNDP2 on 13 primary UM tumours of patients that developed metastatic disease (mUM) and 13 primary UM tumours of patients that did not develop metastasis (nmUM) did not show any statistically significant difference of expression between the two groups. A trend towards lower expression in mUM was found, with 46% of mUM tumours demonstrating no CNDP2 expression (no staining) while all nmUM tumours showed positive staining for CNDP2. However, no significant difference was seen when comparing the intensity or percentage of staining between mUM and nmUM. No significant correlation between CNDP2 score and survival in patients with metastatic disease was found, but higher expression significantly correlated with disomy/trisomy 3 tumours compared to monosomy 3. No other significant correlation between CNDP2 score and clinicopathological factors were found. Apart from correlation with chromosome 3 status, the lack of significant results of CNDP2 expression may be explained by the relatively small sample size of 26 tumours. Due to a relatively weak staining in both mUM and nmUM tissues, CNDP2 was not evaluated further in the larger cohort of UM microarray samples.

CNDP2 is a nonspecific dipeptidase that is widely distributed in central and peripheral human tissues of adults (595). It is predominantly involved in amino acid metabolism and hydrolyses a variety of dipeptides including L-carnosine, but has a strong preference for Cys-Gly and hydrophobic dipeptides including prolyl amino acids. It exists in 2 isoforms; isoform 1 and isoform 2. CNDP2 is mainly implicated in the susceptibility of developing diabetic nephropathy with conflicting results (596–598), and in Parkinsons disease, where it was found to be elevated (599). Only 2 published reports directly implicate low expression of CNDP2 with malignancies, suggesting that it may exert tumour-

suppressive effects (600,601). However, CNDP2 has also been identified in various genomic and proteomic studies in cancer, though it has never directly implicated in cancer development or progression (602–607).

Deletion of CNDP2 gene was observed in 27.2% cancer specimens from an aCGH study containing more than 3,000 cancer specimens where high frequency of copy number loss was observed in oesophageal squamous cell carcinoma (63.6%) and colorectal cancer (50.9%), suggesting that deletion of this gene is common in several gastrointestinal cancer types (602). CNDP2 was identified as one of 95 genes that were differentially upregulated in a study comparing secondary metastatic oral squamous carcinoma to primary tumours (603). This gene signature was also found to be strongly associated with poor patient outcome in an independent cohort of patients. A recent microarray study compared gene expression profiles of normal CD34+ bone marrow cells to those from patients with myelodysplastic syndrome (MDS) to identify gene signatures for classification of different subtypes of the disease (607). Different gene signatures were found to distinguish MDS from normal, aggressive MDS from normal, stable MDS from normal and del(5q) MDS from normal. The del(5q) subtype is classified as low-risk category and is treated with lenalidomide as standard practice (608). Of the 4 categories studied, overexpression of CNDP2 was one of 33 member gene signature identified that distinguished between del(5q) MDS and normal subjects. Since CNDP2 wasn't identified in the gene signature of more aggressive subtypes, its overexpression in low-risk MDS may correlate with our findings of higher expression in primary UM that did not metastasise.

In cutaneous melanoma, a GEP study comparing invasive vs. non-invasive mouse xenograft models identified CNDP2 to be upregulated in the invasive model (606). However, this opposite relationship to our results may not be of any significance, since the molecular characteristics between cutaneous melanoma and UM differ significantly. It is known that these are 2 separate disease entities, with almost exclusive cytogenetic and molecular characteristics.

Genetic mutations associated with cutaneous melanoma such as BRAF and NRAS are rare in UM, while mutations in GNAQ and BAP1 are absent in cutaneous melanoma (609,610). Clinically, uveal melanoma spreads haematogenously, while cutaneous melanoma also spread via the lymphatic system. Therefore, it is likely that CNDP2 may play different roles in different cancer types.

In order to derive an objective method to grading of clear cell renal carcinoma, LC-MS/MS study of 50 cancer samples equally distributed among normal tissues and Fuhrman grades 1–4 was performed by Perroud et al (605). Grade 1 tumours have the most favorable prognosis with lowest risk for metastasis while grade 4 is associated with high-metastatic risk (611). CNDP2 was identified as the most statistically significant protein to be overexpressed in grade 1 and 2, while the abundance of this protein was uniformly low across normal, grade 3 and 4 samples. However, the authors did not further investigate the specific properties of CNDP2 in this disease. A recent 2D-DIGE proteomic analysis identified CNDP2 as one of 68 proteins that were underexpressed in cholangiocarcinoma compared to paired non-tumoral liver tissue from the same patients (604). Parallel significance in UM may be inferred from these proteomic studies. The higher expression of CNDP2 in UM that did not metastasize may represent less aggressive disease with low metastatic potential.

A large-scale cDNA transfection study on human hepatoma cells showed that CNDP2 isoform-2 gene underexpression was significantly associated with tumor microsatellite formation and venous invasion, which are features of metastasis in hepatocellular carcinoma (HCC) (600). HCC cell line transfected with this gene was found to suppress invasion, suggesting that it may play a role as a metastasis-suppressor. Furthermore, significant induction of G1 arrest, sensitization to cell apoptosis, inhibition of cell growth, and tumour formation was observed in nude mice transfected with the CNDP2 isoform-2 gene. Significant downregulation of other proteins associated with invasion and metastasis formation, such as CXCR3, MMP11, and CD44s was also observed in transfected HCC cells. The authors conclude that CNDP2 isoform-2 plays a

significant inhibitory role in the formation, growth and metastasis in HCC. While these associations were found in HCC, this may have implications in UM given that 90% of UM preferentially metastasises to the liver. Thus, it is tempting to postulate that CNDP2 may exert a protective role in the development of liver metastasis in UM. However, the downregulation of CNDP2 in primary UM samples that metastasised to the liver were variable in our study. Half of the samples metastasised to the liver (4/8), while another metastasised to both the liver and lung. The mean raw abundance of CNDP2 in samples that developed hepatic metastases was higher than that of samples that developed extrahepatic metastases (357600 SIV vs. 231385 SIV). Nevertheless, the expression levels of CNDP2 in hepatic metastases, and it potential effects on cell lines derived from hepatic metastasis should be investigated. This may provide further insights into targeted therapy for patients with hepatic metastases.

An array CGH study identified deletion of CNDP2 gene in pancreatic carcinoma tissues (601). Deletion of this gene was an independent poor prognostic marker for overall survival after adjusting for other factors associated with patient outcome. The median overall survival of patients without deletion of CNDP2 gene was significantly longer compared to those with deletion of this gene (30.3 months vs. 16.0 month). Furthermore, a significant association between deletion of the CNDP2 gene and high grade of tumours was also observed. *In vitro* studies of the effect of CNDP2 demonstrated that cells expressing CNDP2 had significantly lower proliferation rate than CNDP2-knockdown cells. Furthermore, a significant increase of G0/G1 cell cycle phase and attenuated cell migration was also observed. Based on these findings, the authors suggest that CNDP2 may function as a growth suppressor, which may not be related to its enzymatic activity.

Elevated levels of CNDP2 may indicate the absence of metastases, and may be useful as a biomarker to monitor patients at high risk for metastasis. However, the validity of CNDP2 as a biomarker needs to be investigated in patients by comparing class 1 low risk patients and class 2 high risk/patients that have developed metastatic disease. The use of CNDP as a biomarker to determine the response to currently used chemotherapeutic agents for the treatment of metastatic disease should also be investigated. Its role to guide selection of patients for adjuvant treatment is also necessary. CNDP2 was found in an unpublished qualitative proteomic study of human normal vitreous humour (612). Its presence in normal vitreous raises the possibility of the use of CNDP2 as a vitreous biomarker in UM patients treated with modalities other than enucleation. Aspiration of vitreous fluid is an invasive but relatively safe and simple technique. Serial measurement of CNDP2 in vitreous may be used to monitor response to treatment, disease progression, and more importantly the onset and development of distant metastasis. The presence, expression and variations of CNDP2 in vitreous fluid of enucleated UM specimens of different disease stages needs to be determined to explore its use as a biomarker.

## 4.5. Signal-induced proliferation-associated 1-like protein 2 (SIPA1L2)

Bioinformatic reanalysis of gene expression microarray data of monosomy 3 tumours with metastasis (M3M) versus disomy 3 tumours without metastasis (D3NM) identified differential upregulation of signal-induced proliferation-associated 1-like protein 2 (SIPA1L2) in M3M. It had the fifth most significant p value (p: 0.001) where it was 1.516 fold differentially upregulated in M3M compared to D3NM. It is located in cytoband 1q42 and positively regulates GTPase activity and small GTPase-mediated signal transduction (613). Otherwise, very little is known about SIPA1L2. However, immunohistochemical staining of SIPA1L2 on 13 primary UM tumours of patients that developed metastatic disease (mUM) and 13 primary UM tumours of patients that did not develop metastasis (nmUM) did not show any statistically significant difference of expression between the two groups. No identifiable trend of expression was seen in either group, which may reflect the modest fold change that was found in the microarray analysis. No significant difference was seen when comparing the intensity or percentage of staining between mUM and nmUM. SIPA1L2 expression did not correlate with clinicopathological factors such as survival, chromosome 3 status, cell type or tumour size. Similar to the other selected targets, the lack of significant results of SIPA1L2 expression may be explained by the relatively small sample size of 26 tumours. Thus, SIPA1L2 was not evaluated further in the larger cohort of UM microarray samples.

SIPA1L2 was identified to be upregulated by McCannel et al in their study of 3 aggressive primary UM cell lines with monosomy 3 loss (407), while van Gils et al also reported upregulated SIPA1L2 as a classifier gene associated with poor prognosis in UM (408). Gene expression profiling of prostate cancer versus normal prostate tissue identified SIPA1L2 as one of 28 transcripts significantly associated with recurrence after radical prostatectomy (520). Interestingly, this study also identified THBS2 among the 28 transcripts. However, neither of these

were followed-up. Significant and consistent over expression of SIPA1L2 and many other genes was shown in astrocytic cancer cells (614). SIPA1L2 was also identified as one of top 50 genes that were overexpressed in aggressive, therapy-resistant prostate cancer cells that were initially androgen-dependent but eventually survived and resumed growth under androgen-deprived conditions (615). Fibroblasts constitute the majority of tumour stroma and have been suggested to be prominent modifiers of cancer progression, with a specific subpopulation designated as cancer-associated fibroblasts (CAFs) that play a key role in promoting tumor initiation and progression. Compared to normal prostate tissue fibroblast, gene expression profiling identified upregulation of SIPA1L2 and 72 other genes in prostate carcinoma fibroblast (616).

Signal transducer and activator of transcription 3 (STAT3) is a latent cytoplasmic transcription factor that it regulates transcription of target genes, induced by a variety of upstream signals, including growth factors, cytokines and non-receptor tyrosine kinases (617–620). Constitutive STAT3 activation has been demonstrated in a variety of cancers such as cutaneous melanoma (621), lymphoma (622), myeloma (623), squamous cell (624), prostate (625) and breast carcinoma (626). In order to identify genes regulated by STAT3, fibroblast cells constitutively expressing STAT3 were shown to downregulate SIPA1L2 expression amongst numerous other genes (627). It is likely that our finding of upregulated SIPA1L2 in aggressive UM plays a role that is independent of STAT3 regulation. In support of this, only one study that sought to determine whether UM cells require Notch activity for growth, reported STAT3 expression in UM (461). Notch blockade using the γ-secretase inhibitor (GSI) MRK003 was shown to inhibit UM cell growth and invasion by inhibiting AKT, Erk, and STAT3. Both AKT and Erk pathways are known to be involved in UM (33,34,154,155), but the significance of STAT3 is unknown.

### 4.5.1. SIPA1L2 may inhibit apoptosis via the extrinsic pathway

Expression of RAS oncogene occurs in about 30% of human tumours, including cutaneous melanoma (628–630). SIPA1L2, along with 27 other genes was shown to be involved in a complex pathway in RAS-mediated epigenetic silencing of Fas (631). In the extrinsic apoptotic pathway, activation of one of the death receptors signalling pathways such as Fas triggers upstream signalling caspases that leads to apoptosis (632). Fas interacts with Fas ligand (FasL) and recruits the adaptor molecule Fas-associated death domain (FADD) (633). FADD also has another domain called the death effector domain, which in turn recruits pro-caspase-8 and/or pro-caspase-10 to the receptor (633). The resulting protein complex activates these initiator caspases and triggers further increased caspase activity that leads to the activation of effector caspases such as caspase-3, -6 and -7. Effector caspases selectively cleave a restricted set of target proteins that ultimately leads to apoptosis. Tumour cells have been shown to be resistant to Fas-mediated apoptosis, with molecular defects being identified at several levels of the apoptotic signalling pathway (634). Indeed, tumours demonstrate resistance to apoptosis in a manner that evades surveillance by the host immune system and leads to uncontrolled growth (550). As an anti-tumour immune response, infiltrating T cells and NK cells express FasL as a cytotoxic mediator (635). However, resistance to Fas-mediated apoptosis protects cancer cells against the anti-tumour response (635). In colorectal tumours, decreased Fas expression was only observed in a small number of adenomas, while carcinomas demonstrated reduced Fas expression and was associated with tumour progression (636). Furthermore, complete loss of Fas expression was observed more frequently in tumours that had already metastasised (636). Recently, mesenchymal stem cells were shown to induce apoptosis, inhibit growth and metastasis of multiple myeloma in mice via the Fas/FasL mechanism (637). Decoy receptor 3 (DcR3) protects cells from a wide range of apoptotic stimuli and was

shown to be expressed in pancreatic carcinoma cells (638). These cells demonstrated resistance to FasL-mediated apoptosis and silencing of DcR3 expression enhanced the inhibitory effects of FasL, reduced proliferation and colony formation *in vitro* (638). Further, the downregulation of DcR3 induced FADD, caspase-3 and caspase-8, thus triggering cell apoptosis in these cells (638). Several studies have implicated reduced Fas levels with lymph node involvement, bone metastases, recurrences and poor prognosis in breast cancer (639–643). Low Fas expression in osteosarcoma was shown to correlate with increased metastatic propensity (644). Interestingly, Fas -negative tumour cells gained the ability to evade the host defence mechanism and form lung metastases (644). In mice with lung metastases, aerosol treatment with chemotherapeutic agents known to upregulate Fas expression, such as liposomal 9-Nitrocamptothecin and Gemcitabine induced tumor regression in wild type mice. However, lung metastases in FasL-deficient mice did not respond to the treatment. Chemotherapeutic drugs can upregulate Fas and FasL expression in tumour cells and induce Fas-mediated apoptosis and lead to tumour regression (645). Cytotoxic drug-induced activation of the Fas/FasL pathway has been shown in leukaemia cells, hepatoblastoma, neuroblastoma and brain tumours (646,647). Chemotherapeutic agents such as etoposide and cisplatin has been shown to upregulate FasL expression at therapeutic concentrations and are capable of inducing tumour cell death in a Fas-dependent manner (648,649). In medulloblastoma and glioblastoma, γ-irradiation was shown to cause cell death by a Fas/FasL-dependent mechanism (650). Kallikrein-binding protein (KBP), a serine proteinase inhibitor, decreased cell viability and induced apoptosis of colorectal carcinoma cells by increasing expression of FasL and activated caspase-8 (651).

Although mutations of the RAS family of oncogenes in UM are rare (652–656), an immunohistochemical study showed that both Fas and FasL was expressed in UM tumours (657). It was also demonstrated that low expression of FasL was associated with an increased risk for metastasis. In another study, depsipeptide, a HDAC inhibitor was shown to inhibit proliferation and growth by

increasing expression of Fas and FasL in 3 UM cell lines derived from primary tumour and 2 cell lines derived from liver metastasis. Depsipeptide induced gene upregulation of both Fas and FasL in these cells, and an increase in activated caspase-3, apoptosis and cell-cycle arrest was observed in treated cells compared to non-treated cells (97). Given the current evidence of Fas in cancer, it may be hypothesised that increased SIPA1L2 expression in aggressive UM may inhibit apoptosis, promote tumour growth and metastatic formation via this mechanism. While it has been shown that SIPA1L2 is involved in RAS-mediated epigenetic silencing of Fas (631), whether it silences Fas via RAS-independent manner needs further investigation to test this hypothesis.

### 4.5.2. Upregulation of SIPA1L2 due to loss of pRB and TFAP2A may cause deregulation of cellular homeostasis

Recently, SIPA1L2 was identified as one of 21 target genes for the transcription factor activator protein-2 gamma (TFAP2C) in a breast cancer cell line (658). Activator protein-2 (AP-2) regulates gene expression by binding to a GC-rich recognition sequence in the regulatory regions of many genes (659,660). AP-2 regulates various signaling pathways involved in development (including the eye), cell growth, differentiation and apoptosis (661–665) and plays a crucial role in cellular homeostasis between normal cell growth and neoplastic formation (666,667). Several studies have shown AP-2 to exert both positive and negative regulatory roles in breast cancer initiation, growth and metastatic progression (668–672). In acute myeloid leukemia, transcription factor activator protein-2 alpha (TFAP2A) upregulated other target genes that stimulated cancer cell proliferation and survival (673). Conversely, reduced expression of TFAP2A was associated with poor prognosis in gastric adenocarcinoma (674), and glioma (675) while overexpression in pancreatic cancer could be exploited to decrease *in vivo* tumour growth and resistance to gemcitabine (676). In cutaneous melanoma, TFAP2A acts as a tumour-suppressor gene by inducing cell-cycle

arrest and apoptosis, with loss of expression of nuclear TFAP2A correlated to melanoma progression (677–680). Conversely, re-expression of TFAP2A in highly metastatic cutaneous melanoma cell lines significantly reduced tumor growth and decreased experimental lung metastasis *in vivo* (681). Penna et al demonstrated that miR-214 contributed to cutaneous melanoma progression and metastatic formation through suppression of the TFAP2C gene (682). Further, TFAP2C mRNA was downregulated in melanoma but expressed in skin as well as nevus samples. In a more recent study, Penna et al also identified indirect downregulation of TFAP2A by miR-214, which may be as a consequence of downregulated TFAP2C (683). Indeed, it is known that TFAP2C silencing reduces TFAP2A protein levels (683) and that TFAP2 family members regulate each other transcriptionally (684). This was confirmed in an immunohistochemical study, with low expression of TFAP2A and TFAP2C associated with poor prognosis in cutaneous melanoma (685).

Interestingly, TFAP2A inactivation was observed as a consequence of loss of RB1 function in retinoblastoma. When TFAP2A expression was restored, apoptosis and inhibition of proliferation was induced in retinoblastoma cells (686). In the initial study by Onken and Harbour et al that led to the identification of class 1 low-risk and class 2 high-risk UM, TFAP2A was identified as one of 62 discriminating genes that accurately distinguished between the two groups (687). This finding is also supported by an earlier study by that identified chromosome 3 loss as a molecular classifier for adverse outcome, which also found underexpression of TFAP2A in aggressive UM. In our study, TFAP2A was found to be downregulated by 1.403 fold (p: 0.004). TFAP2A has been shown to interact with pRB *in vitro*, and associates with pRB *in vivo* (688). As pRB is constitutively hyperphosphorylated and functionally inactivated in UM (689–691), it is possible that SIPA1L2 is upregulated by loss of pRB and TFAP2A in UM, leading to aggressive, metastatic phenotype.

## 4.6. Contactin 3 (CNTN3)

In the bioinformatic reanalysis of gene expression microarray data, Contactin 3 showed the third most significant p value (p: 0.000807) where it was 3.1 fold differentially downregulated in monosomy 3 tumours with metastasis (M3M) compared to disomy 3 tumours without metastasis (D3NM). It is located at cytoband 3p12.3 and is involved in cell adhesion, although its exact function is poorly understood. Tumours with chromosome 3 monosomy are associated with high risk for metastasis. Thus, the downregulation of CNTN3 in aggressive UM is an interesting finding, and may function as a metastasis suppressor gene. However, immunohistochemical staining of CNTN3 on 13 primary UM tumours of patients that developed metastatic disease (mUM) and 13 primary UM tumours of patients that did not develop metastasis (nmUM) did not show any statistically significant difference of expression between the two groups. A trend towards lower expression in mUM was found, with 46% of mUM tumours demonstrating no CNTN3 expression (no staining) while all nmUM tumours showed positive staining for CNTN3. No significant difference was seen when comparing the intensity or percentage of staining between mUM and nmUM. CNTN3 expression did not correlate with clinicopathological factors such as survival, chromosome 3 status, cell type or tumour size. The lack of significant results of CNTN3 expression may be explained by the relatively small sample size of 26 tumours. Furthermore, the majority of tumours only showed relatively weak staining in both mUM and nmUM tissues. Thus, immunohistochemical expression of CNTN3 was not evaluated further in the larger cohort of UM tissue microarray samples.

In a GEP microarray study of 46 UM tumours, van Gils et al identified downregulation of 2 small regions in chromosome 3, associated with shorter survival; 3p12-14 and 3p23-25 (692). This finding is also supported by a microsatellite analysis of 52 primary tumours that identified deletions in regions 3p11-14 and 3p25-26 (693). This suggests that these regions harbour tumour suppressor genes, and loss of these genes lead to the aggressive, metastatic

phenotype observed. Contactins belong to the immunoglobulin superfamily and are involved in cell adhesion. They are located in the cell membrane, and have also been found to be expressed in microtubules and occasionally, nucleoli. It has only been reported by a few studies. Alterations in CNTN3 gene expression is predominantly reported in autistic spectral disorders (694). Loss of heterozygosity in chromosome 3p, including CNTN3 has also been described in familial renal cell carcinoma (695) while another study identified a variant on chromosome 3p12.3 as significantly associated with abdominal aortic aneurysm (696) though this was later disputed (697). A study of endometrial carcinoma identified CNTN3 to be upregulated in early stage compared to late stage disease (698).

Contactin 1 has been shown to promote metastasis in several malignancies. The gene encoding for CNTN1 is located in chromosome 12, unlike CNTN3. Contactin 1 expression correlated with the expression of VEGF-C and VEGF-R-3 in gastric carcinoma (699). This was associated with the presence of lymphatic invasion and poor prognosis, suggesting its use as a biomarker to predict patients at risk for mortality from lymphatic metastasis. Overexpression CNTN1 was also associated with the regional lymph node metastasis of patients with oral squamous cell carcinoma (700). In lung adenocarcinoma, several studies have shown CNTN1 to promote invasion and metastasis (701–703).

### 4.6.1. CNTN3 and PTPRG as tumour suppressors

Although this study did not identify receptor-type protein-tyrosine phosphatase gamma (PTPRG), CNTN3 has been shown to bind to PTPRG *in vitro* (704,705). Protein-tyrosine phosphatases (PTPases) play an essential role in the regulation of cell activation, proliferation and differentiation, since they counterbalance the growth-promoting effects of protein-tyrosine kinases (706). PTPRG is a member of the protein tyrosine phosphatase family, located at chromosome 3p14.21. Deletions and translocations in this region have been

observed in familial renal cell carcinoma (707,708) and breast cancer (709). Its expression was also reduced in gastric cancers (710). PTPRG was expressed in both normal human lung tissue and non-tumour cells of lung adenocarcinoma while in 50% of the lung adenocarcinoma, PTPRG was absent (711). Furthermore, mutations of PTPRG were also identified in colorectal carcinomas, suggesting that PTPs are tumour suppressor genes regulating cellular pathways (712). PTPRG promoter hypermethylation was observed in T-cell lymphomas (713), gastric cancer (714), and melanoma cell lines (715), suggesting promoter hypermethylation is an important mechanism to silence PTPRG expression. In nasopharyngeal carcinoma, decreased expression of PTPRG was associated with tumourigenicity while overexpression inhibited cell growth by inducing G1 arrest through inhibition of pRB phosphorylation and down-regulation of cyclin D1 (716). This observation in nasopharyngeal carcinoma is significant, as pRB is constitutively hyperphosphorylated and functionally inactivated in UM, with cyclin D1 overexpression in about 65% of cases (689–691). Furthermore, increased cyclin D1 protein expression has been associated with larger tumour basal diameter, epithelioid cell type, and poor prognosis (691). Thus, CNTN3 and PTPRG may play a critical role as tumour suppressors in UM.

In breast cancer cells, PTPRG was downregulated in more aggressive phenotype and was shown to prolong doubling times and colony sizes, indicating tumour suppressive characteristics (717). Importantly, PTPRG was shown to inhibit breast tumour formation *in vivo* via the ERK1/2 pathway (718). The most common known oncogenic mutations occur in GNAQ or GNA11, found in about 85% of all primary UM irrespective of tumour class or stage (23,24). Constitutive activation of the MAP-kinases ERK1/2 plays a crucial role in UM development, likely as a consequence of active mutations in the G-proteins GNAQ and GNA11 (24,34,36,37). Several studies have also found activation of ERK1/2 in UM, independent of GNAQ, RAS or BRAF mutational status (34,36,39). Knockdown of mutant GNAQ in UM cells resulted in MAP-kinase inhibition and decrease in pERK expression, accompanied by reduced growth and induced apoptosis (37,38). In an on-going phase II clinical trial of selumetinib (MEK inhibitor) versus

temozolomide in patients with metastatic uveal melanoma (clinicaltrials.gov # NCT01143402), preliminary results show sustained inhibition of pERK and suppression of cyclin D1 in matched tumour biopsies of patients that showed stabilisation and partial response in liver metastases, while progression of metastatic disease was observed in a patient that did not demonstrate pERK inhibition and cyclin D1 suppression (38). Two different protein kinase C (PKC) inhibitors, AEB071 and enzastaurin, were shown to independently increase the accumulation of $p27^{Kip1}$, while decreasing the expression of cyclin D1in three GNAQ-mutated cell lines, leading to G1 cell-cycle arrest (40,41). Several studies have demonstrated that G1 arrest induced by MEK inhibitors is mediated via inhibition of ERK1/2, characterized by decreased expression of cyclin D1 and accumulation of $p27^{Kip1}$ (42–44). The PKC inhibitors also demonstrated antiproliferative effects on these cell lines, suggesting that the suppression of Erk1/2 phosphorylation may be critical to inhibit proliferation through altering the expression of p27, cyclin D1, Bcl-2 and survivin.

Taken together, altered PTPRG expression associated with CNTN3 downregulation may lead to uncontrolled tumour growth and metastatic dissemination in UM. It may be hypothesised that one of the events that enables tumours with loss of heterozygosity/loss of chromosome 3 to acquire its metastatic propensity is via the loss of this tumour suppressor gene. However, the expression or function of CNTN3 or PTPRG has never been studied in UM before. Moreover, CNTN3 is a novel gene and its functions are poorly understood. Despite the lack of significant difference of immunohistochemical expression in this pilot study, future studies to determine its functional properties in UM cell lines are warranted. Specifically, the effect of CNTN3 knockdown on invasion and migration properties of non-invasive cell lines should be determined. Currently, no adjuvant therapies are available to decrease the risk of metastatic disease following treatment of the primary tumour. This is an area with potential clinical significance, as CNTN3/PTPRG may be an important target for therapeutic intervention in post-operative high-risk UM patients with chromosome 3 abnormalities.

## 4.7. Advantages, limitations and future work

There are several advantages of this study compared to previous proteomic studies using cell lines. Cell line models lack the intrinsic tumour microenvironment, where cells interact with a plethora of stromal elements. Furthermore, the functional significance of biomarkers identified *in vitro* may not be consistent with those identified in *in vivo* models (606). Tumour microenvironment also has a large influence on gene expression (719). *In vitro* culture conditions and long-term cell passages are known to greatly change the gene and consequently protein expression patterns for such artificial environments (720,721). Due to these intrinsic differences between cell culture and tissue studies, biomarkers identified in *in vitro* studies may not demonstrate the desired phenotype in *in vivo* studies. Short of using *in vivo* models, UM tissue proteomics may facilitate the identification of biomarkers that may be more translationally relevant and reliable. This however inevitably also introduces other technical difficulties that may yield confounding results due to potential contamination of tumour tissues with surrounding non-neoplastic ocular structures. Specifically, contamination of UM tissue with blood is difficult to avoid and remains a challenge. Techniques such as laser microdissection may minimise contamination of tumour samples with surrounding ocular structures. Likewise, this technique may also be used to compare tumour tissue to adjacent normal uveal tissue as control, which may reveal biomarkers that are intrinsically involved in the developmental biology of UM.

The immunohistochemical study of 26 whole UM tissue samples used for validation of both proteomic and gene microarray targets did not show any substantial statistical significance due to the small sample size. This was intended as a pilot study in order to identify targets that showed adequate and heterogenous staining that was suitable for assessment and grading. Based on this, PRDX3 was selected for validation in the larger cohort of tissue microarray samples. However, both proteomic and bioinformatic gene microarray studies

have identified other novel and interesting molecular candidates. Further investigations into the properties and effects of these proteins and genes are necessary.

To date, tissue studies have only been performed on enucleated samples. As these tumours represent advanced disease, future studies using fine needle aspiration biopsy samples may further our understanding of the early molecular events governing tumour growth, progression and metastasis. Recent advances in proteomic profiling of formalin-fixed, paraffin-embedded tissue would provide an opportunity to greatly expand the range, variety and availability of both primary and metastatic UM tissues available for proteomics analysis. Proteomic analysis of other biological material such as matched serum, vitreous and tumour tissue would also provide insights into the individual molecular characteristics of this disease. This would be an important step towards the identification of effective biomarkers and therapeutic targets for personalised medicine in uveal melanoma.

Specific areas for further research arising from this project are:

1. Investigate the effects of PRDX3 inhibition and overexpression in cell lines of different metastatic propensity
2. Investigate the expression of PRDX3 in metastatic uveal melanoma tissue samples
3. Investigate the expression of CNTN3 in a larger cohort of tumour samples, given its localisation to chromosome 3
4. Investigate the effects of CNTN3 inhibition and overexpression in cell lines of different metastatic propensity

# 5. Conclusion

To identify differentially expressed proteins between primary uveal melanoma tissue of patients that developed metastasis and primary uveal melanoma tissues of patients that did not develop metastasis, quantitative label-free LC-MS proteomic analysis was performed. Thioredoxin-dependant peroxidase reductase (PRDX3) was upregulated and cytosolic non-specific dipeptidase (CNDP2) was downregulated in primary tumours that developed metastasis. To identify differential expressed genes between chromosome 3 monosomy tumours with metastasis and chromosome 3 disomy tumours without metastasis, bioinformatic reanalysis of publically available gene expression microarray datasets was performed. Signal-induced proliferation-associated 1-like protein 2 (SIPA1L2) was upregulated and contactin 3 (CNTN3) was downregulated in monosomy 3 tumours with metastasis. Pilot immunohistochemical validation studies of all 4 targets were not statistically significant. In a larger cohort of primary uveal melanoma tissues, significant difference of PRDX3 expression was observed in tissues of patients that did and did not develop metastasis. High PRDX3 expression was significantly associated with shorter survival, and is predictive of the development of metastatic disease. PRDX3 may play a role in the development of metastatic disease by stimulating proliferation and inhibiting apoptosis of UM cells. Further, its interaction with the MYC and MAPK pathways likely promotes tumour cell survival, proliferation and eventually metastatic dissemination. Other proteins and genes that are known to be involved in uveal melanoma were also found in this study, along with several novel targets for further research.

# 6. Bibliography


1. Egan KM, Seddon JM, Glynn RJ, Gragoudas ES, Albert DM. Epidemiologic aspects of uveal melanoma. Surv Ophthalmol. 1988 Feb;32(4):239–51.

2. Singh AD, Topham A. Survival rates with uveal melanoma in the United States: 1973-1997. Ophthalmology. 2003 May;110(5):962–5.

3. Jensen OA. Malignant melanomas of the human uvea: 25-year follow-up of cases in Denmark, 1943--1952. Acta Ophthalmol (Copenh). 1982 Apr;60(2):161–82.

4. Raivio I. Uveal melanoma in Finland. An epidemiological, clinical, histological and prognostic study. Acta Ophthalmol Suppl. 1977;(133):1–64.

5. Bedikian AY. Metastatic uveal melanoma therapy: current options. Int Ophthalmol Clin. 2006;46(1):151–66.

6. Ehlers JP, Harbour JW. Molecular pathobiology of uveal melanoma. Int Ophthalmol Clin. 2006;46(1):167–80.

7. Singh AD, Borden EC. Metastatic uveal melanoma. Ophthalmol Clin N Am. 2005 Mar;18(1):143–150, ix.

8. Lorigan JG, Wallace S, Mavligit GM. The prevalence and location of metastases from ocular melanoma: imaging study in 110 patients. AJR Am J Roentgenol. 1991 Dec;157(6):1279–81.

9. Eskelin S, Pyrhönen S, Summanen P, Hahka-Kemppinen M, Kivelä T. Tumor doubling times in metastatic malignant melanoma of the uvea: tumor progression before and after treatment. Ophthalmology. 2000 Aug;107(8):1443–9.

10. Triozzi PL, Eng C, Singh AD. Targeted therapy for uveal melanoma. Cancer Treat Rev. 2008 May;34(3):247–58.

11. Jemal A, Siegel R, Ward E, Murray T, Xu J, Smigal C, et al. Cancer statistics, 2006. CA Cancer J Clin. 2006 Apr;56(2):106–30.

12. Singh AD, Bergman L, Seregard S. Uveal melanoma: epidemiologic aspects. Ophthalmol Clin N Am. 2005 Mar;18(1):75–84, viii.

13. Becher R, Korn WM, Prescher G. Use of fluorescence in situ hybridization and comparative genomic hybridization in the cytogenetic analysis of testicular germ cell tumors and uveal melanomas. Cancer Genet Cytogenet. 1997 Jan;93(1):22–8.

14. Prescher G, Bornfeld N, Hirche H, Horsthemke B, Jöckel KH, Becher R. Prognostic implications of monosomy 3 in uveal melanoma. Lancet. 1996 May 4;347(9010):1222–5.

15. Sisley K, Parsons MA, Garnham J, Potter AM, Curtis D, Rees RC, et al. Association of specific chromosome alterations with tumour phenotype in posterior uveal melanoma. Br J Cancer. 2000 Jan;82(2):330–8.

16. Damato B, Duke C, Coupland SE, Hiscott P, Smith PA, Campbell I, et al. Cytogenetics of uveal melanoma: a 7-year clinical experience. Ophthalmology. 2007 Oct;114(10):1925–31.

17. Kilic E, Naus NC, van Gils W, Klaver CC, van Til ME, Verbiest MM, et al. Concurrent loss of chromosome arm 1p and chromosome 3 predicts a decreased disease-free survival in uveal melanoma patients. Invest Ophthalmol Vis Sci. 2005 Jul;46(7):2253–7.

18. Häusler T, Stang A, Anastassiou G, Jöckel K-H, Mrzyk S, Horsthemke B, et al. Loss of heterozygosity of 1p in uveal melanomas with monosomy 3. Int J Cancer J Int Cancer. 2005 Oct 10;116(6):909–13.

19. Griffin CA, Long PP, Schachat AP. Trisomy 6p in an ocular melanoma. Cancer Genet Cytogenet. 1988 May;32(1):129–32.

20. Parrella P, Sidransky D, Merbs SL. Allelotype of posterior uveal melanoma: implications for a bifurcated tumor progression pathway. Cancer Res. 1999 Jul 1;59(13):3032–7.

21. Onken MD, Worley LA, Ehlers JP, Harbour JW. Gene expression profiling in uveal melanoma reveals two molecular classes and predicts metastatic death. Cancer Res. 2004 Oct 15;64(20):7205–9.

22. Tschentscher F, Hüsing J, Hölter T, Kruse E, Dresen IG, Jöckel K-H, et al. Tumor classification based on gene expression profiling shows that uveal melanomas with and without monosomy 3 represent two distinct entities. Cancer Res. 2003 May 15;63(10):2578–84.

23. Onken MD, Worley LA, Long MD, Duan S, Council ML, Bowcock AM, et al. Oncogenic mutations in GNAQ occur early in uveal melanoma. Invest Ophthalmol Vis Sci. 2008 Dec;49(12):5230–4.

24. Van Raamsdonk CD, Griewank KG, Crosby MB, Garrido MC, Vemula S, Wiesner T, et al. Mutations in GNA11 in uveal melanoma. N Engl J Med. 2010 Dec 2;363(23):2191–9.

25. Harbour JW, Onken MD, Roberson EDO, Duan S, Cao L, Worley LA, et al. Frequent mutation of BAP1 in metastasizing uveal melanomas. Science. 2010 Dec 3;330(6009):1410–3.

26. Harbour JW. The genetics of uveal melanoma: an emerging framework for targeted therapy. Pigment Cell Melanoma Res. 2012 Mar;25(2):171–81.

27. Harbour JW, Roberson EDO, Anbunathan H, Onken MD, Worley LA, Bowcock AM. Recurrent mutations at codon 625 of the splicing factor SF3B1 in uveal melanoma. Nat Genet. 2013 Feb;45(2):133–5.

28. Sodhi A, Merbs S. Chapter 141 - Molecular Genetics of Choroidal Melanoma. In: Ryan SJ, Sadda SR, Hinton DR, Schachat AP, Sadda SR, Wilkinson CP, et al., editors. Retina (Fifth Edition) [Internet]. London: W.B. Saunders; 2013 [cited 2014 Jun 11]. p. 2247–53. Available from: http://www.sciencedirect.com/science/article/pii/B9781455707379001417

29. Laurent C, Valet F, Planque N, Silveri L, Maacha S, Anezo O, et al. High PTP4A3 phosphatase expression correlates with metastatic risk in uveal melanoma patients. Cancer Res. 2011 Feb 1;71(3):666–74.

30. Aoki H, Yamada Y, Hara A, Kunisada T. Two distinct types of mouse melanocyte: differential signaling requirement for the maintenance of non-cutaneous and dermal versus epidermal melanocytes. Dev Camb Engl. 2009 Aug;136(15):2511–21.

31. Van Raamsdonk CD, Fitch KR, Fuchs H, de Angelis MH, Barsh GS. Effects of G-protein mutations on skin color. Nat Genet. 2004 Sep;36(9):961–8.

32. Woodman SE. Metastatic uveal melanoma: biology and emerging treatments. Cancer J Sudbury Mass. 2012 Apr;18(2):148–52.

33. Weber A, Hengge UR, Urbanik D, Markwart A, Mirmohammadsaegh A, Reichel MB, et al. Absence of mutations of the BRAF gene and constitutive activation of extracellular-regulated kinase in malignant melanomas of the uvea. Lab Investig J Tech Methods Pathol. 2003 Dec;83(12):1771–6.

34. Zuidervaart W, van Nieuwpoort F, Stark M, Dijkman R, Packer L, Borgstein A-M, et al. Activation of the MAPK pathway is a common event in uveal melanomas although it rarely occurs through mutation of BRAF or RAS. Br J Cancer. 2005 Jun 6;92(11):2032–8.

35. Daniels AB, Lee J-E, MacConaill LE, Palescandolo E, Van Hummelen P, Adams SM, et al. High throughput mass spectrometry-based mutation profiling of primary uveal melanoma. Invest Ophthalmol Vis Sci. 2012 Oct;53(11):6991–6.

36. Rimoldi D, Salvi S, Liénard D, Lejeune FJ, Speiser D, Zografos L, et al. Lack of BRAF mutations in uveal melanoma. Cancer Res. 2003 Sep 15;63(18):5712–5.

37. Van Raamsdonk CD, Bezrookove V, Green G, Bauer J, Gaugler L, O'Brien JM, et al. Frequent somatic mutations of GNAQ in uveal melanoma and blue naevi. Nature. 2009 Jan 29;457(7229):599–602.

38. Ambrosini G, Pratilas CA, Qin L-X, Tadi M, Surriga O, Carvajal RD, et al. Identification of unique MEK-dependent genes in GNAQ mutant uveal melanoma involved in cell growth, tumor cell invasion, and MEK resistance. Clin Cancer Res Off J Am Assoc Cancer Res. 2012 Jul 1;18(13):3552–61.

39. Pópulo H, Vinagre J, Lopes JM, Soares P. Analysis of GNAQ mutations, proliferation and MAPK pathway activation in uveal melanomas. Br J Ophthalmol. 2011 May;95(5):715–9.

40. Wu X, Zhu M, Fletcher JA, Giobbie-Hurder A, Hodi FS. The protein kinase C inhibitor enzastaurin exhibits antitumor activity against uveal melanoma. PloS One. 2012;7(1):e29622.

41. Wu X, Li J, Zhu M, Fletcher JA, Hodi FS. Protein kinase C inhibitor AEB071 targets ocular melanoma harboring GNAQ mutations via effects on the PKC/Erk1/2 and PKC/NF-κB pathways. Mol Cancer Ther. 2012 Sep;11(9):1905–14.

42. Ciuffreda L, Del Bufalo D, Desideri M, Di Sanza C, Stoppacciaro A, Ricciardi MR, et al. Growth-inhibitory and antiangiogenic activity of the MEK inhibitor PD0325901 in malignant melanoma with or without BRAF mutations. Neoplasia N Y N. 2009 Aug;11(8):720–31.

43. Philipp A, Schneider A, Väsrik I, Finke K, Xiong Y, Beach D, et al. Repression of cyclin D1: a novel function of MYC. Mol Cell Biol. 1994 Jun;14(6):4032–43.

44. Kortylewski M, Heinrich PC, Kauffmann ME, Böhm M, MacKiewicz A, Behrmann I. Mitogen-activated protein kinases control p27/Kip1 expression and growth of human melanoma cells. Biochem J. 2001 Jul 1;357(Pt 1):297–303.

45. Chen X, Wu Q, Tan L, Porter D, Jager MJ, Emery C, et al. Combined PKC and MEK inhibition in uveal melanoma with GNAQ and GNA11 mutations. Oncogene. 2013 Oct 21;

46. Manning BD, Cantley LC. AKT/PKB signaling: navigating downstream. Cell. 2007 Jun 29;129(7):1261–74.

47. Scheid MP, Woodgett JR. PKB/AKT: functional insights from genetic models. Nat Rev Mol Cell Biol. 2001 Oct;2(10):760–8.

48. Abdel-Rahman MH, Yang Y, Zhou X-P, Craig EL, Davidorf FH, Eng C. High frequency of submicroscopic hemizygous deletion is a major mechanism of loss of expression of PTEN in uveal melanoma. J Clin Oncol Off J Am Soc Clin Oncol. 2006 Jan 10;24(2):288–95.

49. Saraiva VS, Caissie AL, Segal L, Edelstein C, Burnier MN Jr. Immunohistochemical expression of phospho-Akt in uveal melanoma. Melanoma Res. 2005 Aug;15(4):245–50.

50. Babchia N, Calipel A, Mouriaux F, Faussat A-M, Mascarelli F. The PI3K/Akt and mTOR/P70S6K signaling pathways in human uveal melanoma cells: interaction with B-Raf/ERK. Invest Ophthalmol Vis Sci. 2010 Jan;51(1):421–9.

51. Naus NC, Zuidervaart W, Rayman N, Slater R, van Drunen E, Ksander B, et al. Mutation analysis of the PTEN gene in uveal melanoma cell lines. Int J Cancer J Int Cancer. 2000 Jul 1;87(1):151–3.

52. Ballou LM, Chattopadhyay M, Li Y, Scarlata S, Lin RZ. Galphaq binds to p110alpha/p85alpha phosphoinositide 3-kinase and displaces Ras. Biochem J. 2006 Mar 15;394(Pt 3):557–62.

53. Howes AL, Miyamoto S, Adams JW, Woodcock EA, Brown JH. Galphaq expression activates EGFR and induces Akt mediated cardiomyocyte survival: dissociation from Galphaq mediated hypertrophy. J Mol Cell Cardiol. 2006 May;40(5):597–604.

54. Khalili JS, Yu X, Wang J, Hayes BC, Davies MA, Lizee G, et al. Combination Small Molecule MEK and PI3K Inhibition Enhances Uveal Melanoma Cell Death in a Mutant GNAQ and GNA11 Dependent Manner. Clin Cancer Res Off J Am Assoc Cancer Res. 2012 Aug 15;18(16):4345–55.

55. Musi E, Ambrosini G, De Stanchina E, Schwartz GK. The Phosphoinositide 3-Kinaseα Selective Inhibitor, BYL719, Enhances the Effect of the Protein Kinase C Inhibitor, AEB071, in GNAQ/GNA11 Mutant Uveal Melanoma Cells. Mol Cancer Ther. 2014 Mar 11;

56. Mast/stem cell growth factor receptor Kit [Internet]. Uniprot KB. Available from: http://www.uniprot.org/uniprot/P10721

57. Mouriaux F, Chahud F, Maurage CA, Malecaze F, Labalette P. Implication of stem cell factor in the proliferation of choroidal melanocytes. Exp Eye Res. 2001 Aug;73(2):151–7.

58. Pereira PR, Odashiro AN, Marshall JC, Correa ZM, Belfort R Jr, Burnier MN Jr. The role of c-kit and imatinib mesylate in uveal melanoma. J Carcinog. 2005 Oct 19;4:19.

59. All-Ericsson C, Girnita L, Müller-Brunotte A, Brodin B, Seregard S, Ostman A, et al. c-Kit-dependent growth of uveal melanoma cells: a potential therapeutic target? Invest Ophthalmol Vis Sci. 2004 Jul;45(7):2075–82.

60. Lefevre G, Glotin A-L, Calipel A, Mouriaux F, Tran T, Kherrouche Z, et al. Roles of stem cell factor/c-Kit and effects of Glivec/STI571 in human uveal melanoma cell tumorigenesis. J Biol Chem. 2004 Jul 23;279(30):31769–79.

61. Pache M, Glatz K, Bösch D, Dirnhofer S, Mirlacher M, Simon R, et al. Sequence analysis and high-throughput immunohistochemical profiling of KIT (CD 117) expression in uveal melanoma using tissue microarrays. Virchows Arch Int J Pathol. 2003 Dec;443(6):741–4.

62. Bottaro DP, Rubin JS, Faletto DL, Chan AM, Kmiecik TE, Vande Woude GF, et al. Identification of the hepatocyte growth factor receptor as the c-met proto-oncogene product. Science. 1991 Feb 15;251(4995):802–4.

63. Furge KA, Zhang YW, Vande Woude GF. Met receptor tyrosine kinase: enhanced signaling through adapter proteins. Oncogene. 2000 Nov 20;19(49):5582–9.

64. Birchmeier C, Birchmeier W, Gherardi E, Vande Woude GF. Met, metastasis, motility and more. Nat Rev Mol Cell Biol. 2003 Dec;4(12):915–25.

65. Zhang Y-W, Vande Woude GF. HGF/SF-met signaling in the control of branching morphogenesis and invasion. J Cell Biochem. 2003 Feb 1;88(2):408–17.

66. Topcu-Yilmaz P, Kiratli H, Saglam A, Söylemezoglu F, Hascelik G. Correlation of clinicopathological parameters with HGF, c-Met, EGFR, and IGF-1R expression in uveal melanoma. Melanoma Res. 2010 Apr;20(2):126–32.

67. Abdel-Rahman MH, Boru G, Massengill J, Salem MM, Davidorf FH. MET oncogene inhibition as a potential target of therapy for uveal melanomas. Invest Ophthalmol Vis Sci. 2010 Jul;51(7):3333–9.

68. Economou MA, All-Ericsson C, Bykov V, Girnita L, Bartolazzi A, Larsson O, et al. Receptors for the liver synthesized growth factors IGF-1 and HGF/SF in uveal melanoma: intercorrelation and prognostic implications. Invest Ophthalmol Vis Sci. 2005 Dec;46(12):4372–5.

69. Mallikarjuna K, Pushparaj V, Biswas J, Krishnakumar S. Expression of epidermal growth factor receptor, ezrin, hepatocyte growth factor, and c-Met in uveal melanoma: an immunohistochemical study. Curr Eye Res. 2007 Mar;32(3):281–90.

70. Ye M, Hu D, Tu L, Zhou X, Lu F, Wen B, et al. Involvement of PI3K/Akt signaling pathway in hepatocyte growth factor-induced migration of uveal melanoma cells. Invest Ophthalmol Vis Sci. 2008 Feb;49(2):497–504.

71. Di Cesare S, Marshall J-C, Logan P, Antecka E, Faingold D, Maloney SC, et al. Expression and migratory analysis of 5 human uveal melanoma cell lines for CXCL12, CXCL8, CXCL1, and HGF. J Carcinog. 2007;6:2.

72. Yan D, Zhou X, Chen X, Hu D-N, Dong XD, Wang J, et al. MicroRNA-34a inhibits uveal melanoma cell proliferation and migration through downregulation of c-Met. Invest Ophthalmol Vis Sci. 2009 Apr;50(4):1559–65.

73. Adhami VM, Afaq F, Mukhtar H. Insulin-like growth factor-I axis as a pathway for cancer chemoprevention. Clin Cancer Res Off J Am Assoc Cancer Res. 2006 Oct 1;12(19):5611–4.

74. Leventhal PS, Feldman EL. Insulin-like Growth Factors as Regulators of Cell Motility Signaling Mechanisms. Trends Endocrinol Metab TEM. 1997 Feb;8(1):1–6.

75. Zhang D, Bar-Eli M, Meloche S, Brodt P. Dual regulation of MMP-2 expression by the type 1 insulin-like growth factor receptor: the phosphatidylinositol 3-kinase/Akt and Raf/ERK pathways transmit opposing signals. J Biol Chem. 2004 May 7;279(19):19683–90.

76. All-Ericsson C, Girnita L, Seregard S, Bartolazzi A, Jager MJ, Larsson O. Insulin-like growth factor-1 receptor in uveal melanoma: a predictor for metastatic disease and a potential therapeutic target. Invest Ophthalmol Vis Sci. 2002 Jan;43(1):1–8.

77. Girnita A, All-Ericsson C, Economou MA, Aström K, Axelson M, Seregard S, et al. The insulin-like growth factor-I receptor inhibitor picropodophyllin causes tumor regression and attenuates mechanisms involved in invasion of uveal melanoma cells. Clin Cancer Res Off J Am Assoc Cancer Res. 2006 Feb 15;12(4):1383–91.

78. Economou MA, Andersson S, Vasilcanu D, All-Ericsson C, Menu E, Girnita A, et al. Oral picropodophyllin (PPP) is well tolerated in vivo and inhibits IGF-1R expression and growth of uveal melanoma. Invest Ophthalmol Vis Sci. 2008 Jun;49(6):2337–42.

79. Patel M, Smyth E, Chapman PB, Wolchok JD, Schwartz GK, Abramson DH, et al. Therapeutic implications of the emerging molecular biology of uveal melanoma. Clin Cancer Res Off J Am Assoc Cancer Res. 2011 Apr 15;17(8):2087–100.

80. Onken MD, Ehlers JP, Worley LA, Makita J, Yokota Y, Harbour JW. Functional gene expression analysis uncovers phenotypic switch in aggressive uveal melanomas. Cancer Res. 2006 May 1;66(9):4602–9.

81. Trolet J, Hupé P, Huon I, Lebigot I, Decraene C, Delattre O, et al. Genomic profiling and identification of high-risk uveal melanoma by array CGH analysis of primary tumors and liver metastases. Invest Ophthalmol Vis Sci. 2009 Jun;50(6):2572–80.

82. Johnston SC, Larsen CN, Cook WJ, Wilkinson KD, Hill CP. Crystal structure of a deubiquitinating enzyme (human UCH-L3) at 1.8 A resolution. EMBO J. 1997 Jul 1;16(13):3787–96.

83. Scheuermann JC, de Ayala Alonso AG, Oktaba K, Ly-Hartig N, McGinty RK, Fraterman S, et al. Histone H2A deubiquitinase activity of the Polycomb repressive complex PR-DUB. Nature. 2010 May 13;465(7295):243–7.

84. Yu H, Mashtalir N, Daou S, Hammond-Martel I, Ross J, Sui G, et al. The ubiquitin carboxyl hydrolase BAP1 forms a ternary complex with YY1 and HCF-1 and is a critical regulator of gene expression. Mol Cell Biol. 2010 Nov;30(21):5071–85.

85. Wilkinson KD. Regulation of ubiquitin-dependent processes by deubiquitinating enzymes. FASEB J Off Publ Fed Am Soc Exp Biol. 1997 Dec;11(14):1245–56.

86. Wilkinson KD. Ubiquitination and deubiquitination: targeting of proteins for degradation by the proteasome. Semin Cell Dev Biol. 2000 Jun;11(3):141–8.

87. Angeloni D. Molecular analysis of deletions in human chromosome 3p21 and the role of resident cancer genes in disease. Brief Funct Genomic Proteomic. 2007 Mar;6(1):19–39.

88. Hershko A, Ciechanover A. The ubiquitin system. Annu Rev Biochem. 1998;67:425–79.

89. Jensen DE, Proctor M, Marquis ST, Gardner HP, Ha SI, Chodosh LA, et al. BAP1: a novel ubiquitin hydrolase which binds to the BRCA1 RING finger and enhances BRCA1-mediated cell growth suppression. Oncogene. 1998 Mar 5;16(9):1097–112.

90. Buchhagen DL, Qiu L, Etkind P. Homozygous deletion, rearrangement and hypermethylation implicate chromosome region 3p14.3-3p21.3 in sporadic breast-cancer development. Int J Cancer J Int Cancer. 1994 May 15;57(4):473–9.

91. Abdel-Rahman MH, Pilarski R, Cebulla CM, Massengill JB, Christopher BN, Boru G, et al. Germline BAP1 mutation predisposes to uveal melanoma, lung adenocarcinoma, meningioma, and other cancers. J Med Genet. 2011 Dec;48(12):856–9.

92. Wiesner T, Obenauf AC, Murali R, Fried I, Griewank KG, Ulz P, et al. Germline mutations in BAP1 predispose to melanocytic tumors. Nat Genet. 2011 Oct;43(10):1018–21.

93. Testa JR, Cheung M, Pei J, Below JE, Tan Y, Sementino E, et al. Germline BAP1 mutations predispose to malignant mesothelioma. Nat Genet. 2011 Oct;43(10):1022–5.

94. Njauw C-NJ, Kim I, Piris A, Gabree M, Taylor M, Lane AM, et al. Germline BAP1 inactivation is preferentially associated with metastatic ocular melanoma and cutaneous-ocular melanoma families. PloS One. 2012;7(4):e35295.

95. Carbone M, Ferris LK, Baumann F, Napolitano A, Lum CA, Flores EG, et al. BAP1 cancer syndrome: malignant mesothelioma, uveal and cutaneous melanoma, and MBAITs. J Transl Med. 2012;10:179.

96. Ventii KH, Devi NS, Friedrich KL, Chernova TA, Tighiouart M, Van Meir EG, et al. BRCA1-associated protein-1 is a tumor suppressor that requires deubiquitinating activity and nuclear localization. Cancer Res. 2008 Sep 1;68(17):6953–62.

97. Klisovic DD, Katz SE, Effron D, Klisovic MI, Wickham J, Parthun MR, et al. Depsipeptide (FR901228) inhibits proliferation and induces apoptosis in primary and metastatic human uveal melanoma cell lines. Invest Ophthalmol Vis Sci. 2003 Jun;44(6):2390–8.

98. Landreville S, Agapova OA, Matatall KA, Kneass ZT, Onken MD, Lee RS, et al. Histone deacetylase inhibitors induce growth arrest and differentiation in uveal melanoma. Clin Cancer Res Off J Am Assoc Cancer Res. 2012 Jan 15;18(2):408–16.

99. Furney SJ, Pedersen M, Gentien D, Dumont AG, Rapinat A, Desjardins L, et al. SF3B1 mutations are associated with alternative splicing in uveal melanoma. Cancer Discov. 2013 Jul 16;CD–13–0330.

100. Martin M, Maßhöfer L, Temming P, Rahmann S, Metz C, Bornfeld N, et al. Exome sequencing identifies recurrent somatic mutations in EIF1AX and SF3B1 in uveal melanoma with disomy 3. Nat Genet. 2013 Aug;45(8):933–6.

101. Harbour JW, Chao DL. A Molecular Revolution in Uveal Melanoma: Implications for Patient Care and Targeted Therapy. Ophthalmology. 2014 Jan 28;

102. Leiserson MDM, Blokh D, Sharan R, Raphael BJ. Simultaneous identification of multiple driver pathways in cancer. PLoS Comput Biol. 2013;9(5):e1003054.

103. Mariani P, Piperno-Neumann S, Servois V, Berry MG, Dorval T, Plancher C, et al. Surgical management of liver metastases from uveal melanoma: 16 years' experience at the Institut Curie. Eur J Surg Oncol J Eur Soc Surg Oncol Br Assoc Surg Oncol. 2009 Nov;35(11):1192–7.

104. Frenkel S, Nir I, Hendler K, Lotem M, Eid A, Jurim O, et al. Long-term survival of uveal melanoma patients after surgery for liver metastases. Br J Ophthalmol. 2009 Aug;93(8):1042–6.

105. Aubin J-M, Rekman J, Vandenbroucke-Menu F, Lapointe R, Fairfull-Smith RJ, Mimeault R, et al. Systematic review and meta-analysis of liver resection for metastatic melanoma. Br J Surg. 2013 Aug;100(9):1138–47.

106. Alexander HR, Libutti SK, Bartlett DL, Puhlmann M, Fraker DL, Bachenheimer LC. A phase I-II study of isolated hepatic perfusion using melphalan with or without tumor necrosis factor for patients with ocular melanoma metastatic to liver. Clin Cancer Res Off J Am Assoc Cancer Res. 2000 Aug;6(8):3062–70.

107. Alexander HR Jr, Libutti SK, Pingpank JF, Steinberg SM, Bartlett DL, Helsabeck C, et al. Hyperthermic isolated hepatic perfusion using melphalan for patients with ocular melanoma metastatic to liver. Clin Cancer Res Off J Am Assoc Cancer Res. 2003 Dec 15;9(17):6343–9.

108. Noter SL, Rothbarth J, Pijl MEJ, Keunen JEE, Hartgrink HH, Tijl FGJ, et al. Isolated hepatic perfusion with high-dose melphalan for the treatment of uveal melanoma metastases confined to the liver. Melanoma Res. 2004 Feb;14(1):67–72.

109. Van Etten B, de Wilt JHW, Brunstein F, Eggermont AMM, Verhoef C. Isolated hypoxic hepatic perfusion with melphalan in patients with irresectable ocular melanoma metastases. Eur J Surg Oncol J Eur Soc Surg Oncol Br Assoc Surg Oncol. 2009 May;35(5):539–45.

110. Olofsson R, Cahlin C, All-Ericsson C, Hashimi F, Mattsson J, Rizell M, et al. Isolated Hepatic Perfusion for Ocular Melanoma Metastasis: Registry Data Suggests a Survival Benefit. Ann Surg Oncol. 2013 Oct 19;

111. LIVER21G.jpg [Internet]. Available from: http://media.jsonline.com/images/LIVER21G.jpg

112. Egerer G, Lehnert T, Max R, Naeher H, Keilholz U, Ho AD. Pilot study of hepatic intraarterial fotemustine chemotherapy for liver metastases from uveal melanoma: a single-center experience with seven patients. Int J Clin Oncol. 2001 Feb;6(1):25–8.

113. Leyvraz S, Spataro V, Bauer J, Pampallona S, Salmon R, Dorval T, et al. Treatment of ocular melanoma metastatic to the liver by hepatic arterial chemotherapy. J Clin Oncol Off J Am Soc Clin Oncol. 1997 Jul;15(7):2589–95.

114. Peters S, Voelter V, Zografos L, Pampallona S, Popescu R, Gillet M, et al. Intra-arterial hepatic fotemustine for the treatment of liver metastases from uveal melanoma: experience in 101 patients. Ann Oncol Off J Eur Soc Med Oncol ESMO. 2006 Apr;17(4):578–83.

115. Voelter V, Schalenbourg A, Pampallona S, Peters S, Halkic N, Denys A, et al. Adjuvant intra-arterial hepatic fotemustine for high-risk uveal melanoma patients. Melanoma Res. 2008 Jun;18(3):220–4.

116. Melichar B, Voboril Z, Lojík M, Krajina A. Liver metastases from uveal melanoma: clinical experience of hepatic arterial infusion of cisplatin, vinblastine and dacarbazine. Hepatogastroenterology. 2009 Aug;56(93):1157–62.

117. Sullivan K L. Immunoembolization for melanoma. New York, NY: Cambridge University Press; 2008. p. 311–5.

118. Sato T, Eschelman DJ, Gonsalves CF, Terai M, Chervoneva I, McCue PA, et al. Immunoembolization of malignant liver tumors, including uveal melanoma, using granulocyte-macrophage colony-stimulating factor. J Clin Oncol Off J Am Soc Clin Oncol. 2008 Nov 20;26(33):5436–42.

119. Yamamoto A, Chervoneva I, Sullivan KL, Eschelman DJ, Gonsalves CF, Mastrangelo MJ, et al. High-dose immunoembolization: survival benefit in patients with hepatic metastases from uveal melanoma. Radiology. 2009 Jul;252(1):290–8.

120. Eschelman DJ, Gonsalves CF, Terai M, Laudadio M, Sullivan KL, Mastrangelo MJ, et al. The results of a randomized phase II study using embolization with or without granulocyte-macrophage colony-stimulating factor (GM-CSF) in uveal melanoma patients with hepatic metastasis. J Clin Oncol [Internet]. 2011 [cited 2014 Apr 8];29: 2011 (suppl; abstr 8577)(suppl; abstr 8577). Available from: http://meetinglibrary.asco.org/content/82857-102

121. Patel K, Sullivan K, Berd D, Mastrangelo MJ, Shields CL, Shields JA, et al. Chemoembolization of the hepatic artery with BCNU for metastatic uveal melanoma: results of a phase II study. Melanoma Res. 2005 Aug;15(4):297–304.

122. Vogl T, Eichler K, Zangos S, Herzog C, Hammerstingl R, Balzer J, et al. Preliminary experience with transarterial chemoembolization (TACE) in liver metastases of uveal malignant melanoma: local tumor control and survival. J Cancer Res Clin Oncol. 2007 Mar 1;133(3):177–84.

123. Ronny Schuster ML. Transarterial chemoembolization of liver metastases from uveal melanoma after failure of systemic therapy: toxicity and outcome. Melanoma Res. 2010;20(3):191–6.

124. Huppert PE, Fierlbeck G, Pereira P, Schanz S, Duda SH, Wietholtz H, et al. Transarterial chemoembolization of liver metastases in patients with uveal melanoma. Eur J Radiol. 2010 Jun;74(3):e38–44.

125. Fiorentini G, Aliberti C, Del Conte A, Tilli M, Rossi S, Ballardini P, et al. Intra-arterial hepatic chemoembolization (TACE) of liver metastases from ocular melanoma with slow-release irinotecan-eluting beads. Early results of a phase II clinical study. Vivo Athens Greece. 2009 Feb;23(1):131–7.

126. Venturini M, Pilla L, Agostini G, Cappio S, Losio C, Orsi M, et al. Transarterial chemoembolization with drug-eluting beads preloaded with irinotecan as a first-line approach in uveal melanoma liver metastases: tumor response and predictive value of diffusion-weighted MR imaging in five patients. J Vasc Interv Radiol JVIR. 2012 Jul;23(7):937–41.

127. Edelhauser G, Schicher N, Berzaczy D, Beitzke D, Höeller C, Lammer J, et al. Fotemustine chemoembolization of hepatic metastases from uveal melanoma: a retrospective single-center analysis. AJR Am J Roentgenol. 2012 Dec;199(6):1387–92.

128. deb-tace slide 3_500x415 [Internet]. Available from: http://transplant.surgery.ucsf.edu/media/2967111/deb-tace%20slide%203_500x415.jpg

129. Lane AM, Egan KM, Harmon D, Holbrook A, Munzenrider JE, Gragoudas ES. Adjuvant interferon therapy for patients with uveal melanoma at high risk of metastasis. Ophthalmology. 2009 Nov;116(11):2206–12.

130. Salmon RJ, Levy C, Plancher C, Dorval T, Desjardins L, Leyvraz S, et al. Treatment of liver metastases from uveal melanoma by combined surgery-chemotherapy. Eur J Surg Oncol J Eur Soc Surg Oncol Br Assoc Surg Oncol. 1998 Apr;24(2):127–30.

131. Buder K, Gesierich A, Gelbrich G, Goebeler M. Systemic treatment of metastatic uveal melanoma: review of literature and future perspectives. Cancer Med. 2013 Oct;2(5):674–86.

132. Kelderman S, van der Kooij MK, van den Eertwegh AJM, Soetekouw PMMB, Jansen RLH, van den Brom RRH, et al. Ipilimumab in pretreated metastastic uveal melanoma patients. Results of the Dutch Working group on Immunotherapy of Oncology (WIN-O). Acta Oncol. 2013 Nov;52(8):1786–8.

133. Tarhini AA, Frankel P, Margolin KA, Christensen S, Ruel C, Shipe-Spotloe J, et al. Aflibercept (VEGF Trap) in inoperable stage III or stage iv melanoma of cutaneous or uveal origin. Clin Cancer Res Off J Am Assoc Cancer Res. 2011 Oct 15;17(20):6574–81.

134. Sacco JJ, Nathan PD, Danson S, Lorigan P, Nicholson S, Ottensmeier C, et al. Sunitinib versus dacarbazine as first-line treatment in patients with metastatic uveal melanoma. J Clin Oncol [Internet]. 2013 [cited 2014 Apr 9];31(suppl; abstr 9031). Available from: http://meetinglibrary.asco.org/content/114030-132

135. Schmittel A, Schmidt-Hieber M, Martus P, Bechrakis NE, Schuster R, Siehl JM, et al. A randomized phase II trial of gemcitabine plus treosulfan versus treosulfan alone in patients with metastatic uveal melanoma. Ann Oncol Off J Eur Soc Med Oncol ESMO. 2006 Dec;17(12):1826–9.

136. Bedikian AY, Papadopoulos N, Plager C, Eton O, Ring S. Phase II evaluation of temozolomide in metastatic choroidal melanoma. Melanoma Res. 2003 Jun;13(3):303–6.

137. Reiriz AB, Richter MF, Fernandes S, Cancela AI, Costa TD, Di Leone LP, et al. Phase II study of thalidomide in patients with metastatic malignant melanoma. Melanoma Res. 2004 Dec;14(6):527–31.

138. Zeldis J., Heller C, Seidel G, Yuldasheva N, Shutack Y, Libutti SK. A randomized phase II trial comparing two doses of lenalidomide for the treatment of stage IV ocular melanoma. J Clin Oncol [Internet]. 2009 [cited 2014 Apr 9];27(suppl; abstr e20012). Available from: http://meetinglibrary.asco.org/content/31252-65

139. Homsi J, Bedikian AY, Papadopoulos NE, Kim KB, Hwu W-J, Mahoney SL, et al. Phase 2 open-label study of weekly docosahexaenoic acid-paclitaxel in patients with metastatic uveal melanoma. Melanoma Res. 2010 Dec;20(6):507–10.

140. Bedikian AY, Papadopoulos NE, Kim KB, Vardeleon A, Smith T, Lu B, et al. A pilot study with vincristine sulfate liposome infusion in patients with metastatic melanoma. Melanoma Res. 2008 Dec;18(6):400–4.

141. Spagnolo F, Grosso M, Picasso V, Tornari E, Pesce M, Queirolo P. Treatment of metastatic uveal melanoma with intravenous fotemustine. Melanoma Res. 2013 Jun;23(3):196–8.

142. Leyvraz S, Suciu S, Piperno-Neumann S, Baurain J-F, Zdzienicki M, Testori A, et al. Randomized phase III trial of intravenous (IV) versus hepatic intra-arterial (HIA) fotemustine in patients with liver metastases from uveal melanoma: Final results of the EORTC 18021 study. J Clin Oncol [Internet]. 2012 [cited 2013 Nov 28];30(suppl; abstr 8532). Available from: http://meetinglibrary.asco.org/content/95725-114

143. Schmidt-Hieber M, Schmittel A, Thiel E, Keilholz U. A phase II study of bendamustine chemotherapy as second-line treatment in metastatic uveal melanoma. Melanoma Res. 2004 Dec;14(6):439–42.

144. Pföhler C, Cree IA, Ugurel S, Kuwert C, Haass N, Neuber K, et al. Treosulfan and gemcitabine in metastatic uveal melanoma patients: results of a multicenter feasibility study. Anticancer Drugs. 2003 Jun;14(5):337–40.

145. Keilholz U, Schuster R, Schmittel A, Bechrakis N, Siehl J, Foerster MH, et al. A clinical phase I trial of gemcitabine and treosulfan in uveal melanoma and other solid tumours. Eur J Cancer Oxf Engl 1990. 2004 Sep;40(14):2047–52.

146. Terheyden P, Bröcker EB, Becker JC. Clinical evaluation of in vitro chemosensitivity testing: the example of uveal melanoma. J Cancer Res Clin Oncol. 2004 Jul;130(7):395–9.

147. Corrie PG, Shaw J, Spanswick VJ, Sehmbi R, Jonson A, Mayer A, et al. Phase I trial combining gemcitabine and treosulfan in advanced cutaneous and uveal melanoma patients. Br J Cancer. 2005 Jun 6;92(11):1997–2003.

148. Schmittel A, Scheulen ME, Bechrakis NE, Strumberg D, Baumgart J, Bornfeld N, et al. Phase II trial of cisplatin, gemcitabine and treosulfan in patients with metastatic uveal melanoma. Melanoma Res. 2005 Jun;15(3):205–7.

149. Kivelä T, Suciu S, Hansson J, Kruit WHJ, Vuoristo M-S, Kloke O, et al. Bleomycin, vincristine, lomustine and dacarbazine (BOLD) in combination with recombinant interferon alpha-2b for metastatic uveal melanoma. Eur J Cancer Oxf Engl 1990. 2003 May;39(8):1115–20.

150. Nathan FE, Berd D, Sato T, Shield JA, Shields CL, De Potter P, et al. BOLD+interferon in the treatment of metastatic uveal melanoma: first report of active systemic therapy. J Exp Clin Cancer Res CR. 1997 Jun;16(2):201–8.

151. Pyrhönen S, Hahka-Kemppinen M, Muhonen T, Nikkanen V, Eskelin S, Summanen P, et al. Chemoimmunotherapy with bleomycin, vincristine, lomustine, dacarbazine (BOLD), and human leukocyte interferon for metastatic uveal melanoma. Cancer. 2002 Dec 1;95(11):2366–72.

152. Solti M, Berd D, Mastrangelo MJ, Sato T. A pilot study of low-dose thalidomide and interferon alpha-2b in patients with metastatic melanoma who failed prior treatment. Melanoma Res. 2007 Aug;17(4):225–31.

153. Becker JC, Terheyden P, Kämpgen E, Wagner S, Neumann C, Schadendorf D, et al. Treatment of disseminated ocular melanoma with sequential fotemustine, interferon alpha, and interleukin 2. Br J Cancer. 2002 Oct 7;87(8):840–5.

154. Pópulo H, Soares P, Rocha AS, Silva P, Lopes JM. Evaluation of the mTOR pathway in ocular (uvea and conjunctiva) melanoma. Melanoma Res. 2010 Apr;20(2):107–17.

155. Saraiva VS, Caissie AL, Segal L, Edelstein C, Burnier MN Jr. Immunohistochemical expression of phospho-Akt in uveal melanoma. Melanoma Res. 2005 Aug;15(4):245–50.

156. Matatall KA, Agapova OA, Onken MD, Worley LA, Bowcock AM, Harbour JW. BAP1 deficiency causes loss of melanocytic cell identity in uveal melanoma. BMC Cancer. 2013 Aug 5;13(1):371.

157. Falchook GS, Lewis KD, Infante JR, Gordon MS, Vogelzang NJ, DeMarini DJ, et al. Activity of the oral MEK inhibitor trametinib in patients with advanced melanoma: a phase 1 dose-escalation trial. Lancet Oncol. 2012 Aug;13(8):782–9.

158. Kirkwood JM, Bastholt L, Robert C, Sosman J, Larkin J, Hersey P, et al. Phase II, open-label, randomized trial of the MEK1/2 inhibitor selumetinib as monotherapy versus temozolomide in patients with advanced melanoma. Clin Cancer Res Off J Am Assoc Cancer Res. 2012 Jan 15;18(2):555–67.

159. Carvajal RD, Sosman JA, Quevedo JF, Milhem MM, Joshua AM, Kudchadkar RR, et al. Effect of selumetinib vs chemotherapy on progression-free survival in uveal melanoma: a randomized clinical trial. JAMA. 2014 Jun 18;311(23):2397–405.

160. Penel N, Delcambre C, Durando X, Clisant S, Hebbar M, Negrier S, et al. O-Mel-Inib: a Cancéro-pôle Nord-Ouest multicenter phase II trial of high-dose imatinib mesylate in metastatic uveal melanoma. Invest New Drugs. 2008 Dec;26(6):561–5.

161. Hofmann UB, Kauczok-Vetter CS, Houben R, Becker JC. Overexpression of the KIT/SCF in Uveal Melanoma Does Not Translate into Clinical Efficacy of Imatinib Mesylate. Clin Cancer Res. 2009 Jan 1;15(1):324–9.

162. Nathan PD, Marshall E, Smith CT, Bickerstaff M, Escriu C, Marples M, et al. A Cancer Research UK two-stage multicenter phase II study of imatinib in the treatment of patients with c-kit positive metastatic uveal melanoma (ITEM). J Clin Oncol [Internet]. 2012 [cited 2014 Apr 8];30(suppl; abstr 8523). Available from: http://meetinglibrary.asco.org/content/99652-114

163. El Filali M, Missotten GSOA, Maat W, Ly LV, Luyten GPM, van der Velden PA, et al. Regulation of VEGF-A in uveal melanoma. Invest Ophthalmol Vis Sci. 2010 May;51(5):2329–37.

164. Ijland SA, Jager MJ, Heijdra BM, Westphal JR, Peek R. Expression of angiogenic and immunosuppressive factors by uveal melanoma cell lines. Melanoma Res. 1999 Oct;9(5):445–50.

165. Missotten GSO, Notting IC, Schlingemann RO, Zijlmans HJ, Lau C, Eilers PHC, et al. Vascular endothelial growth factor a in eyes with uveal melanoma. Arch Ophthalmol. 2006 Oct;124(10):1428–34.

166. Boyd SR, Tan D, Bunce C, Gittos A, Neale MH, Hungerford JL, et al. Vascular endothelial growth factor is elevated in ocular fluids of eyes harbouring uveal melanoma: identification of a potential therapeutic window. Br J Ophthalmol. 2002 Apr;86(4):448–52.

167. Crosby MB, Yang H, Gao W, Zhang L, Grossniklaus HE. Serum vascular endothelial growth factor (VEGF) levels correlate with number and location of micrometastases in a murine model of uveal melanoma. Br J Ophthalmol. 2011 Jan;95(1):112–7.

168. El Filali M, Ly LV, Luyten GPM, Versluis M, Grossniklaus HE, van der Velden PA, et al. Bevacizumab and intraocular tumors: an intriguing paradox. Mol Vis. 2012;18:2454–67.

169. Guenterberg KD, Grignol VP, Relekar KV, Varker KA, Chen HX, Kendra KL, et al. A pilot study of bevacizumab and interferon-α2b in ocular melanoma. Am J Clin Oncol. 2011 Feb;34(1):87–91.

170. Piperno-Neumann S, Servois V, Bidard F-C, Mariani P, Plancher C, Asselain B, et al. BEVATEM: Phase II single-center study of bevacizumab in combination with temozolomide in patients (pts) with first-line metastatic uveal melanoma (MUM): First-step results. J Clin Oncol [Internet]. 2012 [cited 2014 Apr 8];30(suppl; abstr 8546). Available from: http://meetinglibrary.asco.org/content/95035-114

171. Mahipal A, Tijani L, Chan K, Laudadio M, Mastrangelo MJ, Sato T. A pilot study of sunitinib malate in patients with metastatic uveal melanoma. Melanoma Res. 2012 Dec;22(6):440–6.

172. Kaempgen E, Schmid M, Erdmann M, Keikavoussi P, Strobel D, Schuler-Thurner B, et al. Predictable clinical responses to sorafenib in stage IV uveal melanoma. J Clin Oncol [Internet]. 2012 [cited 2014 Apr 8];30(suppl; abstr e19032). Available from: http://meetinglibrary.asco.org/content/97643-114

173. Hodi FS, O'Day SJ, McDermott DF, Weber RW, Sosman JA, Haanen JB, et al. Improved survival with ipilimumab in patients with metastatic melanoma. N Engl J Med. 2010 Aug 19;363(8):711–23.

174. Khattak MA, Fisher R, Hughes P, Gore M, Larkin J. Ipilimumab activity in advanced uveal melanoma. Melanoma Res. 2013 Feb;23(1):79–81.

175. Maio M, Danielli R, Chiarion-Sileni V, Pigozzo J, Parmiani G, Ridolfi R, et al. Efficacy and safety of ipilimumab in patients with pre-treated, uveal melanoma. Ann Oncol Off J Eur Soc Med Oncol ESMO. 2013 Nov;24(11):2911–5.

176. Khan SA, Callahan M, Postow MA, Chapman PB, Schwartz GK, Dickson MA, et al. Ipilimumab in the treatment of uveal melanoma: The Memorial Sloan-Kettering Cancer Center experience. J Clin Oncol [Internet]. 2012 [cited 2014 Apr 8];30(suppl; abstr 8549). Available from: http://meetinglibrary.asco.org/content/95579-114

177. Luke JJ, Callahan MK, Postow MA, Romano E, Ramaiya N, Bluth M, et al. Clinical activity of ipilimumab for metastatic uveal melanoma: a retrospective review of the Dana-Farber Cancer Institute, Massachusetts General Hospital, Memorial Sloan-Kettering Cancer Center, and University Hospital of Lausanne experience. Cancer. 2013 Oct 15;119(20):3687–95.

178. Flaherty LE, Unger JM, Liu PY, Mertens WC, Sondak VK. Metastatic melanoma from intraocular primary tumors: the Southwest Oncology Group experience in phase II advanced melanoma clinical trials. Am J Clin Oncol. 1998 Dec;21(6):568–72.

179. Bhatia S, Moon J, Margolin KA, Weber JS, Lao CD, Othus M, et al. Phase II trial of sorafenib in combination with carboplatin and paclitaxel in patients with metastatic uveal melanoma: SWOG S0512. PloS One. 2012;7(11):e48787.

180. Atzpodien J, Terfloth K, Fluck M, Reitz M. Cisplatin, gemcitabine and treosulfan is effective in chemotherapy-pretreated relapsed stage IV uveal melanoma patients. Cancer Chemother Pharmacol. 2008 Sep;62(4):685–8.

181. O'Neill PA, Butt M, Eswar CV, Gillis P, Marshall E. A prospective single arm phase II study of dacarbazine and treosulfan as first-line therapy in metastatic uveal melanoma. Melanoma Res. 2006 Jun;16(3):245–8.

182. Danielli R, Ridolfi R, Chiarion-Sileni V, Queirolo P, Testori A, Plummer R, et al. Ipilimumab in pretreated patients with metastatic uveal melanoma: safety and clinical efficacy. Cancer Immunol Immunother CII. 2012 Jan;61(1):41–8.

183. Ellerhorst JA, Bedikian AY, Smith TM, Papadopoulos NE, Plager C, Eton O. Phase II trial of 9-nitrocamptothecin (RFS 2000) for patients with metastatic cutaneous or uveal melanoma. Anticancer Drugs. 2002 Feb;13(2):169–72.

184. Gygi SP, Rochon Y, Franza BR, Aebersold R. Correlation between protein and mRNA abundance in yeast. Mol Cell Biol. 1999 Mar;19(3):1720–30.

185. Mádi A, Pusztahelyi T, Punyiczki M, Fésüs L. The biology of the post-genomic era: the proteomics. Acta Biol Hung. 2003;54(1):1–14.

186. Srinivas PR, Srivastava S, Hanash S, Wright GL Jr. Proteomics in early detection of cancer. Clin Chem. 2001 Oct;47(10):1901–11.

187. Fabian MR, Sundermeier TR, Sonenberg N. Understanding how miRNAs post-transcriptionally regulate gene expression. Prog Mol Subcell Biol. 2010;50:1–20.

188. Woodman SE. Metastatic uveal melanoma: biology and emerging treatments. Cancer J Sudbury Mass. 2012 Apr;18(2):148–52.

189. Boja ES, Rodriguez H. The path to clinical proteomics research: integration of proteomics, genomics, clinical laboratory and regulatory science. Korean J Lab Med. 2011 Apr;31(2):61–71.

190. Celis JE, Ostergaard M, Jensen NA, Gromova I, Rasmussen HH, Gromov P. Human and mouse proteomic databases: novel resources in the protein universe. FEBS Lett. 1998 Jun 23;430(1-2):64–72.

191. Desmetz C, Lacombe J, Mange A, Maudelonde T, Solassol J. [Serum autoantibodies profiling and early-stage cancer detection]. Médecine Sci MS. 2011 Jul;27(6-7):633–8.

192. Emmert-Buck MR, Gillespie JW, Paweletz CP, Ornstein DK, Basrur V, Appella E, et al. An approach to proteomic analysis of human tumors. Mol Carcinog. 2000 Mar;27(3):158–65.

193. Guo H, Zhu Y-P, Li D, He F-C. [Identification, modeling and simulation of key pathways underlying certain cancers]. Yi Chuan Hered Zhongguo Yi Chuan Xue Hui Bian Ji. 2011 Aug;33(8):809–19.

194. Baskın Y, Yiğitbaşı T. Clinical proteomics of breast cancer. Curr Genomics. 2010 Nov;11(7):528–36.

195. Hassanein M, Rahman JSM, Chaurand P, Massion PP. Advances in proteomic strategies toward the early detection of lung cancer. Proc Am Thorac Soc. 2011 May;8(2):183–8.

196. Mehrotra R, Gupta DK. Exciting new advances in oral cancer diagnosis: avenues to early detection. Head Neck Oncol. 2011;3:33.

197. Bosch LJW, Carvalho B, Fijneman RJA, Jimenez CR, Pinedo HM, van Engeland M, et al. Molecular tests for colorectal cancer screening. Clin Colorectal Cancer. 2011 Mar 1;10(1):8–23.

198. Wright PC, Noirel J, Ow S-Y, Fazeli A. A review of current proteomics technologies with a survey on their widespread use in reproductive biology investigations. Theriogenology. 2012 Mar 1;77(4):738–765.e52.

199. Bogdanov B, Smith RD. Proteomics by FTICR mass spectrometry: top down and bottom up. Mass Spectrom Rev. 2005 Apr;24(2):168–200.

200. Gevaert K, Van Damme P, Ghesquière B, Impens F, Martens L, Helsens K, et al. A la carte proteomics with an emphasis on gel-free techniques. Proteomics. 2007 Aug;7(16):2698–718.

201. Lane CS. Mass spectrometry-based proteomics in the life sciences. Cell Mol Life Sci CMLS. 2005 Apr;62(7-8):848–69.

202. Merril CR. Gel-staining techniques. Methods Enzymol. 1990;182:477–88.

203. Alban A, David SO, Bjorkesten L, Andersson C, Sloge E, Lewis S, et al. A novel experimental design for comparative two-dimensional gel analysis: two-dimensional difference gel electrophoresis incorporating a pooled internal standard. Proteomics. 2003 Jan;3(1):36–44.

204. Fenn JB, Mann M, Meng CK, Wong SF, Whitehouse CM. Electrospray ionization for mass spectrometry of large biomolecules. Science. 1989 Oct 6;246(4926):64–71.

205. Hillenkamp F, Karas M, Beavis RC, Chait BT. Matrix-assisted laser desorption/ionization mass spectrometry of biopolymers. Anal Chem. 1991 Dec 15;63(24):1193A–1203A.

206. Mallick P, Kuster B. Proteomics: a pragmatic perspective. Nat Biotechnol. 2010 Jul;28(7):695–709.

207. Guerrera IC, Kleiner O. Application of mass spectrometry in proteomics. Biosci Rep. 2005 Apr;25(1-2):71–93.

208. Yates JR 3rd. Mass spectrometry. From genomics to proteomics. Trends Genet TIG. 2000 Jan;16(1):5–8.

209. Ong S-E, Blagoev B, Kratchmarova I, Kristensen DB, Steen H, Pandey A, et al. Stable isotope labeling by amino acids in cell culture, SILAC, as a simple and accurate approach to expression proteomics. Mol Cell Proteomics MCP. 2002 May;1(5):376–86.

210. Beynon RJ, Pratt JM. Metabolic labeling of proteins for proteomics. Mol Cell Proteomics MCP. 2005 Jul;4(7):857–72.

211. Dowling P, Meleady P, Henry M, Clynes M. Recent advances in clinical proteomics using mass spectrometry. Bioanalysis. 2010 Sep;2(9):1609–15.

212. Gerber SA, Rush J, Stemman O, Kirschner MW, Gygi SP. Absolute quantification of proteins and phosphoproteins from cell lysates by tandem MS. Proc Natl Acad Sci U S A. 2003 Jun 10;100(12):6940–5.

213. Bantscheff M, Schirle M, Sweetman G, Rick J, Kuster B. Quantitative mass spectrometry in proteomics: a critical review. Anal Bioanal Chem. 2007 Oct;389(4):1017–31.

214. Vaudel M, Sickmann A, Martens L. Peptide and protein quantification: a map of the minefield. Proteomics. 2010 Feb;10(4):650–70.

215. Ramos-Fernández A, López-Ferrer D, Vázquez J. Improved method for differential expression proteomics using trypsin-catalyzed 18O labeling with a correction for labeling efficiency. Mol Cell Proteomics MCP. 2007 Jul;6(7):1274–86.

216. Nahnsen S, Bielow C, Reinert K, Kohlbacher O. Tools for label-free peptide quantification. Mol Cell Proteomics MCP. 2013 Mar;12(3):549–56.

217. Bantscheff M, Schirle M, Sweetman G, Rick J, Kuster B. Quantitative mass spectrometry in proteomics: a critical review. Anal Bioanal Chem. 2007 Oct;389(4):1017–31.

218. Tate S, Larsen B, Bonner R, Gingras A-C. Label-free quantitative proteomics trends for protein-protein interactions. J Proteomics. 2013 Apr 9;81:91–101.

219. Lundgren DH, Hwang S-I, Wu L, Han DK. Role of spectral counting in quantitative proteomics. Expert Rev Proteomics. 2010 Feb;7(1):39–53.

220. Megger DA, Bracht T, Meyer HE, Sitek B. Label-free quantification in clinical proteomics. Biochim Biophys Acta. 2013 Aug;1834(8):1581–90.

221. Lu P, Vogel C, Wang R, Yao X, Marcotte EM. Absolute protein expression profiling estimates the relative contributions of transcriptional and translational regulation. Nat Biotechnol. 2007 Jan;25(1):117–24.

222. Florens L, Carozza MJ, Swanson SK, Fournier M, Coleman MK, Workman JL, et al. Analyzing chromatin remodeling complexes using shotgun proteomics and normalized spectral abundance factors. Methods San Diego Calif. 2006 Dec;40(4):303–11.

223. Zybailov B, Mosley AL, Sardiu ME, Coleman MK, Florens L, Washburn MP. Statistical analysis of membrane proteome expression changes in Saccharomyces cerevisiae. J Proteome Res. 2006 Sep;5(9):2339–47.

224. Griffin NM, Yu J, Long F, Oh P, Shore S, Li Y, et al. Label-free, normalized quantification of complex mass spectrometry data for proteomic analysis. Nat Biotechnol. 2010 Jan;28(1):83–9.

225. Asara JM, Christofk HR, Freimark LM, Cantley LC. A label-free quantification method by MS/MS TIC compared to SILAC and spectral counting in a proteomics screen. Proteomics. 2008 Mar;8(5):994–9.

226. Bondarenko PV, Chelius D, Shaler TA. Identification and Relative Quantitation of Protein Mixtures by Enzymatic Digestion Followed by Capillary Reversed-Phase Liquid Chromatography−Tandem Mass Spectrometry. Anal Chem. 2002 Sep 1;74(18):4741–9.

227. Chelius D, Bondarenko PV. Quantitative profiling of proteins in complex mixtures using liquid chromatography and mass spectrometry. J Proteome Res. 2002 Aug;1(4):317–23.

228. Callister SJ, Barry RC, Adkins JN, Johnson ET, Qian W-J, Webb-Robertson B-JM, et al. Normalization approaches for removing systematic biases associated with mass spectrometry and label-free proteomics. J Proteome Res. 2006 Feb;5(2):277–86.

229. America AHP, Cordewener JHG. Comparative LC-MS: a landscape of peaks and valleys. Proteomics. 2008 Feb;8(4):731–49.

230. Podwojski K, Eisenacher M, Kohl M, Turewicz M, Meyer HE, Rahnenführer J, et al. Peek a peak: a glance at statistics for quantitative label-free proteomics. Expert Rev Proteomics. 2010 Apr;7(2):249–61.

231. Neilson KA, Ali NA, Muralidharan S, Mirzaei M, Mariani M, Assadourian G, et al. Less label, more free: approaches in label-free quantitative mass spectrometry. Proteomics. 2011 Feb;11(4):535–53.

232. Cox J, Mann M. Quantitative, high-resolution proteomics for data-driven systems biology. Annu Rev Biochem. 2011 Jun 7;80:273–99.

233. Chiou S-H, Wu C-Y. Clinical proteomics: current status, challenges, and future perspectives. Kaohsiung J Med Sci. 2011 Jan;27(1):1–14.

234. Anderson L, Hunter CL. Quantitative mass spectrometric multiple reaction monitoring assays for major plasma proteins. Mol Cell Proteomics MCP. 2006 Apr;5(4):573–88.

235. Arnett SD, Lunte CE. Investigation of the mechanism of pH-mediated stacking of anions for the analysis of physiological samples by capillary electrophoresis. Electrophoresis. 2003 Jun;24(11):1745–52.

236. Whiteaker JR, Zhao L, Anderson L, Paulovich AG. An automated and multiplexed method for high throughput peptide immunoaffinity enrichment and multiple reaction monitoring mass spectrometry-based quantification of protein biomarkers. Mol Cell Proteomics MCP. 2010 Jan;9(1):184–96.

237. Pardo M, García A, Antrobus R, Blanco MJ, Dwek RA, Zitzmann N. Biomarker discovery from uveal melanoma secretomes: identification of gp100 and cathepsin D in patient serum. J Proteome Res. 2007 Jul;6(7):2802–11.

238. Pardo M, García A, Thomas B, Piñeiro A, Akoulitchev A, Dwek RA, et al. The characterization of the invasion phenotype of uveal melanoma tumour cells shows the presence of MUC18 and HMG-1 metastasis markers and leads to the identification of DJ-1 as a potential serum biomarker. Int J Cancer J Int Cancer. 2006 Sep 1;119(5):1014–22.

239. Pardo M, García A, Thomas B, Piñeiro A, Akoulitchev A, Dwek RA, et al. Proteome analysis of a human uveal melanoma primary cell culture by 2-DE and MS. Proteomics. 2005 Dec;5(18):4980–93.

240. Wang F, Bing Z, Zhang Y, Ao B, Zhang S, Ye C, et al. Quantitative proteomic analysis for radiation-induced cell cycle suspension in 92-1 melanoma cell line. J Radiat Res (Tokyo). 2013 Jul 1;54(4):649–62.

241. Yan L-B, Shi K, Bing Z-T, Sun Y-L, Shen Y. Proteomic analysis of energy metabolism and signal transduction in irradiated melanoma cells. Int J Ophthalmol. 2013;6(3):286–94.

242. Zuidervaart W, Hensbergen PJ, Wong M-C, Deelder AM, Tensen CP, Jager MJ, et al. Proteomic analysis of uveal melanoma reveals novel potential markers involved in tumor progression. Invest Ophthalmol Vis Sci. 2006 Mar;47(3):786–93.

243. Coupland SE, Vorum H, Mandal N, Kalirai H, Honoré B, Urbak SF, et al. Proteomics of uveal melanomas suggests HSP-27 as a possible surrogate marker of chromosome 3 loss. Invest Ophthalmol Vis Sci. 2010 Jan;51(1):12–20.

244. Linge A, Kennedy S, O'Flynn D, Beatty S, Moriarty P, Henry M, et al. Differential expression of fourteen proteins between uveal melanoma from patients who subsequently developed distant metastases versus those who did Not. Invest Ophthalmol Vis Sci. 2012;53(8):4634–43.

245. Albelda SM, Oliver PD, Romer LH, Buck CA. EndoCAM: a novel endothelial cell-cell adhesion molecule. J Cell Biol. 1990 Apr;110(4):1227–37.

246. Reeves R, Edberg DD, Li Y. Architectural transcription factor HMGI(Y) promotes tumor progression and mesenchymal transition of human epithelial cells. Mol Cell Biol. 2001 Jan;21(2):575–94.

247. Hod Y. Differential control of apoptosis by DJ-1 in prostate benign and cancer cells. J Cell Biochem. 2004 Aug 15;92(6):1221–33.

248. MacKeigan JP, Clements CM, Lich JD, Pope RM, Hod Y, Ting JP-Y. Proteomic profiling drug-induced apoptosis in non-small cell lung carcinoma: identification of RS/DJ-1 and RhoGDIalpha. Cancer Res. 2003 Oct 15;63(20):6928–34.

249. Kim RH, Peters M, Jang Y, Shi W, Pintilie M, Fletcher GC, et al. DJ-1, a novel regulator of the tumor suppressor PTEN. Cancer Cell. 2005 Mar;7(3):263–73.

250. He XY, Liu BY, Yao WY, Zhao XJ, Zheng Z, Li JF, et al. Serum DJ-1 as a diagnostic marker and prognostic factor for pancreatic cancer. J Dig Dis. 2011 Apr;12(2):131–7.

251. Bande MF, Santiago M, Blanco MJ, Mera P, Capeans C, Rodríguez-Alvarez MX, et al. Serum DJ-1/PARK 7 is a potential biomarker of choroidal nevi transformation. Invest Ophthalmol Vis Sci. 2012 Jan;53(1):62–7.

252. Bartenjev I, Rudolf Z, Stabuc B, Vrhovec I, Perkovic T, Kansky A. Cathepsin D expression in early cutaneous malignant melanoma. Int J Dermatol. 2000 Aug;39(8):599–602.

253. Lou X, Xiao T, Zhao K, Wang H, Zheng H, Lin D, et al. Cathepsin D is secreted from M-BE cells: its potential role as a biomarker of lung cancer. J Proteome Res. 2007 Mar;6(3):1083–92.

254. Borthwick NJ, Thombs J, Polak M, Gabriel FG, Hungerford JL, Damato B, et al. The biology of micrometastases from uveal melanoma. J Clin Pathol. 2011 Aug;64(8):666–71.

255. De Vries TJ, Trancikova D, Ruiter DJ, van Muijen GN. High expression of immunotherapy candidate proteins gp100, MART-1, tyrosinase and TRP-1 in uveal melanoma. Br J Cancer. 1998 Nov;78(9):1156–61.

256. Luyten GP, van der Spek CW, Brand I, Sintnicolaas K, de Waard-Siebinga I, Jager MJ, et al. Expression of MAGE, gp100 and tyrosinase genes in uveal melanoma cell lines. Melanoma Res. 1998 Feb;8(1):11–6.

257. Mulcahy KA, Rimoldi D, Brasseur F, Rodgers S, Liénard D, Marchand M, et al. Infrequent expression of the MAGE gene family in uveal melanomas. Int J Cancer J Int Cancer. 1996 Jun 11;66(6):738–42.

258. Gangemi R, Mirisola V, Barisione G, Fabbi M, Brizzolara A, Lanza F, et al. Mda-9/syntenin is expressed in uveal melanoma and correlates with metastatic progression. PloS One. 2012;7(1):e29989.

259. Das SK, Bhutia SK, Azab B, Kegelman TP, Peachy L, Santhekadur PK, et al. MDA-9/syntenin and IGFBP-2 promote angiogenesis in human melanoma. Cancer Res. 2013 Jan 15;73(2):844–54.

260. Das SK, Bhutia SK, Kegelman TP, Peachy L, Oyesanya RA, Dasgupta S, et al. MDA-9/syntenin: a positive gatekeeper of melanoma metastasis. Front Biosci Landmark Ed. 2012;17:1–15.

261. Helmke BM, Polychronidis M, Benner A, Thome M, Arribas J, Deichmann M. Melanoma metastasis is associated with enhanced expression of the syntenin gene. Oncol Rep. 2004 Aug;12(2):221–8.

262. Boukerche H, Su Z, Prévot C, Sarkar D, Fisher PB. mda-9/Syntenin promotes metastasis in human melanoma cells by activating c-Src. Proc Natl Acad Sci U S A. 2008 Oct 14;105(41):15914–9.

263. Das SK, Bhutia SK, Sokhi UK, Azab B, Su Z-Z, Boukerche H, et al. Raf kinase inhibitor RKIP inhibits MDA-9/syntenin-mediated metastasis in melanoma. Cancer Res. 2012 Dec 1;72(23):6217–26.

264. Maat W, el Filali M, Dirks-Mulder A, Luyten GPM, Gruis NA, Desjardins L, et al. Episodic Src activation in uveal melanoma revealed by kinase activity profiling. Br J Cancer. 2009 Jul 21;101(2):312–9.

265. Versluis M, El Filali M, Bronkhorst I, Baghat A, Luyten G, Jager M, et al. ERK activation and monosomy 3 are associated with Src expression in uveal melanoma and may serve as biomarkers for Dasatinib treatment. Acta Ophthalmol (Copenh). 2011;89:0–0.

266. Ohashi K, Nagata K, Maekawa M, Ishizaki T, Narumiya S, Mizuno K. Rho-associated kinase ROCK activates LIM-kinase 1 by phosphorylation at threonine 508 within the activation loop. J Biol Chem. 2000 Feb 4;275(5):3577–82.

267. Pavey S, Zuidervaart W, van Nieuwpoort F, Packer L, Jager M, Gruis N, et al. Increased p21-activated kinase-1 expression is associated with invasive potential in uveal melanoma. Melanoma Res. 2006 Aug;16(4):285–96.

268. Keezer SM, Ivie SE, Krutzsch HC, Tandle A, Libutti SK, Roberts DD. Angiogenesis inhibitors target the endothelial cell cytoskeleton through altered regulation of heat shock protein 27 and cofilin. Cancer Res. 2003 Oct 1;63(19):6405–12.

269. Rehman I, Azzouzi A-R, Cross SS, Deloulme JC, Catto JWF, Wylde N, et al. Dysregulated expression of S100A11 (calgizzarin) in prostate cancer and precursor lesions. Hum Pathol. 2004 Nov;35(11):1385–91.

270. Yao R, Davidson DD, Lopez-Beltran A, MacLennan GT, Montironi R, Cheng L. The S100 proteins for screening and prognostic grading of bladder cancer. Histol Histopathol. 2007 Sep;22(9):1025–32.

271. Wang G, Wang X, Wang S, Song H, Sun H, Yuan W, et al. Colorectal cancer progression correlates with upregulation of S100A11 expression in tumor tissues. Int J Colorectal Dis. 2008 Jul;23(7):675–82.

272. Cross SS, Hamdy FC, Deloulme JC, Rehman I. Expression of S100 proteins in normal human tissues and common cancers using tissue microarrays: S100A6, S100A8, S100A9 and S100A11 are all overexpressed in common cancers. Histopathology. 2005 Mar;46(3):256–69.

273. Barak V, Kaiserman I, Frenkel S, Hendler K, Kalickman I, Pe'er J. The dynamics of serum tumor markers in predicting metastatic uveal melanoma (part 1). Anticancer Res. 2011 Jan;31(1):345–9.

274. Barak V, Frenkel S, Kalickman I, Maniotis AJ, Folberg R, Pe'er J. Serum markers to detect metastatic uveal melanoma. Anticancer Res. 2007 Aug;27(4A):1897–900.

275. Artal-Sanz M, Tavernarakis N. Prohibitin and mitochondrial biology. Trends Endocrinol Metab TEM. 2009 Oct;20(8):394–401.

276. Sievers C, Billig G, Gottschalk K, Rudel T. Prohibitins are required for cancer cell proliferation and adhesion. PloS One. 2010;5(9):e12735.

277. Nan Y, Yang S, Tian Y, Zhang W, Zhou B, Bu L, et al. Analysis of the expression protein profiles of lung squamous carcinoma cell using shot-gun proteomics strategy. Med Oncol Northwood Lond Engl. 2009;26(2):215–21.

278. Sato T, Sakamoto T, Takita K, Saito H, Okui K, Nakamura Y. The human prohibitin (PHB) gene family and its somatic mutations in human tumors. Genomics. 1993 Sep;17(3):762–4.

279. Ummanni R, Junker H, Zimmermann U, Venz S, Teller S, Giebel J, et al. Prohibitin identified by proteomic analysis of prostate biopsies distinguishes hyperplasia and cancer. Cancer Lett. 2008 Aug 8;266(2):171–85.

280. Kang X, Zhang L, Sun J, Ni Z, Ma Y, Chen X, et al. Prohibitin: a potential biomarker for tissue-based detection of gastric cancer. J Gastroenterol. 2008;43(8):618–25.

281. Ryu J-W, Kim H-J, Lee Y-S, Myong N-H, Hwang C-H, Lee G-S, et al. The proteomics approach to find biomarkers in gastric cancer. J Korean Med Sci. 2003 Aug;18(4):505–9.

282. He J, Li J, Ye C, Zhou L, Zhu J, Wang J, et al. Cell cycle suspension: a novel process lurking in $G_2$ arrest. Cell Cycle Georget Tex. 2011 May 1;10(9):1468–76.

283. Rayamajhi M, Zhang Y, Miao EA. Detection of pyroptosis by measuring released lactate dehydrogenase activity. Methods Mol Biol Clifton NJ. 2013;1040:85–90.

284. Chen Y, Zhang H, Xu A, Li N, Liu J, Liu C, et al. Elevation of serum l-lactate dehydrogenase B correlated with the clinical stage of lung cancer. Lung Cancer Amst Neth. 2006 Oct;54(1):95–102.

285. Leiblich A, Cross SS, Catto JWF, Phillips JT, Leung HY, Hamdy FC, et al. Lactate dehydrogenase-B is silenced by promoter hypermethylation in human prostate cancer. Oncogene. 2006 May 11;25(20):2953–60.

286. Kami K, Fujimori T, Sato H, Sato M, Yamamoto H, Ohashi Y, et al. Metabolomic profiling of lung and prostate tumor tissues by capillary electrophoresis time-of-flight mass spectrometry. Metabolomics Off J Metabolomic Soc. 2013 Apr;9(2):444–53.

287. Novellasdemunt L, Tato I, Navarro-Sabate A, Ruiz-Meana M, Méndez-Lucas A, Perales JC, et al. Akt-dependent activation of the heart 6-phosphofructo-2-kinase/fructose-2,6-bisphosphatase (PFKFB2) isoenzyme by amino acids. J Biol Chem. 2013 Apr 12;288(15):10640–51.

288. Selumetinib shows promise in metastatic uveal melanoma. Cancer Discov. 2013 Jul;3(7):OF8.

289. Jmor F, Kalirai H, Taktak A, Damato B, Coupland SE. HSP-27 protein expression in uveal melanoma: correlation with predicted survival. Acta Ophthalmol (Copenh). 2012 Sep;90(6):534–9.

290. Kostenko S, Moens U. Heat shock protein 27 phosphorylation: kinases, phosphatases, functions and pathology. Cell Mol Life Sci CMLS. 2009 Oct;66(20):3289–307.

291. Lanneau D, Brunet M, Frisan E, Solary E, Fontenay M, Garrido C. Heat shock proteins: essential proteins for apoptosis regulation. J Cell Mol Med. 2008 Jun;12(3):743–61.

292. Cornford PA, Dodson AR, Parsons KF, Desmond AD, Woolfenden A, Fordham M, et al. Heat shock protein expression independently predicts clinical outcome in prostate cancer. Cancer Res. 2000 Dec 15;60(24):7099–105.

293. Kapranos N, Kominea A, Konstantinopoulos PA, Savva S, Artelaris S, Vandoros G, et al. Expression of the 27-kDa heat shock protein (HSP27) in gastric carcinomas and adjacent normal, metaplastic, and dysplastic gastric mucosa, and its prognostic significance. J Cancer Res Clin Oncol. 2002 Aug;128(8):426–32.

294. Thanner F, Sütterlin MW, Kapp M, Rieger L, Morr AK, Kristen P, et al. Heat shock protein 27 is associated with decreased survival in node-negative breast cancer patients. Anticancer Res. 2005 Jun;25(3A):1649–53.

295. Geisler JP, Tammela JE, Manahan KJ, Geisler HE, Miller GA, Zhou Z, et al. HSP27 in patients with ovarian carcinoma: still an independent prognostic indicator at 60 months follow-up. Eur J Gynaecol Oncol. 2004;25(2):165–8.

296. Malusecka E, Krzyzowska-Gruca S, Gawrychowski J, Fiszer-Kierzkowska A, Kolosza Z, Krawczyk Z. Stress proteins HSP27 and HSP70i predict survival in non-small cell lung carcinoma. Anticancer Res. 2008 Feb;28(1B):501–6.

297. Missotten GS, Journée-de Korver JG, de Wolff-Rouendaal D, Keunen JE, Schlingemann RO, Jager MJ. Heat shock protein expression in the eye and in uveal melanoma. Invest Ophthalmol Vis Sci. 2003 Jul;44(7):3059–65.

298. Aldrian S, Trautinger F, Fröhlich I, Berger W, Micksche M, Kindas-Mügge I. Overexpression of Hsp27 affects the metastatic phenotype of human melanoma cells in vitro. Cell Stress Chaperones. 2002 Apr;7(2):177–85.

299. Storch J, Thumser AE. The fatty acid transport function of fatty acid-binding proteins. Biochim Biophys Acta. 2000 Jun 26;1486(1):28–44.

300. Lichtenfels R, Dressler SP, Zobawa M, Recktenwald CV, Ackermann A, Atkins D, et al. Systematic comparative protein expression profiling of clear cell renal cell carcinoma: a pilot study based on the separation of tissue specimens by two-dimensional gel electrophoresis. Mol Cell Proteomics MCP. 2009 Dec;8(12):2827–42.

301. Zhang L, Cilley RE, Chinoy MR. Suppression subtractive hybridization to identify gene expressions in variant and classic small cell lung cancer cell lines. J Surg Res. 2000 Sep;93(1):108–19.

302. Okano T, Kondo T, Fujii K, Nishimura T, Takano T, Ohe Y, et al. Proteomic signature corresponding to the response to gefitinib (Iressa, ZD1839), an epidermal growth factor receptor tyrosine kinase inhibitor in lung adenocarcinoma. Clin Cancer Res Off J Am Assoc Cancer Res. 2007 Feb 1;13(3):799–805.

303. Hashimoto T, Kusakabe T, Sugino T, Fukuda T, Watanabe K, Sato Y, et al. Expression of heart-type fatty acid-binding protein in human gastric carcinoma and its association with tumor aggressiveness, metastasis and poor prognosis. Pathobiol J Immunopathol Mol Cell Biol. 2004;71(5):267–73.

304. Yang Y, Spitzer E, Kenney N, Zschiesche W, Li M, Kromminga A, et al. Members of the fatty acid binding protein family are differentiation factors for the mammary gland. J Cell Biol. 1994 Nov;127(4):1097–109.

305. Albery WJ, Knowles JR. Free-energy profile of the reaction catalyzed by triosephosphate isomerase. Biochemistry (Mosc). 1976 Dec 14;15(25):5627–31.

306. Bui T, Thompson CB. Cancer's sweet tooth. Cancer Cell. 2006 Jun;9(6):419–20.

307. Lee W-H, Choi J-S, Byun M-R, Koo K-T, Shin S, Lee S-K, et al. Functional inactivation of triosephosphate isomerase through phosphorylation during etoposide-induced apoptosis in HeLa cells: potential role of Cdk2. Toxicology. 2010 Dec 5;278(2):224–8.

308. Selicharova I, Sanda M, Mladkova J, Ohri SS, Vashishta A, Fusek M, et al. 2-DE analysis of breast cancer cell lines 1833 and 4175 with distinct metastatic organ-specific potentials: comparison with parental cell line MDA-MB-231. Oncol Rep. 2008 May;19(5):1237–44.

309. Chen G, Gharib TG, Huang C-C, Thomas DG, Shedden KA, Taylor JMG, et al. Proteomic analysis of lung adenocarcinoma: identification of a highly expressed set of proteins in tumors. Clin Cancer Res Off J Am Assoc Cancer Res. 2002 Jul;8(7):2298–305.

310. Kim JE, Koo KH, Kim YH, Sohn J, Park YG. Identification of potential lung cancer biomarkers using an in vitro carcinogenesis model. Exp Mol Med. 2008 Dec 31;40(6):709–20.

311. Qian X-L, Shi Q-G, Pang B, Wu R-Q, Yu L, Li S-H, et al. [Identification and expression of two new secretory proteins associated with prostate cancer]. Yi Chuan Hered Zhongguo Yi Chuan Xue Hui Bian Ji. 2010 Mar;32(3):235–41.

312. Bioethics IC for. Human biological material : recommendations for collection, use and storage in research 2005 /. Irish Council for Bioethics,; 2005. http://www.bioethics.ie/pdfs/BioEthics_fin.pdf

313. Huang DW, Sherman BT, Lempicki RA. Bioinformatics enrichment tools: paths toward the comprehensive functional analysis of large gene lists. Nucleic Acids Res. 2009 Jan;37(1):1–13.

314. Huang DW, Sherman BT, Lempicki RA. Systematic and integrative analysis of large gene lists using DAVID bioinformatics resources. Nat Protoc. 2009;4(1):44–57.

315. Mi H, Muruganujan A, Thomas PD. PANTHER in 2013: modeling the evolution of gene function, and other gene attributes, in the context of phylogenetic trees. Nucleic Acids Res. 2013 Jan;41(Database issue):D377–386.

316. Mi H, Muruganujan A, Casagrande JT, Thomas PD. Large-scale gene function analysis with the PANTHER classification system. Nat Protoc. 2013 Aug;8(8):1551–66.

317. Mi H, Thomas P. PANTHER pathway: an ontology-based pathway database coupled with data analysis tools. Methods Mol Biol Clifton NJ. 2009;563:123–40.

318. Remmele W, Stegner HE. [Recommendation for uniform definition of an immunoreactive score (IRS) for immunohistochemical estrogen receptor detection (ER-ICA) in breast cancer tissue]. Pathol. 1987 May;8(3):138–40.

319. Onken MD, Worley LA, Tuscan MD, Harbour JW. An accurate, clinically feasible multi-gene expression assay for predicting metastasis in uveal melanoma. J Mol Diagn JMD. 2010 Jul;12(4):461–8.

320. Hanahan D, Weinberg RA. The hallmarks of cancer. Cell. 2000 Jan 7;100(1):57–70.

321. Adams JM, Cory S. The Bcl-2 apoptotic switch in cancer development and therapy. Oncogene. 2007 Feb 26;26(9):1324–37.

322. Lowe SW, Cepero E, Evan G. Intrinsic tumour suppression. Nature. 2004 Nov 18;432(7015):307–15.

323. Evan G, Littlewood T. A matter of life and cell death. Science. 1998 Aug 28;281(5381):1317–22.

324. Coupland SE, Lake SL, Zeschnigk M, Damato BE. Molecular pathology of uveal melanoma. Eye Lond Engl. 2013 Feb;27(2):230–42.

325. PARK7 parkinson protein 7 [ Homo sapiens (human) ] [Internet]. Gene Entrez. Available from: http://www.ncbi.nlm.nih.gov/gene/11315

326. Emons G, Pahwa GS, Brack C, Sturm R, Oberheuser F, Knuppen R. Gonadotropin releasing hormone binding sites in human epithelial ovarian carcinomata. Eur J Cancer Clin Oncol. 1989 Feb;25(2):215–21.

327. Irmer G, Bürger C, Müller R, Ortmann O, Peter U, Kakar SS, et al. Expression of the messenger RNAs for luteinizing hormone-releasing hormone (LHRH) and its receptor in human ovarian epithelial carcinoma. Cancer Res. 1995 Feb 15;55(4):817–22.

328. Cheung LWT, Mak ASC, Cheung ANY, Ngan HYS, Leung PCK, Wong AST. P-cadherin cooperates with insulin-like growth factor-1 receptor to promote metastatic signaling of gonadotropin-releasing hormone in ovarian cancer via p120 catenin. Oncogene. 2011 Jun 30;30(26):2964–74.

329. Cheung LWT, Leung PCK, Wong AST. Cadherin switching and activation of p120 catenin signaling are mediators of gonadotropin-releasing hormone to promote tumor cell migration and invasion in ovarian cancer. Oncogene. 2010 Apr 22;29(16):2427–40.

330. Cheung LWT, Leung PCK, Wong AST. Gonadotropin-releasing hormone promotes ovarian cancer cell invasiveness through c-Jun NH2-terminal kinase-mediated activation of matrix metalloproteinase (MMP)-2 and MMP-9. Cancer Res. 2006 Nov 15;66(22):10902–10.

331. Cheung LW, Yung S, Chan T-M, Leung PC, Wong AS. Targeting Gonadotropin-releasing Hormone Receptor Inhibits the Early Step of Ovarian Cancer Metastasis by Modulating Tumor-mesothelial Adhesion. Mol Ther. 2013 Jan;21(1):78–90.

332. Nagy A, Schally AV. Targeting of cytotoxic luteinizing hormone-releasing hormone analogs to breast, ovarian, endometrial, and prostate cancers. Biol Reprod. 2005 Nov;73(5):851–9.

333. Von Alten J, Fister S, Schulz H, Viereck V, Frosch K-H, Emons G, et al. GnRH analogs reduce invasiveness of human breast cancer cells. Breast Cancer Res Treat. 2006 Nov;100(1):13–21.

334. Schubert A, Hawighorst T, Emons G, Gründker C. Agonists and antagonists of GnRH-I and -II reduce metastasis formation by triple-negative human breast cancer cells in vivo. Breast Cancer Res Treat. 2011 Dec;130(3):783–90.

335. Davidson L, Pawson AJ, Millar RP, Maudsley S. Cytoskeletal reorganization dependence of signaling by the gonadotropin-releasing hormone receptor. J Biol Chem. 2004 Jan 16;279(3):1980–93.

336. Enomoto M, Utsumi M, Park MK. Gonadotropin-releasing hormone induces actin cytoskeleton remodeling and affects cell migration in a cell-type-specific manner in TSU-Pr1 and DU145 cells. Endocrinology. 2006 Jan;147(1):530–42.

337. Yates C, Wells A, Turner T. Luteinising hormone-releasing hormone analogue reverses the cell adhesion profile of EGFR overexpressing DU-145 human prostate carcinoma subline. Br J Cancer. 2005 Jan 31;92(2):366–75.

338. Dobkin-Bekman M, Naidich M, Rahamim L, Przedecki F, Almog T, Lim S, et al. A preformed signaling complex mediates GnRH-activated ERK phosphorylation of paxillin and FAK at focal adhesions in L beta T2 gonadotrope cells. Mol Endocrinol Baltim Md. 2009 Nov;23(11):1850–64.

339. Miller WR, Scott WN, Morris R, Fraser HM, Sharpe RM. Growth of human breast cancer cells inhibited by a luteinizing hormone-releasing hormone agonist. Nature. 1985 Jan 17;313(5999):231–3.

340. Kahán Z, Nagy A, Schally AV, Halmos G, Arencibia JM, Groot K. Administration of a targeted cytotoxic analog of luteinizing hormone-releasing hormone inhibits growth of estrogen-independent MDA-MB-231 human breast cancers in nude mice. Breast Cancer Res Treat. 2000 Feb;59(3):255–62.

341. Kahán Z, Nagy A, Schally AV, Halmos G, Arencibia JM, Groot K. Complete regression of MX-1 human breast carcinoma xenografts after targeted chemotherapy with a cytotoxic analog of luteinizing hormone-releasing hormone, AN-207. Cancer. 1999 Jun 15;85(12):2608–15.

342. Aguilar-Rojas A, Huerta-Reyes M, Maya-Núñez G, Arechavaleta-Velásco F, Conn PM, Ulloa-Aguirre A, et al. Gonadotropin-releasing hormone receptor activates GTPase RhoA and inhibits cell invasion in the breast cancer cell line MDA-MB-231. BMC Cancer. 2012 Nov 23;12(1):550.

343. Vallar L, Spada A, Giannattasio G. Altered Gs and adenylate cyclase activity in human GH-secreting pituitary adenomas. Nature. 1987 Dec 10;330(6148):566–8.

344. Lehnerdt GF, Franz P, Winterhoff S, Bankfalvi A, Grehl S, Lang S, et al. The GNAS1 T393C polymorphism predicts survival in patients with advanced squamous cell carcinoma of the larynx. The Laryngoscope. 2008 Dec;118(12):2172–6.

345. Maudsley S, Davidson L, Pawson AJ, Chan R, López de Maturana R, Millar RP. Gonadotropin-releasing hormone (GnRH) antagonists promote proapoptotic signaling in peripheral reproductive tumor cells by activating a Galphai-coupling state of the type I GnRH receptor. Cancer Res. 2004 Oct 15;64(20):7533–44.

346. Gründker C, Völker P, Emons G. Antiproliferative signaling of luteinizing hormone-releasing hormone in human endometrial and ovarian cancer cells through G protein alpha(I)-mediated activation of phosphotyrosine phosphatase. Endocrinology. 2001 Jun;142(6):2369–80.

347. Kan Z, Jaiswal BS, Stinson J, Janakiraman V, Bhatt D, Stern HM, et al. Diverse somatic mutation patterns and pathway alterations in human cancers. Nature. 2010 Aug 12;466(7308):869–73.

348. Tominaga E, Tsuda H, Arao T, Nishimura S, Takano M, Kataoka F, et al. Amplification of GNAS may be an independent, qualitative, and reproducible biomarker to predict progression-free survival in epithelial ovarian cancer. Gynecol Oncol. 2010 Aug 1;118(2):160–6.

349. Alakus H, Warnecke-Eberz U, Bollschweiler E, Mönig SP, Vallböhmer D, Brabender J, et al. GNAS1 T393C polymorphism is associated with histopathological response to neoadjuvant radiochemotherapy in esophageal cancer. Pharmacogenomics J. 2009 Jun;9(3):202–7.

350. Otterbach F, Callies R, Frey UH, Schmitz KJ, Wreczycki C, Kimmig R, et al. The T393C polymorphism in the gene GNAS1 of G protein is associated with survival of patients with invasive breast carcinoma. Breast Cancer Res Treat. 2007 Nov;105(3):311–7.

351. Tominaga E, Tsuda H, Arao T, Nishimura S, Takano M, Kataoka F, et al. Amplification of GNAS may be an independent, qualitative, and reproducible biomarker to predict progression-free survival in epithelial ovarian cancer. Gynecol Oncol. 2010 Aug 1;118(2):160–6.

352. Xie F-J, Zhao P, Kou J-Y, Hong W, Fu L, Hu L, et al. The T393C polymorphism of GNAS1 as a predictor for chemotherapy sensitivity and survival in advanced non-small-cell lung cancer patients treated with gemcitabine plus platinum. Cancer Chemother Pharmacol. 2012 Jun;69(6):1443–8.

353. Hanahan D, Weinberg RA. Hallmarks of cancer: the next generation. Cell. 2011 Mar 4;144(5):646–74.

354. Kroemer G, Pouyssegur J. Tumor cell metabolism: cancer's Achilles' heel. Cancer Cell. 2008 Jun;13(6):472–82.

355. Mazurek S, Boschek CB, Hugo F, Eigenbrodt E. Pyruvate kinase type M2 and its role in tumor growth and spreading. Semin Cancer Biol. 2005 Aug;15(4):300–8.

356. Guo W, Giancotti FG. Integrin signalling during tumour progression. Nat Rev Mol Cell Biol. 2004 Oct;5(10):816–26.

357. Mitra SK, Schlaepfer DD. Integrin-regulated FAK-Src signaling in normal and cancer cells. Curr Opin Cell Biol. 2006 Oct;18(5):516–23.

358. Stupack DG, Puente XS, Boutsaboualoy S, Storgard CM, Cheresh DA. Apoptosis of adherent cells by recruitment of caspase-8 to unligated integrins. J Cell Biol. 2001 Oct 29;155(3):459–70.

359. Zhao H, Ross FP, Teitelbaum SL. Unoccupied alpha(v)beta3 integrin regulates osteoclast apoptosis by transmitting a positive death signal. Mol Endocrinol Baltim Md. 2005 Mar;19(3):771–80.

360. Stupack DG, Teitz T, Potter MD, Mikolon D, Houghton PJ, Kidd VJ, et al. Potentiation of neuroblastoma metastasis by loss of caspase-8. Nature. 2006 Jan 5;439(7072):95–9.

361. Kanamori M, Vanden Berg SR, Bergers G, Berger MS, Pieper RO. Integrin beta3 overexpression suppresses tumor growth in a human model of gliomagenesis: implications for the role of beta3 overexpression in glioblastoma multiforme. Cancer Res. 2004 Apr 15;64(8):2751–8.

362. Danen EH, van Kraats AA, Cornelissen IM, Ruiter DJ, van Muijen GN. Integrin beta 3 cDNA transfection into a highly metastatic alpha v beta 3-negative human melanoma cell line inhibits invasion and experimental metastasis. Biochem Biophys Res Commun. 1996 Sep 4;226(1):75–81.

363. Zutter MM, Santoro SA, Staatz WD, Tsung YL. Re-expression of the alpha 2 beta 1 integrin abrogates the malignant phenotype of breast carcinoma cells. Proc Natl Acad Sci U S A. 1995 Aug 1;92(16):7411–5.

364. Kren A, Baeriswyl V, Lehembre F, Wunderlin C, Strittmatter K, Antoniadis H, et al. Increased tumor cell dissemination and cellular senescence in the absence of beta1-integrin function. EMBO J. 2007 Jun 20;26(12):2832–42.

365. Varner JA, Emerson DA, Juliano RL. Integrin alpha 5 beta 1 expression negatively regulates cell growth: reversal by attachment to fibronectin. Mol Biol Cell. 1995 Jun;6(6):725–40.

366. Giancotti FG, Ruoslahti E. Elevated levels of the alpha 5 beta 1 fibronectin receptor suppress the transformed phenotype of Chinese hamster ovary cells. Cell. 1990 Mar 9;60(5):849–59.

367. Negrutskii BS, El'skaya AV. Eukaryotic translation elongation factor 1 alpha: structure, expression, functions, and possible role in aminoacyl-tRNA channeling. Prog Nucleic Acid Res Mol Biol. 1998;60:47–78.

368. Proud CG. Peptide-chain elongation in eukaryotes. Mol Biol Rep. 1994 May;19(3):161–70.

369. Sang Lee J, Gyu Park S, Park H, Seol W, Lee S, Kim S. Interaction network of human aminoacyl-tRNA synthetases and subunits of elongation factor 1 complex. Biochem Biophys Res Commun. 2002 Feb 15;291(1):158–64.

370. Janssen GM, Morales J, Schipper A, Labbé JC, Mulner-Lorillon O, Bellé R, et al. A major substrate of maturation promoting factor identified as elongation factor 1 beta gamma delta in Xenopus laevis. J Biol Chem. 1991 Aug 15;266(23):14885–8.

371. Kung AL, Sherwood SW, Schimke RT. Cell line-specific differences in the control of cell cycle progression in the absence of mitosis. Proc Natl Acad Sci U S A. 1990 Dec;87(24):9553–7.

372. Lew Y, Jones DV, Mars WM, Evans D, Byrd D, Frazier ML. Expression of elongation factor-1 gamma-related sequence in human pancreatic cancer. Pancreas. 1992;7(2):144–52.

373. Mimori K, Mori M, Inoue H, Ueo H, Mafune K, Akiyoshi T, et al. Elongation factor 1 gamma mRNA expression in oesophageal carcinoma. Gut. 1996 Jan;38(1):66–70.

374. Mimori K, Mori M, Tanaka S, Akiyoshi T, Sugimachi K. The overexpression of elongation factor 1 gamma mRNA in gastric carcinoma. Cancer. 1995 Mar 15;75(6 Suppl):1446–9.

375. Chi K, Jones DV, Frazier ML. Expression of an elongation factor 1 gamma-related sequence in adenocarcinomas of the colon. Gastroenterology. 1992 Jul;103(1):98–102.

376. Ender B, Lynch P, Kim YH, Inamdar NV, Cleary KR, Frazier ML. Overexpression of an elongation factor-1 gamma-hybridizing RNA in colorectal adenomas. Mol Carcinog. 1993;7(1):18–20.

377. Mathur S, Cleary KR, Inamdar N, Kim YH, Steck P, Frazier ML. Overexpression of elongation factor-1gamma protein in colorectal carcinoma. Cancer. 1998 Mar 1;82(5):816–21.

378. Ivaska J, Pallari H-M, Nevo J, Eriksson JE. Novel functions of vimentin in cell adhesion, migration, and signaling. Exp Cell Res. 2007 Jun 10;313(10):2050–62.

379. Tang HL, Lung HL, Wu KC, Le A-HP, Tang HM, Fung MC. Vimentin supports mitochondrial morphology and organization. Biochem J. 2008 Feb 15;410(1):141–6.

380. Morris EJ, Evason K, Wiand C, L'Ecuyer TJ, Fulton AB. Misdirected vimentin messenger RNA alters cell morphology and motility. J Cell Sci. 2000 Jul;113 ( Pt 13):2433–43.

381. Katsumoto T, Mitsushima A, Kurimura T. The role of the vimentin intermediate filaments in rat 3Y1 cells elucidated by immunoelectron microscopy and computer-graphic reconstruction. Biol Cell Auspices Eur Cell Biol Organ. 1990;68(2):139–46.

382. Singh S, Sadacharan S, Su S, Belldegrun A, Persad S, Singh G. Overexpression of vimentin: role in the invasive phenotype in an androgen-independent model of prostate cancer. Cancer Res. 2003 May 1;63(9):2306–11.

383. Zhao Y, Yan Q, Long X, Chen X, Wang Y. Vimentin affects the mobility and invasiveness of prostate cancer cells. Cell Biochem Funct. 2008 Oct;26(5):571–7.

384. Wu M, Bai X, Xu G, Wei J, Zhu T, Zhang Y, et al. Proteome analysis of human androgen-independent prostate cancer cell lines: variable metastatic potentials correlated with vimentin expression. Proteomics. 2007 Jun;7(12):1973–83.

385. Sethi S, Macoska J, Chen W, Sarkar FH. Molecular signature of epithelial-mesenchymal transition (EMT) in human prostate cancer bone metastasis. Am J Transl Res. 2010;3(1):90–9.

386. Fuyuhiro Y, Yashiro M, Noda S, Kashiwagi S, Matsuoka J, Doi Y, et al. Clinical significance of vimentin-positive gastric cancer cells. Anticancer Res. 2010 Dec;30(12):5239–43.

387. Takemura K, Hirayama R, Hirokawa K, Inagaki M, Tsujimura K, Esaki Y, et al. Expression of vimentin in gastric cancer: a possible indicator for prognosis. Pathobiol J Immunopathol Mol Cell Biol. 1994;62(3):149–54.

388. Jin H, Morohashi S, Sato F, Kudo Y, Akasaka H, Tsutsumi S, et al. Vimentin expression of esophageal squamous cell carcinoma and its aggressive potential for lymph node metastasis. Biomed Res Tokyo Jpn. 2010 Apr;31(2):105–12.

389. Hu L, Lau SH, Tzang C-H, Wen J-M, Wang W, Xie D, et al. Association of Vimentin overexpression and hepatocellular carcinoma metastasis. Oncogene. 2004 Jan 8;23(1):298–302.

390. Alfonso P, Núñez A, Madoz-Gurpide J, Lombardia L, Sánchez L, Casal JI. Proteomic expression analysis of colorectal cancer by two-dimensional differential gel electrophoresis. Proteomics. 2005 Jul;5(10):2602–11.

391. Korsching E, Packeisen J, Liedtke C, Hungermann D, Wülfing P, van Diest PJ, et al. The origin of vimentin expression in invasive breast cancer: epithelial-mesenchymal transition, myoepithelial histogenesis or histogenesis from progenitor cells with bilinear differentiation potential? J Pathol. 2005 Aug;206(4):451–7.

392. Gilles C, Polette M, Mestdagt M, Nawrocki-Raby B, Ruggeri P, Birembaut P, et al. Transactivation of vimentin by beta-catenin in human breast cancer cells. Cancer Res. 2003 May 15;63(10):2658–64.

393. Li M, Zhang B, Sun B, Wang X, Ban X, Sun T, et al. A novel function for vimentin: the potential biomarker for predicting melanoma hematogenous metastasis. J Exp Clin Cancer Res CR. 2010;29:109.

394. Chu YW, Seftor EA, Romer LH, Hendrix MJ. Experimental coexpression of vimentin and keratin intermediate filaments in human melanoma cells augments motility. Am J Pathol. 1996 Jan;148(1):63–9.

395. Hendrix MJ, Seftor EA, Chu YW, Seftor RE, Nagle RB, McDaniel KM, et al. Coexpression of vimentin and keratins by human melanoma tumor cells: correlation with invasive and metastatic potential. J Natl Cancer Inst. 1992 Feb 5;84(3):165–74.

396. Ben-Ze'ev A, Raz A. Relationship between the organization and synthesis of vimentin and the metastatic capability of B16 melanoma cells. Cancer Res. 1985 Jun;45(6):2632–41.

397. Caselitz J, Jänner M, Breitbart E, Weber K, Osborn M. Malignant melanomas contain only the vimentin type of intermediate filaments. Virchows Arch A Pathol Anat Histopathol. 1983;400(1):43–51.

398. Corbi N, Batassa EM, Pisani C, Onori A, Di Certo MG, Strimpakos G, et al. The eEF1? Subunit Contacts RNA Polymerase II and Binds Vimentin Promoter Region. PLoS ONE [Internet]. 2010 Dec 31 [cited 2013 Oct 24];5(12). Available from: http://www.ncbi.nlm.nih.gov/pmc/articles/PMC3013090/

399. Wang H-Q, Du Z-X, Liu B-Q, Gao Y-Y, Meng X, Guan Y, et al. TNF-related apoptosis-inducing ligand suppresses PRDX4 expression. FEBS Lett. 2009 May 6;583(9):1511–5.

400. Whitaker HC, Patel D, Howat WJ, Warren AY, Kay JD, Sangan T, et al. Peroxiredoxin-3 is overexpressed in prostate cancer and promotes cancer cell survival by protecting cells from oxidative stress. Br J Cancer. 2013 Jul 23;

401. Ladd AN, Charlet N, Cooper TA. The CELF family of RNA binding proteins is implicated in cell-specific and developmentally regulated alternative splicing. Mol Cell Biol. 2001 Feb;21(4):1285–96.

402. Mukhopadhyay D, Jung J, Murmu N, Houchen CW, Dieckgraefe BK, Anant S. CUGBP2 plays a critical role in apoptosis of breast cancer cells in response to genotoxic injury. Ann N Y Acad Sci. 2003 Dec;1010:504–9.

403. Natarajan G, Ramalingam S, Ramachandran I, May R, Queimado L, Houchen CW, et al. CUGBP2 downregulation by prostaglandin E2 protects colon cancer cells from radiation-induced mitotic catastrophe. Am J Physiol Gastrointest Liver Physiol. 2008 May;294(5):G1235–1244.

404. Ramalingam S, Ramamoorthy P, Subramaniam D, Anant S. Reduced Expression of RNA Binding Protein CELF2, a Putative Tumor Suppressor Gene in Colon Cancer. Immuno-Gastroenterol. 2012;1(1):27–33.

405. Subramaniam D, Ramalingam S, Linehan DC, Dieckgraefe BK, Postier RG, Houchen CW, et al. RNA binding protein CUGBP2/CELF2 mediates curcumin-induced mitotic catastrophe of pancreatic cancer cells. PloS One. 2011;6(2):e16958.

406. Burgess BL, Rao NP, Eskin A, Nelson SF, McCannel TA. Characterization of three cell lines derived from fine needle biopsy of choroidal melanoma with metastatic outcome. Mol Vis. 2011;17:607–15.

407. McCannel TA, Burgess BL, Rao NP, Nelson SF, Straatsma BR. Identification of candidate tumor oncogenes by integrative molecular analysis of choroidal melanoma fine-needle aspiration biopsy specimens. Arch Ophthalmol. 2010 Sep;128(9):1170–7.

408. Gils W van, Lodder EM, Mensink HW, Kiliç E, Naus NC, Brüggenwirth HT, et al. Gene Expression Profiling in Uveal Melanoma: Two Regions on 3p Related to Prognosis. Invest Ophthalmol Vis Sci. 2008 Oct 1;49(10):4254–62.

409. Worby CA, Gentry MS, Dixon JE. Malin decreases glycogen accumulation by promoting the degradation of protein targeting to glycogen (PTG). J Biol Chem. 2008 Feb 15;283(7):4069–76.

410. Doherty MJ, Young PR, Cohen PT. Amino acid sequence of a novel protein phosphatase 1 binding protein (R5) which is related to the liver- and muscle-specific glycogen binding subunits of protein phosphatase 1. FEBS Lett. 1996 Dec 16;399(3):339–43.

411. Papandreou I, Cairns RA, Fontana L, Lim AL, Denko NC. HIF-1 mediates adaptation to hypoxia by actively downregulating mitochondrial oxygen consumption. Cell Metab. 2006 Mar;3(3):187–97.

412. Beyer S, Kristensen MM, Jensen KS, Johansen JV, Staller P. The histone demethylases JMJD1A and JMJD2B are transcriptional targets of hypoxia-inducible factor HIF. J Biol Chem. 2008 Dec 26;283(52):36542–52.

413. Shen G-M, Zhang F-L, Liu X-L, Zhang J-W. Hypoxia-inducible factor 1-mediated regulation of PPP1R3C promotes glycogen accumulation in human MCF-7 cells under hypoxia. FEBS Lett. 2010 Oct 22;584(20):4366–72.

414. Bonazzi VF, Irwin D, Hayward NK. Identification of candidate tumor suppressor genes inactivated by promoter methylation in melanoma. Genes Chromosomes Cancer. 2009 Jan;48(1):10–21.

415. Kim JH, Dhanasekaran SM, Prensner JR, Cao X, Robinson D, Kalyana-Sundaram S, et al. Deep sequencing reveals distinct patterns of DNA methylation in prostate cancer. Genome Res. 2011 Jul;21(7):1028–41.

416. Kim Y-H, Lee HC, Kim S-Y, Yeom YI, Ryu KJ, Min B-H, et al. Epigenomic Analysis of Aberrantly Methylated Genes in Colorectal Cancer Identifies Genes Commonly Affected by Epigenetic Alterations. Ann Surg Oncol. 2011 Aug;18(8):2338–47.

417. Zhou D, Yang L, Zheng L, Ge W, Li D, Zhang Y, et al. Exome Capture Sequencing of Adenoma Reveals Genetic Alterations in Multiple Cellular Pathways at the Early Stage of Colorectal Tumorigenesis. PLoS ONE [Internet]. 2013 Jan 2 [cited 2013 Sep 15];8(1). Available from: http://www.ncbi.nlm.nih.gov/pmc/articles/PMC3534699/

418. Vogt PK. Jun, the oncoprotein. Oncogene. 2001 Apr 30;20(19):2365–77.

419. Vasilevskaya I, O'Dwyer PJ. Role of Jun and Jun kinase in resistance of cancer cells to therapy. Drug Resist Updat Rev Comment Antimicrob Anticancer Chemother. 2003 Jun;6(3):147–56.

420. DLC1 deleted in liver cancer 1 [ Homo sapiens (human) ] [Internet]. Gene Entrez. Available from: http://www.ncbi.nlm.nih.gov/gene/10395

421. Durkin ME, Yuan B-Z, Zhou X, Zimonjic DB, Lowy DR, Thorgeirsson SS, et al. DLC-1:a Rho GTPase-activating protein and tumour suppressor. J Cell Mol Med. 2007 Oct;11(5):1185–207.

422. Tripathi V, Popescu NC, Zimonjic DB. DLC1 Interaction with ?-Catenin Stabilizes Adherens Junctions and Enhances DLC1 Antioncogenic Activity. Mol Cell Biol. 2012 Jun;32(11):2145–59.

423. Kim TY, Vigil D, Der CJ, Juliano RL. Role of DLC-1, a tumor suppressor protein with RhoGAP activity, in regulation of the cytoskeleton and cell motility. Cancer Metastasis Rev. 2009 Jun;28(1-2):77–83.

424. Shih Y-P, Liao Y-C, Lin Y, Lo SH. DLC1 negatively regulates angiogenesis in a paracrine fashion. Cancer Res. 2010 Nov 1;70(21):8270–5.

425. Chung GE, Yoon J-H, Lee J-H, Kim HY, Myung SJ, Yu SJ, et al. Ursodeoxycholic acid-induced inhibition of DLC1 protein degradation leads to suppression of hepatocellular carcinoma cell growth. Oncol Rep. 2011 Jun;25(6):1739–46.

426. Zhou X, Zimonjic DB, Park S-W, Yang X-Y, Durkin ME, Popescu NC. DLC1 suppresses distant dissemination of human hepatocellular carcinoma cells in nude mice through reduction of RhoA GTPase activity, actin cytoskeletal disruption and down-regulation of genes involved in metastasis. Int J Oncol. 2008 Jun;32(6):1285–91.

427. Wong C-M, Yam JW-P, Ching Y-P, Yau T-O, Leung TH-Y, Jin D-Y, et al. Rho GTPase-activating protein deleted in liver cancer suppresses cell proliferation and invasion in hepatocellular carcinoma. Cancer Res. 2005 Oct 1;65(19):8861–8.

428. Xue W, Krasnitz A, Lucito R, Sordella R, Vanaelst L, Cordon-Cardo C, et al. DLC1 is a chromosome 8p tumor suppressor whose loss promotes hepatocellular carcinoma. Genes Dev. 2008 Jun 1;22(11):1439–44.

429. Zhou X, Thorgeirsson SS, Popescu NC. Restoration of DLC-1 gene expression induces apoptosis and inhibits both cell growth and tumorigenicity in human hepatocellular carcinoma cells. Oncogene. 2004 Feb 12;23(6):1308–13.

430. Ullmannova V, Popescu NC. Expression profile of the tumor suppressor genes DLC-1 and DLC-2 in solid tumors. Int J Oncol. 2006 Nov;29(5):1127–32.

431. Low JSW, Tao Q, Ng KM, Goh HK, Shu X-S, Woo WL, et al. A novel isoform of the 8p22 tumor suppressor gene DLC1 suppresses tumor growth and is frequently silenced in multiple common tumors. Oncogene. 2011 Apr 21;30(16):1923–35.

432. Feng Y, Zhou H, Li J, Li Z, Cheng W, Jin M, et al. [Expression of deleted in liver cancer 1 and phosphorelated focal adhesion kinase in breast cancer]. Nan Fang Yi Ke Da Xue Xue Bao. 2011 Aug;31(8):1448–51.

433. Guan C-N, Zhang P-W, Lou H-Q, Liao X-H, Chen B-Y. DLC-1 expression levels in breast cancer assessed by qRT- PCR are negatively associated with malignancy. Asian Pac J Cancer Prev APJCP. 2012;13(4):1231–3.

434. Goodison S, Yuan J, Sloan D, Kim R, Li C, Popescu NC, et al. The RhoGAP protein DLC-1 functions as a metastasis suppressor in breast cancer cells. Cancer Res. 2005 Jul 15;65(14):6042–53.

435. Yang X, Popescu NC, Zimonjic DB. DLC1 interaction with S100A10 mediates inhibition of in vitro cell invasion and tumorigenicity of lung cancer cells through a RhoGAP-independent mechanism. Cancer Res. 2011 Apr 15;71(8):2916–25.

436. Healy KD, Hodgson L, Kim T-Y, Shutes A, Maddileti S, Juliano RL, et al. DLC-1 suppresses non-small cell lung cancer growth and invasion by RhoGAP-dependent and independent mechanisms. Mol Carcinog. 2008 May;47(5):326–37.

437. Yuan B-Z, Jefferson AM, Millecchia L, Popescu NC, Reynolds SH. Morphological changes and nuclear translocation of DLC1 tumor suppressor protein precede apoptosis in human non-small cell lung carcinoma cells. Exp Cell Res. 2007 Nov 1;313(18):3868–80.

438. Guan M, Tripathi V, Zhou X, Popescu NC. Adenovirus-mediated restoration of expression of the tumor suppressor gene DLC1 inhibits the proliferation and tumorigenicity of aggressive, androgen-independent human prostate cancer cell lines: prospects for gene therapy. Cancer Gene Ther. 2008 Jun;15(6):371–81.

439. Zhou X, Yang X-Y, Popescu NC. Synergistic antineoplastic effect of DLC1 tumor suppressor protein and histone deacetylase inhibitor, suberoylanilide hydroxamic acid (SAHA), on prostate and liver cancer cells: perspectives for therapeutics. Int J Oncol. 2010 Apr;36(4):999–1005.

440. Guan M, Zhou X, Soulitzis N, Spandidos DA, Popescu NC. Aberrant methylation and deacetylation of deleted in liver cancer-1 gene in prostate cancer: potential clinical applications. Clin Cancer Res Off J Am Assoc Cancer Res. 2006 Mar 1;12(5):1412–9.

441. Ullmannova-Benson V, Guan M, Zhou X, Tripathi V, Yang X-Y, Zimonjic DB, et al. DLC1 tumor suppressor gene inhibits migration and invasion of multiple myeloma cells through RhoA GTPase pathway. Leukemia. 2009 Feb;23(2):383–90.

442. Tripathi SC, Kaur J, Matta A, Gao X, Sun B, Chauhan SS, et al. Loss of DLC1 is an independent prognostic factor in patients with oral squamous cell carcinoma. Mod Pathol Off J U S Can Acad Pathol Inc. 2012 Jan;25(1):14–25.

443. Dai Z, Jin Y. Promoter methylation of the DLC-1 gene and its inhibitory effect on human colon cancer. Oncol Rep. 2013 Jun 19;

444. Feng X, Li C, Liu W, Chen H, Zhou W, Wang L, et al. DLC-1, a candidate tumor suppressor gene, inhibits the proliferation, migration and tumorigenicity of human nasopharyngeal carcinoma cells. Int J Oncol. 2013 Jun;42(6):1973–84.

445. Cao X, Voss C, Zhao B, Kaneko T, Li SS-C. Differential regulation of the activity of deleted in liver cancer 1 (DLC1) by tensins controls cell migration and transformation. Proc Natl Acad Sci U S A. 2012 Jan 31;109(5):1455–60.

446. Qian X, Li G, Asmussen HK, Asnaghi L, Vass WC, Braverman R, et al. Oncogenic inhibition by a deleted in liver cancer gene requires cooperation between tensin binding and Rho-specific GTPase-activating protein activities. Proc Natl Acad Sci U S A. 2007 May 22;104(21):9012–7.

447. Hynes NE, MacDonald G. ErbB receptors and signaling pathways in cancer. Curr Opin Cell Biol. 2009 Apr;21(2):177–84.

448. Onken MD, Worley LA, Harbour JW. A Metastasis Modifier Locus on Human Chromosome 8p in Uveal Melanoma Identified by Integrative Genomic Analysis. Clin Cancer Res. 2008 Jun 15;14(12):3737–45.

449. Trolet J, Hupé P, Huon I, Lebigot I, Decraene C, Delattre O, et al. Genomic Profiling and Identification of High-Risk Uveal Melanoma by Array CGH Analysis of Primary Tumors and Liver Metastases. Invest Ophthalmol Vis Sci. 2009 Jun 1;50(6):2572–80.

450. Ewens KG, Kanetsky PA, Richards-Yutz J, Al-Dahmash S, De Luca MC, Bianciotto CG, et al. Genomic profile of 320 uveal melanoma cases: chromosome 8p-loss and metastatic outcome. Invest Ophthalmol Vis Sci. 2013 Aug;54(8):5721–9.

451. Moss ML, Stoeck A, Yan W, Dempsey PJ. ADAM10 as a target for anti-cancer therapy. Curr Pharm Biotechnol. 2008 Feb;9(1):2–8.

452. Gangemi R, Amaro A, Gino A, Barisione G, Fabbi M, Pfeffer U, et al. ADAM10 correlates with uveal melanoma metastasis and promotes in vitro invasion. Pigment Cell Melanoma Res. 2014 Nov;27(6):1138–48.

453. Paris D, Quadros A, Patel N, DelleDonne A, Humphrey J, Mullan M. Inhibition of angiogenesis and tumor growth by beta and gamma-secretase inhibitors. Eur J Pharmacol. 2005 May 2;514(1):1–15.

454. Wang Z, Zhang Y, Li Y, Banerjee S, Liao J, Sarkar FH. Down-regulation of Notch-1 contributes to cell growth inhibition and apoptosis in pancreatic cancer cells. Mol Cancer Ther. 2006 Mar;5(3):483–93.

455. Wang Z, Zhang Y, Banerjee S, Li Y, Sarkar FH. Notch-1 down-regulation by curcumin is associated with the inhibition of cell growth and the induction of apoptosis in pancreatic cancer cells. Cancer. 2006 Jun 1;106(11):2503–13.

456. Van Es JH, van Gijn ME, Riccio O, van den Born M, Vooijs M, Begthel H, et al. Notch/gamma-secretase inhibition turns proliferative cells in intestinal crypts and adenomas into goblet cells. Nature. 2005 Jun 16;435(7044):959–63.

457. Van Es JH, Clevers H. Notch and Wnt inhibitors as potential new drugs for intestinal neoplastic disease. Trends Mol Med. 2005 Nov;11(11):496–502.

458. Asnaghi L, Lin MH, Lim KS, Lim KJ, Tripathy A, Wendeborn M, et al. Hypoxia promotes uveal melanoma invasion through enhanced Notch and MAPK activation. PloS One. 2014;9(8):e105372.

459. Asnaghi L, Handa JT, Merbs SL, Harbour JW, Eberhart CG. A role for Jag2 in promoting uveal melanoma dissemination and growth. Invest Ophthalmol Vis Sci. 2013 Jan;54(1):295–306.

460. Huang X, Wang L, Zhang H, Wang H, Zhao X, Qian G, et al. Therapeutic efficacy by targeting correction of Notch1-induced aberrants in uveal tumors. PloS One. 2012;7(8):e44301.

461. Asnaghi L, Ebrahimi KB, Schreck KC, Bar EE, Coonfield ML, Bell WR, et al. Notch signaling promotes growth and invasion in uveal melanoma. Clin Cancer Res Off J Am Assoc Cancer Res. 2012 Feb 1;18(3):654–65.

462. Brueckl WM, Grombach J, Wein A, Ruckert S, Porzner M, Dietmaier W, et al. Alterations in the tissue inhibitor of metalloproteinase-3 (TIMP-3) are found frequently in human colorectal tumours displaying either microsatellite stability (MSS) or instability (MSI). Cancer Lett. 2005 Jun 1;223(1):137–42.

463. Van der Velden PA, Zuidervaart W, Hurks MHMH, Pavey S, Ksander BR, Krijgsman E, et al. Expression profiling reveals that methylation of TIMP3 is involved in uveal melanoma development. Int J Cancer J Int Cancer. 2003 Sep 10;106(4):472–9.

464. Bange FC, Flohr T, Buwitt U, Böttger EC. An interferon-induced protein with release factor activity is a tryptophanyl-tRNA synthetase. FEBS Lett. 1992 Mar 30;300(2):162–6.

465. Tzima E, Reader JS, Irani-Tehrani M, Ewalt KL, Schwartz MA, Schimmel P. Biologically active fragment of a human tRNA synthetase inhibits fluid shear stress-activated responses of endothelial cells. Proc Natl Acad Sci U S A. 2003 Dec 9;100(25):14903–7.

466. Rubin BY, Anderson SL, Xing L, Powell RJ, Tate WP. Interferon induces tryptophanyl-tRNA synthetase expression in human fibroblasts. J Biol Chem. 1991 Dec 25;266(36):24245–8.

467. Yu Y, Liu Y, Shen N, Xu X, Xu F, Jia J, et al. Crystal structure of human tryptophanyl-tRNA synthetase catalytic fragment: insights into substrate recognition, tRNA binding, and angiogenesis activity. J Biol Chem. 2004 Feb 27;279(9):8378–88.

468. Wakasugi K, Slike BM, Hood J, Otani A, Ewalt KL, Friedlander M, et al. A human aminoacyl-tRNA synthetase as a regulator of angiogenesis. Proc Natl Acad Sci U S A. 2002 Jan 8;99(1):173–7.

469. Salvucci O, Basik M, Yao L, Bianchi R, Tosato G. Evidence for the involvement of SDF-1 and CXCR4 in the disruption of endothelial cell-branching morphogenesis and angiogenesis by TNF-alpha and IFN-gamma. J Leukoc Biol. 2004 Jul;76(1):217–26.

470. Otani A, Slike BM, Dorrell MI, Hood J, Kinder K, Ewalt KL, et al. A fragment of human TrpRS as a potent antagonist of ocular angiogenesis. Proc Natl Acad Sci U S A. 2002 Jan 8;99(1):178–83.

471. Ghanipour A, Jirström K, Pontén F, Glimelius B, Påhlman L, Birgisson H. The prognostic significance of tryptophanyl-tRNA synthetase in colorectal cancer. Cancer Epidemiol Biomark Prev Publ Am Assoc Cancer Res Cosponsored Am Soc Prev Oncol. 2009 Nov;18(11):2949–56.

472. Paley EL, Paley DE, Merkulova-Rainon T, Subbarayan PR. Hypoxia signature of splice forms of tryptophanyl-tRNA synthetase marks pancreatic cancer cells with distinct metastatic abilities. Pancreas. 2011 Oct;40(7):1043–56.

473. Yang H, Jager MJ, Grossniklaus HE. Bevacizumab suppression of establishment of micrometastases in experimental ocular melanoma. Invest Ophthalmol Vis Sci. 2010 Jun;51(6):2835–42.

474. Notting IC, Missotten GSOA, Sijmons B, Boonman ZFHM, Keunen JEE, van der Pluijm G. Angiogenic profile of uveal melanoma. Curr Eye Res. 2006 Sep;31(9):775–85.

475. BCAT1 branched chain amino-acid transaminase 1, cytosolic [ Homo sapiens (human) ] [Internet]. Gene Entrez. Available from: http://www.ncbi.nlm.nih.gov/gene/586

476. Ben-Yosef T, Eden A, Benvenisty N. Characterization of murine BCAT genes: Bcat1, a c-Myc target, and its homolog, Bcat2. Mamm Genome Off J Int Mamm Genome Soc. 1998 Jul;9(7):595–7.

477. Yoshikawa R, Yanagi H, Shen C-S, Fujiwara Y, Noda M, Yagyu T, et al. ECA39 is a novel distant metastasis-related biomarker in colorectal cancer. World J Gastroenterol WJG. 2006 Sep 28;12(36):5884–9.

478. Benvenisty N, Leder A, Kuo A, Leder P. An embryonically expressed gene is a target for c-Myc regulation via the c-Myc-binding sequence. Genes Dev. 1992 Dec;6(12B):2513–23.

479. Ben-Yosef T, Yanuka O, Benvenisty N. ECA39 is regulated by c-Myc in human and by a Jun/Fos homolog, Gcn4, in yeast. Oncogene. 1996 Nov 7;13(9):1859–66.

480. Schuldiner O, Eden A, Ben-Yosef T, Yanuka O, Simchen G, Benvenisty N. ECA39, a conserved gene regulated by c-Myc in mice, is involved in G1/S cell cycle regulation in yeast. Proc Natl Acad Sci U S A. 1996 Jul 9;93(14):7143–8.

481. Zhou W, Feng X, Ren C, Jiang X, Liu W, Huang W, et al. Over-expression of BCAT1, a c-Myc target gene, induces cell proliferation, migration and invasion in nasopharyngeal carcinoma. Mol Cancer. 2013 Jun 8;12:53.

482. Zhou W, Feng X, Li H, Wang L, Li H, Zhu B, et al. Functional evidence for a nasopharyngeal carcinoma-related gene BCAT1 located at 12p12. Oncol Res. 2007;16(9):405–13.

483. Sisley K, Rennie IG, Parsons MA, Jacques R, Hammond DW, Bell SM, et al. Abnormalities of chromosomes 3 and 8 in posterior uveal melanoma correlate with prognosis. Genes Chromosomes Cancer. 1997 May;19(1):22–8.

484. Wonsey DR, Zeller KI, Dang CV. The c-Myc target gene PRDX3 is required for mitochondrial homeostasis and neoplastic transformation. Proc Natl Acad Sci U S A. 2002 May 14;99(10):6649–54.

485. SDC2 syndecan 2 [ Homo sapiens (human) ] [Internet]. Gene Entrez. Available from: http://www.ncbi.nlm.nih.gov/gene?cmd=Retrieve&dopt=full_report&list_uids=6383

486. Zimmermann P, Zhang Z, Degeest G, Mortier E, Leenaerts I, Coomans C, et al. Syndecan recycling [corrected] is controlled by syntenin-PIP2 interaction and Arf6. Dev Cell. 2005 Sep;9(3):377–88.

487. Grootjans JJ, Zimmermann P, Reekmans G, Smets A, Degeest G, Dürr J, et al. Syntenin, a PDZ protein that binds syndecan cytoplasmic domains. Proc Natl Acad Sci U S A. 1997 Dec 9;94(25):13683–8.

488. Lee H, Kim Y, Choi Y, Choi S, Hong E, Oh E-S. Syndecan-2 cytoplasmic domain regulates colon cancer cell migration via interaction with syntenin-1. Biochem Biophys Res Commun. 2011 May 27;409(1):148–53.

489. Pardo M, García A, Antrobus R, Blanco MJ, Dwek RA, Zitzmann N. Biomarker discovery from uveal melanoma secretomes: identification of gp100 and cathepsin D in patient serum. J Proteome Res. 2007 Jul;6(7):2802–11.

490. Gangemi R, Mirisola V, Barisione G, Fabbi M, Brizzolara A, Lanza F, et al. Mda-9/syntenin is expressed in uveal melanoma and correlates with metastatic progression. PloS One. 2012;7(1):e29989.

491. Thies A, Schachner M, Moll I, Berger J, Schulze H-J, Brunner G, et al. Overexpression of the cell adhesion molecule L1 is associated with metastasis in cutaneous malignant melanoma. Eur J Cancer Oxf Engl 1990. 2002 Sep;38(13):1708–16.

492. Zecchini S, Bianchi M, Colombo N, Fasani R, Goisis G, Casadio C, et al. The differential role of L1 in ovarian carcinoma and normal ovarian surface epithelium. Cancer Res. 2008 Feb 15;68(4):1110–8.

493. Rökman A, Baffoe-Bonnie AB, Gillanders E, Fredriksson H, Autio V, Ikonen T, et al. Hereditary prostate cancer in Finland: fine-mapping validates 3p26 as a major predisposition locus. Hum Genet. 2005 Jan;116(1-2):43–50.

494. Gavert N, Conacci-Sorrell M, Gast D, Schneider A, Altevogt P, Brabletz T, et al. L1, a novel target of beta-catenin signaling, transforms cells and is expressed at the invasive front of colon cancers. J Cell Biol. 2005 Feb 14;168(4):633–42.

495. Qin YR, Fu L, Sham PC, Kwong DLW, Zhu CL, Chu KKW, et al. Single-nucleotide polymorphism-mass array reveals commonly deleted regions at 3p22 and 3p14.2 associate with poor clinical outcome in esophageal squamous cell carcinoma. Int J Cancer J Int Cancer. 2008 Aug 15;123(4):826–30.

496. Uchida K, Oga A, Nakao M, Mano T, Mihara M, Kawauchi S, et al. Loss of 3p26.3 is an independent prognostic factor in patients with oral squamous cell carcinoma. Oncol Rep. 2011 Aug;26(2):463–9.

497. Chen J, Fu L, Zhang L-Y, Kwong DL, Yan L, Guan X-Y. Tumor suppressor genes on frequently deleted chromosome 3p in nasopharyngeal carcinoma. Chin J Cancer. 2012 May;31(5):215–22.

498. He L-H, Ma Q, Shi Y-H, Ge J, Zhao H-M, Li S-F, et al. CHL1 is involved in human breast tumorigenesis and progression. Biochem Biophys Res Commun. 2013 Aug 23;438(2):433–8.

499. Huang X, Zhu L, Zhao T, Wu L, Wu K, Schachner M, et al. CHL1 negatively regulates the proliferation and neuronal differentiation of neural progenitor cells through activation of the ERK1/2 MAPK pathway. Mol Cell Neurosci. 2011 Jan;46(1):296–307.

500. Senchenko VN, Krasnov GS, Dmitriev AA, Kudryavtseva AV, Anedchenko EA, Braga EA, et al. Differential expression of CHL1 gene during development of major human cancers. PloS One. 2011;6(3):e15612.

501. Long M-J, Wu F-X, Li P, Liu M, Li X, Tang H. MicroRNA-10a targets CHL1 and promotes cell growth, migration and invasion in human cervical cancer cells. Cancer Lett. 2012 Nov 28;324(2):186–96.

502. Zeschnigk M, Tschentscher F, Lich C, Brandt B, Horsthemke B, Lohmann DR. Methylation analysis of several tumour suppressor genes shows a low frequency of methylation of CDKN2A and RARB in uveal melanomas. Comp Funct Genomics. 2003;4(3):329–36.

503. Jannie KM, Stipp CS, Weiner JA. ALCAM regulates motility, invasiveness, and adherens junction formation in uveal melanoma cells. PloS One. 2012;7(6):e39330.

504. Beutel J, Wegner J, Wegner R, Ziemssen F, Nassar K, Rohrbach JM, et al. Possible implications of MCAM expression in metastasis and non-metastatic of primary uveal melanoma patients. Curr Eye Res. 2009 Nov;34(11):1004–9.

505. Anastassiou G, Schilling H, Stang A, Djakovic S, Heiligenhaus A, Bornfeld N. Expression of the cell adhesion molecules ICAM-1, VCAM-1 and NCAM in uveal melanoma: a clinicopathological study. Oncology. 2000;58(1):83–8.

506. Mooy CM, Luyten GP, de Jong PT, Jensen OA, Luider TM, van der Ham F, et al. Neural cell adhesion molecule distribution in primary and metastatic uveal melanoma. Hum Pathol. 1995 Nov;26(11):1185–90.

507. Tschentscher F, Hüsing J, Hölter T, Kruse E, Dresen IG, Jöckel K-H, et al. Tumor Classification Based on Gene Expression Profiling Shows That Uveal Melanomas with and without Monosomy 3 Represent Two Distinct Entities. Cancer Res. 2003 May 15;63(10):2578–84.

508. Sorbin and SH3 domain-containing protein 2 - Homo sapiens (Human) [Internet]. Uniprot KB. Available from: http://www.uniprot.org/uniprot/O94875

509. Cestra G, Toomre D, Chang S, De Camilli P. The Abl/Arg substrate ArgBP2/nArgBP2 coordinates the function of multiple regulatory mechanisms converging on the actin cytoskeleton. Proc Natl Acad Sci U S A. 2005 Feb 1;102(5):1731–6.

510. Yuan Z, Kim D, Kaneko S, Sussman M, Bokoch GM, Kruh GD, et al. ArgBP2gamma interacts with Akt and p21-activated kinase-1 and promotes cell survival. J Biol Chem. 2005 Jun 3;280(22):21483–90.

511. Pavey S, Zuidervaart W, van Nieuwpoort F, Packer L, Jager M, Gruis N, et al. Increased p21-activated kinase-1 expression is associated with invasive potential in uveal melanoma. Melanoma Res. 2006 Aug;16(4):285–96.

512. Samadi AK, Cohen SM, Mukerji R, Chaguturu V, Zhang X, Timmermann BN, et al. Natural withanolide withaferin A induces apoptosis in uveal melanoma cells by suppression of Akt and c-MET activation. Tumour Biol J Int Soc Oncodevelopmental Biol Med. 2012 Aug;33(4):1179–89.

513. Backsch C, Rudolph B, Steinbach D, Scheungraber C, Liesenfeld M, Häfner N, et al. An integrative functional genomic and gene expression approach revealed SORBS2 as a putative tumour suppressor gene involved in cervical carcinogenesis. Carcinogenesis. 2011 Jul;32(7):1100–6.

514. Mestre-Escorihuela C, Rubio-Moscardo F, Richter JA, Siebert R, Climent J, Fresquet V, et al. Homozygous deletions localize novel tumor suppressor genes in B-cell lymphomas. Blood. 2007 Jan 1;109(1):271–80.

515. Taieb D, Roignot J, André F, Garcia S, Masson B, Pierres A, et al. ArgBP2-Dependent Signaling Regulates Pancreatic Cell Migration, Adhesion, and Tumorigenicity. Cancer Res. 2008 Jun 15;68(12):4588–96.

516. THBS2 thrombospondin 2 [ Homo sapiens (human) ] [Internet]. Gene Entrez. Available from: http://www.ncbi.nlm.nih.gov/gene/7058

517. Yang Z, Kyriakides TR, Bornstein P. Matricellular proteins as modulators of cell-matrix interactions: adhesive defect in thrombospondin 2-null fibroblasts is a consequence of increased levels of matrix metalloproteinase-2. Mol Biol Cell. 2000 Oct;11(10):3353–64.

518. Kim H, Watkinson J, Varadan V, Anastassiou D. Multi-cancer computational analysis reveals invasion-associated variant of desmoplastic reaction involving INHBA, THBS2 and COL11A1. BMC Med Genomics. 2010;3:51.

519. Peng Z-M, Tang F-Q, Wu E-S. [Study of gene expression difference in lung carcinogenesis by cDNA microarray]. Ai Zheng Aizheng Chin J Cancer. 2004 Feb;23(2):150–4.

520. Gulzar ZG, McKenney JK, Brooks JD. Increased expression of NuSAP in recurrent prostate cancer is mediated by E2F1. Oncogene. 2013 Jan 3;32(1):70–7.

521. Farrow B, Berger DH, Rowley D. Tumor-derived pancreatic stellate cells promote pancreatic cancer cell invasion through release of thrombospondin-2. J Surg Res. 2009 Sep;156(1):155–60.

522. Kodama J, Hashimoto I, Seki N, Hongo A, Yoshinouchi M, Okuda H, et al. Thrombospondin-1 and -2 messenger RNA expression in epithelial ovarian tumor. Anticancer Res. 2001 Aug;21(4B):2983–7.

523. Kunz M, Koczan D, Ibrahim SM, Gillitzer R, Gross G, Thiesen HJ. Differential expression of thrombospondin 2 in primary and metastatic malignant melanoma. Acta Derm Venereol. 2002;82(3):163–9.

524. Chijiwa T, Abe Y, Ikoma N, Yamazaki H, Tsukamoto H, Suemizu H, et al. Thrombospondin 2 inhibits metastasis of human malignant melanoma through microenvironment-modification in NOD/SCID/gammaCnull (NOG) mice. Int J Oncol. 2009 Jan;34(1):5–13.

525. Bornstein P. Thrombospondins function as regulators of angiogenesis. J Cell Commun Signal. 2009 Dec;3(3-4):189–200.

526. Streit M, Riccardi L, Velasco P, Brown LF, Hawighorst T, Bornstein P, et al. Thrombospondin-2: a potent endogenous inhibitor of tumor growth and angiogenesis. Proc Natl Acad Sci U S A. 1999 Dec 21;96(26):14888–93.

527. Hawighorst T, Velasco P, Streit M, Hong YK, Kyriakides TR, Brown LF, et al. Thrombospondin-2 plays a protective role in multistep carcinogenesis: a novel host anti-tumor defense mechanism. EMBO J. 2001 Jun 1;20(11):2631–40.

528. Ordonez JL, Paraoan L, Hiscott P, Gray D, García-Fiñana M, Grierson I, et al. Differential expression of angioregulatory matricellular proteins in posterior uveal melanoma. Melanoma Res. 2005 Dec;15(6):495–502.

529. Wang S, Neekhra A, Albert DM, Sorenson CM, Sheibani N. Suppression of thrombospondin-1 expression during uveal melanoma progression and its potential therapeutic utility. Arch Ophthalmol. 2012 Mar;130(3):336–41.

530. MEGF10 multiple EGF-like-domains 10 [ Homo sapiens (human) ] [Internet]. Gene Entrez. Available from: http://www.ncbi.nlm.nih.gov/gene/84466

531. Kay JN, Chu MW, Sanes JR. MEGF10 and MEGF11 mediate homotypic interactions required for mosaic spacing of retinal neurons. Nature. 2012 Mar 22;483(7390):465–9.

532. Suzuki E, Nakayama M. The mammalian Ced-1 ortholog MEGF10/KIAA1780 displays a novel adhesion pattern. Exp Cell Res. 2007 Jul 1;313(11):2451–64.

533. Boyden SE, Mahoney LJ, Kawahara G, Myers JA, Mitsuhashi S, Estrella EA, et al. Mutations in the satellite cell gene MEGF10 cause a recessive congenital myopathy with minicores. Neurogenetics. 2012 May;13(2):115–24.

534. Logan CV, Lucke B, Pottinger C, Abdelhamed ZA, Parry DA, Szymanska K, et al. Mutations in MEGF10, a regulator of satellite cell myogenesis, cause early onset myopathy, areflexia, respiratory distress and dysphagia (EMARDD). Nat Genet. 2011 Dec;43(12):1189–92.

535. Pierson TM, Markello T, Accardi J, Wolfe L, Adams D, Sincan M, et al. Novel SNP array analysis and exome sequencing detect a homozygous exon 7 deletion of MEGF10 causing early onset myopathy, areflexia, respiratory distress and dysphagia (EMARDD). Neuromuscul Disord NMD. 2013 Jun;23(6):483–8.

536. Orentas RJ, Yang JJ, Wen X, Wei JS, Mackall CL, Khan J. Identification of Cell Surface Proteins as Potential Immunotherapy Targets in 12 Pediatric Cancers. Front Oncol [Internet]. 2012 Dec 17 [cited 2013 Sep 8];2. Available from: http://www.ncbi.nlm.nih.gov/pmc/articles/PMC3523547/

537. De la Bletiere DR, Blanchet O, Cornillet-Lefebvre P, Coutolleau A, Baranger L, Genevieve F, et al. Routine use of microarray-based gene expression profiling to identify patients with low cytogenetic risk acute myeloid leukemia: accurate results can be obtained even with suboptimal samples. BMC Med Genomics. 2012 Jan 30;5:6.

538. Hofmann B, Hecht H-J, Flohé L. Peroxiredoxins. Biol Chem. 2002 Apr;383(3-4):347–64.

539. Bryk R, Griffin P, Nathan C. Peroxynitrite reductase activity of bacterial peroxiredoxins. Nature. 2000 Sep 14;407(6801):211–5.

540. Peshenko IV, Shichi H. Oxidation of active center cysteine of bovine 1-Cys peroxiredoxin to the cysteine sulfenic acid form by peroxide and peroxynitrite. Free Radic Biol Med. 2001 Aug 1;31(3):292–303.

541. Butterfield LH, Merino A, Golub SH, Shau H. From cytoprotection to tumor suppression: the multifactorial role of peroxiredoxins. Antioxid Redox Signal. 1999;1(4):385–402.

542. Fujii J, Ikeda Y. Advances in our understanding of peroxiredoxin, a multifunctional, mammalian redox protein. Redox Rep Commun Free Radic Res. 2002;7(3):123–30.

543. Chance B, Sies H, Boveris A. Hydroperoxide metabolism in mammalian organs. Physiol Rev. 1979 Jul;59(3):527–605.

544. Cadenas E. Mitochondrial free radical production and cell signaling. Mol Aspects Med. 2004 Apr;25(1-2):17–26.

545. Chang T-S, Cho C-S, Park S, Yu S, Kang SW, Rhee SG. Peroxiredoxin III, a mitochondrion-specific peroxidase, regulates apoptotic signaling by mitochondria. J Biol Chem. 2004 Oct 1;279(40):41975–84.

546. Seo MS, Kang SW, Kim K, Baines IC, Lee TH, Rhee SG. Identification of a new type of mammalian peroxiredoxin that forms an intramolecular disulfide as a reaction intermediate. J Biol Chem. 2000 Jul 7;275(27):20346–54.

547. Chae HZ, Robison K, Poole LB, Church G, Storz G, Rhee SG. Cloning and sequencing of thiol-specific antioxidant from mammalian brain: alkyl hydroperoxide reductase and thiol-specific antioxidant define a large family of antioxidant enzymes. Proc Natl Acad Sci U S A. 1994 Jul 19;91(15):7017–21.

548. Chae HZ, Kim HJ, Kang SW, Rhee SG. Characterization of three isoforms of mammalian peroxiredoxin that reduce peroxides in the presence of thioredoxin. Diabetes Res Clin Pract. 1999 Sep;45(2-3):101–12.

549. Rhee SG, Kang SW, Chang TS, Jeong W, Kim K. Peroxiredoxin, a novel family of peroxidases. IUBMB Life. 2001 Jul;52(1-2):35–41.

550. Igney FH, Krammer PH. Death and anti-death: tumour resistance to apoptosis. Nat Rev Cancer. 2002 Apr;2(4):277–88.

551. Wallace DC. Mitochondrial diseases in man and mouse. Science. 1999 Mar 5;283(5407):1482–8.

552. Newmeyer DD, Ferguson-Miller S. Mitochondria: releasing power for life and unleashing the machineries of death. Cell. 2003 Feb 21;112(4):481–90.

553. Garg AK, Aggarwal BB. Reactive oxygen intermediates in TNF signaling. Mol Immunol. 2002 Dec;39(9):509–17.

554. Kruman I, Guo Q, Mattson MP. Calcium and reactive oxygen species mediate staurosporine-induced mitochondrial dysfunction and apoptosis in PC12 cells. J Neurosci Res. 1998 Feb 1;51(3):293–308.

555. Tan S, Sagara Y, Liu Y, Maher P, Schubert D. The regulation of reactive oxygen species production during programmed cell death. J Cell Biol. 1998 Jun 15;141(6):1423–32.

556. Saito Y, Nishio K, Ogawa Y, Kimata J, Kinumi T, Yoshida Y, et al. Turning point in apoptosis/necrosis induced by hydrogen peroxide. Free Radic Res. 2006 Jun;40(6):619–30.

557. Ryter SW, Kim HP, Hoetzel A, Park JW, Nakahira K, Wang X, et al. Mechanisms of cell death in oxidative stress. Antioxid Redox Signal. 2007 Jan;9(1):49–89.

558. Burkitt M, Jones C, Lawrence A, Wardman P. Activation of cytochrome c to a peroxidase compound I-type intermediate by H2O2: relevance to redox signalling in apoptosis. Biochem Soc Symp. 2004;(71):97–106.

559. Nonn L, Berggren M, Powis G. Increased expression of mitochondrial peroxiredoxin-3 (thioredoxin peroxidase-2) protects cancer cells against hypoxia and drug-induced hydrogen peroxide-dependent apoptosis. Mol Cancer Res MCR. 2003 Jul;1(9):682–9.

560. Chowdhury SKR, Raha S, Tarnopolsky MA, Singh G. Increased expression of mitochondrial glycerophosphate dehydrogenase and antioxidant enzymes in prostate cancer cell lines/cancer. Free Radic Res. 2007 Oct;41(10):1116–24.

561. Basu A, Banerjee H, Rojas H, Martinez SR, Roy S, Jia Z, et al. Differential expression of peroxiredoxins in prostate cancer: consistent upregulation of PRDX3 and PRDX4. The Prostate. 2011 May 15;71(7):755–65.

562. Ummanni R, Barreto F, Venz S, Scharf C, Barett C, Mannsperger HA, et al. Peroxiredoxins 3 and 4 are overexpressed in prostate cancer tissue and affect the proliferation of prostate cancer cells in vitro. J Proteome Res. 2012 Apr 6;11(4):2452–66.

563. Chua P-J, Lee E-H, Yu Y, Yip GW-C, Tan P-H, Bay B-H. Silencing the Peroxiredoxin III gene inhibits cell proliferation in breast cancer. Int J Oncol. 2010 Feb;36(2):359–64.

564. Noh DY, Ahn SJ, Lee RA, Kim SW, Park IA, Chae HZ. Overexpression of peroxiredoxin in human breast cancer. Anticancer Res. 2001 Jun;21(3B):2085–90.

565. Karihtala P, Mäntyniemi A, Kang SW, Kinnula VL, Soini Y. Peroxiredoxins in breast carcinoma. Clin Cancer Res Off J Am Assoc Cancer Res. 2003 Aug 15;9(9):3418–24.

566. Park JH, Kim YS, Lee HL, Shim JY, Lee KS, Oh YJ, et al. Expression of peroxiredoxin and thioredoxin in human lung cancer and paired normal lung. Respirol Carlton Vic. 2006 May;11(3):269–75.

567. Walsh B, Pearl A, Suchy S, Tartaglio J, Visco K, Phelan SA. Overexpression of Prdx6 and resistance to peroxide-induced death in Hepa1-6 cells: Prdx suppression increases apoptosis. Redox Rep Commun Free Radic Res. 2009;14(6):275–84.

568. De Simoni S, Goemaere J, Knoops B. Silencing of peroxiredoxin 3 and peroxiredoxin 5 reveals the role of mitochondrial peroxiredoxins in the protection of human neuroblastoma SH-SY5Y cells toward MPP+. Neurosci Lett. 2008 Mar 15;433(3):219–24.

569. Li M, Han X, Yu B. Synthesis of monomethylated dioscin derivatives and their antitumor activities. Carbohydr Res. 2003 Jan 20;338(2):117–21.

570. Cai J, Liu M, Wang Z, Ju Y. Apoptosis induced by dioscin in Hela cells. Biol Pharm Bull. 2002 Feb;25(2):193–6.

571. Wang Y, Cheung YH, Yang Z, Chiu J-F, Che C-M, He Q-Y. Proteomic approach to study the cytotoxicity of dioscin (saponin). Proteomics. 2006 Apr;6(8):2422–32.

572. Wang Z, Cheng Y, Wang N, Wang DM, Li YW, Han F, et al. Dioscin induces cancer cell apoptosis through elevated oxidative stress mediated by downregulation of peroxiredoxins. Cancer Biol Ther. 2012 Feb 1;13(3):138–47.

573. Singh AD, Tubbs R, Biscotti C, Schoenfield L, Trizzoi P. Chromosomal 3 and 8 status within hepatic metastasis of uveal melanoma. Arch Pathol Lab Med. 2009 Aug;133(8):1223–7.

574. Parrella P, Caballero OL, Sidransky D, Merbs SL. Detection of c-myc amplification in uveal melanoma by fluorescent in situ hybridization. Invest Ophthalmol Vis Sci. 2001 Jul;42(8):1679–84.

575. Royds JA, Sharrard RM, Parsons MA, Lawry J, Rees R, Cottam D, et al. C-myc oncogene expression in ocular melanomas. Graefes Arch Clin Exp Ophthalmol Albrecht Von Graefes Arch Für Klin Exp Ophthalmol. 1992;230(4):366–71.

576. Mooy CM, Luyten GP, de Jong PT, Luider TM, Stijnen T, van de Ham F, et al. Immunohistochemical and prognostic analysis of apoptosis and proliferation in uveal melanoma. Am J Pathol. 1995 Oct;147(4):1097–104.

577. Chana JS, Cree IA, Foss AJ, Hungerford JL, Wilson GD. The prognostic significance of c-myc oncogene expression in uveal melanoma. Melanoma Res. 1998 Apr;8(2):139–44.

578. Chana JS, Wilson GD, Cree IA, Alexander RA, Myatt N, Neale M, et al. c-myc, p53, and Bcl-2 expression and clinical outcome in uveal melanoma. Br J Ophthalmol. 1999 Jan;83(1):110–4.

579. Tulley PN, Neale M, Jackson D, Chana JS, Grover R, Cree I, et al. The relation between c-myc expression and interferon sensitivity in uveal melanoma. Br J Ophthalmol. 2004 Dec;88(12):1563–7.

580. Ehlers JP, Worley L, Onken MD, Harbour JW. DDEF1 is located in an amplified region of chromosome 8q and is overexpressed in uveal melanoma. Clin Cancer Res Off J Am Assoc Cancer Res. 2005 May 15;11(10):3609–13.

581. Dang CV. MYC on the path to cancer. Cell. 2012 Mar 30;149(1):22–35.

582. Wise DR, DeBerardinis RJ, Mancuso A, Sayed N, Zhang X-Y, Pfeiffer HK, et al. Myc regulates a transcriptional program that stimulates mitochondrial glutaminolysis and leads to glutamine addiction. Proc Natl Acad Sci U S A. 2008 Dec 2;105(48):18782–7.

583. Gao P, Tchernyshyov I, Chang T-C, Lee Y-S, Kita K, Ochi T, et al. c-Myc suppression of miR-23a/b enhances mitochondrial glutaminase expression and glutamine metabolism. Nature. 2009 Apr 9;458(7239):762–5.

584. Egler RA, Fernandes E, Rothermund K, Sereika S, de Souza-Pinto N, Jaruga P, et al. Regulation of reactive oxygen species, DNA damage, and c-Myc function by peroxiredoxin 1. Oncogene. 2005 Dec 1;24(54):8038–50.

585. Vafa O, Wade M, Kern S, Beeche M, Pandita TK, Hampton GM, et al. c-Myc can induce DNA damage, increase reactive oxygen species, and mitigate p53 function: a mechanism for oncogene-induced genetic instability. Mol Cell. 2002 May;9(5):1031–44.

586. Zhang H, Gao P, Fukuda R, Kumar G, Krishnamachary B, Zeller KI, et al. HIF-1 inhibits mitochondrial biogenesis and cellular respiration in VHL-deficient renal cell carcinoma by repression of C-MYC activity. Cancer Cell. 2007 May;11(5):407–20.

587. Wang H, Mannava S, Grachtchouk V, Zhuang D, Soengas MS, Gudkov AV, et al. c-Myc depletion inhibits proliferation of human tumor cells at various stages of the cell cycle. Oncogene. 2008 Mar 20;27(13):1905–15.

588. Koh CM, Gurel B, Sutcliffe S, Aryee MJ, Schultz D, Iwata T, et al. Alterations in nucleolar structure and gene expression programs in prostatic neoplasia are driven by the MYC oncogene. Am J Pathol. 2011 Apr;178(4):1824–34.

589. Cappellen D, Schlange T, Bauer M, Maurer F, Hynes NE. Novel c-MYC target genes mediate differential effects on cell proliferation and migration. EMBO Rep. 2007 Jan;8(1):70–6.

590. Soucek L, Whitfield J, Martins CP, Finch AJ, Murphy DJ, Sodir NM, et al. Modelling Myc inhibition as a cancer therapy. Nature. 2008 Oct 2;455(7213):679–83.

591. Delmore JE, Issa GC, Lemieux ME, Rahl PB, Shi J, Jacobs HM, et al. BET bromodomain inhibition as a therapeutic strategy to target c-Myc. Cell. 2011 Sep 16;146(6):904–17.

592. Mertz JA, Conery AR, Bryant BM, Sandy P, Balasubramanian S, Mele DA, et al. Targeting MYC dependence in cancer by inhibiting BET bromodomains. Proc Natl Acad Sci U S A. 2011 Oct 4;108(40):16669–74.

593. Kota J, Chivukula RR, O'Donnell KA, Wentzel EA, Montgomery CL, Hwang H-W, et al. Therapeutic microRNA delivery suppresses tumorigenesis in a murine liver cancer model. Cell. 2009 Jun 12;137(6):1005–17.

594. Menssen A, Hermeking H. Characterization of the c-MYC-regulated transcriptome by SAGE: identification and analysis of c-MYC target genes. Proc Natl Acad Sci U S A. 2002 Apr 30;99(9):6274–9.

595. Teufel M, Saudek V, Ledig J-P, Bernhardt A, Boularand S, Carreau A, et al. Sequence identification and characterization of human carnosinase and a closely related non-specific dipeptidase. J Biol Chem. 2003 Feb 21;278(8):6521–31.

596. Kurashige M, Imamura M, Araki S-I, Suzuki D, Babazono T, Uzu T, et al. The influence of a single nucleotide polymorphism within CNDP1 on susceptibility to diabetic nephropathy in Japanese women with type 2 diabetes. PloS One. 2013;8(1):e54064.

597. Wanic K, Placha G, Dunn J, Smiles A, Warram JH, Krolewski AS. Exclusion of polymorphisms in carnosinase genes (CNDP1 and CNDP2) as a cause of diabetic nephropathy in type 1 diabetes: results of large case-control and follow-up studies. Diabetes. 2008 Sep;57(9):2547–51.

598. Ahluwalia TS, Lindholm E, Groop LC. Common variants in CNDP1 and CNDP2, and risk of nephropathy in type 2 diabetes. Diabetologia. 2011 Sep;54(9):2295–302.

599. Licker V, Côte M, Lobrinus JA, Rodrigo N, Kövari E, Hochstrasser DF, et al. Proteomic profiling of the substantia nigra demonstrates CNDP2 overexpression in Parkinson's disease. J Proteomics. 2012 Aug 3;75(15):4656–67.

600. Zhang P, Chan DW, Zhu Y, Li JJ, Ng IO-L, Wan D, et al. Identification of carboxypeptidase of glutamate like-B as a candidate suppressor in cell growth and metastasis in human hepatocellular carcinoma. Clin Cancer Res Off J Am Assoc Cancer Res. 2006 Nov 15;12(22):6617–25.

601. Lee J-H, Giovannetti E, Hwang J-H, Petrini I, Wang Q, Voortman J, et al. Loss of 18q22.3 involving the carboxypeptidase of glutamate-like gene is associated with poor prognosis in resected pancreatic cancer. Clin Cancer Res Off J Am Assoc Cancer Res. 2012 Jan 15;18(2):524–33.

602. Beroukhim R, Mermel CH, Porter D, Wei G, Raychaudhuri S, Donovan J, et al. The landscape of somatic copy-number alteration across human cancers. Nature. 2010 Feb 18;463(7283):899–905.

603. Xu C, Wang P, Liu Y, Zhang Y, Fan W, Upton MP, et al. Integrative genomics in combination with RNA interference identifies prognostic and functionally relevant gene targets for oral squamous cell carcinoma. PLoS Genet. 2013;9(1):e1003169.

604. Darby IA, Vuillier-Devillers K, Pinault E, Sarrazy V, Lepreux S, Balabaud C, et al. Proteomic Analysis of Differentially Expressed Proteins in Peripheral Cholangiocarcinoma. Cancer Microenviron. 2010 Jun 26;4(1):73–91.

605. Perroud B, Ishimaru T, Borowsky AD, Weiss RH. Grade-dependent Proteomics Characterization of Kidney Cancer. Mol Cell Proteomics MCP. 2009 May;8(5):971–85.

606. XI Y, RIKER A, SHEVDE-SAMANT L, SAMANT R, MORRIS C, GAVIN E, et al. Global Comparative Gene Expression Analysis of Melanoma Patient Samples, Derived Cell Lines and Corresponding Tumor Xenografts. Cancer Genomics Proteomics. 2008;5(1):1–35.

607. Sridhar K, Ross DT, Tibshirani R, Butte AJ, Greenberg PL. Relationship of differential gene expression profiles in CD34+ myelodysplastic syndrome marrow cells to disease subtype and progression. Blood. 2009 Nov 26;114(23):4847–58.

608. Komrokji RS, List AF. Lenalidomide for treatment of myelodysplastic syndromes. Curr Pharm Des. 2012;18(22):3198–203.

609. Van den Bosch T, Kilic E, Paridaens D, de Klein A. Genetics of uveal melanoma and cutaneous melanoma: two of a kind? Dermatol Res Pract. 2010;2010:360136.

610. Gaudi S, Messina JL. Molecular bases of cutaneous and uveal melanomas. Pathol Res Int. 2011;2011:159421.

611. Novara G, Martignoni G, Artibani W, Ficarra V. Grading systems in renal cell carcinoma. J Urol. 2007 Feb;177(2):430–6.

612. Goel R, Pandey A. Qualitative proteomic analysis of human normal vitreous humor [Internet]. Available from: http://www.humanproteinpedia.org/Experimental_details?exp_id=TE-142110

613. SIPA1L2 Homo sapiens A7E2F9 [Internet]. Gene Ontology. Available from: http://www.ebi.ac.uk/QuickGO/GProtein?ac=Q9P2F8

614. Gopalakrishna-Pillai S, Iverson LE. Astrocytes derived from trisomic human embryonic stem cells express markers of astrocytic cancer cells and premalignant stem-like progenitors. BMC Med Genomics. 2010 Apr 27;3:12.

615. Marques RB, Dits NF, Erkens-Schulze S, van Weerden WM, Jenster G. Bypass Mechanisms of the Androgen Receptor Pathway in Therapy-Resistant Prostate Cancer Cell Models. PLoS ONE [Internet]. 2010 Oct 19 [cited 2013 Oct 8];5(10). Available from: http://www.ncbi.nlm.nih.gov/pmc/articles/PMC2957443/

616. Madar S, Brosh R, Buganim Y, Ezra O, Goldstein I, Solomon H, et al. Modulated expression of WFDC1 during carcinogenesis and cellular senescence. Carcinogenesis. 2009 Jan;30(1):20–7.

617. Leaman DW, Leung S, Li X, Stark GR. Regulation of STAT-dependent pathways by growth factors and cytokines. FASEB J Off Publ Fed Am Soc Exp Biol. 1996 Dec;10(14):1578–88.

618. Yu H, Jove R. The STATs of cancer--new molecular targets come of age. Nat Rev Cancer. 2004 Feb;4(2):97–105.

619. Darnell JE Jr. STATs and gene regulation. Science. 1997 Sep 12;277(5332):1630–5.

620. Darnell JE Jr, Kerr IM, Stark GR. Jak-STAT pathways and transcriptional activation in response to IFNs and other extracellular signaling proteins. Science. 1994 Jun 3;264(5164):1415–21.

621. Niu G, Heller R, Catlett-Falcone R, Coppola D, Jaroszeski M, Dalton W, et al. Gene therapy with dominant-negative Stat3 suppresses growth of the murine melanoma B16 tumor in vivo. Cancer Res. 1999 Oct 15;59(20):5059–63.

622. Ding BB, Yu JJ, Yu RY-L, Mendez LM, Shaknovich R, Zhang Y, et al. Constitutively activated STAT3 promotes cell proliferation and survival in the activated B-cell subtype of diffuse large B-cell lymphomas. Blood. 2008 Feb 1;111(3):1515–23.

623. Catlett-Falcone R, Landowski TH, Oshiro MM, Turkson J, Levitzki A, Savino R, et al. Constitutive activation of Stat3 signaling confers resistance to apoptosis in human U266 myeloma cells. Immunity. 1999 Jan;10(1):105–15.

624. Grandis JR, Drenning SD, Zeng Q, Watkins SC, Melhem MF, Endo S, et al. Constitutive activation of Stat3 signaling abrogates apoptosis in squamous cell carcinogenesis in vivo. Proc Natl Acad Sci U S A. 2000 Apr 11;97(8):4227–32.

625. Ni Z, Lou W, Leman ES, Gao AC. Inhibition of constitutively activated Stat3 signaling pathway suppresses growth of prostate cancer cells. Cancer Res. 2000 Mar 1;60(5):1225–8.

626. Garcia R, Bowman TL, Niu G, Yu H, Minton S, Muro-Cacho CA, et al. Constitutive activation of Stat3 by the Src and JAK tyrosine kinases participates in growth regulation of human breast carcinoma cells. Oncogene. 2001 May 3;20(20):2499–513.

627. Haviland R, Eschrich S, Bloom G, Ma Y, Minton S, Jove R, et al. Necdin, a Negative Growth Regulator, Is a Novel STAT3 Target Gene Down-Regulated in Human Cancer. PLoS ONE [Internet]. 2011 Oct 27 [cited 2013 Oct 8];6(10). Available from: http://www.ncbi.nlm.nih.gov/pmc/articles/PMC3203112/

628. Giehl K. Oncogenic Ras in tumour progression and metastasis. Biol Chem. 2005 Mar;386(3):193–205.

629. Posch C, Ortiz-Urda S. NRAS mutant melanoma - undrugable? Oncotarget. 2013 Apr 13;4(4):494–5.

630. Kwong LN, Costello JC, Liu H, Genovese G, Jiang S, Jeong JH, et al. Oncogenic NRAS Signaling Differentially Regulates Survival and Proliferation in Melanoma. Nat Med. 2012 Oct;18(10):1503–10.

631. Gazin C, Wajapeyee N, Gobeil S, Virbasius C-M, Green MR. An Elaborate Pathway Required for Ras-Mediated Epigenetic Silencing. Nature. 2007 Oct 25;449(7165):1073–7.

632. Woo M, Hakem R, Soengas MS, Duncan GS, Shahinian A, Kägi D, et al. Essential contribution of caspase 3/CPP32 to apoptosis and its associated nuclear changes. Genes Dev. 1998 Mar 15;12(6):806–19.

633. Houston A, O'Connell J. The Fas signalling pathway and its role in the pathogenesis of cancer. Curr Opin Pharmacol. 2004 Aug;4(4):321–6.

634. O'Connell J, Bennett MW, O'Sullivan GC, Collins JK, Shanahan F. The Fas counterattack: a molecular mechanism of tumor immune privilege. Mol Med Camb Mass. 1997 May;3(5):294–300.

635. Elsässer-Beile U, Gierschner D, Welchner T, Wetterauer U. Different expression of Fas and Fas ligand in tumor infiltrating and peripheral lymphocytes of patients with renal cell carcinomas. Anticancer Res. 2003 Feb;23(1A):433–7.

636. Möller P, Koretz K, Leithäuser F, Brüderlein S, Henne C, Quentmeier A, et al. Expression of APO-1 (CD95), a member of the NGF/TNF receptor superfamily, in normal and neoplastic colon epithelium. Int J Cancer J Int Cancer. 1994 May 1;57(3):371–7.

637. Atsuta I, Liu S, Miura Y, Akiyama K, Chen C, An Y, et al. Mesenchymal stem cells inhibit multiple myeloma cells via the Fas/Fas ligand pathway. Stem Cell Res Ther. 2013 Sep 11;4(5):111.

638. Zhou J, Song S, He S, Wang Z, Zhang B, Li D, et al. Silencing of decoy receptor 3 (DcR3) expression by siRNA in pancreatic carcinoma cells induces Fas ligand-mediated apoptosis in vitro and in vivo. Int J Mol Med. 2013 Sep;32(3):653–60.

639. Mottolese M, Buglioni S, Bracalenti C, Cardarelli MA, Ciabocco L, Giannarelli D, et al. Prognostic relevance of altered Fas (CD95)-system in human breast cancer. Int J Cancer J Int Cancer. 2000 Mar 20;89(2):127–32.

640. Reimer T, Herrnring C, Koczan D, Richter D, Gerber B, Kabelitz D, et al. FasL:Fas ratio--a prognostic factor in breast carcinomas. Cancer Res. 2000 Feb 15;60(4):822–8.

641. Botti C, Buglioni S, Benevolo M, Giannarelli D, Papaldo P, Cognetti F, et al. Altered expression of FAS system is related to adverse clinical outcome in stage I-II breast cancer patients treated with adjuvant anthracycline-based chemotherapy. Clin Cancer Res Off J Am Assoc Cancer Res. 2004 Feb 15;10(4):1360–5.

642. Bebenek M, Duś D, Koźlak J. Fas and Fas ligand as prognostic factors in human breast carcinoma. Med Sci Monit Int Med J Exp Clin Res. 2006 Nov;12(11):CR457–461.

643. Bebenek M, Duś D, Koźlak J. Fas/Fas-ligand expressions in primary breast cancer are significant predictors of its skeletal spread. Anticancer Res. 2007 Feb;27(1A):215–8.

644. Gordon N, Kleinerman ES. The role of Fas/FasL in the metastatic potential of osteosarcoma and targeting this pathway for the treatment of osteosarcoma lung metastases. Cancer Treat Res. 2009;152:497–508.

645. O'Brien DI, Nally K, Kelly RG, O'Connor TM, Shanahan F, O'Connell J. Targeting the Fas/Fas ligand pathway in cancer. Expert Opin Ther Targets. 2005 Oct;9(5):1031–44.

646. Micheau O, Solary E, Hammann A, Martin F, Dimanche-Boitrel MT. Sensitization of cancer cells treated with cytotoxic drugs to fas-mediated cytotoxicity. J Natl Cancer Inst. 1997 Jun 4;89(11):783–9.

647. Fulda S, Sieverts H, Friesen C, Herr I, Debatin KM. The CD95 (APO-1/Fas) system mediates drug-induced apoptosis in neuroblastoma cells. Cancer Res. 1997 Sep 1;57(17):3823–9.

648. Friesen C, Fulda S, Debatin KM. Cytotoxic drugs and the CD95 pathway. Leukemia. 1999 Nov;13(11):1854–8.

649. Friesen C, Herr I, Krammer PH, Debatin KM. Involvement of the CD95 (APO-1/FAS) receptor/ligand system in drug-induced apoptosis in leukemia cells. Nat Med. 1996 May;2(5):574–7.

650. Fulda S, Scaffidi C, Pietsch T, Krammer PH, Peter ME, Debatin KM. Activation of the CD95 (APO-1/Fas) pathway in drug- and gamma-irradiation-induced apoptosis of brain tumor cells. Cell Death Differ. 1998 Oct;5(10):884–93.

651. Yao Y, Li L, Huang X, Gu X, Xu Z, Zhang Y, et al. SERPINA3K induces apoptosis in human colorectal cancer cells via activating the Fas/FasL/caspase-8 signaling pathway. FEBS J. 2013 Jul;280(14):3244–55.

652. Cruz F 3rd, Rubin BP, Wilson D, Town A, Schroeder A, Haley A, et al. Absence of BRAF and NRAS mutations in uveal melanoma. Cancer Res. 2003 Sep 15;63(18):5761–6.

653. Kiliç E, Brüggenwirth HT, Verbiest MMPJ, Zwarthoff EC, Mooy NM, Luyten GPM, et al. The RAS-BRAF kinase pathway is not involved in uveal melanoma. Melanoma Res. 2004 Jun;14(3):203–5.

654. Soparker CN, O'Brien JM, Albert DM. Investigation of the role of the ras protooncogene point mutation in human uveal melanomas. Invest Ophthalmol Vis Sci. 1993 Jun 1;34(7):2203–9.

655. Mooy CM, Van der Helm MJ, Van der Kwast TH, De Jong PT, Ruiter DJ, Zwarthoff EC. No N-ras mutations in human uveal melanoma: the role of ultraviolet light revisited. Br J Cancer. 1991 Aug;64(2):411–3.

656. Zuidervaart W, van Nieuwpoort F, Stark M, Dijkman R, Packer L, Borgstein A-M, et al. Activation of the MAPK pathway is a common event in uveal melanomas although it rarely occurs through mutation of BRAF or RAS. Br J Cancer. 2005 Jun 6;92(11):2032–8.

657. Anastassiou G, Coupland SE, Stang A, Boeloeni R, Schilling H, Bornfeld N. Expression of Fas and Fas ligand in uveal melanoma: biological implication and prognostic value. J Pathol. 2001 Aug;194(4):466–72.

658. Ailan H, Xiangwen X, Daolong R, Lu G, Xiaofeng D, Xi Q, et al. Identification of target genes of transcription factor activator protein 2 gamma in breast cancer cells. BMC Cancer. 2009 Aug 11;9:279.

659. Williams T, Tjian R. Analysis of the DNA-binding and activation properties of the human transcription factor AP-2. Genes Dev. 1991 Apr;5(4):670–82.

660. Williams T, Tjian R. Characterization of a dimerization motif in AP-2 and its function in heterologous DNA-binding proteins. Science. 1991 Mar 1;251(4997):1067–71.

661. Werling U, Schorle H. Transcription factor gene AP-2 gamma essential for early murine development. Mol Cell Biol. 2002 May;22(9):3149–56.

662. Moser M, Pscherer A, Roth C, Becker J, Mücher G, Zerres K, et al. Enhanced apoptotic cell death of renal epithelial cells in mice lacking transcription factor AP-2beta. Genes Dev. 1997 Aug 1;11(15):1938–48.

663. Nottoli T, Hagopian-Donaldson S, Zhang J, Perkins A, Williams T. AP-2-null cells disrupt morphogenesis of the eye, face, and limbs in chimeric mice. Proc Natl Acad Sci U S A. 1998 Nov 10;95(23):13714–9.

664. Zhang J, Hagopian-Donaldson S, Serbedzija G, Elsemore J, Plehn-Dujowich D, McMahon AP, et al. Neural tube, skeletal and body wall defects in mice lacking transcription factor AP-2. Nature. 1996 May 16;381(6579):238–41.

665. Schorle H, Meier P, Buchert M, Jaenisch R, Mitchell PJ. Transcription factor AP-2 essential for cranial closure and craniofacial development. Nature. 1996 May 16;381(6579):235–8.

666. Hilger-Eversheim K, Moser M, Schorle H, Buettner R. Regulatory roles of AP-2 transcription factors in vertebrate development, apoptosis and cell-cycle control. Gene. 2000 Dec 30;260(1-2):1–12.

667. Eckert D, Buhl S, Weber S, Jäger R, Schorle H. The AP-2 family of transcription factors. Genome Biol. 2005;6(13):246.

668. Pellikainen JM, Kosma V-M. Activator protein-2 in carcinogenesis with a special reference to breast cancer--a mini review. Int J Cancer J Int Cancer. 2007 May 15;120(10):2061–7.

669. Turner BC, Zhang J, Gumbs AA, Maher MG, Kaplan L, Carter D, et al. Expression of AP-2 transcription factors in human breast cancer correlates with the regulation of multiple growth factor signalling pathways. Cancer Res. 1998 Dec 1;58(23):5466–72.

670. Zhu C-H, Domann FE. Dominant negative interference of transcription factor AP-2 causes inhibition of ErbB-3 expression and suppresses malignant cell growth. Breast Cancer Res Treat. 2002 Jan;71(1):47–57.

671. McPherson LA, Weigel RJ. AP2alpha and AP2gamma: a comparison of binding site specificity and trans-activation of the estrogen receptor promoter and single site promoter constructs. Nucleic Acids Res. 1999 Oct 15;27(20):4040–9.

672. Pellikainen J, Kataja V, Ropponen K, Kellokoski J, Pietiläinen T, Böhm J, et al. Reduced nuclear expression of transcription factor AP-2 associates with aggressive breast cancer. Clin Cancer Res Off J Am Assoc Cancer Res. 2002 Nov;8(11):3487–95.

673. Ding X, Yang Z, Zhou F, Wang F, Li X, Chen C, et al. Transcription factor AP-2α regulates acute myeloid leukemia cell proliferation by influencing Hoxa gene expression. Int J Biochem Cell Biol. 2013 Aug;45(8):1647–56.

674. Wang W, Lv L, Pan K, Zhang Y, Zhao J, Chen J, et al. Reduced expression of transcription factor AP-2α is associated with gastric adenocarcinoma prognosis. PloS One. 2011;6(9):e24897.

675. Heimberger AB, McGary EC, Suki D, Ruiz M, Wang H, Fuller GN, et al. Loss of the AP-2alpha transcription factor is associated with the grade of human gliomas. Clin Cancer Res Off J Am Assoc Cancer Res. 2005 Jan 1;11(1):267–72.

676. Jonckheere N, Fauquette V, Stechly L, Saint-Laurent N, Aubert S, Susini C, et al. Tumour growth and resistance to gemcitabine of pancreatic cancer cells are decreased by AP-2alpha overexpression. Br J Cancer. 2009 Aug 18;101(4):637–44.

677. Tellez CS, Davis DW, Prieto VG, Gershenwald JE, Johnson MM, McCarty MF, et al. Quantitative analysis of melanocytic tissue array reveals inverse correlation between activator protein-2alpha and protease-activated receptor-1 expression during melanoma progression. J Invest Dermatol. 2007 Feb;127(2):387–93.

678. Berger AJ, Davis DW, Tellez C, Prieto VG, Gershenwald JE, Johnson MM, et al. Automated quantitative analysis of activator protein-2alpha subcellular expression in melanoma tissue microarrays correlates with survival prediction. Cancer Res. 2005 Dec 1;65(23):11185–92.

679. Karjalainen JM, Kellokoski JK, Eskelinen MJ, Alhava EM, Kosma VM. Downregulation of transcription factor AP-2 predicts poor survival in stage I cutaneous malignant melanoma. J Clin Oncol Off J Am Soc Clin Oncol. 1998 Nov;16(11):3584–91.

680. Melnikova VO, Dobroff AS, Zigler M, Villares GJ, Braeuer RR, Wang H, et al. CREB inhibits AP-2alpha expression to regulate the malignant phenotype of melanoma. PloS One. 2010;5(8):e12452.

681. Huang S, Jean D, Luca M, Tainsky MA, Bar-Eli M. Loss of AP-2 results in downregulation of c-KIT and enhancement of melanoma tumorigenicity and metastasis. EMBO J. 1998 Aug 3;17(15):4358–69.

682. Penna E, Orso F, Cimino D, Tenaglia E, Lembo A, Quaglino E, et al. microRNA-214 contributes to melanoma tumour progression through suppression of TFAP2C. EMBO J. 2011 May 18;30(10):1990–2007.

683. Penna E, Orso F, Cimino D, Vercellino I, Grassi E, Quaglino E, et al. miR-214 Coordinates Melanoma Progression by Upregulating ALCAM through TFAP2 and miR-148b Downmodulation. Cancer Res. 2013 Jul 1;73(13):4098–111.

684. Bauer R, Imhof A, Pscherer A, Kopp H, Moser M, Seegers S, et al. The genomic structure of the human AP-2 transcription factor. Nucleic Acids Res. 1994 Apr 25;22(8):1413–20.

685. Osella-Abate S, Novelli M, Quaglino P, Orso F, Ubezio B, Tomasini C, et al. Expression of AP-2α, AP-2γ and ESDN in primary melanomas: Correlation with histopathological features and potential prognostic value. J Dermatol Sci. 2012 Dec;68(3):202–4.

686. Li X, Glubrecht DD, Godbout R. AP2 transcription factor induces apoptosis in retinoblastoma cells. Genes Chromosomes Cancer. 2010 Sep;49(9):819–30.

687. Onken MD, Worley LA, Ehlers JP, Harbour JW. Gene Expression Profiling in Uveal Melanoma Reveals Two Molecular Classes and Predicts Metastatic Death. Cancer Res. 2004 Oct 15;64(20):7205–9.

688. Wu F, Lee AS. Identification of AP-2 as an interactive target of Rb and a regulator of the G1/S control element of the hamster histone H3.2 promoter. Nucleic Acids Res. 1998 Nov 1;26(21):4837–45.

689. Brantley MA Jr, Harbour JW. Inactivation of retinoblastoma protein in uveal melanoma by phosphorylation of sites in the COOH-terminal region. Cancer Res. 2000 Aug 15;60(16):4320–3.

690. Coupland SE, Bechrakis N, Schüler A, Anagnostopoulos I, Hummel M, Bornfeld N, et al. Expression patterns of cyclin D1 and related proteins regulating G1-S phase transition in uveal melanoma and retinoblastoma. Br J Ophthalmol. 1998 Aug;82(8):961–70.

691. Coupland SE, Anastassiou G, Stang A, Schilling H, Anagnostopoulos I, Bornfeld N, et al. The prognostic value of cyclin D1, p53, and MDM2 protein expression in uveal melanoma. J Pathol. 2000 Jun;191(2):120–6.

692. Van Gils W, Lodder EM, Mensink HW, Kiliç E, Naus NC, Brüggenwirth HT, et al. Gene expression profiling in uveal melanoma: two regions on 3p related to prognosis. Invest Ophthalmol Vis Sci. 2008 Oct;49(10):4254–62.

693. Cross NA, Ganesh A, Parpia M, Murray AK, Rennie IG, Sisley K. Multiple locations on chromosome 3 are the targets of specific deletions in uveal melanoma. Eye Lond Engl. 2006 Apr;20(4):476–81.

694. Holt R, Monaco AP. Links between genetics and pathophysiology in the autism spectrum disorders. EMBO Mol Med. 2011 Aug;3(8):438–50.

695. Yusenko MV, Nagy A, Kovacs G. Molecular analysis of germline t(3;6) and t(3;12) associated with conventional renal cell carcinomas indicates their rate-limiting role and supports the three-hit model of carcinogenesis. Cancer Genet Cytogenet. 2010 Aug;201(1):15–23.

696. Elmore JR, Obmann MA, Kuivaniemi H, Tromp G, Gerhard GS, Franklin DP, et al. Identification of a genetic variant associated with abdominal aortic aneurysms on chromosome 3p12.3 by genome wide association. J Vasc Surg. 2009 Jun;49(6):1525–31.

697. Jones GT, van Rij AM. Regarding "Identification of a genetic variant associated with abdominal aortic aneurysms on chromosome 3p12.3 by genome wide association."J Vasc Surg. 2009 Nov;50(5):1246–1247; author reply 1247.

698. Chang S-J, Wang T-Y, Tsai C-Y, Hu T-F, Chang MD-T, Wang H-W. Increased epithelial stem cell traits in advanced endometrial endometrioid carcinoma. BMC Genomics. 2009 Dec 16;10:613.

699. Yu J-W, Wu S-H, Lu R, Wu J, Ni X-C, Zhou G, et al. Expression and Significances of Contactin-1 in Human Gastric Cancer. Gastroenterol Res Pract [Internet]. 2013 [cited 2013 Aug 25];2013. Available from: http://www.ncbi.nlm.nih.gov/pmc/articles/PMC3626361/

700. WU H-M, CAO W, YE D, REN G-X, WU Y-N, GUO W. Contactin 1 (CNTN1) expression associates with regional lymph node metastasis and is a novel predictor of prognosis in patients with oral squamous cell carcinoma. Mol Med Rep. 2012 Aug;6(2):265–70.

701. Su J-L, Yang C-Y, Shih J-Y, Wei L-H, Hsieh C-Y, Jeng Y-M, et al. Knockdown of Contactin-1 Expression Suppresses Invasion and Metastasis of Lung Adenocarcinoma. Cancer Res. 2006 Mar 1;66(5):2553–61.

702. Su J-L, Yang P-C, Shih J-Y, Yang C-Y, Wei L-H, Hsieh C-Y, et al. The VEGF-C/Flt-4 axis promotes invasion and metastasis of cancer cells. Cancer Cell. 2006 Mar;9(3):209–23.

703. Yan J, Wong N, Hung C, Chen WX-Y, Tang D. Contactin-1 Reduces E-Cadherin Expression Via Activating AKT in Lung Cancer. PLoS ONE [Internet]. 2013 May 28 [cited 2013 Aug 25];8(5). Available from: http://www.ncbi.nlm.nih.gov/pmc/articles/PMC3665745/

704. Bouyain S, Watkins DJ. The protein tyrosine phosphatases PTPRZ and PTPRG bind to distinct members of the contactin family of neural recognition molecules. Proc Natl Acad Sci U S A. 2010 Feb 9;107(6):2443–8.

705. Bouyain S, Watkins DJ. Identification of tyrosine phosphatase ligands for contactin cell adhesion molecules. Commun Integr Biol. 2010 May;3(3):284–6.

706. Shock LP, Bare DJ, Klinz SG, Maness PF. Protein tyrosine phosphatases expressed in developing brain and retinal Müller glia. Brain Res Mol Brain Res. 1995 Jan;28(1):110–6.

707. Druck T, Kastury K, Hadaczek P, Podolski J, Toloczko A, Sikorski A, et al. Loss of heterozygosity at the familial RCC t(3;8) locus in most clear cell renal carcinomas. Cancer Res. 1995 Nov 15;55(22):5348–53.

708. Kastury K, Ohta M, Lasota J, Moir D, Dorman T, LaForgia S, et al. Structure of the human receptor tyrosine phosphatase gamma gene (PTPRG) and relation to the familial RCC t(3;8) chromosome translocation. Genomics. 1996 Mar 1;32(2):225–35.

709. Panagopoulos I, Pandis N, Thelin S, Petersson C, Mertens F, Borg A, et al. The FHIT and PTPRG genes are deleted in benign proliferative breast disease associated with familial breast cancer and cytogenetic rearrangements of chromosome band 3p14. Cancer Res. 1996 Nov 1;56(21):4871–5.

710. Wu C-W, Kao H-L, Li AF-Y, Chi C-W, Lin W-C. Protein tyrosine-phosphatase expression profiling in gastric cancer tissues. Cancer Lett. 2006 Oct 8;242(1):95–103.

711. Van Niekerk CC, Poels LG. Reduced expression of protein tyrosine phosphatase gamma in lung and ovarian tumors. Cancer Lett. 1999 Mar 22;137(1):61–73.

712. Wang Z, Shen D, Parsons DW, Bardelli A, Sager J, Szabo S, et al. Mutational analysis of the tyrosine phosphatome in colorectal cancers. Science. 2004 May 21;304(5674):1164–6.

713. Van Doorn R, Zoutman WH, Dijkman R, de Menezes RX, Commandeur S, Mulder AA, et al. Epigenetic profiling of cutaneous T-cell lymphoma: promoter hypermethylation of multiple tumor suppressor genes including BCL7a, PTPRG, and p73. J Clin Oncol Off J Am Soc Clin Oncol. 2005 Jun 10;23(17):3886–96.

714. Wang J-F, Dai D-Q. Metastatic suppressor genes inactivated by aberrant methylation in gastric cancer. World J Gastroenterol WJG. 2007 Nov 21;13(43):5692–8.

715. Furuta J, Nobeyama Y, Umebayashi Y, Otsuka F, Kikuchi K, Ushijima T. Silencing of Peroxiredoxin 2 and aberrant methylation of 33 CpG islands in putative promoter regions in human malignant melanomas. Cancer Res. 2006 Jun 15;66(12):6080–6.

716. Cheung AKL, Lung HL, Hung SC, Law EWL, Cheng Y, Yau WL, et al. Functional analysis of a cell cycle-associated, tumor-suppressive gene, protein tyrosine phosphatase receptor type G, in nasopharyngeal carcinoma. Cancer Res. 2008 Oct 1;68(19):8137–45.

717. Liu S, Sugimoto Y, Sorio C, Tecchio C, Lin YC. Function analysis of estrogenically regulated protein tyrosine phosphatase gamma (PTPgamma) in human breast cancer cell line MCF-7. Oncogene. 2004 Feb 12;23(6):1256–62.

718. Shu ST, Sugimoto Y, Liu S, Chang H-L, Ye W, Wang L-S, et al. Function and regulatory mechanisms of the candidate tumor suppressor receptor protein tyrosine phosphatase gamma (PTPRG) in breast cancer cells. Anticancer Res. 2010 Jun;30(6):1937–46.

719. Allinen M, Beroukhim R, Cai L, Brennan C, Lahti-Domenici J, Huang H, et al. Molecular characterization of the tumor microenvironment in breast cancer. Cancer Cell. 2004 Jul;6(1):17–32.

720. Mazzatti DJ, White A, Forsey RJ, Powell JR, Pawelec G. Gene expression changes in long-term culture of T-cell clones: genomic effects of chronic antigenic stress in aging and immunosenescence. Aging Cell. 2007 Apr;6(2):155–63.

721. Lo M, Bulach DM, Powell DR, Haake DA, Matsunaga J, Paustian ML, et al. Effects of temperature on gene expression patterns in Leptospira interrogans serovar Lai as assessed by whole-genome microarrays. Infect Immun. 2006 Oct;74(10):5848–59.